8. Report MA-129T

7. 15 August 1980

1. Tech. Mon: Merlyn F. Lausten

2. EP22

NASA

(NASA-CR-160906) PHOTOGRAPHIC COMBUSTION CHARACTERIZATION OF LOX/HYDROCARBON TYPE PROPELLANTS Final Report (Aerojet Liquid Rocket Co.) 164 p HC A08/MF A01 CSCL 21D

N81-16310

Unclas
G3/28 41220

3 # PHOTOGRAPHIC COMBUSTION CHARACTERIZATION OF LOX/HYDROCARBON TYPE PROPELLANTS

Final Report

By

4. D. C. Judd

5. AEROJET LIQUID ROCKET COMPANY

Prepared For

NATIONAL AERONAUTICS AND SPACE ADMINISTRATION

NASA-Johnson Space Center

6, Contract NAS 9-15724

PHOTOGRAPHIC COMBUSTION CHARACTERIZATION OF LOX/HYDROCARBON TYPE PROPELLANTS

Contract NAS 9-15724
Final Report MA-129T

15 August 1980

Prepared By:

D. C. Judd
Project Engineer

Aerojet Liquid Rocket Company
P.O. Box 13222
Sacramento, California 95813

FOREWORD

This final report describes the analytical and experimental work conducted to develop techniques for photographing Liquid Oxygen/Hydrocarbon (LOX/HC) phenomena and to identify and characterize potential anomalies (e.g., reactive stream separation [RSS], carbon formation, fuel freezing) in the combustion of LOX/HC propellants operating with a variety of injector elements. The activity was performed by Aerojet Liquid Rocket Company on Contract NAS 9-15724 under the direction of Mr. M. F. Lausten, NASA/JSC Project Manager. Aerojet personnel included Mr. J. W. Salmon, Program Manager, Mr. B. R. Lawver, Project Manager, and Mr. D. C. Judd, Project Engineer. The following individuals also contributed to the success of the program:

Gene Hron	Fabrication
Arnold Keller	Test Engineering
Norm Rowett	Test Instrumentation
Duane Robertson	Test Instrumentation
Lee Lang	Injector Design
Jim Duey	Data Analysis
Anne Johnson	Data Analysis

ABSTRACT

An experimental and analytical program was conducted to determine if previously developed high-speed photography techniques could be utilized to increase the analytical understanding of LOX/HC type propellant combustion. The program was conducted in two phases. The objective of Phase I was to demonstrate the advantages and limitations of using high-speed photography to identify potential combustion anomalies (e.g., pops, fuel freezing, reactive stream separation [RSS], carbon formation). The objective of Phase II, and the primary program end product, was to develop combustion evaluation criteria for evaluating, characterizing, and screening promising low-cost propellant combination(s) and injector element(s) for long-life, reusable engine systems.

Carbon formation and RSS mechanisms and trends were identified by using high-speed color photography at speeds up to 6000 frames/sec. Single element injectors were tested with LOX/RP-1, LOX/Propane, LOX/Methane and LOX/Ammonia propellants. Tests were conducted using seven separate injector elements. Five different conventionally machined elements were tested: OFO Triplet; Rectangular Unlike Doublet (RUD); Unlike Doublet (UD); Like-on-Like Doublet (LOL-EDM); and Slit Triplet. The RUD and Slit Triplet had rectangular orifices; the others were circular. Two platelet injectors were tested: the Transverse Like-on-Like Doublet (TLOL) and the Pre-Atomized Triplet (PAT). Platelet injectors are fabricated by diffusion-bonding a stack of thin metal sheets which have etched flow passages. All seven injectors were fired at main engine conditions. The RUD and LOL-EDM were also fired at gas generator mixture ratios. One hundred and twenty-seven (127) tests were conducted over a chamber pressure range of 125-1500 psia, a fuel temperature range of -245°F to 158°F, and a fuel velocity range of 48-707 ft/sec.

Combustion evaluation criteria were developed at the initiation of Phase II to guide selection of the fuels, injector elements, and operating conditions for testing. Separate criteria were developed for fuel and injector element selection and evaluation.

The fuel selection criteria were divided into two categories: system and test. The system criteria are 1) Specific Impulse, 2) Regenerative Chamber Cooling Capability, 3) Bulk Density, 4) Cost, 5) Toxicity, and 6) Corrosiveness. The selected test criteria are 1) Fuel Freezing, 2) Pops, 3) Carbon Formation, 4) Reactive Stream Separation (RSS), and 5) Supercritical Pressure Operation.

ABSTRACT (cont.)

The injector element selection criteria were 1) Atomization, 2) Mixing (i.e., RSS), 3) Injector Face Compatibility, 4) Chamber Wall Compatibility, 5) Chug Stability, 6) High Frequency Combustion Stability, 7) Injector Momentum Balance, 8) Fuel Freezing, and 9) Meaningful Photographic Results.

After Phase II testing, two additional criteria were added: Carbon Formation and Fabrication Complexity. The Phase II testing provided data for assessment of two of the fuel evaluation criteria: carbon formation and RSS. The gas-side carbon formation criteria proved to be accurate. As the fuel hydrogen/carbon ratio decreased (CH_4 = 4.0, C_3H_8 = 2.67, RP-1 = 2.0), carbon formation increased. The fuel type also influences the fuel vaporization rate, which plays a significant role in carbon formation. As the fuel vaporization rate increases in the injector face near-zone, carbon formation decreases. Mixing limited combustion (i.e., RSS) proved to be sensitive to all parameters that influence fuel vaporization rate. For any operating point, the fuel yielding the more rapid near-zone fuel vaporization will, in general, increase the degree of RSS.

The Phase II testing resulted in definitive data on four of the previously described injection element evaluation criteria: Mixing (i.e., RSS), Injector Momentum Balance, Fuel Freezing, and Carbon Formation. Two factors control mixing: 1) the fuel vaporization rate and 2) the degree of injection orifice or spray fan cant towards the unlike propellant. Unlike spray fan impingement elements (i.e., TLOL, PAT and EDM-LOL) increase the fuel vaporization rate and promote RSS. The testing confirmed the pre-test criteria for injector momentum balance. No incidences of fuel freezing occurred. Fuel freezing is not an important design criteria for injectors in the low-thrust per element design range (approximately 1-50 lbF/element). The photographic test results indicated conclusively that injector element type and design directly influence carbon formation. Unlike spray fan impingement elements reduce carbon formation because they induce a relatively rapid near-zone fuel vaporization rate. Coherent jet impingement elements, on the other hand, exhibit increased carbon formation.

TABLE OF CONTENTS

TABLE OF CONTENTS (cont.)

LIST OF TABLES

LIST OF FIGURES

LIST OF FIGURES (cont.)

I. INTRODUCTION AND SUMMARY

A. INTRODUCTION

Studies to date indicate that two of the major keys to achieving low space transportation costs are minimizing engine development and operational costs. Therefore, major reductions in future space transportation costs will be achieved with highly reusable systems that utilize low-cost propellants. Since the selection of the propellants will have a major impact on the cost of future space transportation, it is imperative that a comprehensive evaluation be conducted prior to the selection of the final propellant combination(s).

The use of high-speed single element photography has been found to be an economical and successful method for evaluating and characterizing hypergolic propellants (Ref. 1). The results have been successfully applied in the following programs: Space Shuttle Orbital Maneuvering Engine Technology, Space Shuttle Orbital Maneuvering Engine Development, Air Force ITIP (Improved Transtage Injector Program), Air Force 5 lbF N_2O_4/MMH, Improved Aerobee, and the Post Boost Propulsion System for the Air Force MX Program. In this study, a number of low-cost propellants (LOX/Hydrocarbon and LOX/Ammonia), injectors, and operating conditions were characterized and screened with a minimum of funding by using a modification of these photographic techniques.

The program had two primary objectives. The first objective, Phase I, was to experimentally demonstrate the advantages and limitations of using high-speed photography to identify and characterize potential anomalies (e.g., pops, fuel freezing, thermal decomposition, and reactive stream separation [RSS]) in the combustion of liquid oxygen/hydrocarbon (LOX/HC) type propellants operating with a variety of injector elements. The second objective, Phase II, was to develop combustion evaluation criteria based on the test results for evaluating, characterizing, and screening promising low-cost LOX/HC type propellants for long-life reusable propulsion systems. The seven injectors and four propellant combinations tested in this program provide much of the needed experimental data necessary to rationally select the most promising propellant combination(s) and injector element(s) for future engine technology efforts and development programs.

B. SUMMARY

The work undertaken in this program resulted in the design and testing of seven single element injectors and four fuels with the aim of photographically characterizing observed combustion phenomena. The seven injectors tested were the OFO Triplet, the Platelet Transverse Like-on-Like Doublet (TLOL), the Rectangular Unlike Doublet (RUD), the Unlike Doublet (UD), the Like-on-Like Doublet Electrode Discharge Machined (LOL-EDM), the

I, B, Summary (cont.)

Platelet Pre-Atomized Triplet (PAT), and the EDM Slit Triplet. The OFO triplet consists of three inline circular orifices. The outside two orifices flow with oxidizer and are canted inboard to impinge the axially directed fuel orifice. Except for the two platelet elements, all of the elements utilize coherent jet impingement. These elements mechanically atomize the propellant prior to impingement. The fuels tested were RP-1, Propane (C_3H_8), Methane (CH_4) and Ammonia (NH_3). The hotfirings were conducted in a specifically constructed chamber fitted with quartz windows for photographically viewing the impingement spray field.

Test photographic results showed that the appearance of LOX/HC combustion is markedly different from previously observed storable propellant combustion (Ref. 1). Figure 1 displays typical photographic results from the program. In the top photograph, black clouds are clearly visible downstream of the impingement zone. The occurrence of these clouds was assumed to indicate the formation of free carbon during the combustion process. The bottom photograph shows striated oxidizer and fuel fans, which indicates relatively poor bipropellant mixing. Carbon formation and mixing were the two combustion processes most thoroughly characterized as a result of the photographic testing.

The Phase I test program consisted of 44 tests. The following main chamber injector/fuel combinations were tested: 1) OFO Triplet/RP-1 Fuel; 2) RUD/RP-1 Fuel; 3) TLOL/RP-1 Fuel; 4) TLOL/Propane Fuel; and 5) RUD/Propane Fuel. The RUD was also tested with propane at gas generator conditions. The Phase I testing resulted in the establishment of a baseline photographic technique for main chamber conditions. The testing indicated that carbon formation and RSS (i.e., mixing) trends could be established by using highspeed photography. The major limitation to proper assessment of gas generator combustion characterization was caused by dense black clouds obscuring the combustion flow field during testing.

The Phase II test program consisted of 83 tests. The fuels, injection elements, and operating conditions were selected with the Phase II combustion evaluation criteria (described below). The following main chamber injector/fuel combinations were tested: 1) UD/Ammonia Fuel; 2) LOL-EDM/Propane Fuel; 3) PAT/Propane Fuel; and, 4) Slit Triplet/Gaseous Methane Fuel. Two gas generator injector/fuel combinations were tested: 1) LOL-EDM/Propane Fuel and 2) LOL-EDM/Liquid Methane Fuel. The Phase II testing yielded important insights leading to preliminary model formulations for carbon formation and RSS.

Carbon formation within the injector spray field was found to be directly related to fuel temperature (T_f), fuel type, chamber pressure

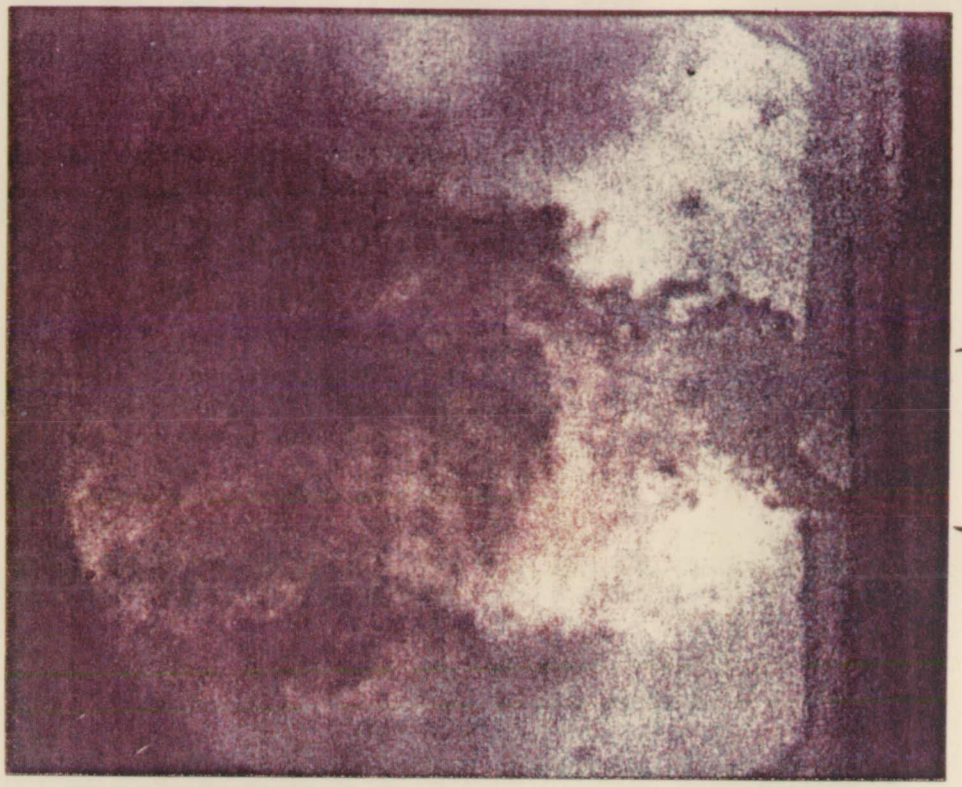

Test No. 172 Pc = 610 psia

Fuel Type: C_3H_8 O/F = 2.95

Injector Element: Like-on-Like EDM

Test No. 187 Pc = 800 psia

Fuel Type: C_3H_8 O/F = 2.90

Injector Element: Pre-Atomized Triplet

Figure 1. High-Speed Photography Shows Carbon Formation and Mixing Trends For Hydrocarbon Fuels

(Pc), and injector type. Distinct regions of carbon formation were identified and correlated with three plots of "Pc-VS-T_f". Each of the data points is a symbol which represents a certain degree of photographic clarity assumed to be indicative of carbon formation. The data indicate that the carbon formation may be related to a flame-quenching or partial reaction mechanism. Development of a physically mechanistic model will require more experimental work. Testing with methane at both main engine and fuel-rich gas generator mixture ratios showed that methane can burn with very little or no carbon deposition.

For the purposes of this report, RSS is defined as any degradation or change in the hotfire spray mixing characteristics as compared to the observed cold-flow mixing characteristics. Some degree of RSS was observed to occur with all of the fuels except ammonia. One hypothesis for its occurrence is vaporization-controlled combustion at the impingement interface. Interface combustion is a function of fuel ignition delay time, chamber pressure, fuel temperature, and fuel type. Impingement angle was also observed to have an influence on HC RSS. A second hypothesis is that the change in mixing characteristics with chamber pressure and temperature is dependent on gas dynamic effects correlated by the Weber Number. The Weber Number effect at higher chamber pressures may cause faster breakup which changes mixing patterns. Further testing is required to clarify the RSS mechanism.

No fuel "freezing" or popping was experienced under any of the test conditions evaluated in this program (orifice diameters from .024 to .045 inches). It is possible, however, that the use of large orifices (e.g., booster engine applications) could promote fuel freezing because of their reduced surface area to volume ratio (i.e., combustion gases would heat larger orifice jets more slowly).

Combustion evaluation criteria were developed at the initiation of Phase II to guide selection of the fuels, injector elements, and operating conditions for testing. The basic sources of data for development of the criteria were recently conducted LOX/HC technology programs, the N_2O_4/Amine fuels "Blowapart" program (Ref. 1), and the Phase I test results. Separate criteria were developed for fuel and injector element selection and evaluation.

The fuel selection criteria were divided into two categories: system and test. The system criteria are 1) Specific Impulse, 2) Regenerative Chamber Cooling Capability, 3) Bulk Density, 4) Cost, 5) Toxicity, and 6) Corrosiveness. The system criteria were used for fuel selection but were not evaluated during the test program. The selected test criteria are 1) Fuel Freezing, 2) Pops, 3) Carbon Formation, 4) Reactive Stream Separation, and 5) Supercritical Pressure Operation.

I, B, Summary (cont.).

The injector element selection criteria were: 1) Atomization, 2) Mixing (i.e., RSS), 3) Injector Face Compatibility, 4) Chamber Wall Compatibility, 5) Chug Stability, 6) High Frequency Combustion Stability, 7) Injector Momentum Balance, 8) Fuel Freezing, and 9) Meaningful Photographic Results.

The fuel and injector element criteria were used to select the fuel and injection elements for Phase II testing. For the most part, qualitative judgments were used to rate the candidate fuels and elements. Based on the criteria, three fuels - propane, methane (gaseous and liquid), and ammonia - and six injector element configurations - LOL-EDM, PAT, UD, Slit Triplet, RUD Gas Generator, and LOL-EDM Gas Generator - were selected.

The Phase II testing provided data for assessment of two of the fuel evaluation criteria: carbon formation and RSS. The gas-side carbon formation criteria proved to be accurate. As the fuel hydrogen/carbon ratio decreased (CH_4 = 4.0, C_3H_8 = 2.67, RP-1 = 2.0), carbon formation increased. The fuel type also influences the fuel vaporization rate, which plays a significant role in carbon formation. As the fuel vaporization rate increases in the injector face near-zone, carbon formation decreases. Mixing limited combustion (i.e., RSS) proved to be sensitive to all parameters that influence fuel vaproization rate. For any operating point, the fuel yielding the more rapid near-zone fuel vaporization will, in general, increase the degree of RSS.

The Phase II testing resulted in definitive data on four of the previously described injection element evaluation criteria: Mixing (i.e., RSS), Injector Momentum Balance, Fuel Freezing, and Meaningful Photographic Results. Additionally, as a result of the testing and a reanalysis of the important considerations pertaining to injector selection, two additional criteria were added: Carbon Formation and Fabrication Complexity. Two factors control mixing: 1) the fuel vaporization rate and 2) the degree of injection orifice or spray fan cant towards the unlike propellant. Unlike spray fan impingement elements (i.e., TLOL, PAT and EDM-LOL) increase the fuel vaporization rate and promote RSS. The testing confirmed the pre-test criteria for injector momentum balance. No incidences of fuel freezing occurred. Fuel freezing is not an important design criteria for injectors in the low-thrust per element design range (approximately 1-50 lbF/element). The photographic test results indicated conclusively that injector element type and design directly influence carbon formation. Unlkike spray fan impingement elements reduce carbon formation because they induce a relatively rapid near-zone fuel vaporization rate. Coherent jet impingement elements, on the other hand, exhibit increased carbon formation.

I, B, Summary (cont.)

Testing to date has increased knowledge of LOX/HC combustion phenomena and has provided much of the necessary data. However, the suggested fuel and injection element selection criteria are still qualitative. Carbon formation and RSS trends and influences are understood. However, mechanistic analytical modeling must still be conducted in order to obtain quantitatively accurate evaluation criteria as well.

II. TECHNICAL APPROACH

The objective of this program was to identify and characterize potential LOX/HC combustion anomalies with various low-cost fuels and injectors to rationally select the most promising combinations for future engine technology and development efforts. This objective was accomplished through high-speed photography and analysis of seven single element injectors and four low-cost propellants (see Table I). The injectors, fuels, and test conditions are representative of advanced OMS and RCS engine applications at both main engine and fuel-rich gas generator conditions.

The program was originally funded for a two-phase program spread over twelve months. This was subsequently changed to a fifteen-month program to allow added-scope testing of additional fuels and injectors. Figure 2 shows the program schedule and the detailed breakdown of Phase I and Phase II events.

The Task I objectives were to conduct all the design, fabrication, testing, and analysis necessary to demonstrate the advantages and limitations of using high-speed photography to identify and characterize potential anomalies (e.g., pops, fuel freezing, stream separation, carbon formation, etc.) in the combustion of LOX/HC type propellants while operating with various injector elements. The work included the following: preparation of a detailed test plan (Ref. 2 and 3); design of an unlike jet impinging injector (Rectangular Unlike Doublet-RUD); design of an unlike spray impinging injector (Transverse Like-on-Like-TLOL); experimental testing and photographic coverage of the RUD and TLOL with RP-1 and propane at main engine conditions; experimental testing and photographic coverage of an existing OFO Triplet injector with RP-1 at main engine conditions, and experimental testing and photographic coverage of the RUD with propane at fuel-rich gas generator conditions.

The Task II objectives were 1) to develop combustion evaluation criteria based on pre-test analysis and Phase I hotfire testing and 2) to evaluate, characterize, and screen several LOX/HC propellants with different injector elements on the basis of the evaluation criteria. The emphasis was directed towards providing data to aid in the rational selection of the most promising propellant combinations(s) and injector element(s) for future engine technology and development efforts. Task II work included the following: 1) preparation of a "Propellant, Injector, and Test Conditions Recommendation" for Phase II testing (Ref. 4), which included the combustion evaluation criteria that had served as a screening guide for fuel and injector selection) and 2) design and testing of the following injector and fuel combinations:

a) Unlike Doublet - LOX/NH_3 as a main engine element.

b) LOL-EDM - LOX/C_3H_8 as a main engine and gas generator element.

TABLE I

SUMMARY OF INJECTORS AND TEST CONDITIONS

INJECTOR ELEMENT	FUEL	CHAMBER PRESSURE (psia)	MR	FUEL VELOCITY (ft/sec)	FUEL TEMPERATURE (°F)	NO. OF TESTS
OFO Triplet	RP-1	450-1500	1.7-2.8	76-200	50-72	16
RUD (Main Engine)	RP-1	130	2.8	57	15	2
RUD (Main Engine)	C_3H_8	150-790	2.6-3.15	63-166	52-68	8
RUD (Gas Generator)	C_3H_8	850-860	0.46-0.5	110-116	59-61	3
TLOL	RP-1	135-800	2.1-3.1	48-95	30-45	11
TLOL	C_3H_8	135-790	2.5-3.0	63-120	43-45	4
UD	NH_3	150-505	1.1-1.67	73-150	45-65	12
LOL-EDM (Main Engine)	C_3H_8	150-800	2.2-4.1	56-165	29-158	20
LOL-EDM (Gas Generator)	C_3H_8	510-810	0.72-0.73	88-113	75-79	2
LOL-EDM (Gas Generator)	ℓCH_4	485-805	0.82-0.44	113-157	-206-245	6
PAT	C_3H_8	150-805	2.2-3.5	69-178	43-120	21
Slit Triplet	gCH_4	125-810	2.75-4.7	174-707	38-73	22
						127

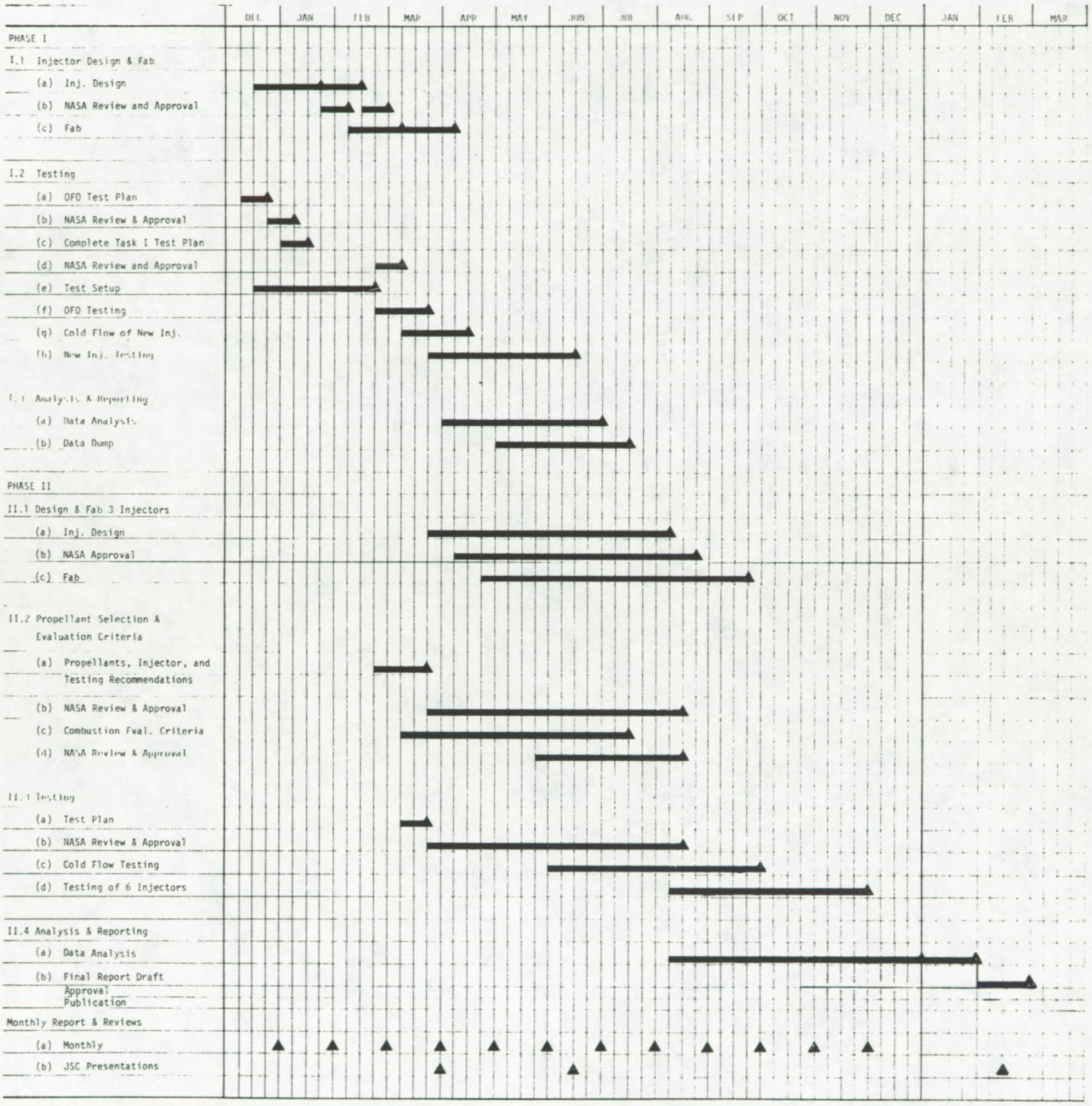

Figure 2. Photographic Characterization of LOX/HC Type Propellants Program Schedule

II, Technical Approach (cont.)

c) LOL-EDM - LOX/$_{\ell}$CH4 as a gas generator element.

d) PAT - LOX/C3H8 as a main engine element.

e) Slit Triplet-LOX/gCH4 as a main engine element.

Task II also included 1) an evaluation and comparison of the test results as per the combustion evaluation criteria, along with pertinent data correlations aiding in the characterization of LOX/HC combustion anomalies (included herein) and 2) a discussion of the unexpected program results/benefits, combined with recommendations for further efforts (included herein).

III. RESULTS AND CONCLUSIONS

A. RESULTS

Distinct regions of carbon formation within the injector sprays were observed and identified for the following fuel/injector combinations using high speed color photography:

Fuel	Injector
RP-1	TLOL, RUD, OFO Triplet
C_3H_8	RUD, LOL-EDM (Short Impingement Height)
C_3H_8	TLOL, PAT (Long Impingement Height)

Carbon formation was found to be directly related to fuel temperature, fuel type, chamber pressure, and injector type. Each test was rated according to the degree of carbon formation observed. Figure 3 illustrates how ratings of "CLEAR," "PARTIALLY OBSCURED," and "OBSCURED" would appear with a single unlike doublet element. The chamber pressure exerts the strongest influence on carbon formation. Increasing chamber pressure reduces carbon formation. Carbon formation is dependent on the fuel types. Carbon formation increases with decreasing molecular hydrogen/carbon ratio. Injector type influences carbon formation. Increasing the fuel free stream length and interfacial surface area available for heating reduces carbon. Figure 4 shows plots that correlate carbon formation, chamber pressure, fuel temperature, fuel type and injector type. This data can be more easily studied in Figures 48, 49 and 50.

RSS was observed in the combustion of LOX/HC type propellants and found to be primarily influenced by chamber pressure, fuel temperature, and injector type. RSS was far more apparent for unlike spray impingement elements (TLOL, PAT, EDM-LOL). RSS was characterized by reduced mixing in the spray field, as shown in Figure 5.

Although RSS trends are observable, more testing at lower pressures, different impingement angles, and varied fuel temperatures is necessary to formulate correlations.

Other significant results and observations are as follows:

1. Fuel freezing and popping was not observed with the injector elements and operating conditions tested to date. However, there is evidence of fuel cooling.

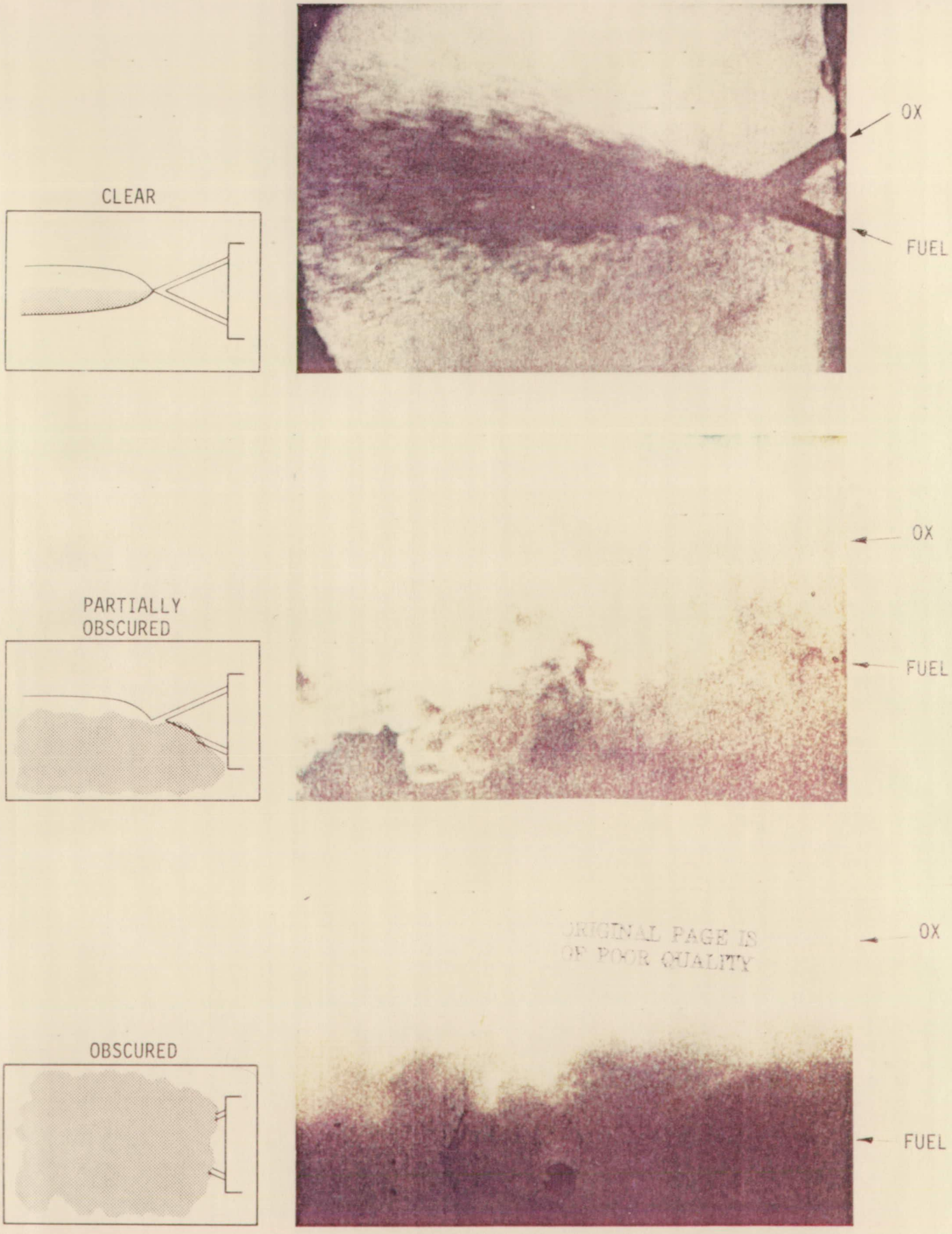

Figure 3. Modes of Carbon Formation

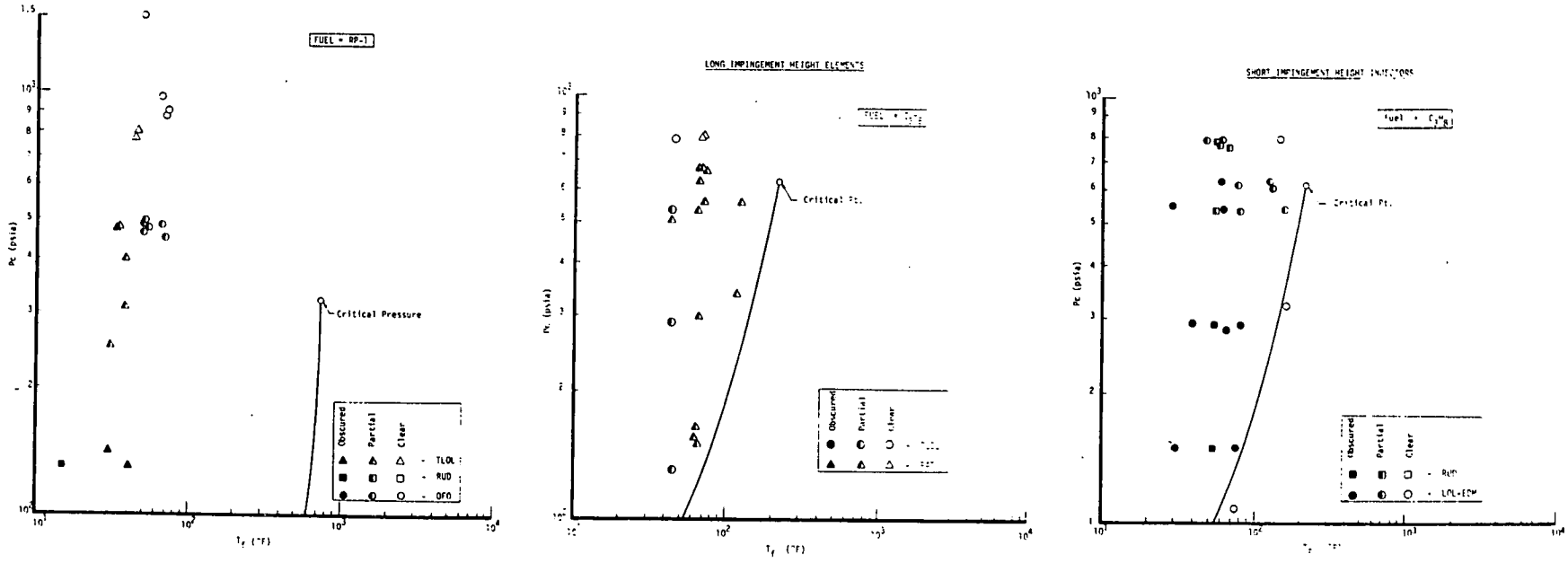

Figure 4. Carbon Formation is Correlated with Chamber Pressure, Fuel Temperature, Fuel Type, and Injector Type

LOW P_c

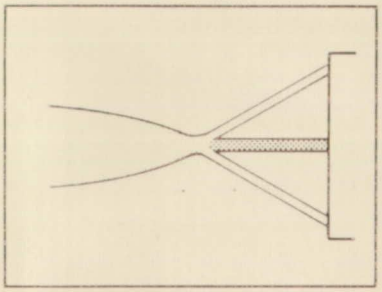

HIGH P_c

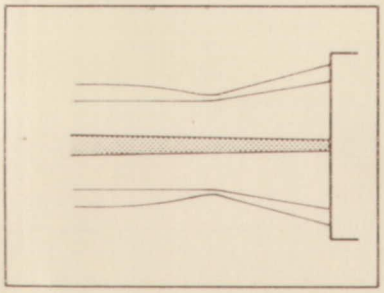

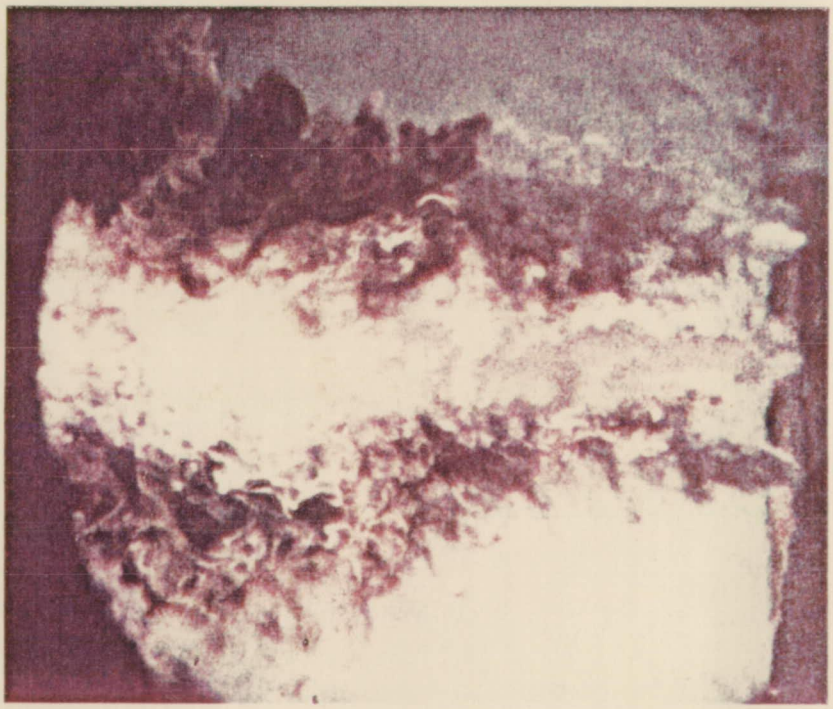

Figure 5. Stream Separation in the Spray Field at High Pc

III, A, Results (cont.)

2. Atomization, vaporization and combustion at supercritical pressure is not noticeably different from combustion at subcritical pressure, except for the continuous influence of chamber pressure on the fuel vaporization rate.

3. Fuel-rich methane gas generator single element combustion was observed to burn cleanly without carbon formation.

4. C* efficiency was observed to increase with increasing chamber pressure and flowrate for all fuels and injectors.

5. Heating the fuel appears to affect liquid phase mixing slightly, as evidenced by a slight decrease in C* (i.e., increased RSS).

6. Effective high-speed color photography techniques have been developed for observing single element LOX/HC combustion.

One of the main objectives of Task II was to develop combustion evaluation criteria, based on analysis and testing, and use it to evaluate, characterize, and screen several LOX/HC propellants in different injector elements (Ref. 4). Fuel and injection element evaluation criteria were defined (see Section V.E). The criteria were applied qualitatively to select fuels and injection elements for Phase II testing. The Phase II test results indicate that carbon formation and RSS trends are understood, but that mechanistic analytical modeling must be conducted to obtain valuable quantitative evaluation criteria.

B. CONCLUSIONS

The following conclusions are drawn from this work.

1. Single element photography has been successfully used to characterize LOX/HC combustion.

2. Qualitative trends are understood for control of carbon formation. Chamber pressure, fuel type, fuel temperature, and injector design influences have been observed. Carbon formation increased for the fuels tested in the following order: ammonia, methane, propane, RP-1.

3. Methane shows significant promise as a non-carbon generating H/C fuel for gas generators and preburners.

III, B, Conclusions (cont.)

4. Ammonia displayed relatively benign combustion that resulted in well-mixed bipropellant spray fans over a wide operating range.

5. Qualitative trends are understood for control of LOX/HC combustion mixing. Chamber pressure, fuel type, fuel temperature and injector design influences have been observed.

6. Preliminary modeling approaches for carbon formation and RSS have been suggested, but physically mechanistic models are not yet developed.

7. The program carbon deposition data could be used to develop models for gas-side carbon deposition for high-pressure LOX/HC thrust chambers.

8. The program RSS data could be used to develop models for injector element mass and mixture ratio distribution control for all advanced engines.

IV. APPLICATION OF RESULTS AND RECOMMENDATIONS

A. APPLICATION OF RESULTS

The primary result of this program is a fundamental understanding of the RSS and carbon formation combustion phenomena associated with LOX/HC combustion. This understanding will be applied to aid the design, testing, and analysis of multi-element LOX/HC injectors and to guide the development of mechanistic analytical models.

B. RECOMMENDATIONS

The following recommendations are made on the basis of the program results:

1. Continued single element cold-flow and hotfire photographic testing is recommended.

   a. Testing of heated propane and RP-1 at gas generator operating conditions is necessary to characterize carbon formation dependence on fuel temperature.

   b. The carbon formation trends should be used as a guide to update the fuel-rich combustion model developed on Contract NAS 3-21753.

   c. High-pressure cold-flow testing should be performed to allow differentiation between gas dynamic (Weber No.) and combustion (RSS) effects.

   d. Further testing at low pressures (100-300 psia) is necessary to determine the influence of fuel type and injector element design parameters on the occurrence of RSS.

2. The results of the Task I cooling analysis of the Combustion Performance and Heat Transfer Characterization of LOX/HC Type Propellants Program (NAS 9-15958) should be reviewed to ensure that all potential thrust chamber assembly operating points have been characterized at single element conditions.

3. Scaling studies should be conducted to determine the applicability of the current data base to high-pressure LOX/HC liquid rocket booster designs.

V. TECHNICAL DISCUSSION

A. EXPERIMENTAL HARDWARE AND TEST SETUP

1. Test Apparatus

The test apparatus consists of a test chamber equipped with transparent viewing ports, a GO_2/GH_2 igniter, removable injectors, and nozzles (see Figure 6). The test chamber was designed during the Task III "Blowapart" program (Ref. 1) and was modified slightly for use on this program.

a. Test Chamber

The test chamber was machined from a 4-inch square x 6-inch long block of 304 CRES. The combustion chamber section is 4 inches (10.16 cm) long, to which a 2-inch (5.08 cm) L* spacer is bolted to increase the combustion zone length to 6 inches (15.2 cm). The block was bored to provide a 2.75 inch (6.99 cm) diameter combustion chamber. Four circular quartz windows were provided to facilitate photographic viewing and to allow flexibility in photographic lighting of the combustion process. The windows are 1/2 inch (1.27 cm) thick to provide a safety margin for 1000 psia (6.89×10^5 N/m^2) operation. The flat quartz windows are sandwiched between durabula gaskets for cushioning against ignition shocks and uneven loading. A silicon "O" ring provides sealing on the window periphery. Quartz windows are used to provide good propellant compatibility and well-defined optical properties. Thin quartz disc inserts are also employed to protect the 1/2" pressure bearing windows from high heat flux and window damage.

The chamber was designed to provide an inert gas (GN_2) film purge to prevent obscuring the view of propellant spray impingement on the windows. The gas purge flow is injected through four inlets into an annular manifold. The gas is directed from the manifold through an annular gap and made to flow around the periphery of the chamber wall. The wall passages were sized such that the GN_2 is injected into the chamber at 50 ft/sec (15.2 m/sec) at 300 psia (2.07×10^6 N/m^2) chamber pressure to minimize mixing with the propellant spray and combustion gas. Storable propellant "Blowapart" testing (Ref. 1) showed that the cold GN_2 purge gas caused poor spray field visibility due to the density gradient created between it and the hot combustion gas. Therefore, all subsequent storable propellant tests were run without purging during hotfire testing. However, it was necessary to reactivate the purge circuit for LOX/HC testing. In place of GN_2, a helium purge is used to protect the windows from the LOX spray during the start transient and from carbon deposits during shutdown. It automatically shuts off during steady-state operation.

Provisions were made for mounting both high and low frequency response pressure transducers and thermocouples. The nozzles consist of removable copper inserts drilled to provide the desired operating pressures. The nozzle configuration and exiting sizes are shown in Figure 7.

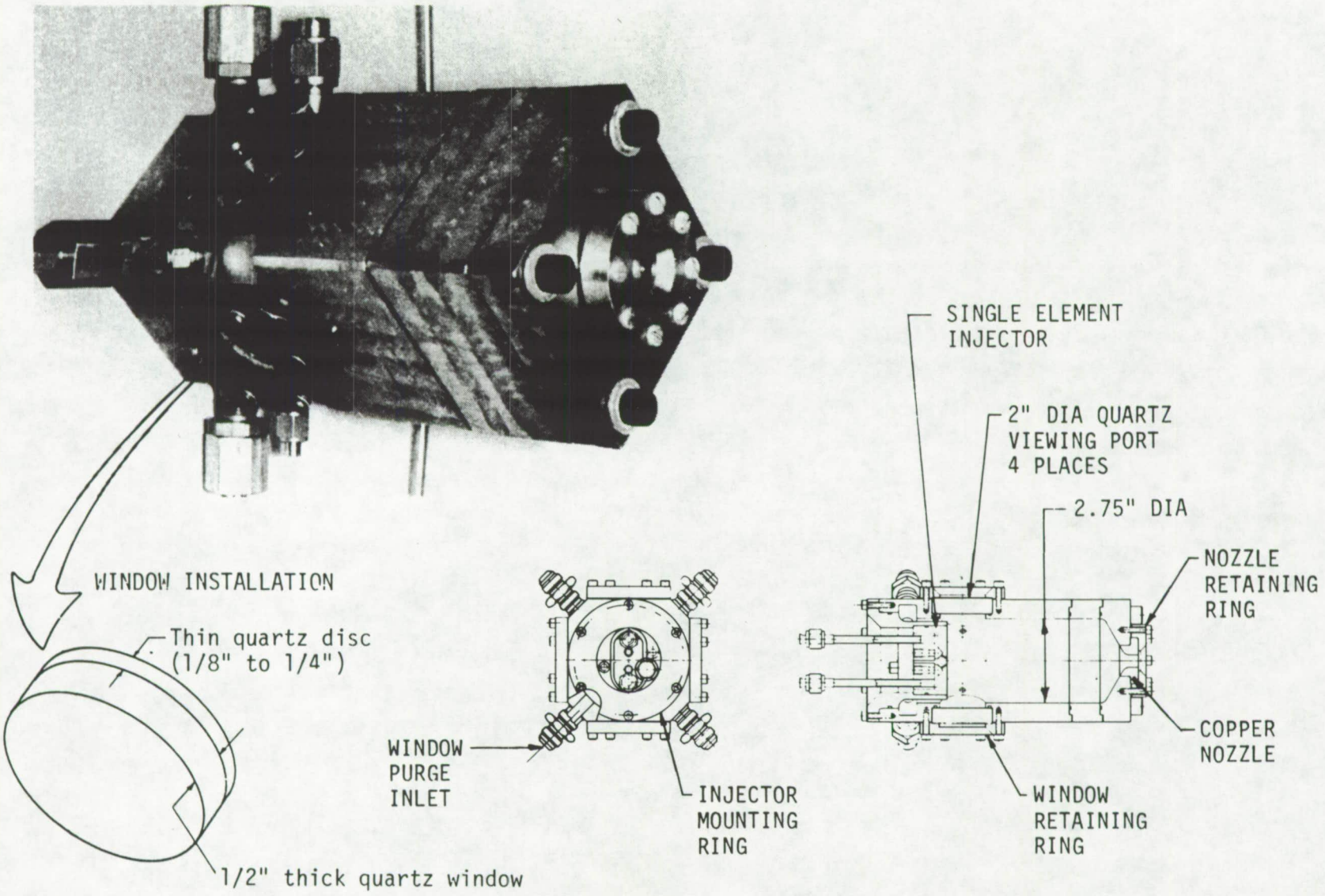

Figure 6. Test Chamber Assembly

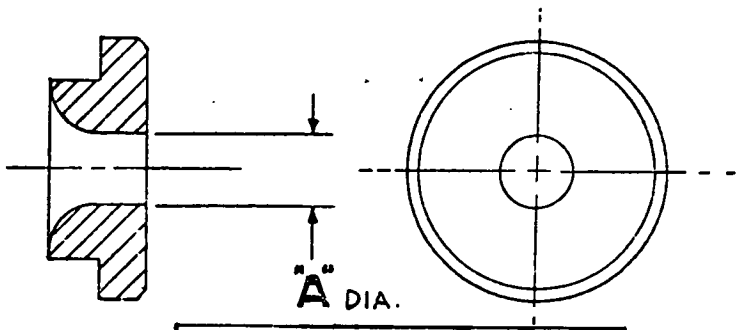

"A" Diameter	
.089	.257"
.1"	.269"
.113	.281
.125	.297
.129	.328
.140	.332
.150	.370
.166	.413
.173	.435
.189	.465
.196	.500
.213	.567
.234	.600
.250	.75 "

Figure 7. Heatsink Copper Nozzles

V, A, Experimental Hardware and Test Setup (cont.)

b. Igniter

The igniter shown in Figure 8 operates on gaseous hydrogen and gaseous oxygen which are ignited by a spark plug. This assembly is an existing igniter that has been used on many high-pressure programs. The igniter is mounted in a port drilled into the L* spacer section by means of an adapter (see Figure 9). The igniter operates at a mixture ratio of 2.0 and a chamber pressure of 250 psia during hotfire testing.

c. Injectors

Seven different injectors (two platelet and five EDM) were tested during the program. All but the OFO Triplet and the Unlike Doublet injectors were designed and fabricated on this program. These two injectors were residual hardware from Contract NAS 9-14186.

All of the injectors were made in a cylindrical "piston" shape to fit into the chamber purge ring located at the forward end of the chamber. The injector is held in the purge ring by allen head screws. A silicon rubber O-ring seals the injector to the purge ring. All of the injectors were cold-flowed prior to hotfire testing to measure Kw's and to verify impingement accuracy. The flow data are discussed in Section V.C.1.

(1) OFO

The OFO Triplet shown in Figure 10 is residual hardware from Contract NAS 9-14186. The OFO arrangement was selected to maximize the oxidizer-to-fuel interface, thereby maximizing the potential for fuel freezing. The fuel is injected axially, and the oxidizer is fed from the inlet tube to a torus which feeds two orifices 180° apart. The impingement half angle is 30°. The .030 inch diameter orifices are EDM'ed in the torus cover which is ED-welded to the body.

(2) TLOL

The Transverse Like-on-Like Element (TLOL), Figure 11, is a photo-etched platelet injector which is a version of the baseline injector element used on the Space Shuttle OMS engine. The OMS-E uses the N_2O_4/MMH storable propellant combination. The TLOL was selected for the following reasons:

(a) Like impingement and self-atomizing injectors were predicted to inhibit fuel freezing.

(b) Based on previous photographic studies with storable propellants (Ref. 1), self-atomizing injectors promote RSS.

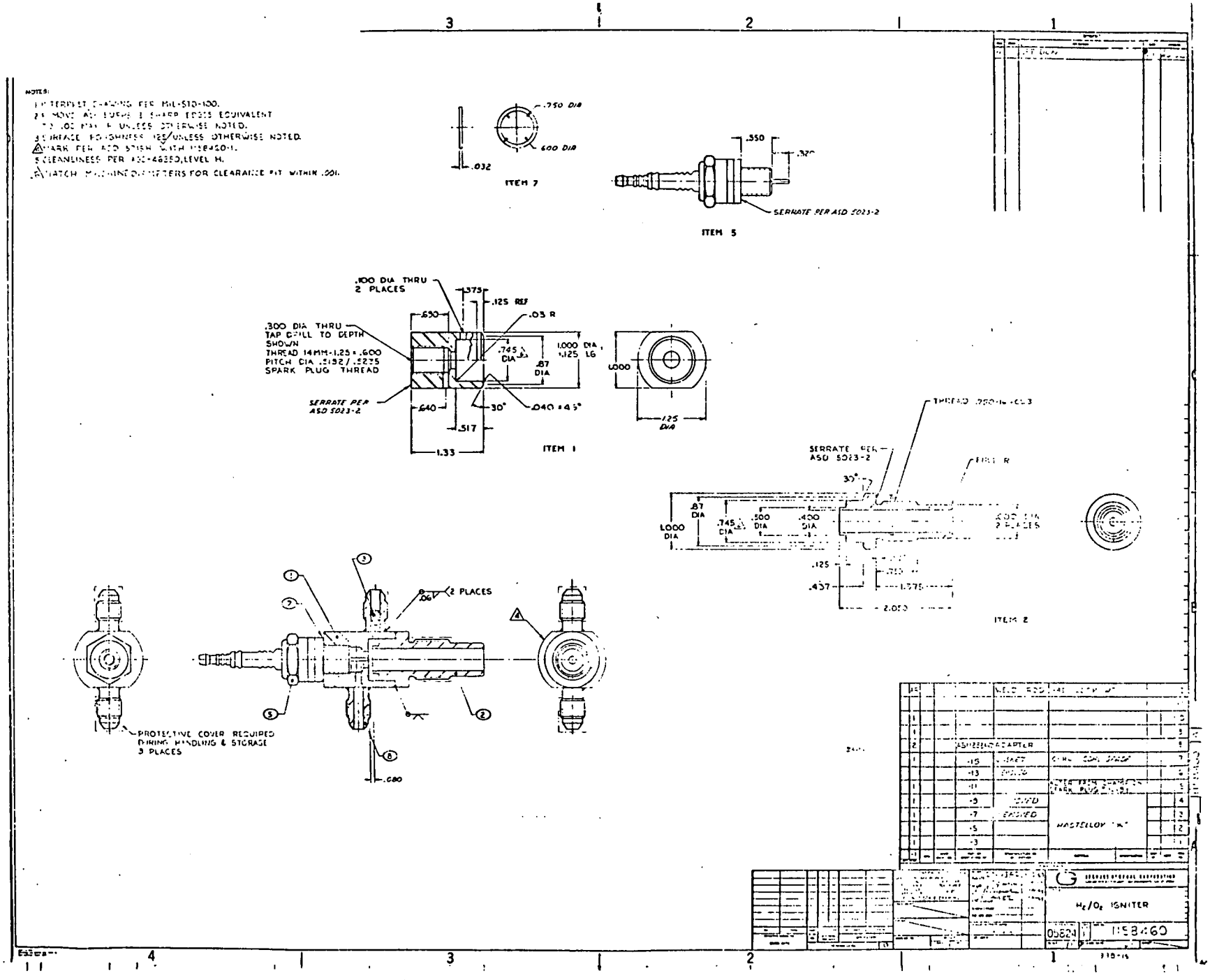

Figure 8. GO_2/GH_2 Torch Igniter

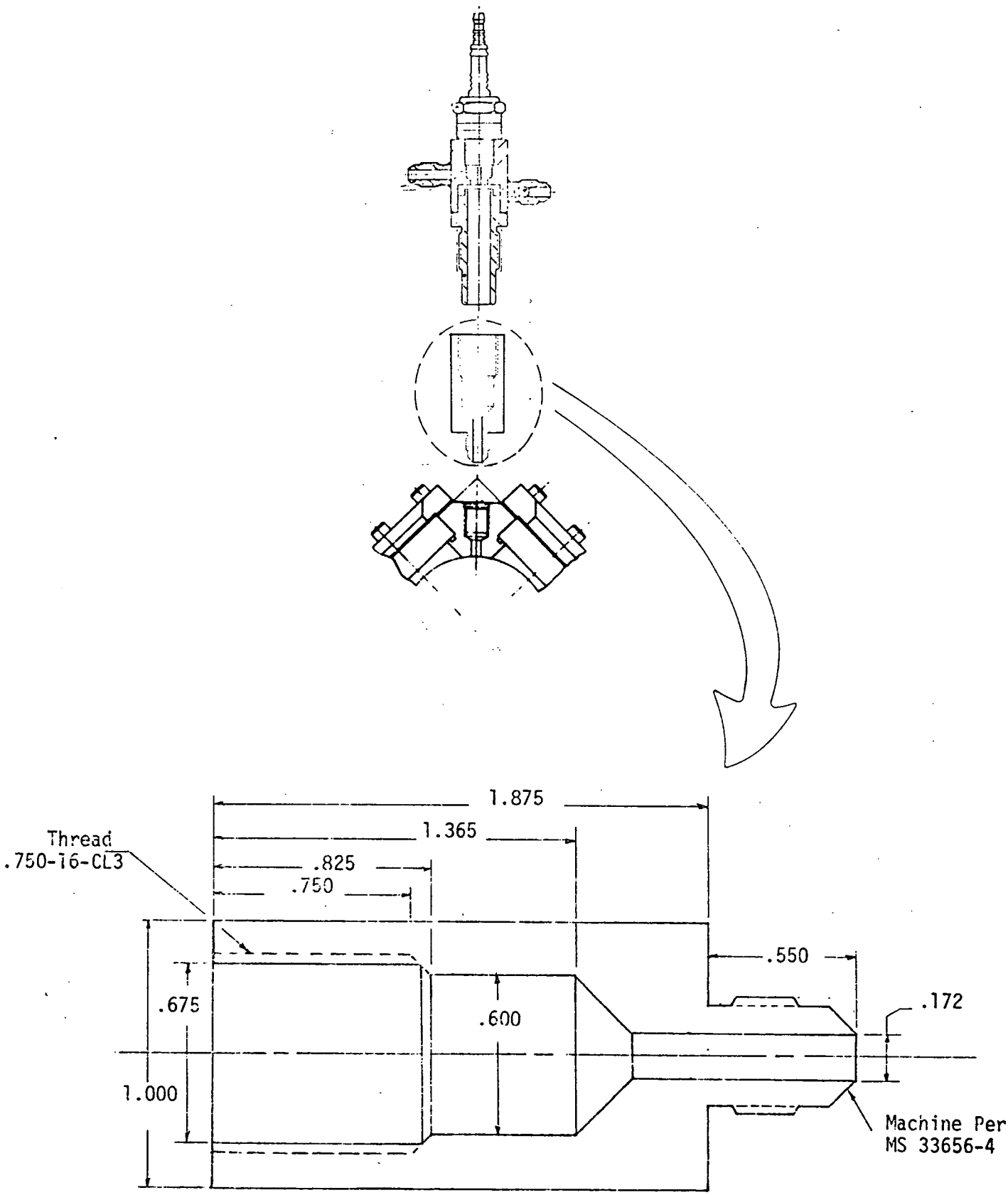

Figure 9. Igniter Mounting Adapter

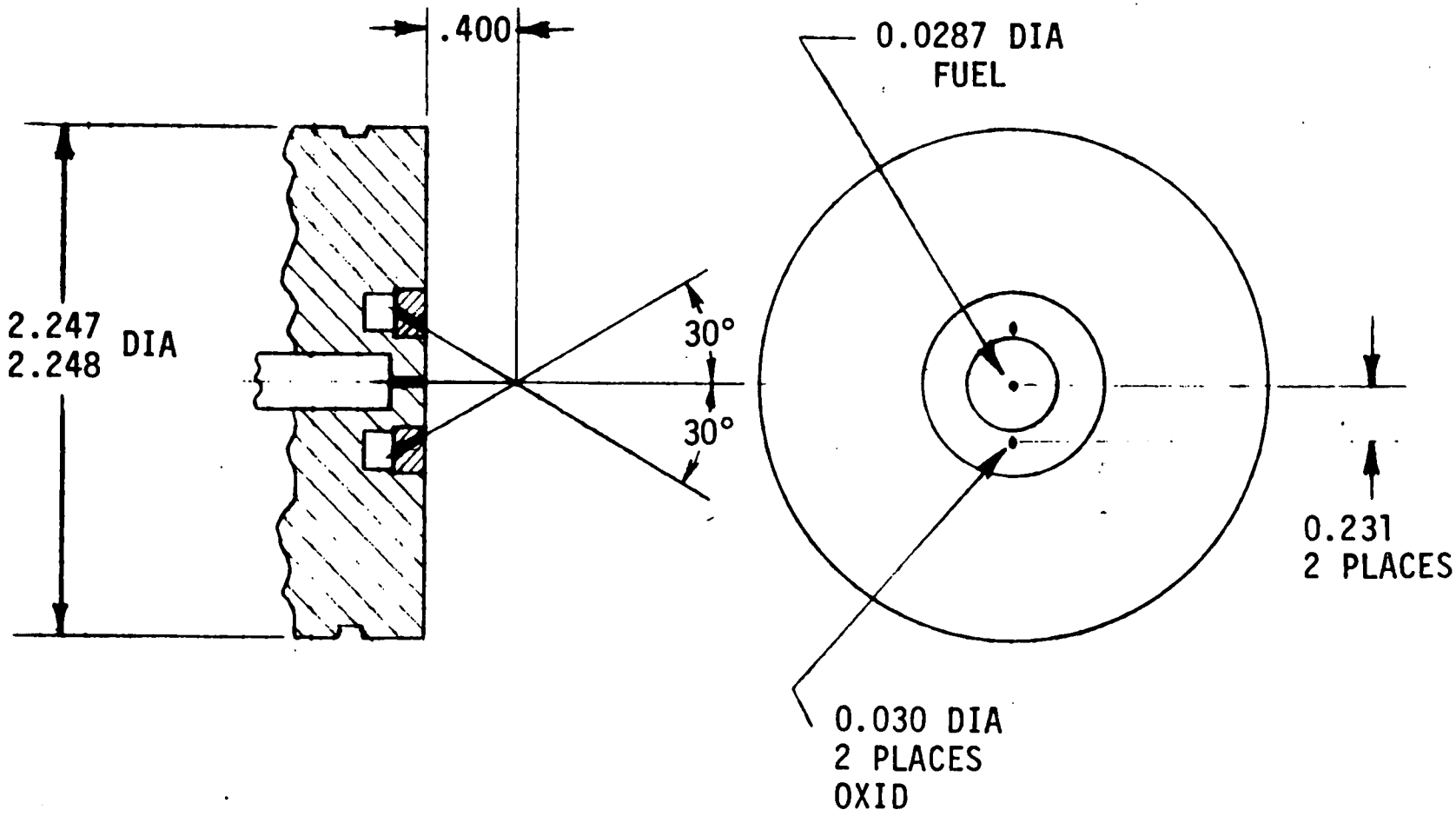

Figure 10. OFO Triplet Injector Configuration

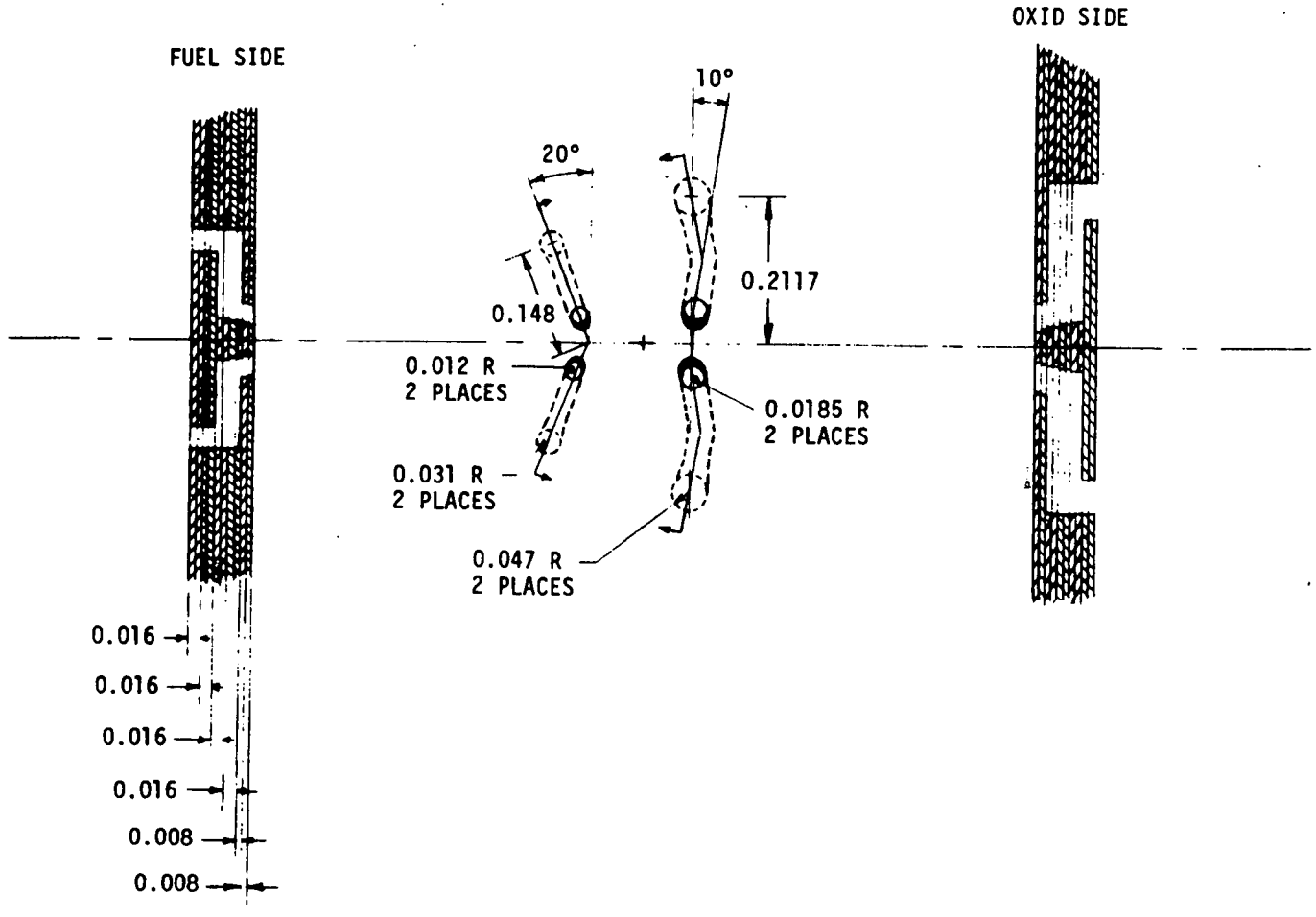

Figure 11. Transverse Like-on-Like (TLOL) Injector Configuration

(c) Like impinging doublets can be operated over a wide range of mixture ratios with little effect on resultant spray angle.

(d) This element has well-characterized predictable combustion stability and performance characteristics with storable propellants.

The TLOL consists of a body, inlet lines, a manifold platelet stack, and an element platelet stack. The manifold stack provides propellant routing and thermal isolation. The element stack contains the transverse inertance channel to the injection orifice. The platelet stacks are diffusion-bonded and then brazed to the body.

(3) RUD

The Rectangular Unlike Doublet (RUD) element (Figure 12) is an EDM'ed injector fed directly from inlet tubes. The injector face is machined so that the propellants are injected in streams normal to the face. A rectangular orifice configuration was selected to avoid the large orifice diameter mismatch associated with LOX/HC circular orifices. The circular orifice diameter mismatch produces a "banana-shaped" spray distribution which is difficult to interpret photographically. The RUD is complementary to the TLOL for the following reasons:

(a) Unlike impingement of coherent jets was predicted to encourage freezing with LOX/RP-1 propellants.

(b) Based on the results of previous work with storable propellants, coherent jets have less interfacial surface area and are not as active in promoting RSS.

(c) Resultant spray angle and mixture ratio distributions are sensitive to mixture ratio.

The RUD injector was designed for the same operating conditions and propellants as the TLOL. The injection angles of 50° for the fuel and 20° for the LOX were selected so that the resultant spray fan would parallel the centerline of the chamber at nominal mixture ratio. Aspect ratios were chosen to keep orifice area and surface tension to a minimum, thus helping to avoid the change in free stream cross section from rectangular to circular. The L:D ratio for both orifices is greater than 6 in order to ensure fully attached flow (Ref. 5).

The inlet lines are fitted with "two-pass" coolant jackets to allow for switching propellant circuits. This switching flexibility allows the RUD to be used as a fuel-rich gas generator element.

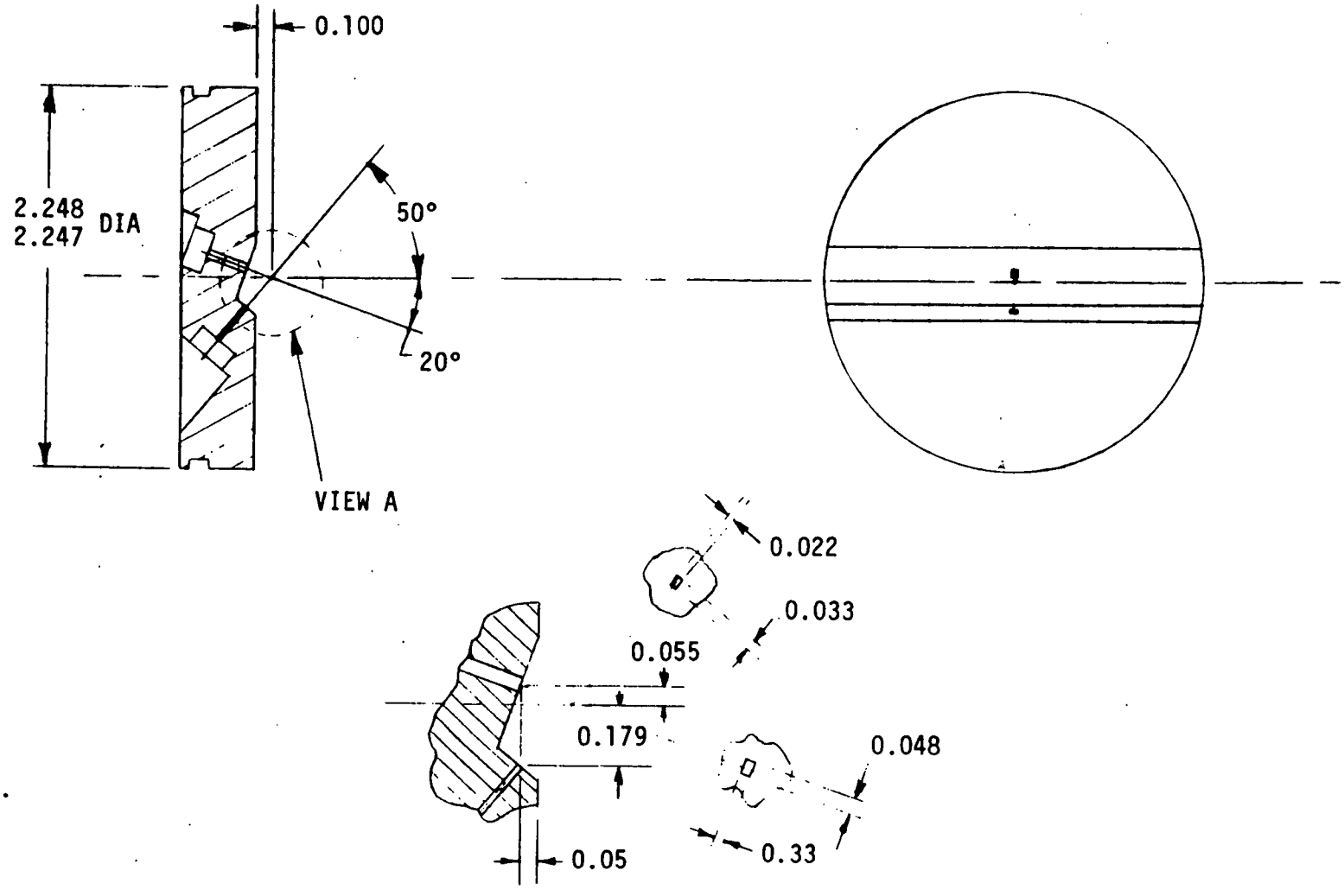

Figure 12. Rectangular Unlike Doublet (RUD) Injector Configuration

V, A, Experimental Hardware and Test Setup (cont.)

(4) UD

The Unlike Doublet (UD) element (Figure 13) is residual hardware from Contract NAS 9-14186 and was adapted for LOX/NH_3 testing by enlarging both the fuel and oxidizer orifices to .045" diameter. This diameter sizing resulted in an optimum mixing condition for LOX/NH_3. This element provided the opportunity to quickly and economically explore LOX/NH_3 combustion phenomena. This element was easily photographed because of the simple unlike impingement and because of the lack of carbon related problems.

(5) LOL-EDM

The EDM Like-on-Like (LOL-EDM) element (Figure 14) was selected partly because of its historically successful use with LOX/HC propellants and partly to gain a comparison with data from the TLOL. The LOL-EDM had a fuel fan angle of 22° and an oxidizer fan angle of 10°. An included angle of 32° was recommended for optimum performance and compatibility in the ITIP Phase Zero Final Report (Ref. 6). The LOL-EDM was designed with piston seals around the inlet manifolds so that it could be used with a reusable injector body. Figure 15 shows the reusable body with its piston seal mating surfaces and two-pass temperature conditioning jackets on both inlet lines.

(6) PAT

The Pre-Atomized Triplet (PAT) element (Figure 16) consists of two fuel splash plate elements which impinge on one centrally located oxidizer x-doublet (XDT) element. Both of these platelet element concepts are well characterized hydraulically. The PAT element was designed for a high-pressure LOX/RP-1 injector or Contract NAS 3-21030. Three of its advantages are that (1) the platelet atomization process is relatively insensitive to orifice alignment, (2) the atomization process is insensitive to propellant injection momentum, and (3) a plugged orifice does not influence the atomization characteristics of the other orifices. A reason for selecting the PAT for this program was that pre-atomization of the propellants prior to impingement would promote propellant heating and prevent possible fuel freezing associated with coherent stream impingement. PAT testing also provided the opportunity to compare combustion data from an FOF triplet with data from the OFO triplet and pre-atomized elements with coherent jet elements.

The PAT was scaled from the Contract NAS 3-21030 PAT by scaling certain metering orifices and transverse leg lengths. This scaling

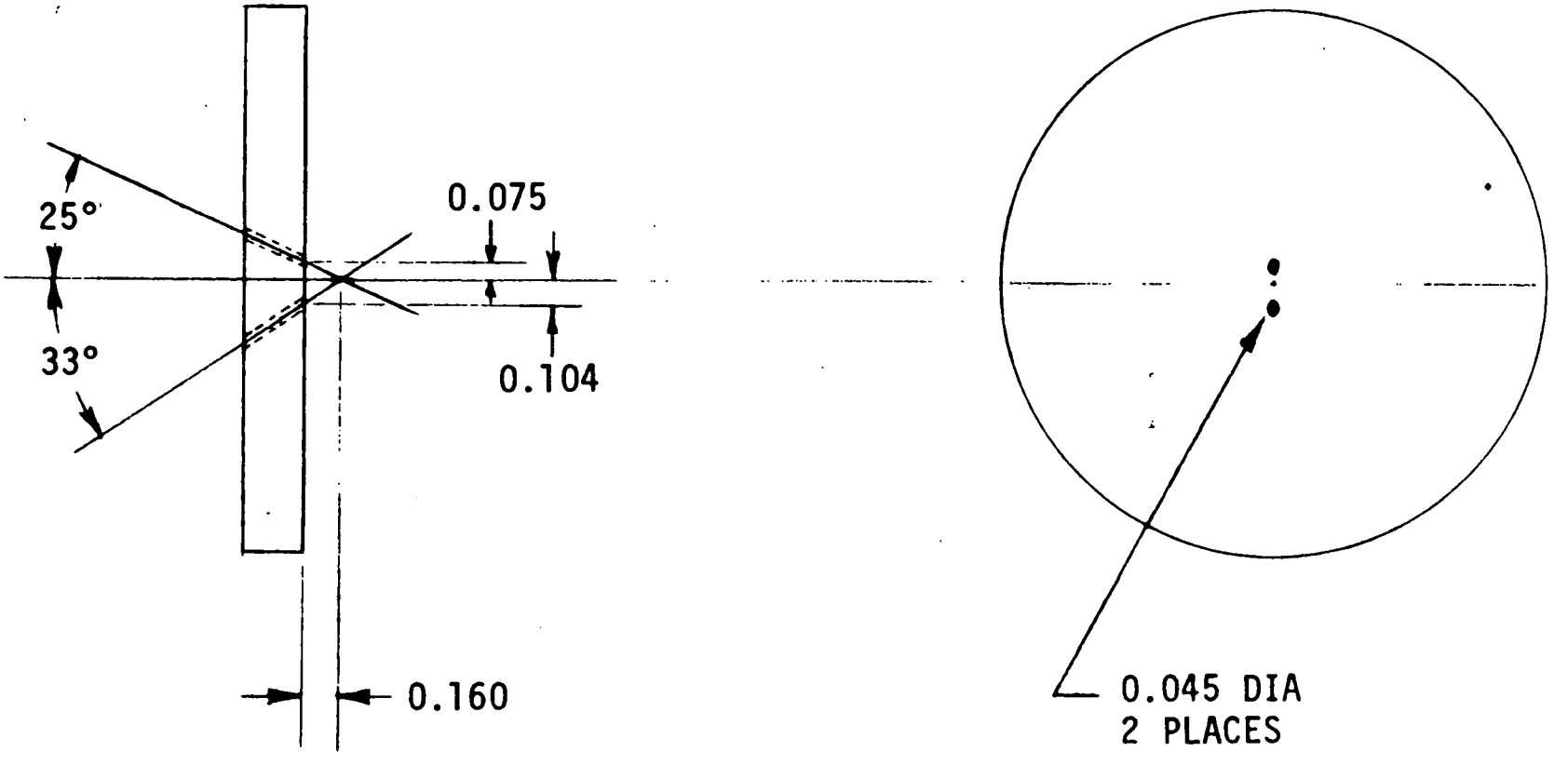

Figure 13. Unlike Doublet (UD) Injector Configuration

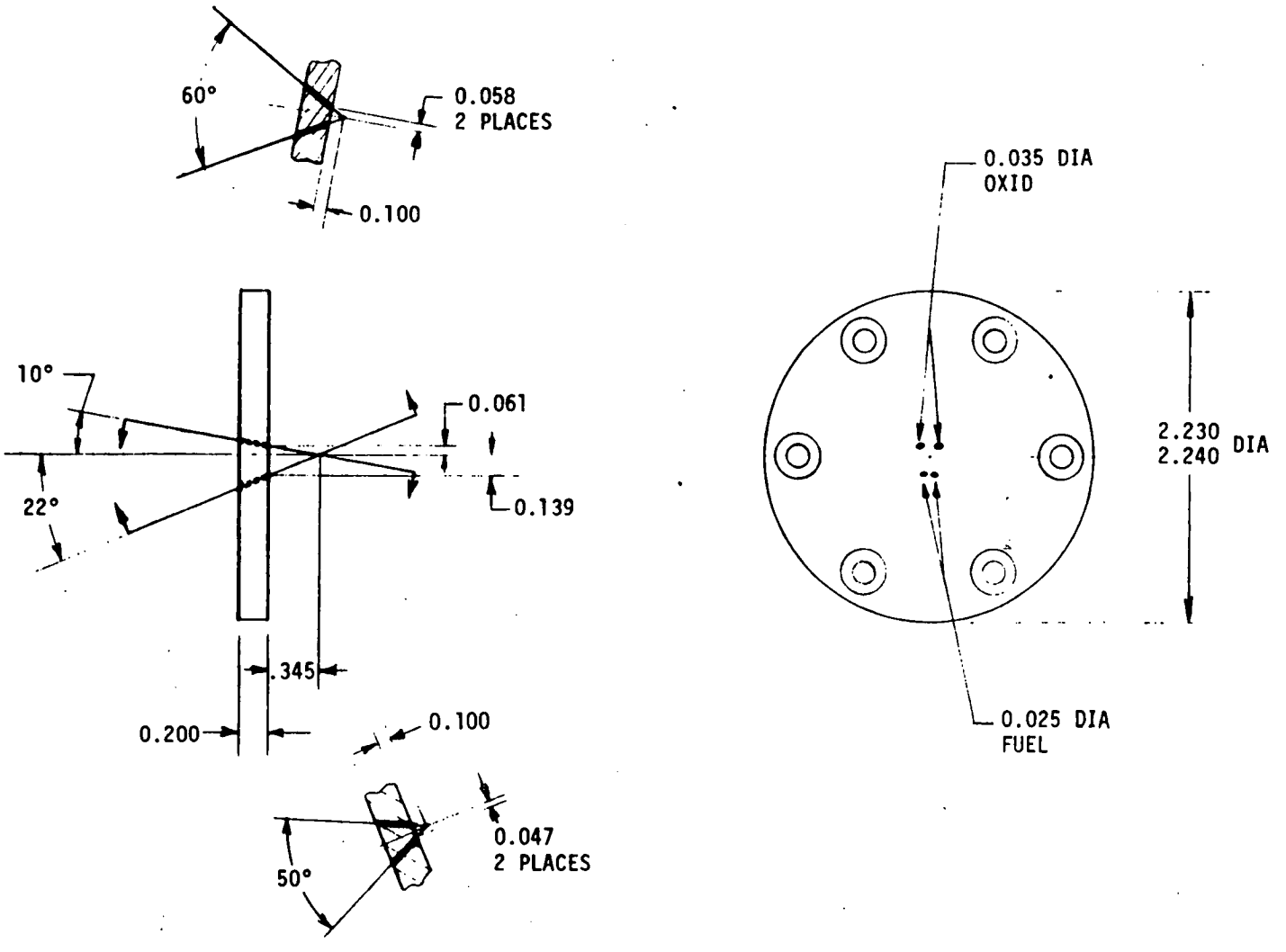

Figure 14. LOL-EDM Injector Configuration

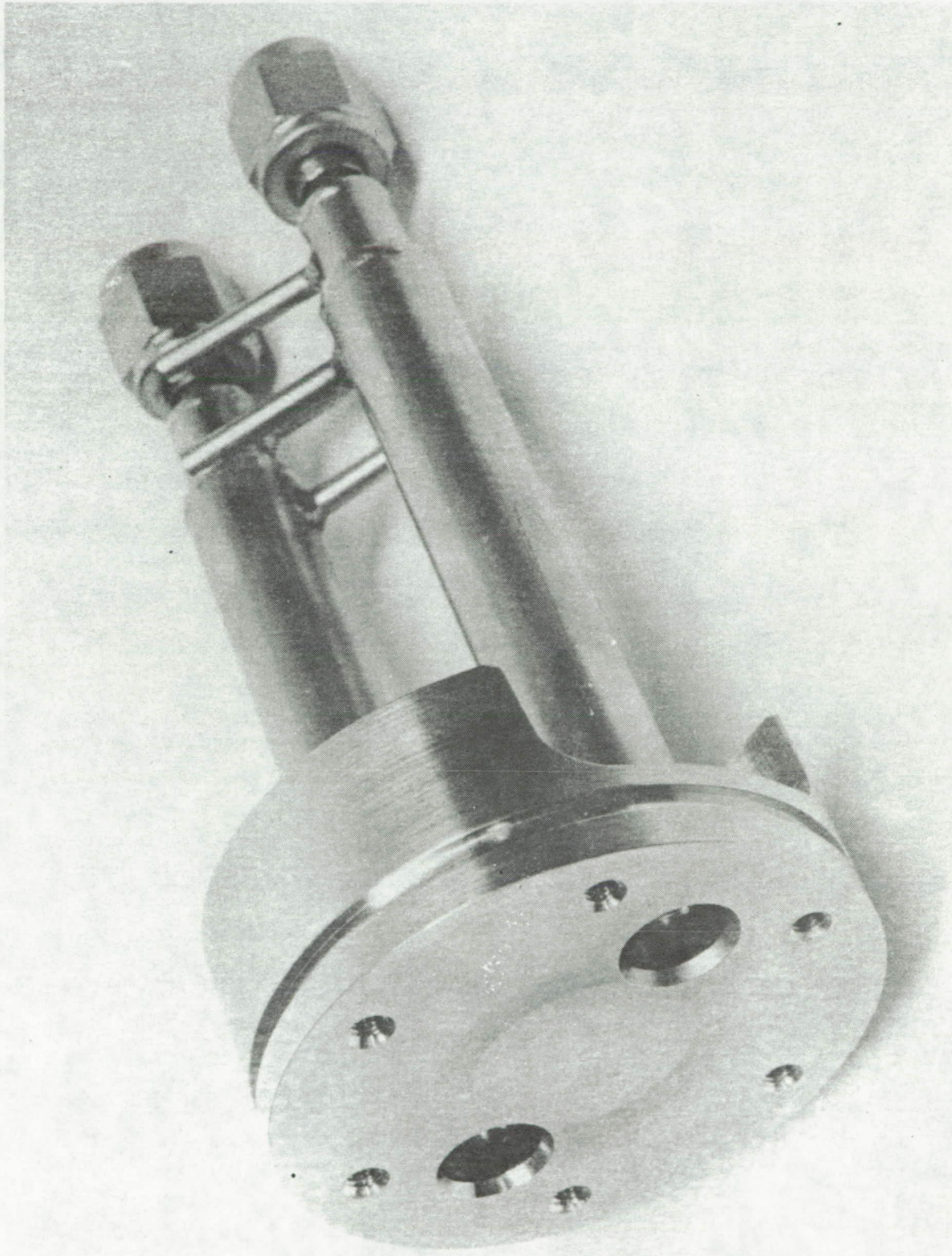

Figure 15. Reusable Injector Body

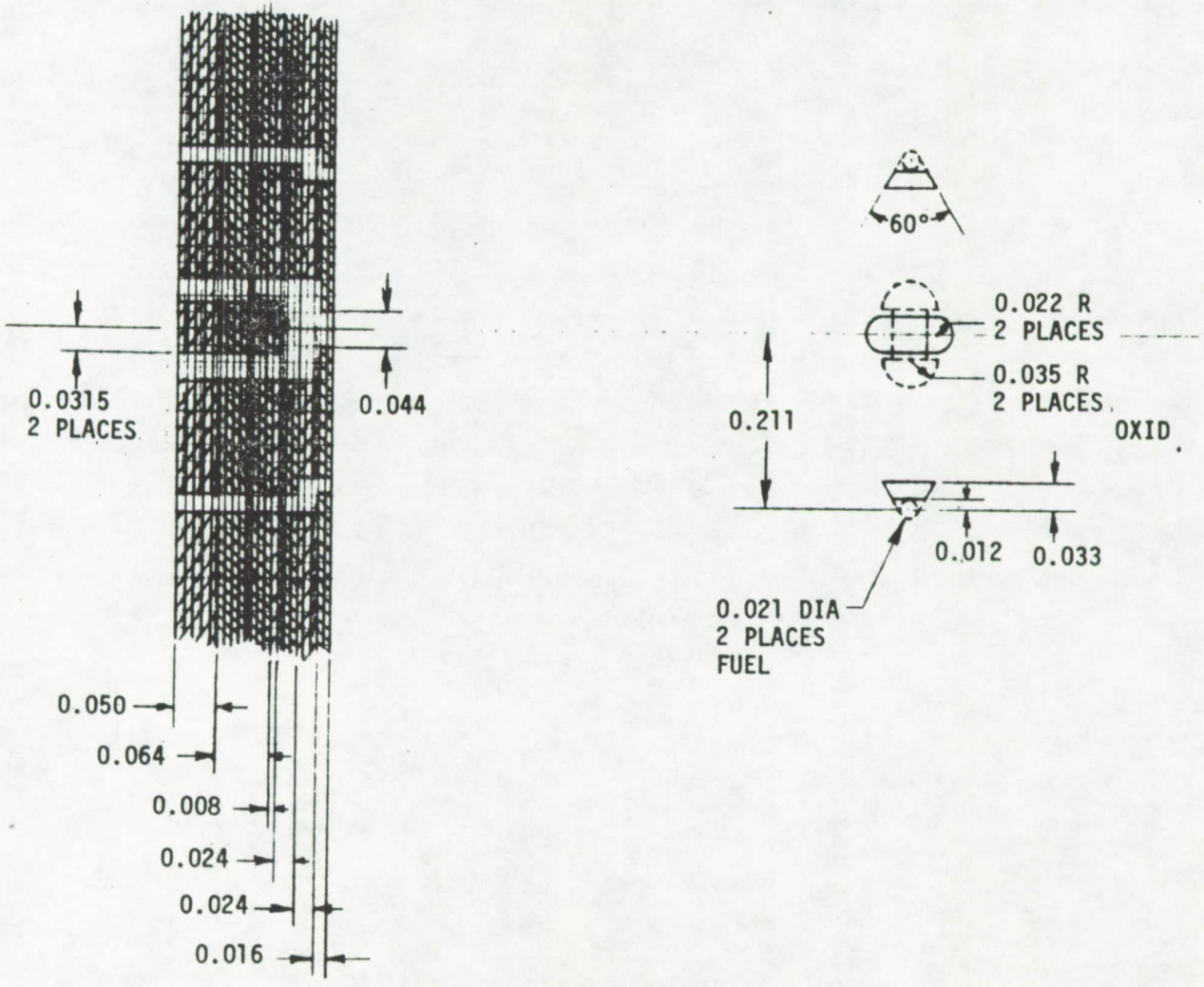

Figure 16. Pre-Atomized Triplet (PAT) Injector Configuration

did not include the top platelets which had a thickness of OsGGK< t& ?tvg injectors. This caused the single element PAT to have nearly twice the vertical L/D of the previous PAT design after impinging against the splashplate and resulted in a much shallower impingement angle for it. (30° included angle for the single element PAT versus 60° included angle for the previous PAT.)

(7) Slit Triplet

The Slit Triplet element (Figure 17) was designed to be used with LOX and gaseous methane. This design features a centrally located rectangular LOX orifice (high aspect ratio) which is impinged upon by gaseous methane exiting from two outside rectangular orifices. The intent was to create an element that would verify whether or not RSS would be observed with impinging gas and liquid streams and that would yield good photographic results.

2. Hotfire Test Facility Setup

The test apparatus was set up in Test Bay 3 of the ALRC Research Physics Lab (see Figure 18). A schematic of the propellant system used is shown in Figure 19. Propellant was stored in one-gallon, 3000 psi run vessels. Gaseous pressurization of these systems was used to provide controlled run conditions over a wide range of chamber pressures. Gaseous helium was used to pressurize the LOX and gaseous nitrogen was used for the liquid RP-1, C_3H_8, CH_4 and NH_3 fuels. The gaseous CH_4 fuel tests were run from pre-loaded pressure bottles.

LOX temperature conditioning was provided by means of the following: (1) LH_2 temperature conditioning jackets surrounding both propellant inlet lines; (2) addition of a LOX bypass circuit to increase LOX mass flow and keep LOX temperatures near -275°F (the bypass was active during the entire test period); and (3) LN_2 temperature conditioning jackets surrounding both thrust chamber valves. Total temperature conditioning capability was from -300°F to 200°F.

Four separate purges were employed during testing: (1) a helium trickle purge was connected to the oxidizer circuit to prevent contamination or propellant migration; (2) a nitrogen purge was connected to the fuel circuit for the same reason; (3) a separately regulated gaseous helium purge was used to provide chamber back pressure as well as window purge for the chamber viewports during the start and shutdown transients; (4) a separately regulated GN_2 supply was used to purge the test chamber after shutdown.

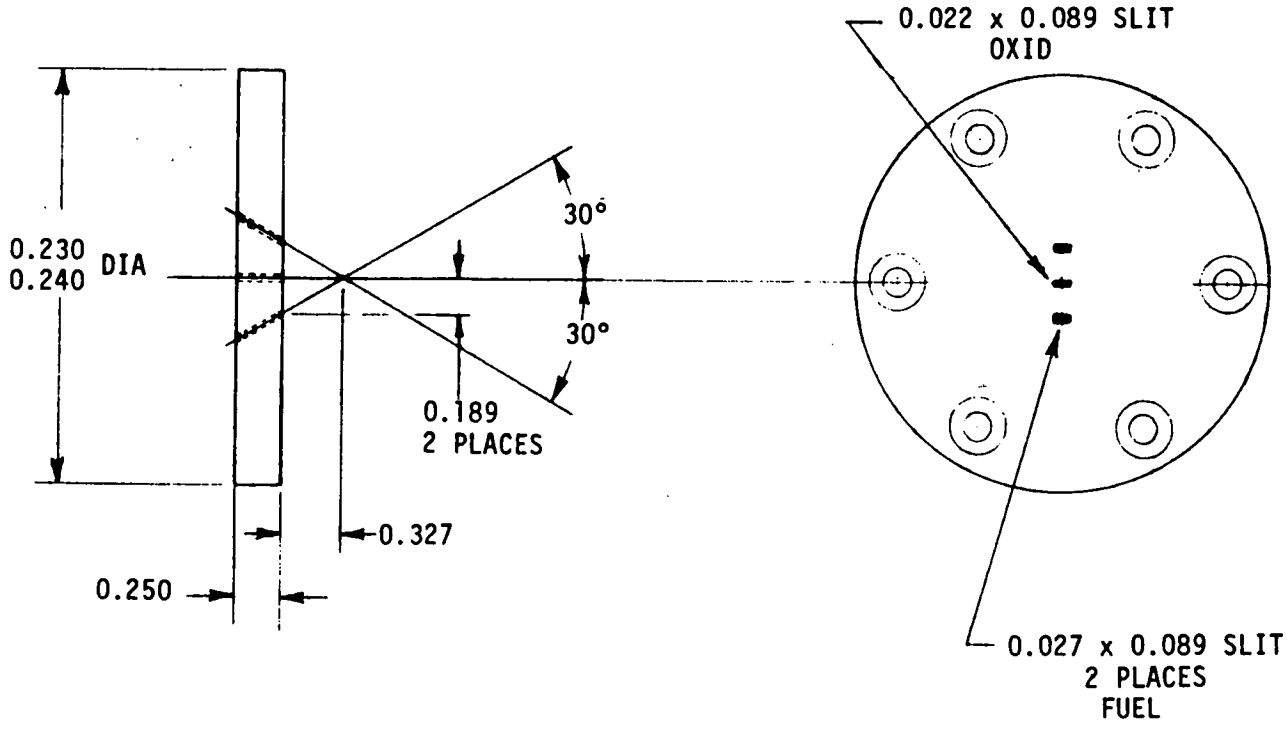

Figure 17. Slit Triplet Injector Configuration

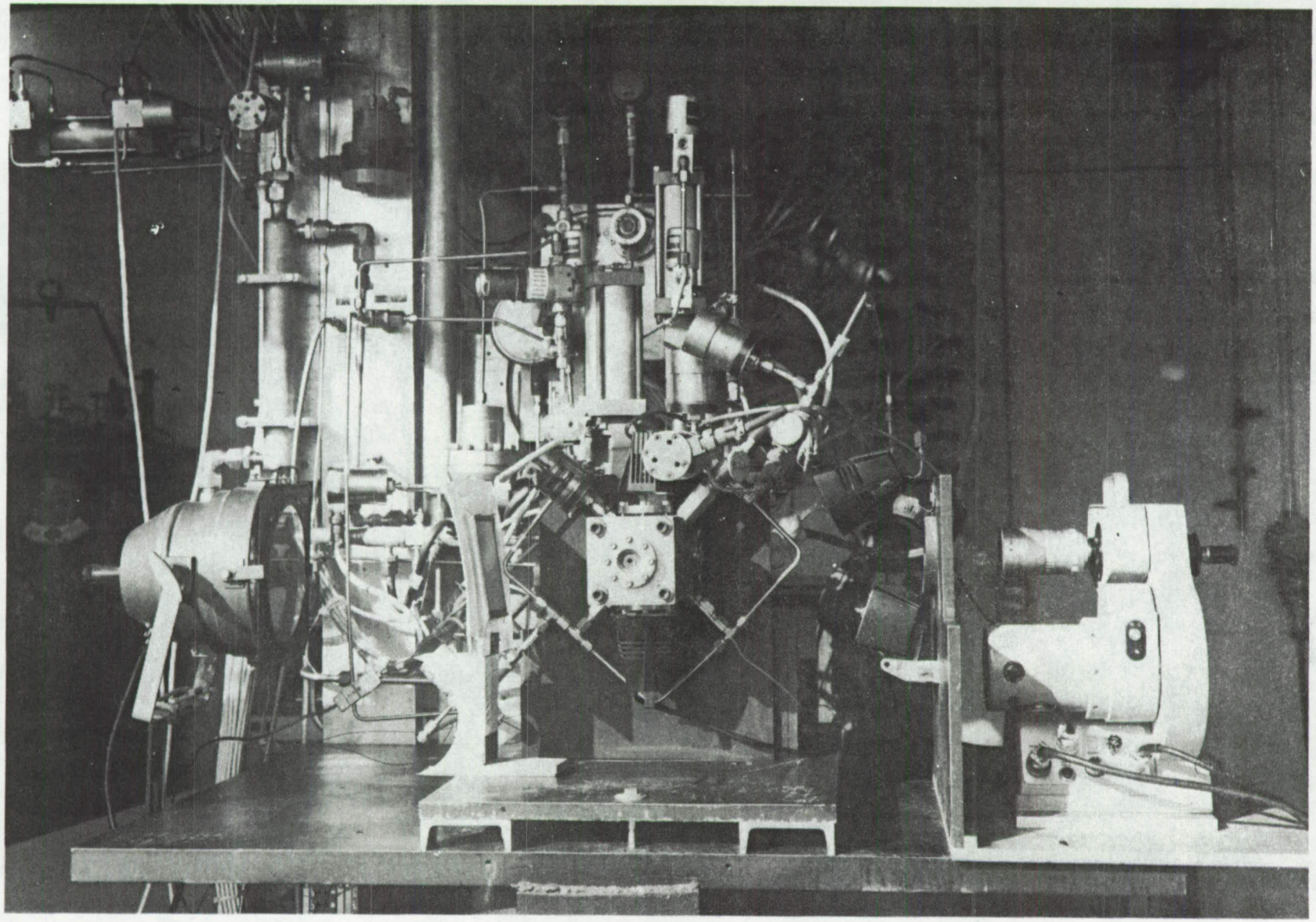

Figure 18. Test Setup

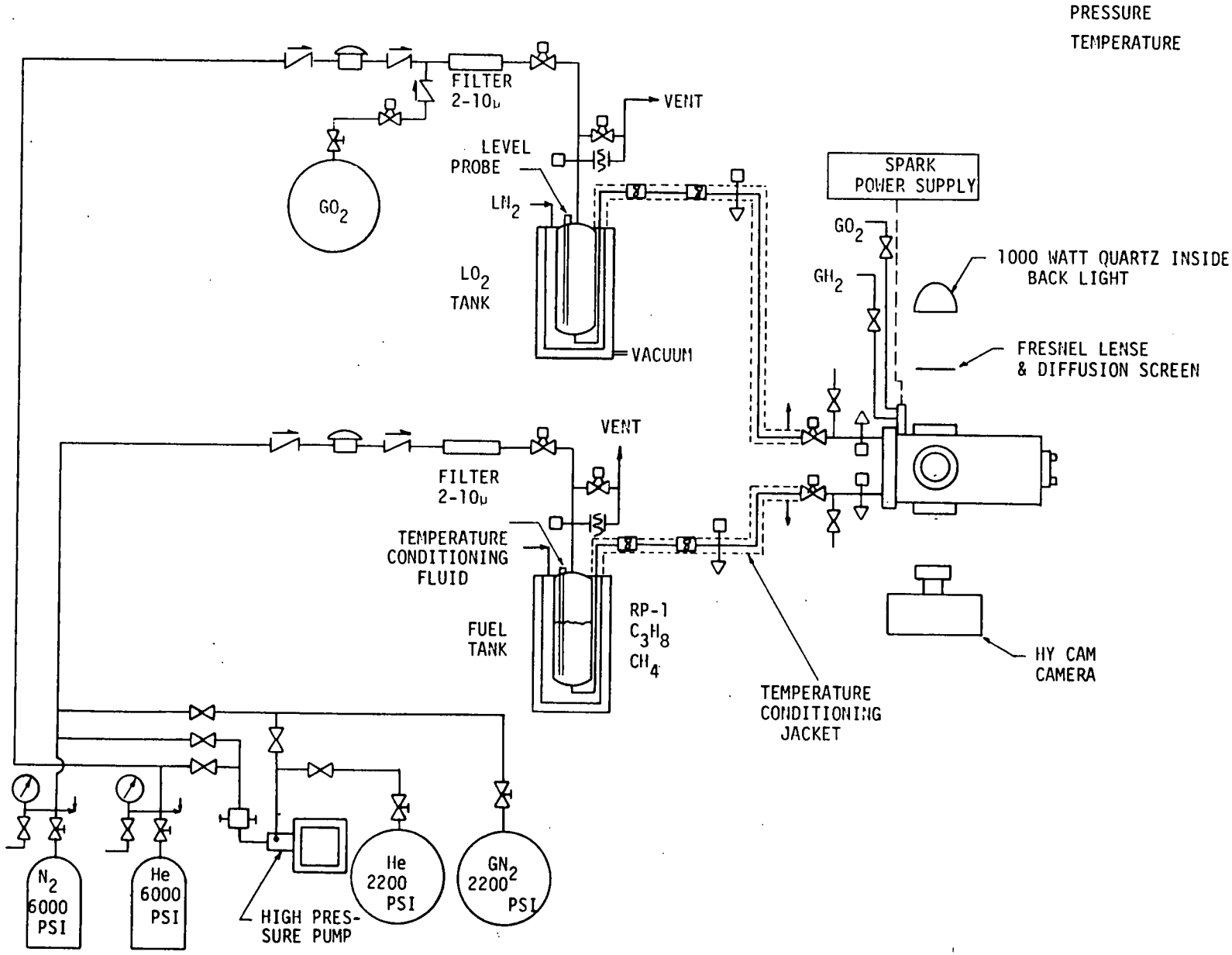

Figure 19. Propellant Flow System Schematic

V, A, Experimental Hardware and Test Setup (cont.)

3. Cold-Flow Test Setup

Two types of cold-flow tests were run in the ALRC Research Physics Laboratory.

The main purpose of the first cold-flow tests was to determine the injector Kw's and to verify impingement accuracy. In these tests, filtered de-ionized water was used as the test fluid. Pressure measurements were made with Heise pressure gages, and flowrate was measured by using a time/volume technique, with run times from 60 to 200 seconds.

The second series of tests used high-speed photography to gain a baseline against which hotfire mixing and combustion phenomena could be compared. In these tests, the injectors were flowed with Freon and blue water.

Kw plots and photographs of the cold-flow tests can be found in Section V.C.1 of this report.

4. Hotfire Instrumentation

The high frequency and low frequency instrumentation listed in Tables II and III were used in the locations shown in the schematic of Figure 20. The high frequency transducers were used to respond to any abnormal combustion occurrences (e.g., pops). The low frequency transducers recorded steady-state manifold and chamber pressures. Low frequency response test parameters were recorded on a Consolidated Electrodynamics Corporation direct writing oscillograph. High frequency response data were recorded on a Sangamo Model 3564 analog tape recorder.

Propellant flowrates were measured by flowmeter as well as calculated by using injector cold-flow Kw's and the measured injection pressure drops. The pressure drops were determined from the oxidizer manifold (POJ), fuel manifold (PFJ), and chamber pressure (Pc) transducers. Transducer bias and zero offsets were accounted for by pretest calibration.

TABLE II

HIGH FREQUENCY RESPONSE INSTRUMENTATION

Test Parameter	Symbol	Instrument Make	Instrument Model	Range	Accuracy
Oxidizer Manifold Pressure	POJHF	Kistler	601	0-3000 psi (P-P)	± 0.5%
Fuel Manifold Pressure	PFJHF	Kistler	601	0-3000 psi (P-P)	± 0.5%
Chamber Pressure	PCHF	Kistler	601	0-3000 psi (P-P)	± 0.5%

TABLE III

LOW FREQUENCY RESPONSE INSTRUMENTATION

Test Parameter	Symbol	Range	Units	Recorder "O" Graph	Recorder Tape	Recorder Digital
Ox Tank Pressure	POT	0-2000	PSIA	X		
Fuel Tank Pressure	PFT	0-2000	PSIA	X		
Ox Injector Pressure	POJ	0-2000	PSIA	X		X
Fuel Injector Pressure	PFJ	0-2000	PSIA	X		X
Chamber Pressure	PC	0-1500	PSIA	X		X
Igniter Chamber Pressure	PCI	0-1500	PSIA	X		X
Ox Flowrate	WO	0-0.2	LB/SEC	X		X
Fuel Flowrate	WF	0-0.2	LB/SEC	X		X
Ox Flowmeter Temp	TOFM	-300-100	°F	X		X
Fuel Flowmeter Temp	TFFM	0-500	°F	X		X
Ox Injector Temp	TOJ	-300-100	°F	X		
Fuel Injector Temp	TFJ	0-500	°F	X		
Ox Valve Voltage	VOV			X		
Fuel Valve Voltage	VFV			X		
Camera Voltage	VCAM				X	
Injector Purge Valve Voltage	VIPV			X		
Igniter Ox Valve Voltage	VOVI			X		
Igniter Fuel Valve Voltage	VFVI			X		

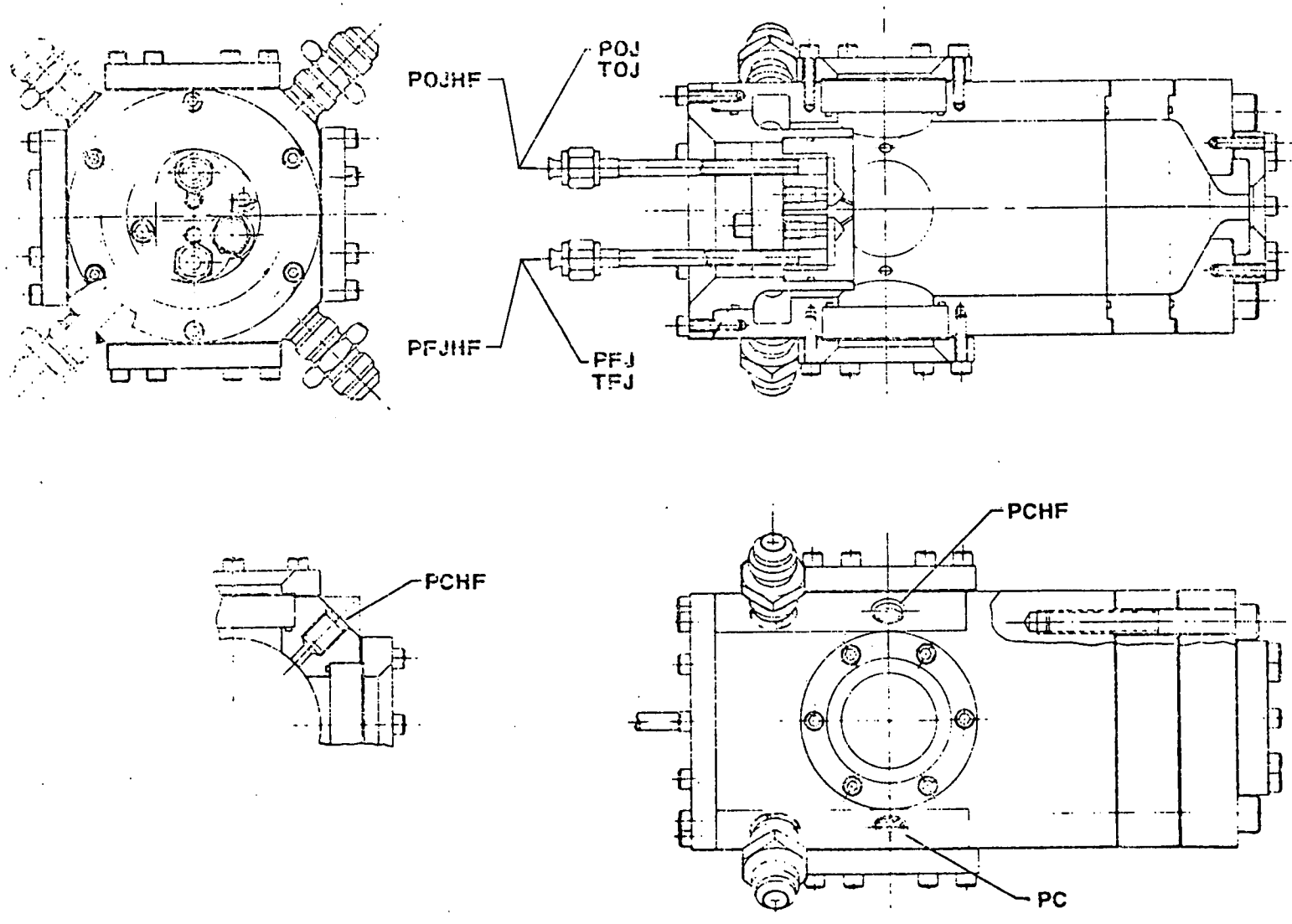

Figure 20. Instrumentation Schematic

V, A, Experimental Hardware and Test Setup (cont.)

The test operating point data were digitized and processed in an on-line HP 2100A computer. The Physics Lab data reduction program for the N_2O_4/Amine test program was modified for use with LOX/HC type propellants (Ref. 7). Curve fits for various LOX/HC properties, such as viscosity, surface tension, density, etc., were incorporated over the range of anticipated temperatures and pressures (see Appendix I).

B. PHOTOGRAPHIC EQUIPMENT AND TECHNIQUES

The intent of photographic characterization of injector element combustion phenomena is to provide an understanding of the physico-chemical processes that are operative at engine operating conditions. This necessitates the ability to "look" through the flame to observe the liquid propellant streams and resultant sprays in order to determine relative spray mass and mixture ratio distributions by observing the liquid propellant colors.

It was found that there are two major problems associated with photographing LOX/HC combustion flow fields. The first was that the combustion flame light emission was so intense that it masked the reflected light necessary to see the propellant streams (see Figure 21). The best technique found for overcoming the intense combustion light was to reduce the film exposure time to where the film, in effect, didn't "see" the flame light and then to provide high intensity external lighting for viewing of the propellant streams. It was found that use of back lighting alone will not provide the lighting balance required to properly interpret the film, since the external lighting must be provided from the back, top, bottom, and front to obtain a balance between reflected and absorbed light.

The second problem concerned obtaining useful photographic data when the chamber was filled with dark, swirling clouds or when the windows became coated with carbon. This problem was alleviated in a limited sense by providing oxidizer-rich transients as well as window purges to protect windows from carbon deposits. Notwithstanding all of the efforts to get good movies, the field of view was almost always obscured at pressures below 300 psia with RP-1 and C_3H_8. Reasons for the carbon formation are discussed in Sections V.C.2 and V.D.1 of this report.

The photographic combustion characterization was accomplished by using the equipment shown in Figure 22. The photographic equipment is centered around a Hycam model 41-0004 rotating prism high-speed movie camera. This unique camera has the capability of varying the frame exposure time independent of the film frame rate through a replaceable rotating shutter. The shutter is mounted to the prism shaft and rotates at the same speed as

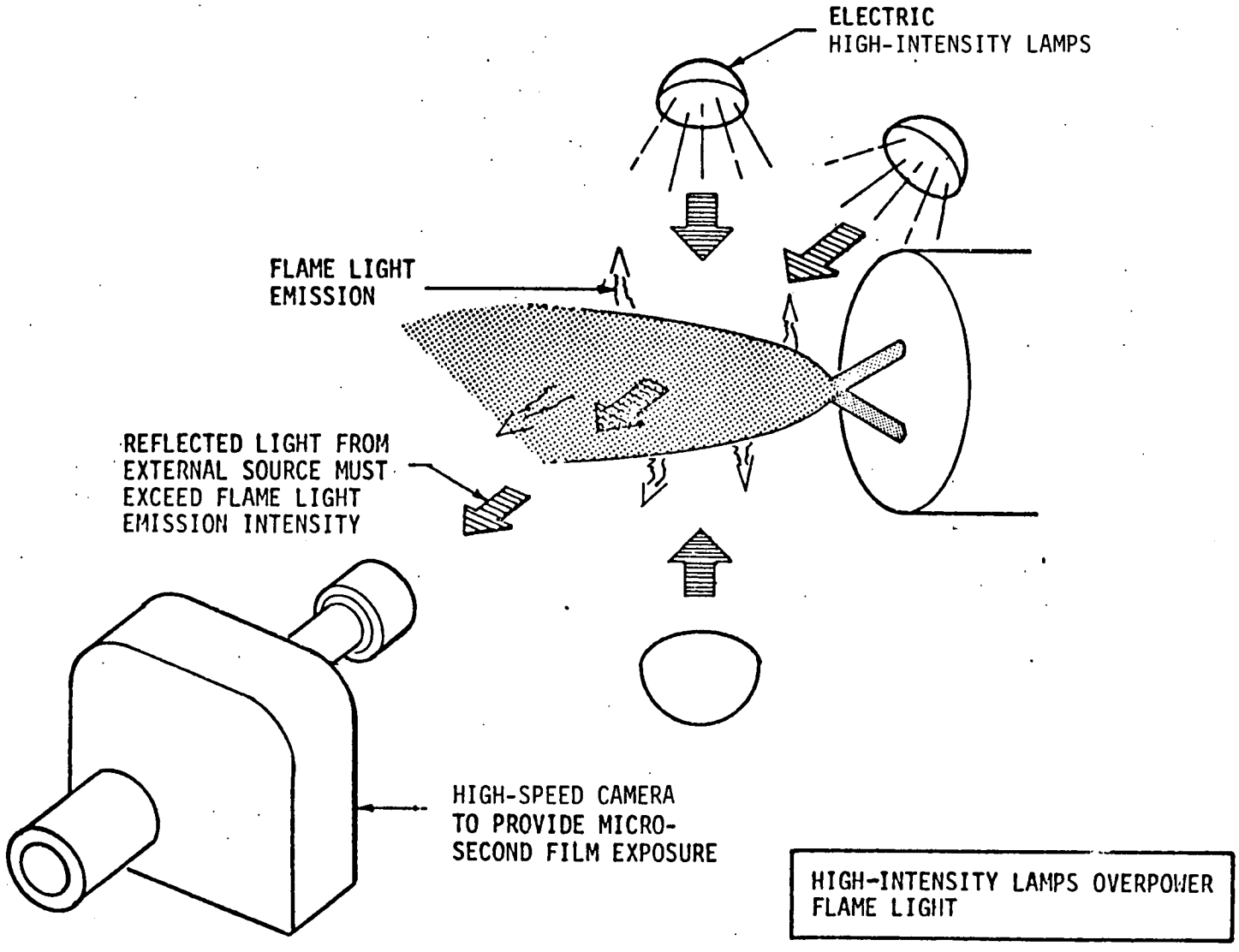

Figure 21. High-Intensity Lamps Overpower Flame Light Emission

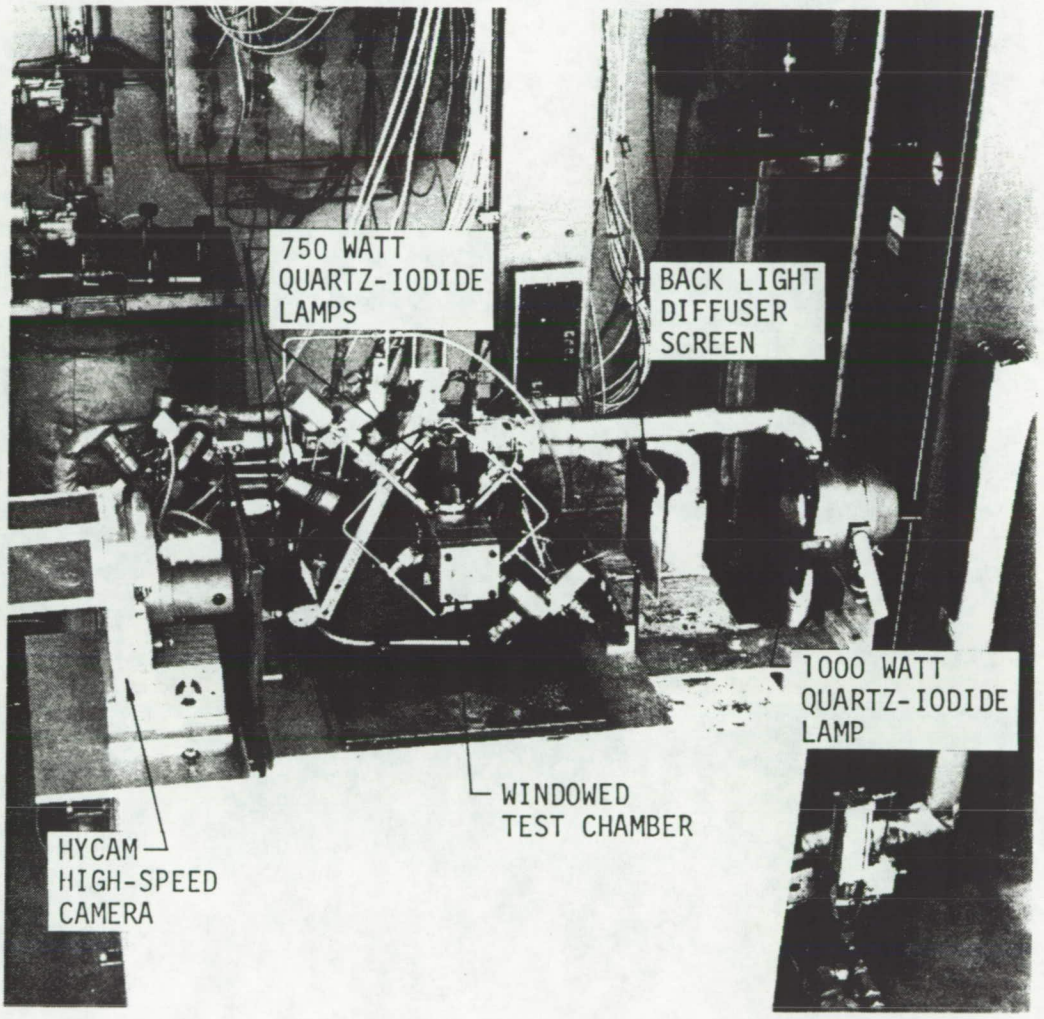

Figure 22. Photographic Equipment Setup

the prism. The light exposure at a given frame rate is controlled by changing the shutter ratio of open time to close time. This is done with interchangeable shutters. The available shutter ratios are:

1/2.5, 1/10, 1/20, 1/50, and 1/100.

The light exposure time is determined by the product of the shutter ratio and the reciprocal of the frame rate:

Exposure time = Shutter ratio x 1/pps (pictures per second).

Thus it is possible to obtain exposures of a few microseconds at relatively low frame rates.

The method of photographic characterization initially used was the one found to be successful in the N_2O_4/MMH "Blowapart" program. Color high-speed photographs of the spray field were taken at a rate of 800 pictures per second and an exposure time of 25μ sec. Ektachrome EF No. 7242 film (400 ft rolls) was used. The spray volume was illuminated with one 1000-watt quartz iodine lamp for back lighting and four 750 watt lamps for side, top, and bottom lighting.

Subsequent testing showed that this method was incapable of "masking" the bright LOX/HC combustion light and "seeing" into the atomization and mixing process. It was soon discovered that one successful light setting would not be possible for each of the test conditions, as had been the case during the storable propellant "Blowapart" program. Instead, the f-stop, camera speed, and external lighting intensity would have to be varied in correspondence to the chamber pressure, fuel type, and mixture ratio. As a result, a new flashbulb lighting technique was employed which proved much more effective in taking clear, discernible photographs. Each of the incandescent photo-floods was replaced with a large flashbulb (5 megalumen on the two front lights and 2 megalumen for the top, bottom, and backlights). The flashbulbs were triggered during steady-state combustion just before shutdown and provided 25 ms of extremely bright light at a film speed of 3200 fps and an f-stop of 16. This technique proved to be much more effective than the previous lighting arrangement with RP-1 and C_3H_8 in masking combustion light and seeing into the mixing process. Tests using CH_4 and NH_3 as fuels gave off far less combustion light and were easily photographed using only photoflood lighting at 800 pps and an f-stop of 4.

C. TEST RESULTS

A total of 127 hotfire tests were conducted with the injector elements and propellants listed in Table I. Cold-flow tests were also

V, C, Test Results (cont.)

conducted to determine the injector element hydraulic resistances and to characterize non-reactive impingement phenomena.

1. Cold-Flow Test Results

a. Hydraulic Characteristics

Each of the injectors were cold-flow tested to determine their hydraulic resistance and to verify impingement accuracy. Filtered, de-ionized water was used as the test fluid on these tests. Pressure measurements were made with Heiss pressure gages, and flowrate was calculated by using a time/volume technique, with run times ranging from 60 to 200 seconds.

The hydraulic resistances for each of the elements were determined from plots of flowrate versus pressure drop, as shown in Figures 23 through 29. The resistance values are summarized in Table IV.

b. Non-Reactive Impingement Phenomena

In the second series of cold-flow tests, the injectors were flowed with Freon and blue water (to represent the oxidizer and fuel, respectively). These tests were photographed with the high-speed camera to gain a baseline against which hotfire mixing and combustion phenomena could be compared. The results of this testing were as follows:

OFO

This particular injector had a very slight misimpingement and was very sensitive to changes in momentum ratio. Figure 30 shows the OFO at a momentum ratio of 0.96 where the spray uniformity reaches a maximum. Other cold-flows at momentum ratios of 1.45 and 0.45 show that the fuel tends to core down the center while the oxidizer either penetrates without mixing or is reflected away unmixed. The fuel orifice flowed detached (due to cavitation) at pressure drops above 60 psi. This detachment phenomenon did not occur during hotfire because of the increased back pressure.

RUD

The RUD appeared fairly well mixed at a momentum ratio of 0.97 (Figure 31). Momentum ratios above and below

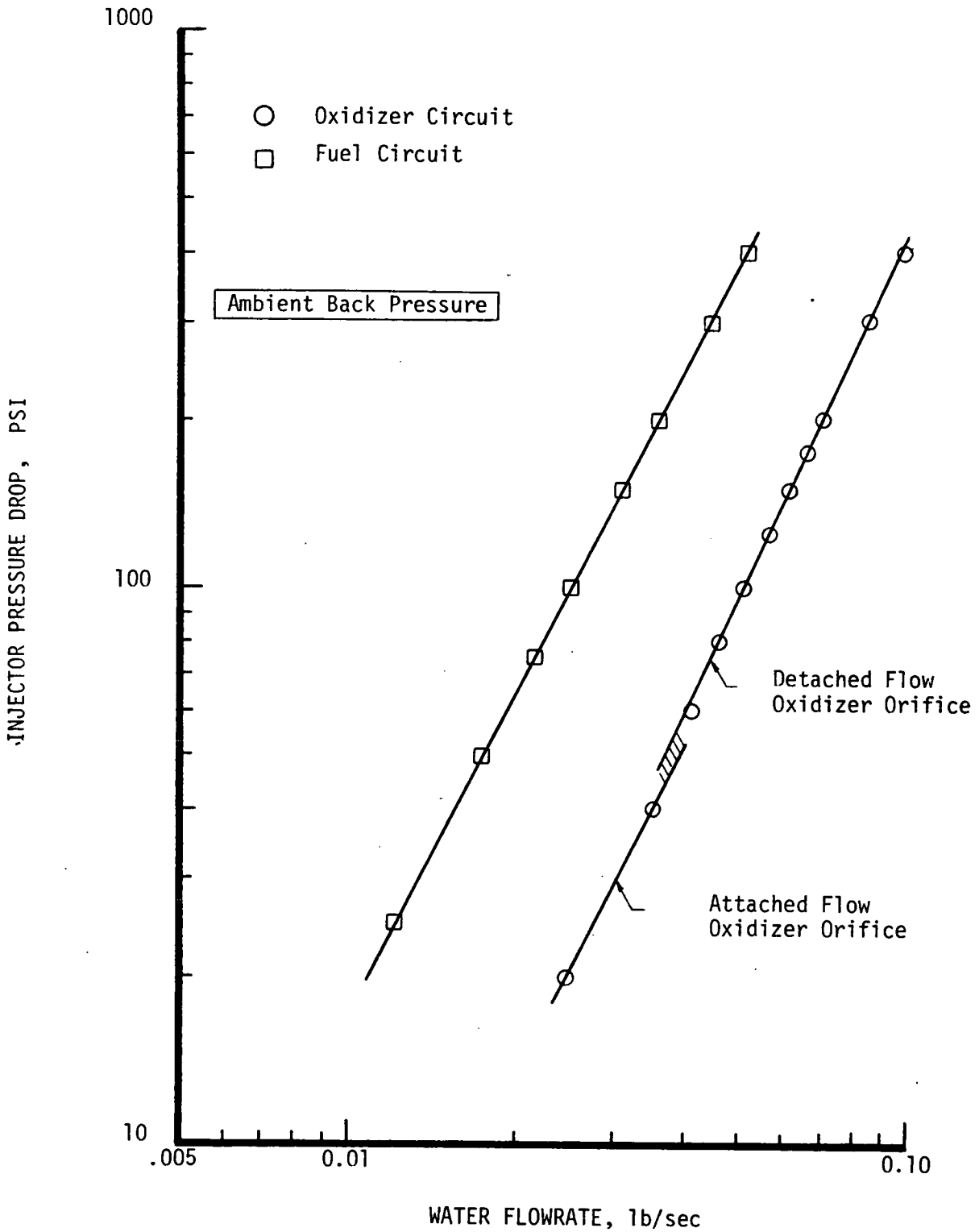

Figure 23. OFO Triplet Pressure Drop Characteristics

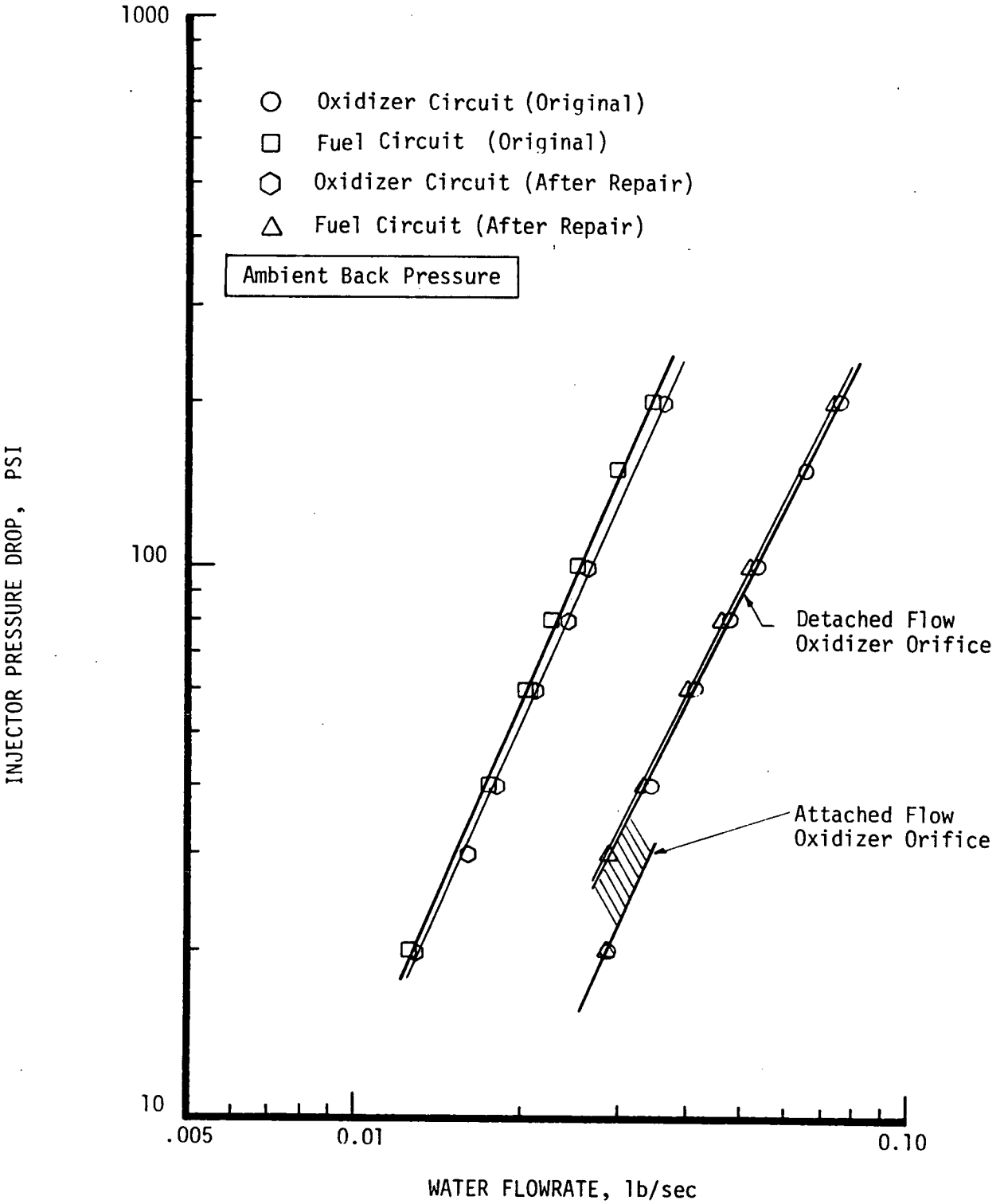

Figure 24. RUD Injector Pressure Drop Characteristics

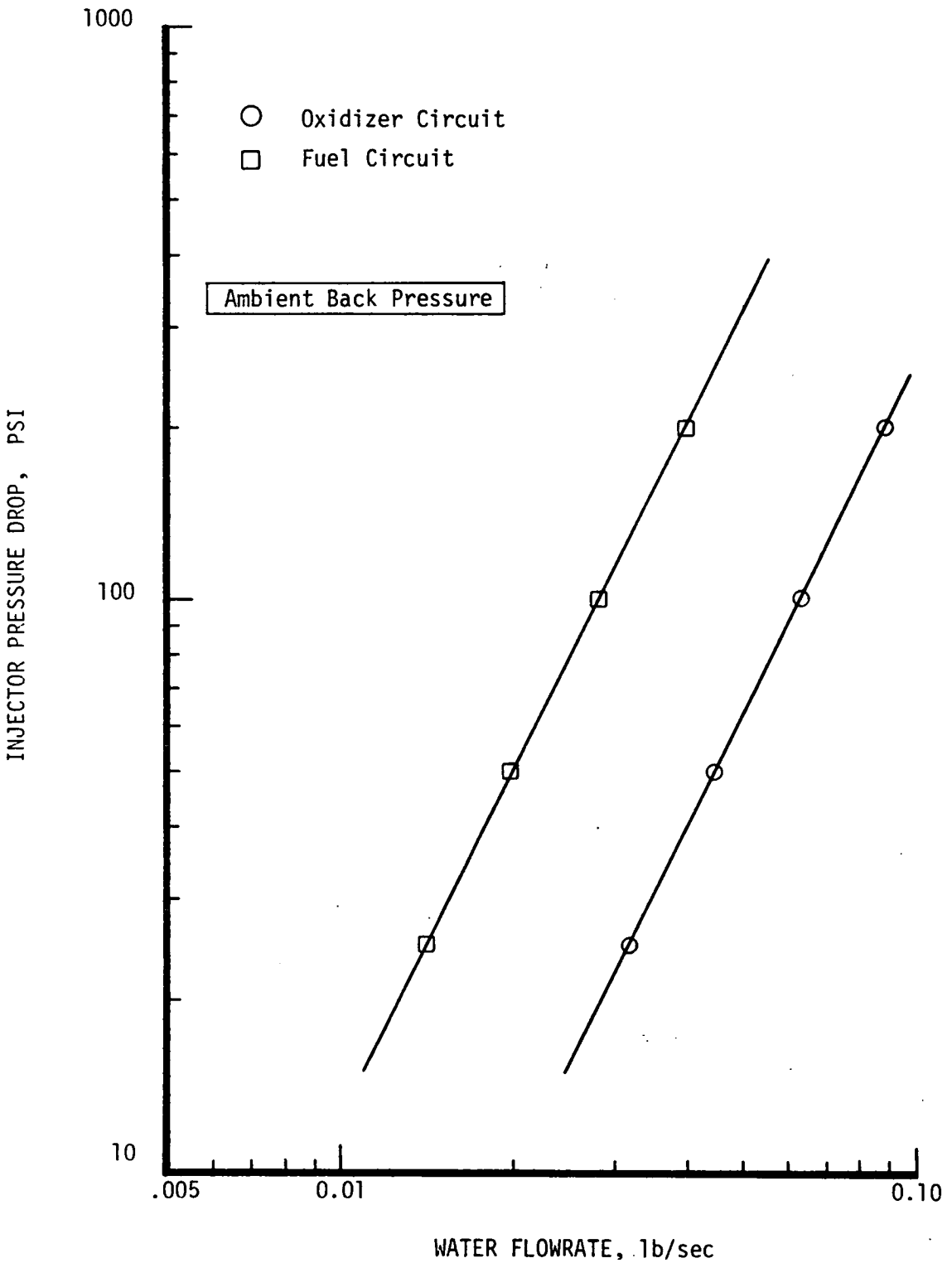

Figure 25. TLOL Injector Pressure Drop Characteristics

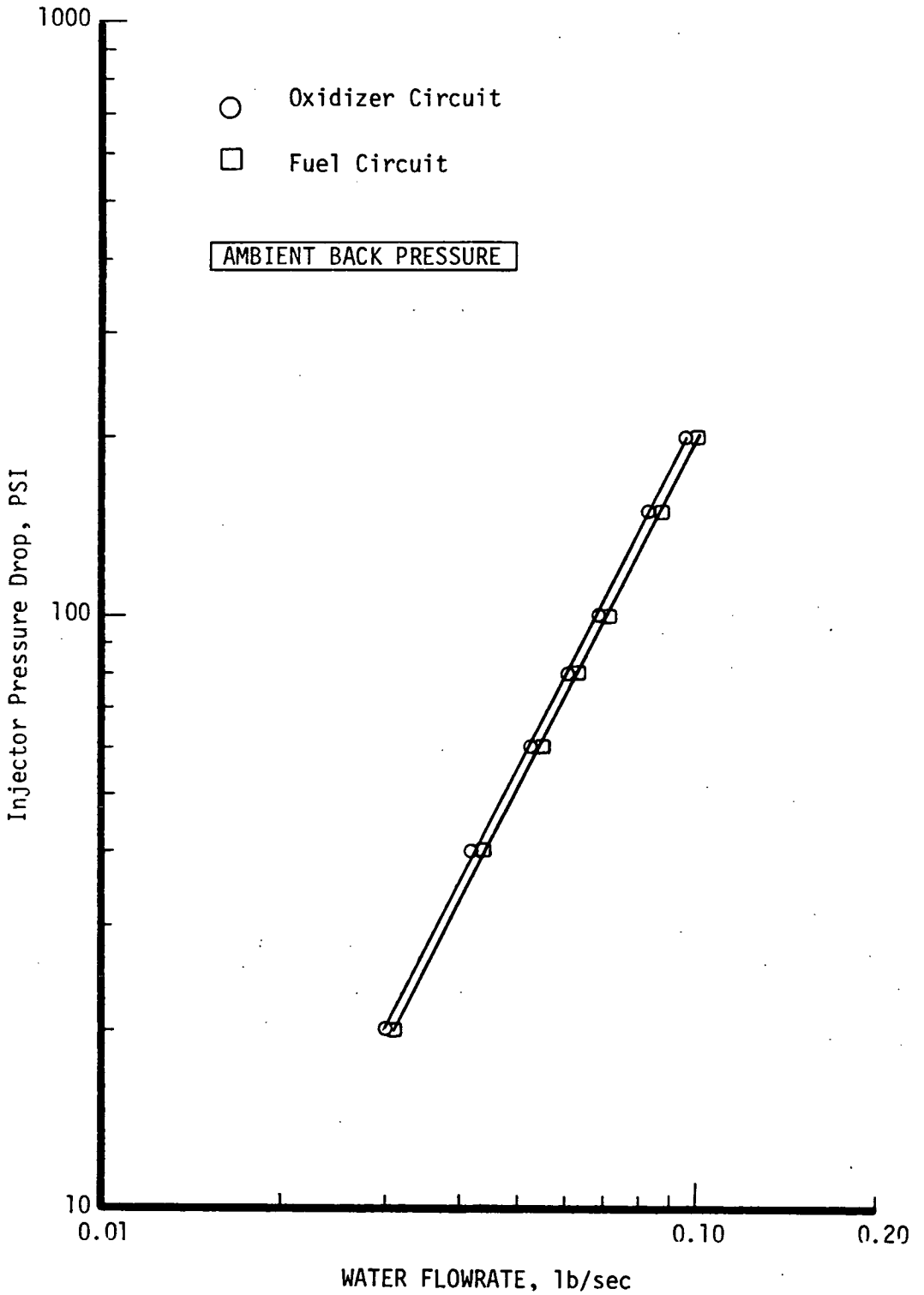

Figure 26. Unlike Doublet Injector Pressure Drop Characteristics

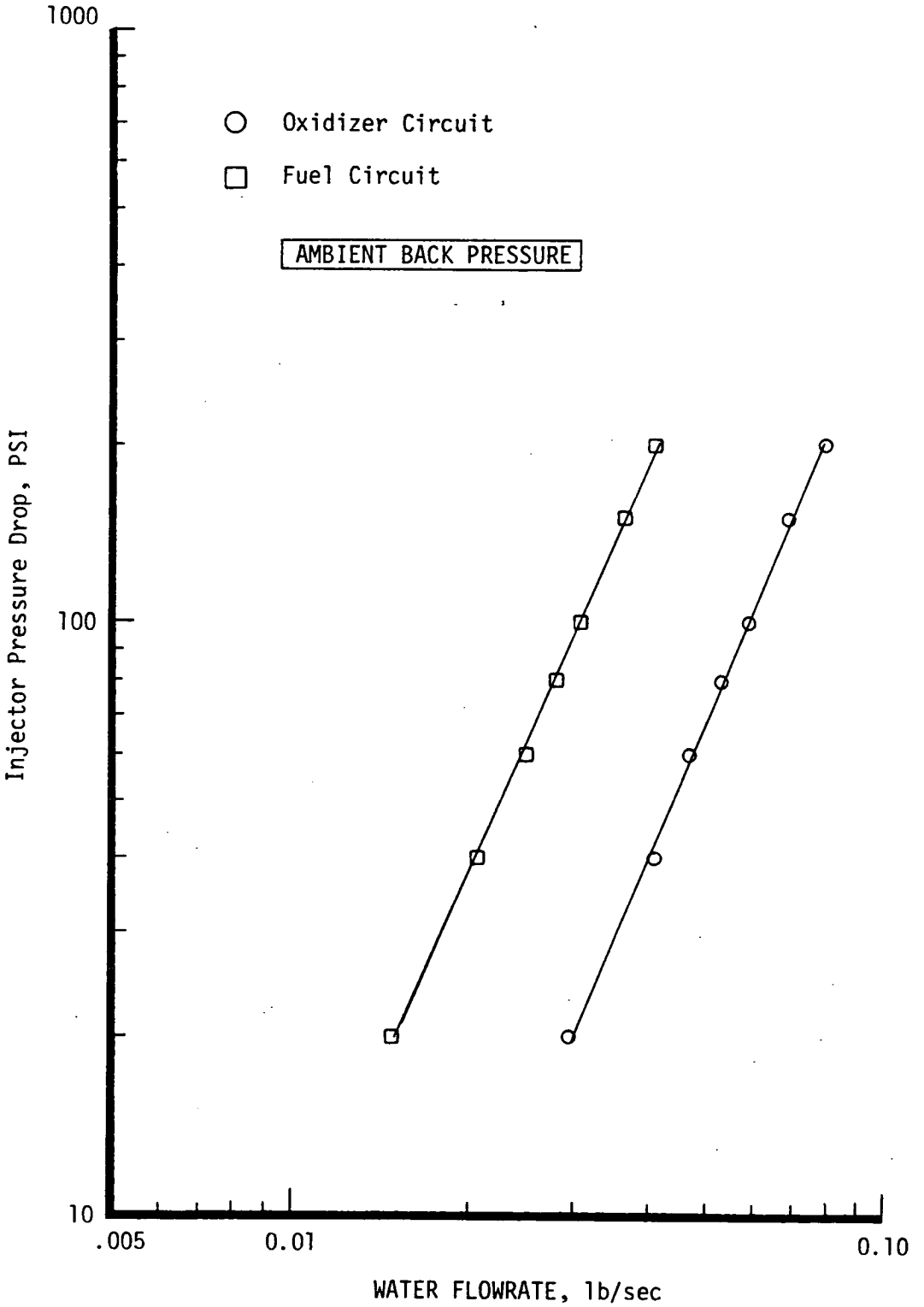

Figure 27. LOL-EDM Injector Pressure Drop Characteristics

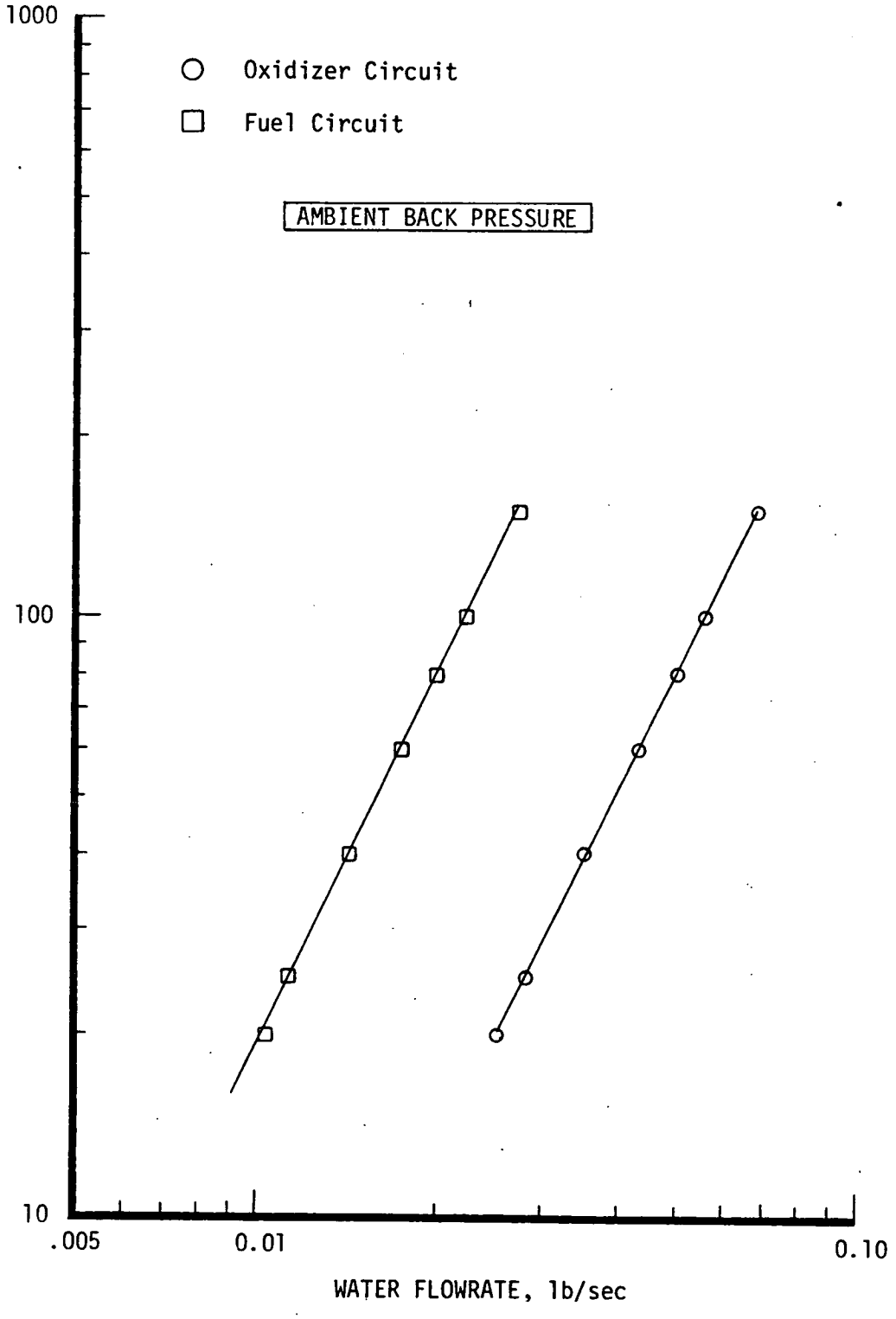

Figure 28. Pre-Atomized Triplet Pressure Drop Characteristics

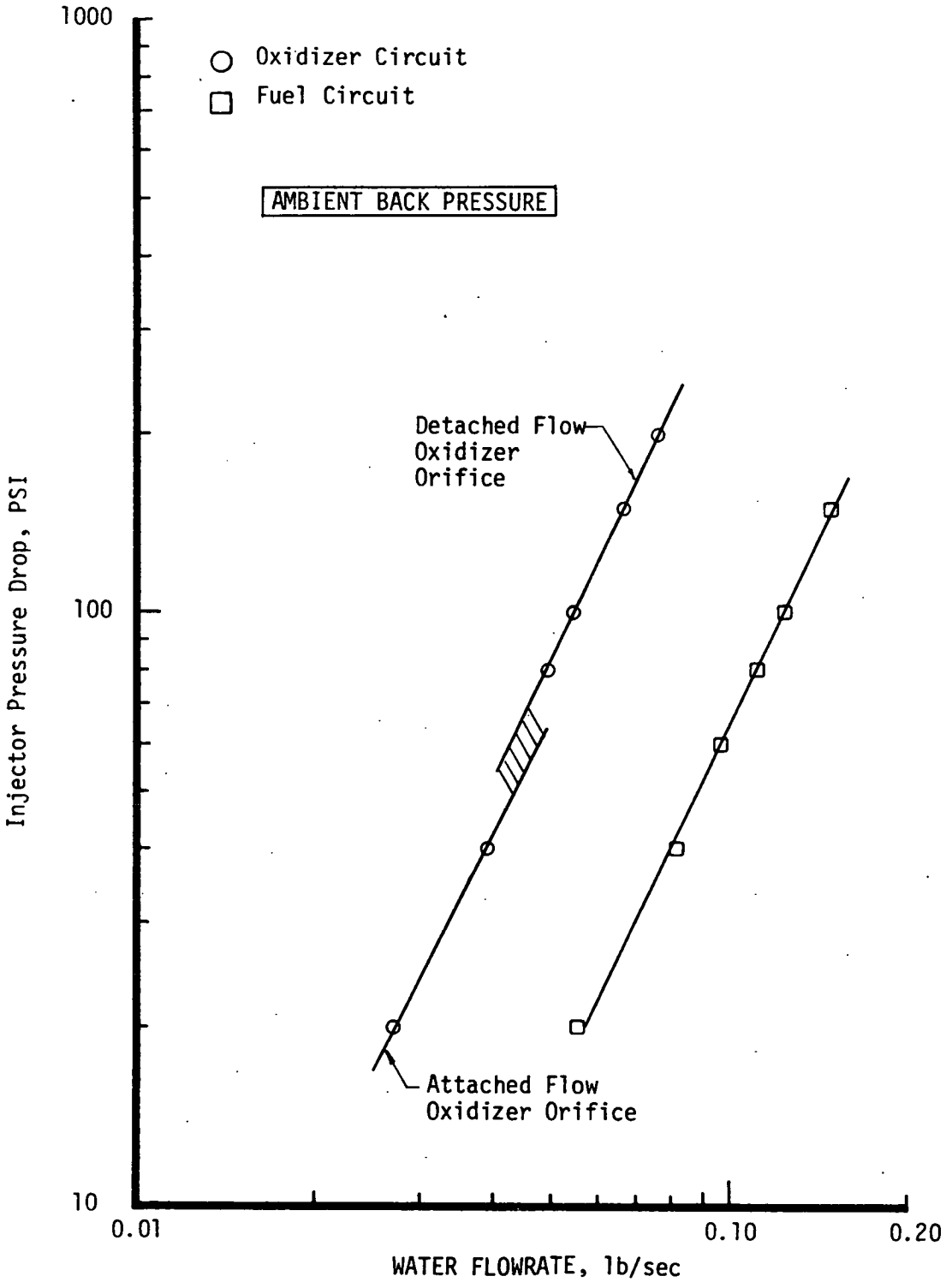

Figure 29. Slit Triplet Pressure Drop Characteristics

TABLE IV

INJECTOR ELEMENT COLD-FLOW DATA SUMMARY

	Fuel Orifice			Oxidizer Orifice		
Injector	D(in.)	$K_w \left(\frac{lbm - in.}{lbF^{1/2} - sec.}\right)$	C_D	D(in.)	$K_w \left(\frac{lbm - in.}{lbF^{1/2} - sec.}\right)$	C_D
OFO Triplet	0.0287	0.002509	0.735	0.030	0.0055	0.737
RUD	0.0264	0.002886	0.7535	0.03911	0.006354	0.7603
TLOL	0.024	0.0028	0.5866	0.037	0.00628	0.5535
UD	0.045	0.0071	0.8461	0.045	0.0068	0.8104
LOL-EDM	0.025	0.003312	0.6394	0.035	0.006590	0.6491
PAT	0.021	0.002266	0.62	0.044	0.005612	0.5494
SLIT TRIPLET	0.041	0.01241	0.4894	0.035	0.006164	0.5967

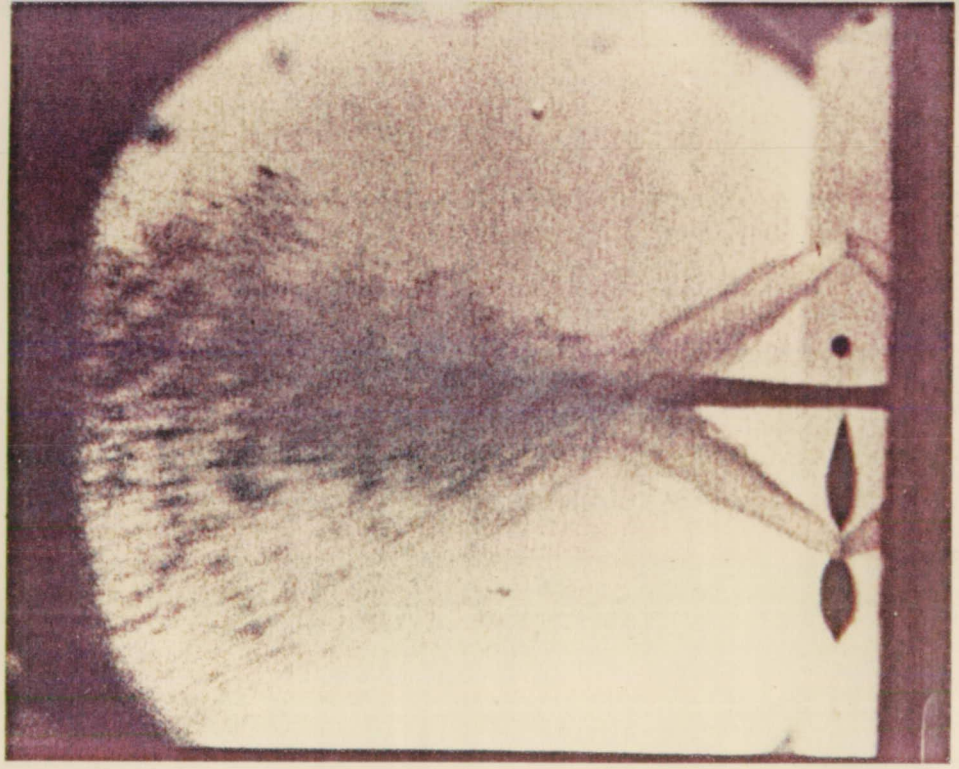

Cold-Flow Test No. 42B
Fluids: Freon/Blue Water
Injector Type: OFO Triplet
Momentum Ratio: 0.96

V_f = 97 fps
V_{ox} = 80 fps

Figure 30. OFO Triplet Injector Cold-Flow Test No. 42B

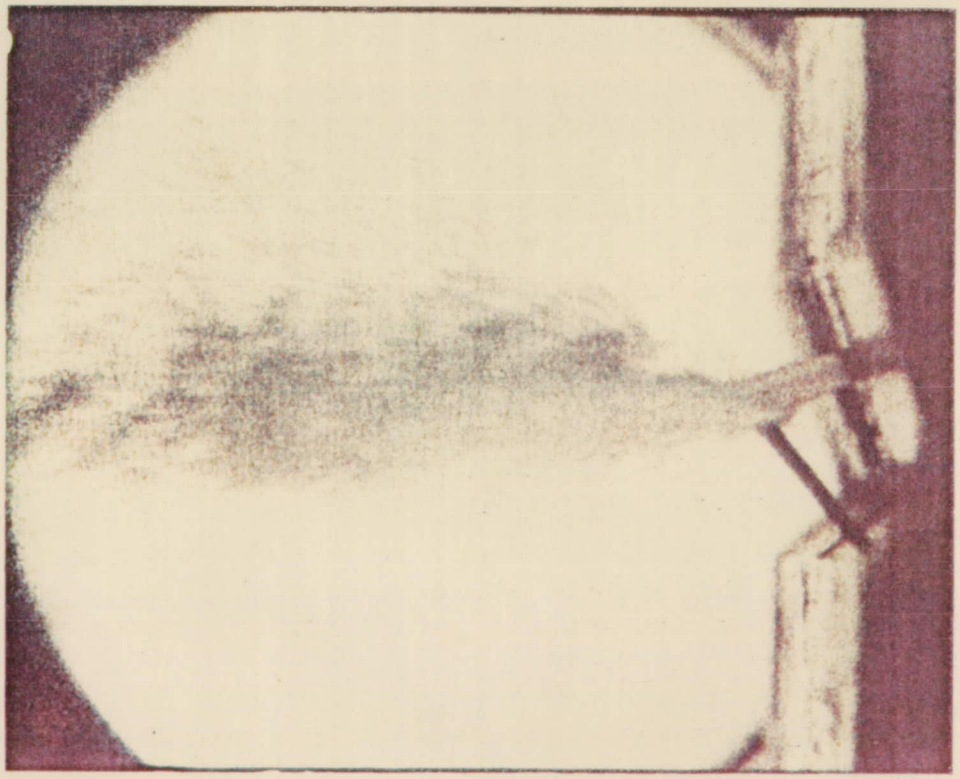

Cold-Flow Test No. 35
Fluids: Freon/Blue Water
Injector: RUD
Momentum Ratio: 0.97

V_f = 107 fps
V_{ox} = 74 fps

Figure 31. RUD Injector Cold-Flow Test No. 35

1.0 encouraged propellant "shoot-through" (i.e., penetration). Both propellant streams largely retained their rectangular shapes to the impingement point. The rectangular orifices avoid the poor mixing experienced with circular unlike doublets due to diameter mismatch.

TLOL

The TLOL was cold-flowed over a momentum ratio range of 0.40 to 1.5. Figure 32 shows the TLOL at a momentum ratio of 0.87. The TLOL showed very little mixing at any momentum ratio because of its small included impingement angle (15°).

UD

The UD had equal orifice sizes and attained good spray uniformity around a momentum ratio of 1.0 (Figure 33). Penetration of both propellants occurred above and below a momentum ratio of 1.0.

LOL-EDM

This injector, although similar to the TLOL in many respects, displayed fairly good mixing characteristics at momentum ratios from 0.45 to 1.37. Figure 34 shows the LOL-EDM at a momentum ratio of 0.99. The reason it mixes better than the TLOL is due to the increased included impingement angle (32°).

PAT

The PAT, as its name implies, produced three finely atomized streams which seemed to mix uniformly at momentum ratios from 0.45 to 1.35. There was a slight tendency for the oxidizer to "blow away" the fuel at high momentum ratios, but overall it seemed to remain well mixed (see Figure 35).

SLIT TRIPLET

The Slit Triplet was a disappointment from an atomization and mixing standpoint. Cold-flow tests with Freon and GN_2 showed that reasonable atomization and mixing

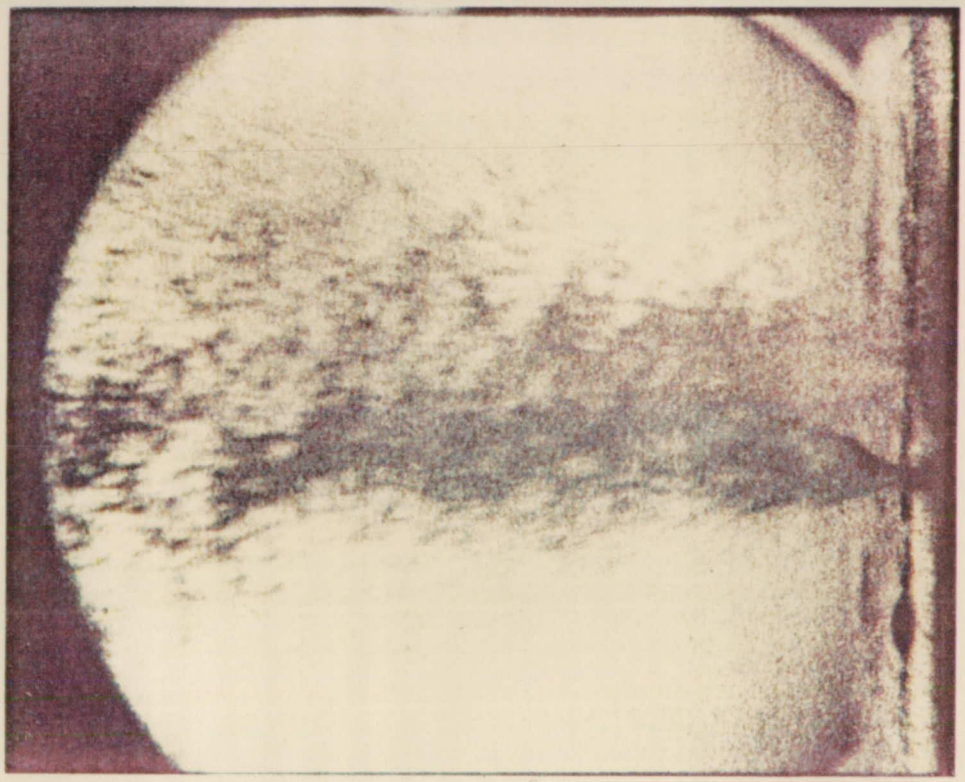

Cold-Flow Test No. 34
Fluids: Freon/Blue Water
Injector: TLOL
Momentum Ratio: 0.87

V_f = 85 fps
V_{ox} = 55 fps

Figure 32. TLOL Injector Cold-Flow Test No. 34

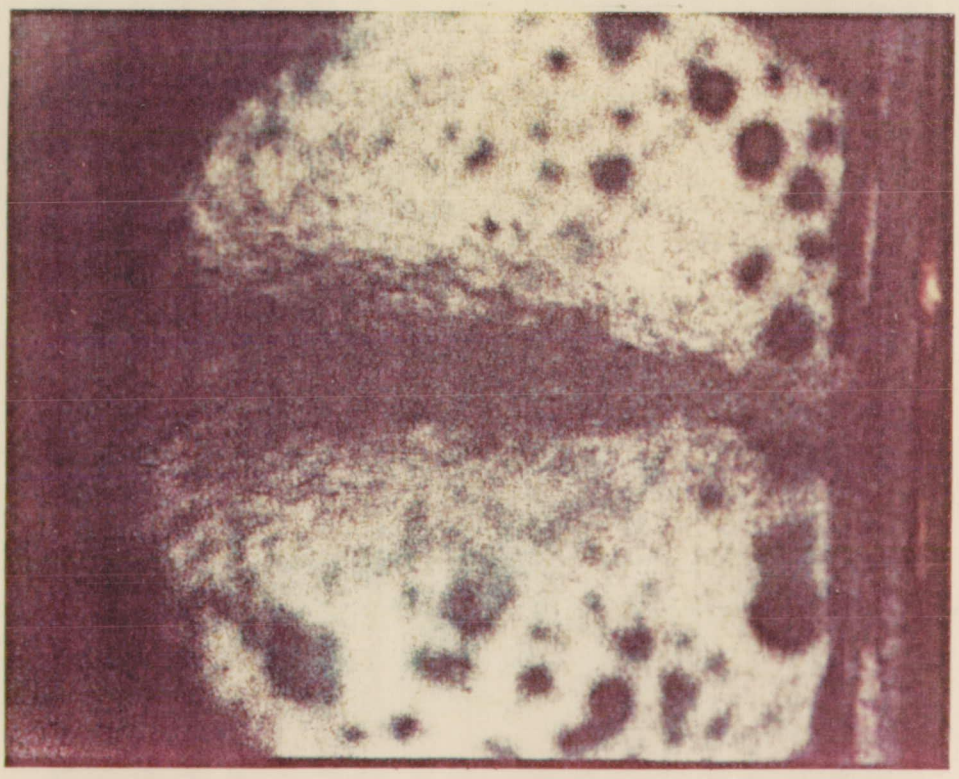

Cold-Flow Test No. 43B
Fluids: Freon/Blue Water
Injector: UD
Momentum Ratio: 0.85

V_f = 101 fps
V_{ox} = 80 fps

Figure 33. UD Injector Cold-Flow Test No. 43B

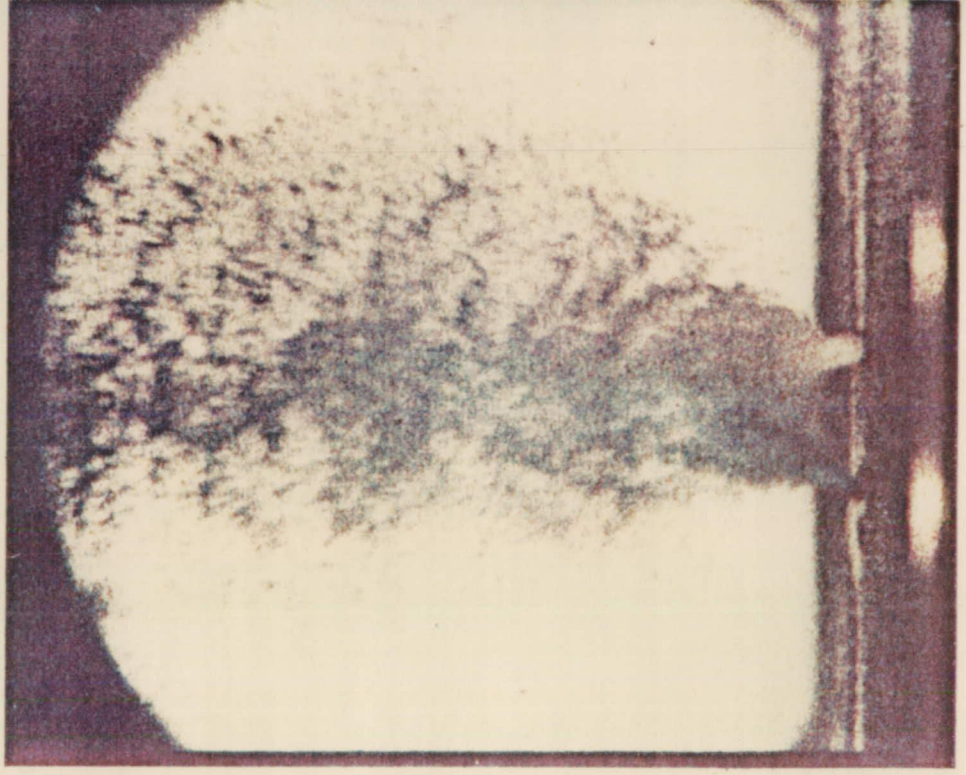

Cold-Flow Test No. 32
Fluids: Freon/Blue Water
Injector: LOL-EDM
Momentum Ratio: 0.99

V_f = 89 fps
V_{ox} = 64 fps

Figure 34. LOL-EDM Injector Cold-Flow Test No. 32

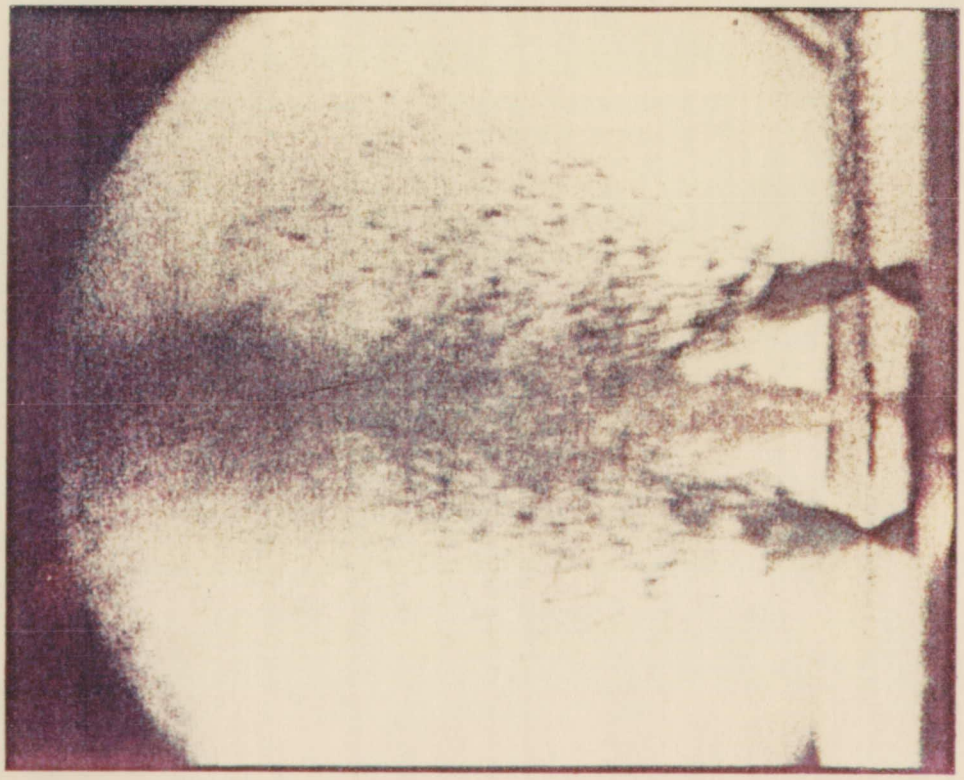

Cold-Flow Test No. 33
Fluids: Freon/Blue Water
Injector: PAT
Momentum Ratio: 0.93

V_f = 95 fps
V_{ox} = 54 fps

Figure 35. PAT Injector Cold-Flow Test No. 33

does not occur until the mometum ratio is less than 0.3. This inability to atomize and mix properly is believed to be related to the high aspect ratio of the orifices (see Figure 36).

Table V, a summary of impingement parameters, presents predicted optimum values for three cold-flow mixing criteria as well as the actual cold-flow and hotfire values over which the testing ranged. These criteria were used as a guide to determine the range of momentum ratio values that were evaluated during cold-flow. The cited OFO stream misimpingement obviously adds uncertainty to the results obtained with that injector. During this testing it was discovered that Rupe's mixing criteria for triplet injectors were more applicable to the OFO and PAT than Elverum and Morey's.

Since both the Rupe and Elverum and Morey criteria apply to fully developed turbulent liquid streams, they were not applied to the gas/liquid Slit Triplet injector. Rather, a simple momentum ratio was used for this injector. The best cold-flow mixing conditions are summarized in Table VI.

2. Hotfire Test Results

A total of 127 hotfire tests of seven injectors and four fuel combinations were conducted between 1 March 1979 and 29 November 1979 (see Table I). The test results are tabulated in Appendix II. The tabulation includes a description of the injector element, chamber pressure, mixture ratio, fuel velocity, fuel temperature, fuel Reynolds number, total weight flow, characteristic velocity, and the mode of operation. The operating mode describes the degree of carbon formation (see Section V.D.1 for definitions) and is identified from the high-speed movies taken during hotfire testing. Photographs taken from selected tests are shown in Figures 37-45. These photos, blowups of the high-speed 16 mm movie film, are included to assist in the description of the test results.

a. OFO Triplet with RP-1

Sixteen tests (Tests 101-116) were conducted with the OFO triplet, using RP-1 as fuel. The chamber pressure was varied from 450 psia to 1505 psia, and the mixture ratio varied from 1.7 to 2.8. These tests were dedicated to checking out the facility and photographic equipment and firming up a successful photographic technique. Representative test photographs are shown in Figure 37.

Early OFO test results showed a very overexposed, turbulent combustion with an extremely bright central flame. Using the baseline

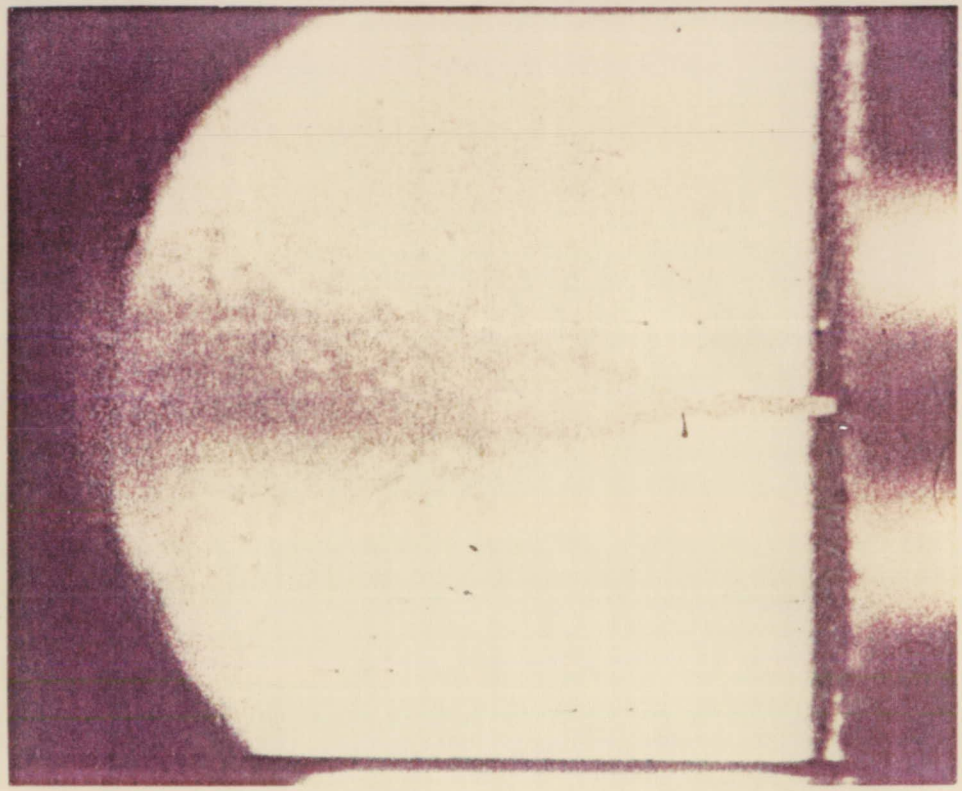

Cold-Flow Test No. 44
Fluids: Freon/GN_2
Injector: Slit Triplet
Momentum Ratio: 0.073

V_f = 1125.8 fps
V_{ox} = 27.9 fps

Figure 36. SLIT Triplet Injector Cold-Flow Test No. 44

TABLE V

IMPINGEMENT PARAMETERS

Injector and Fuel	Predicted Optimum			Cold-Flow			Hotfire		
	Rupe Criteria	Elverum & Morey Crit.	Momentum Ratio	Rupe Criteria	Elverum & Morey Crit.	Momentum Ratio	Rupe Criteria	Elverum & Morey Crit.	Momentum Ratio
OFO - RP1	1.0	0.66		0.45-1.45	0.49-1.52		0.55-1.29	0.638-1.47	
RUD - RP1	1.0			0.45-1.47			2.04		
RUD - C_3H_8	1.0			0.45-1.47			1.041-1.495		
RUD-GG C_3H_8	1.0			0.45-1.47			0.305-0.409		
TLOL - RP1	1.0			0.40-1.50			0.93-1.96		
TLOL-C_3H_8	1.0			0.40-1.50			0.843-1.157		
UD-NH_3	1.0			0.37-1.43			0.755-1.661		
LOL-EDM-C_3H_8	1.0			0.45-1.37			0.84-2.67		
LOL-EDM GG-C_3H_8	1.0			0.45-1.37			0.631-0.719		
LOL-EDM GG-ℓCH_4	1.0			0.45-1.37			0.213-0.705		
PAT - C_3H_8	1.0	0.66		0.45-1.35	1.19-3.51		0.59-1.52	0.066-2.761	
SLIT TRIPLET - gCH_4			1.0			0.073-4.912			0.31-1.291

Rupe Criteria: $$\frac{\rho_{ox} V^2_{ox} D_{ox}}{\rho_f V_f^2 D_f} = 1.0$$

Elverum & Morey Criteria: $$\left(\frac{\dot{w}_1}{\dot{w}_2}\right)^2 \frac{\rho_2}{\rho_1} \left(\frac{A_2}{2A_1}\right)^{1.75} = 0.66$$

Momentum Ratio: $$\frac{\dot{w}_{ox} V_{ox}}{\dot{w}_f V_f}$$

TABLE VI

OBSERVED BEST COLD-FLOW MIXING CONDITIONS

INJECTOR	RUPE	ELVERUM & MOREY	MOMENTUM RATIO
OFO	0.96	1.007	1.94
RUD	0.97	---	1.43
TLOL	0.87	---	1.35
UD	0.85	---	0.85
LOL-EDM	0.99	---	1.38
PAT	0.93	1.75	1.23
SLIT TRIPLET	0.044	1.99	0.073

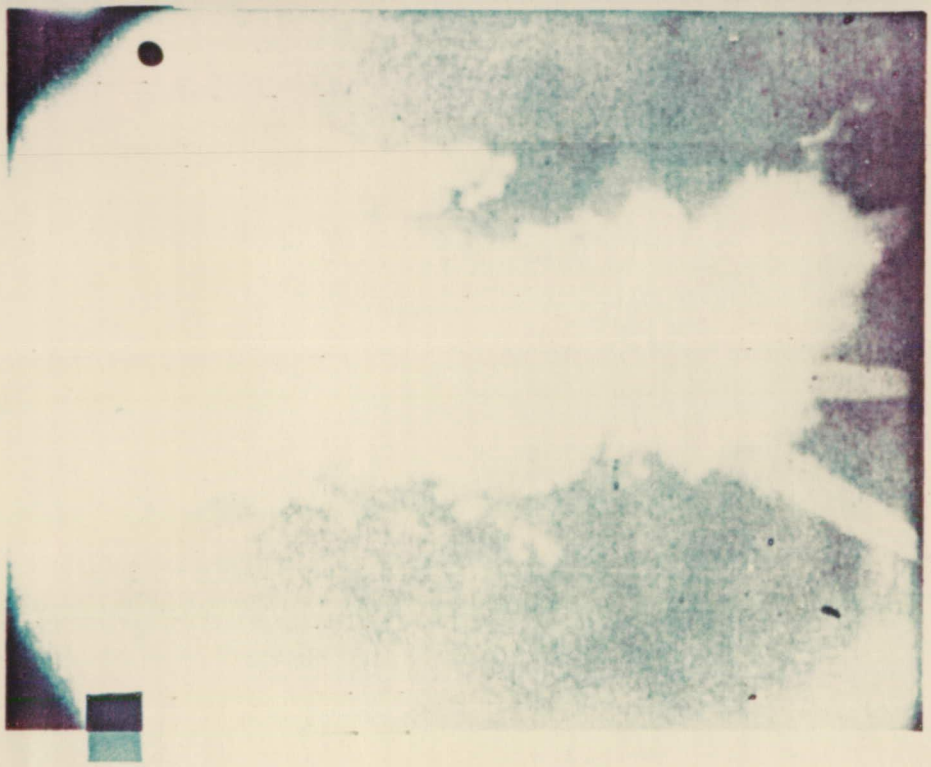

Test No. 101
Fuel Type: RP-1
Injector Element: OFO
Pc = 460 psia
O/F = 2.40

Test No. 105
Fuel Type: RP-1
Injector Element: OF
Pc = 480 psia
O/F = 2.78

Figure 37. OFO Triplet, RP-1 Fuel Combustion (Sheet 1 of 4)

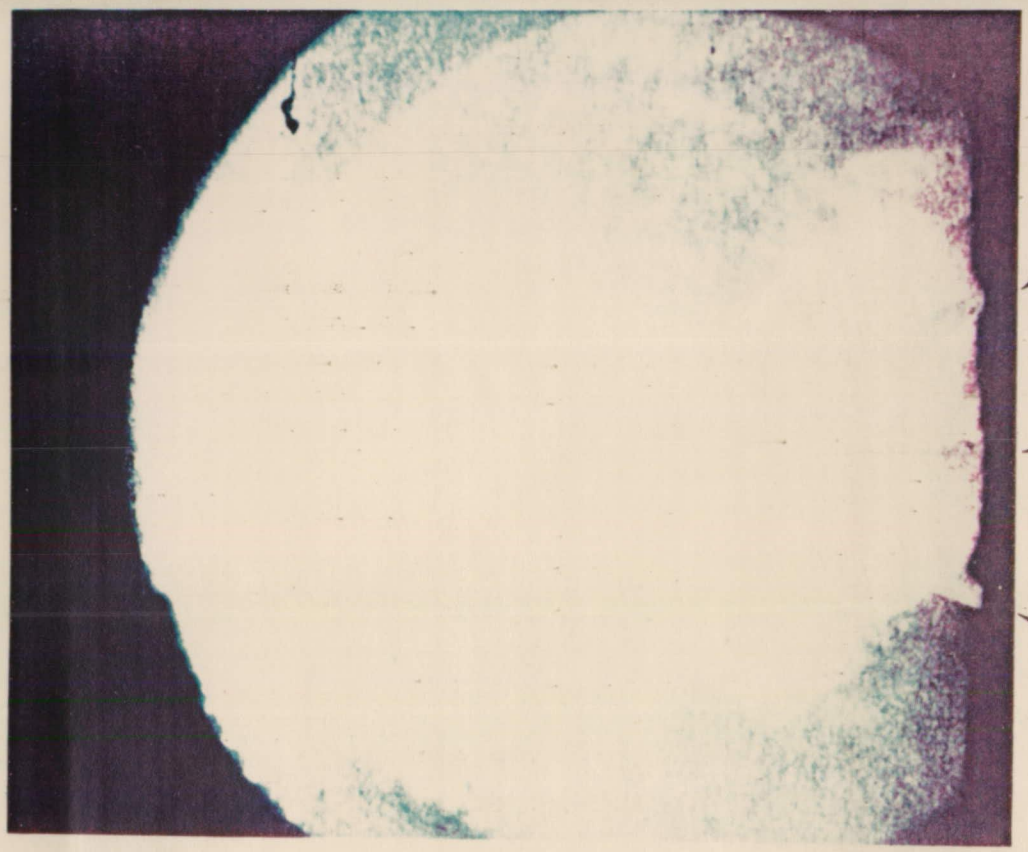

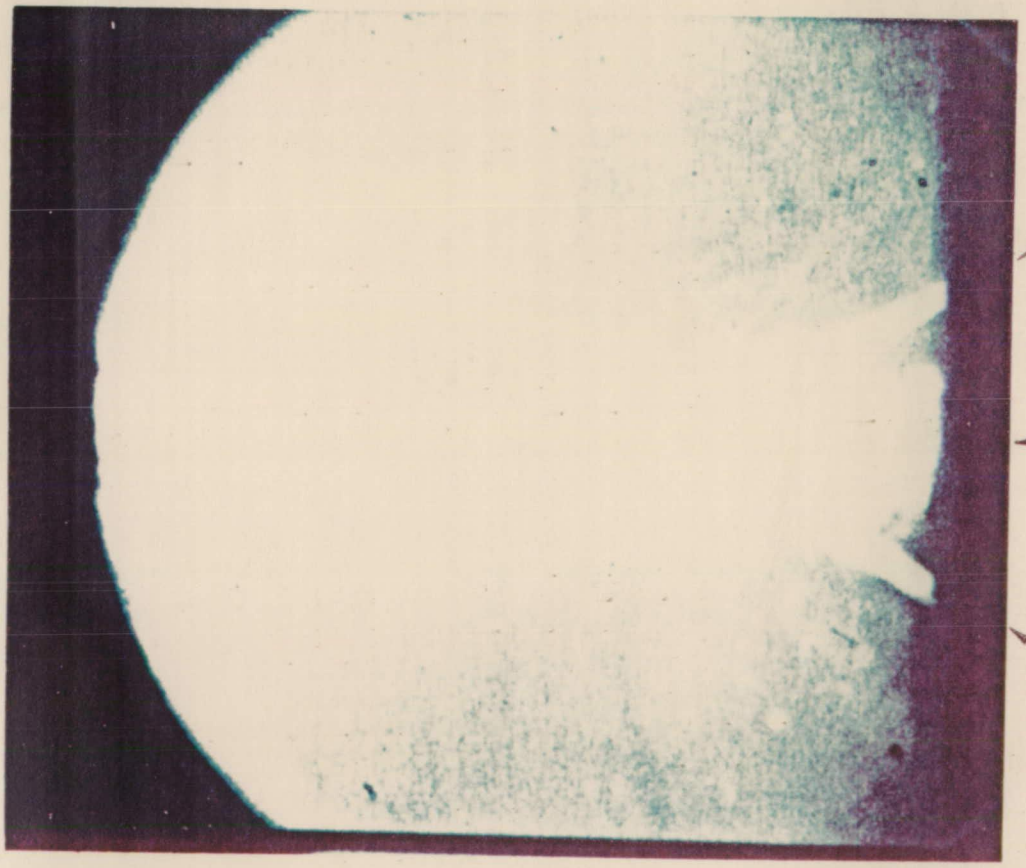

Figure 37. OFO Triplet, RP-1 Fuel Combustion (Sheet 2 of 4)

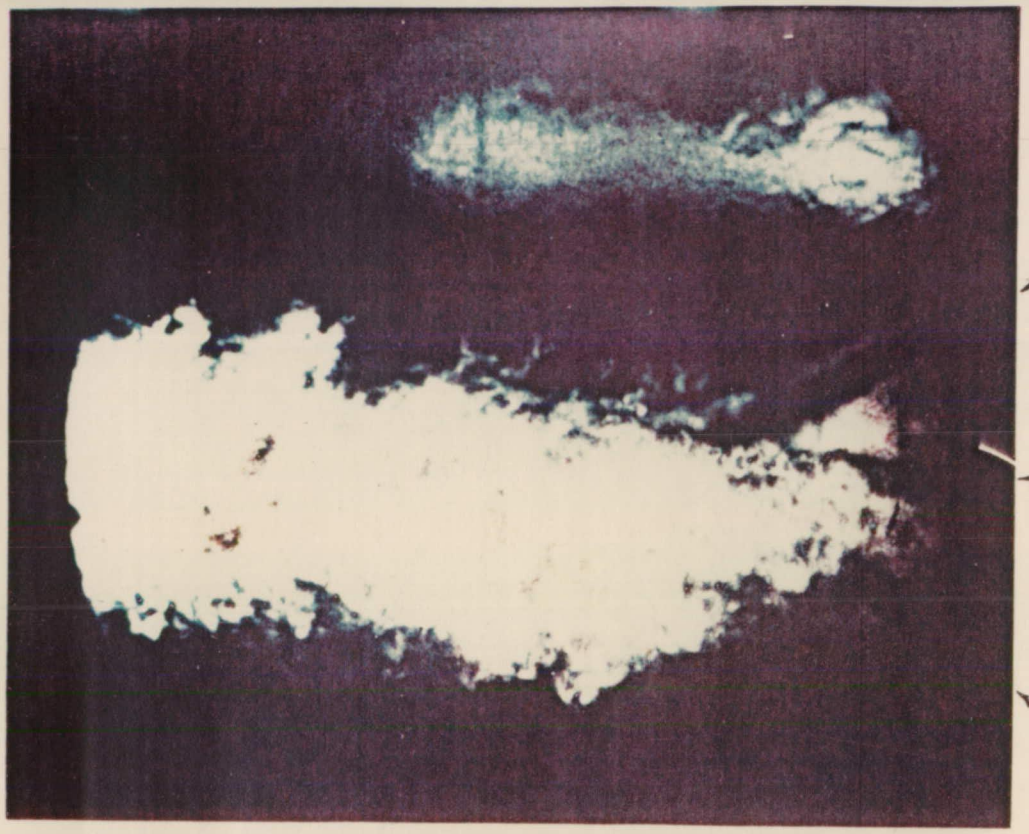

Test No. 110
Fuel Type: RP-1
Injector Element: OFO
Pc = 480 psia
O/F = 2.7

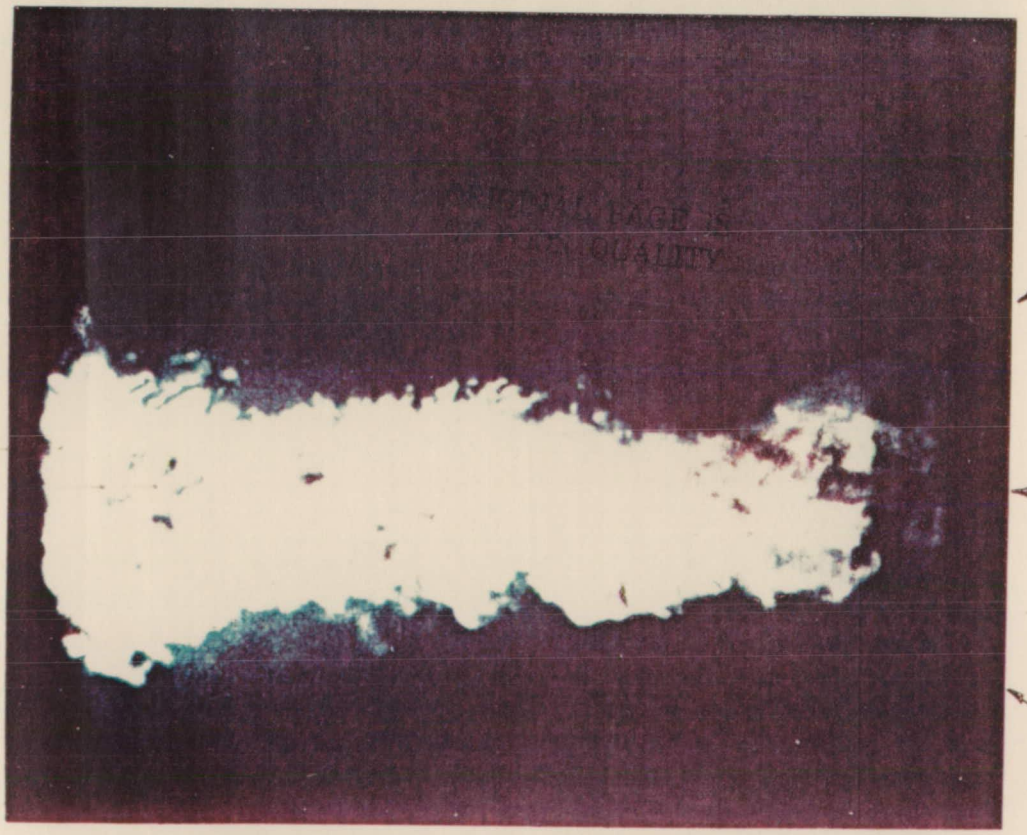

Test No. 114
Fuel Type: RP-1
Injector Element: OFO
Pc = 970 psia
O/F = 2.35

Figure 37. OFO Triplet, RP-1 Fuel Combustion (Sheet 3 of 4)

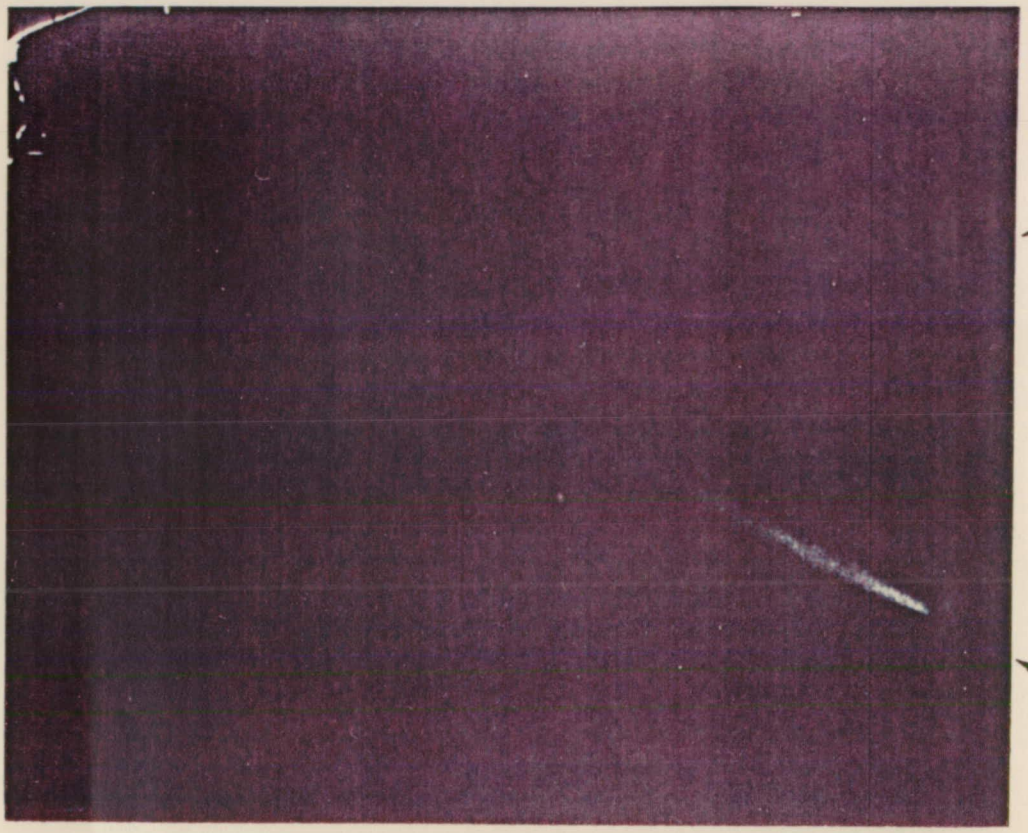

Test No. 115
Fuel Type: RP-1
Injector Element: OFO
Pc = psia
O/F =
Lox Cold Flow

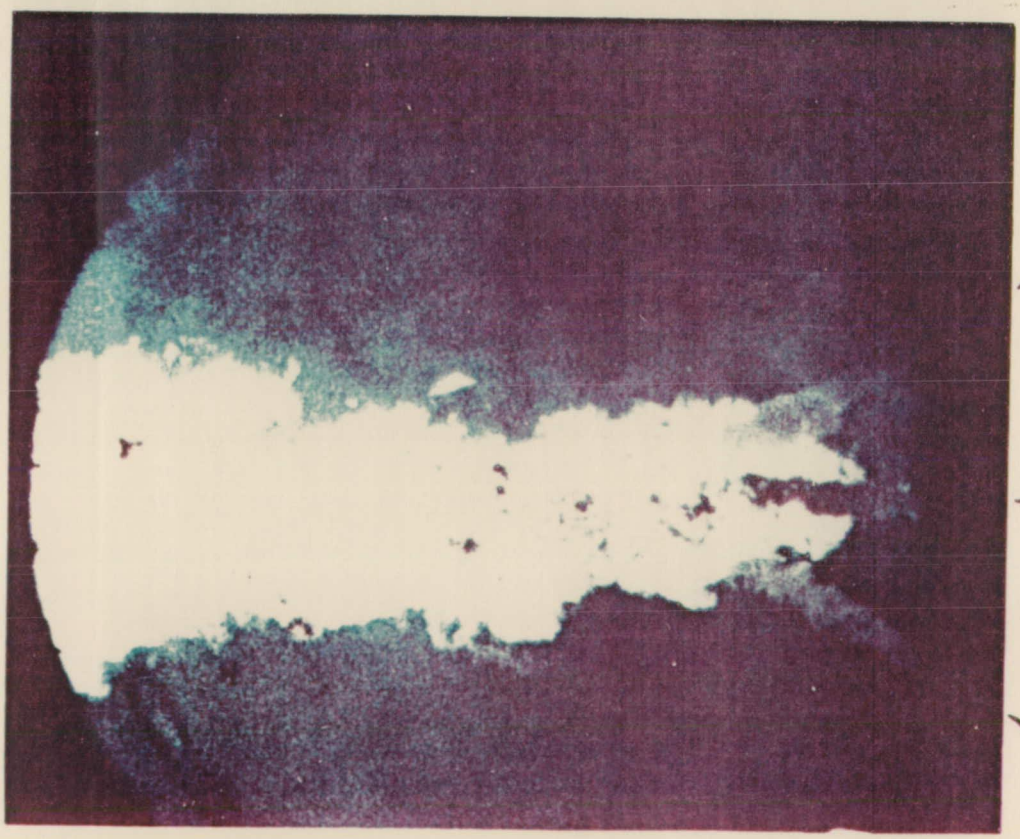

Test No. 116
Fuel Type: RP-1
Injector Element: OFO
Pc = 1505 psia
O/F = 2.60

Figure 37. OFO Triplet, RP-1 Fuel Combustion (Sheet 4 of 4)

camera settings (ASA 125 film, shutter = 1/50, 800 pps, f-4), there was far too much combustion light (Tests 101-107) to see any droplet details. After some test stand and light setting changes, the movies showed greater detail but also indicated a need for increased external light. The bright central flame, white in earlier films, (Tests 101-107) now appeared as a yellow flame interspersed with brownish areas which likely represent decomposing RP-1 and carbon formation (see Tests 110, 114, 115, 116).

The final OFO tests during early April indicated that the light settings in use represented the optimum to be obtained from conventional photoflood lighting. Test 114, at 1000 psia and MR = 2.35, appears as a bright central yellow flame interspersed with decomposing RP-1 and carbon formation. The photo of Test 115 shows a LOX cold-flow due to an igniter malfunction. Test 116, at 1500 psia and MR = 2.6, differs from Test 114 only in its greater flame brilliance.

b. TLOL with RP-1

Eleven tests were conducted with the TLOL injector element, using RP-1 (Tests 119-129). TLOL testing utilized the flashbulb lighting technique described in Section IV.B, which greatly improved picture quality.

The TLOL combustion using RP-1 fuel (Figure 38) was similar to that of the OFO triplet in the following four ways: (1) carbon formation, (2) lack of freezing or popping, (3) increasing flame brilliance with increasing chamber pressure, and (4) recirculation gas flow patterns. Dissimilarities in the spray field uniformity were observed as the result of differences in mixing characteristics. The TLOL appears to exhibit RSS as evidenced by striations of unmixed fuel and oxidizer (Tests 123 and 124). The fuel fan exhibits a brownish-black color even before unlike impingement, indicating thermal decomposition due to propellant stream heating (Tests 128 and 129). The LOX fans exhibit a white-gray color and vaporized more rapidly with increasing chamber pressure. (Compare Tests 128 and 129.)

c. RUD with RP-1

The RUD injector was fired only once (Test 117) with LOX/RP-1 because of test priorities. This test was conducted at a low pressure (130 psia) and encountered difficulty in flowing liquid oxygen. Since the movie from Test 117 was obscured with a great deal of carbon formation, it is not shown.

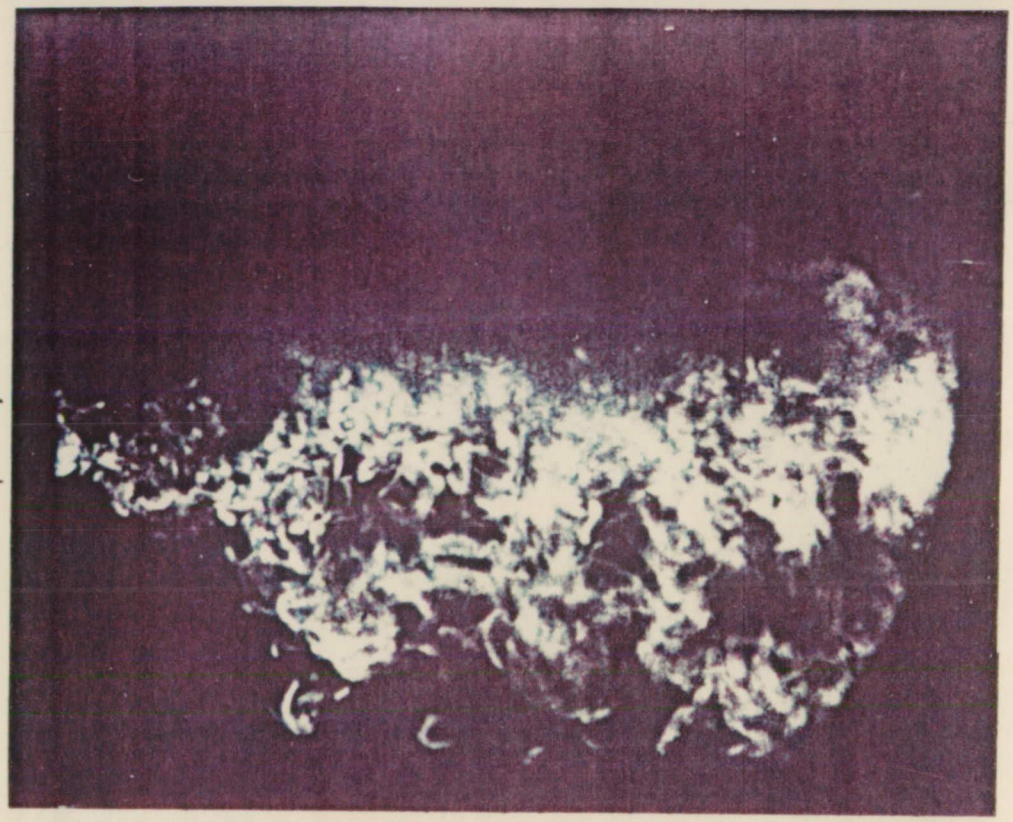

Test No. 121
Fuel Type: RP-1
Injector Element: TLOL
Pc = 310 psia
O/F = 2.80

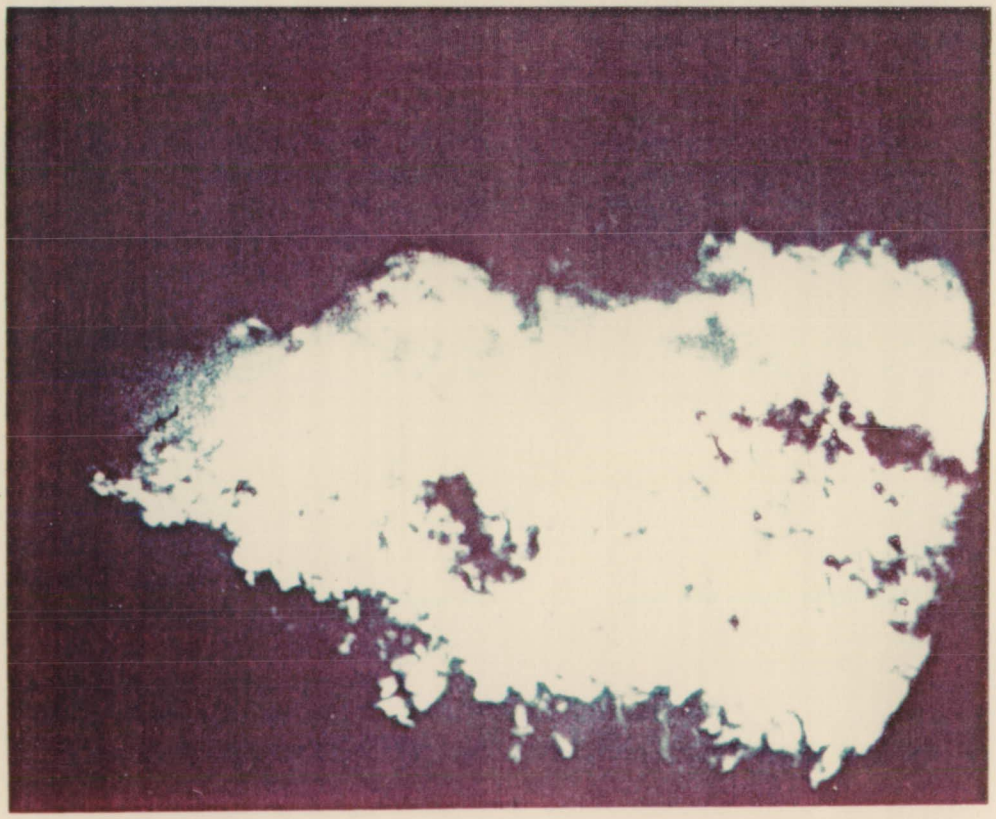

Test No. 122
Fuel Type: RP-1
Injector Element: TLOL
Pc = 785 psia
O/F = 2.70

Figure 38. TLOL, RP-1 Fule Combustion (Sheet 1 of 4)

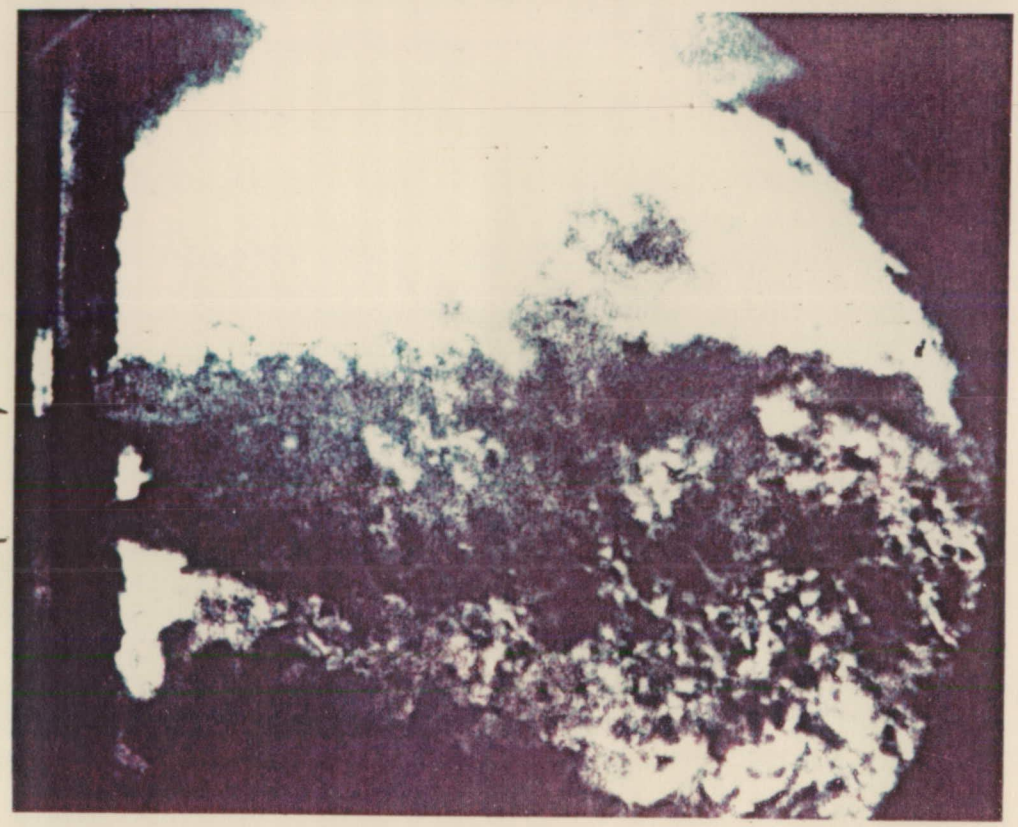

Test No. 123
Fuel Type: RP-1
Injector Element: TLO
Pc = 475 psia
O/F = 2.65

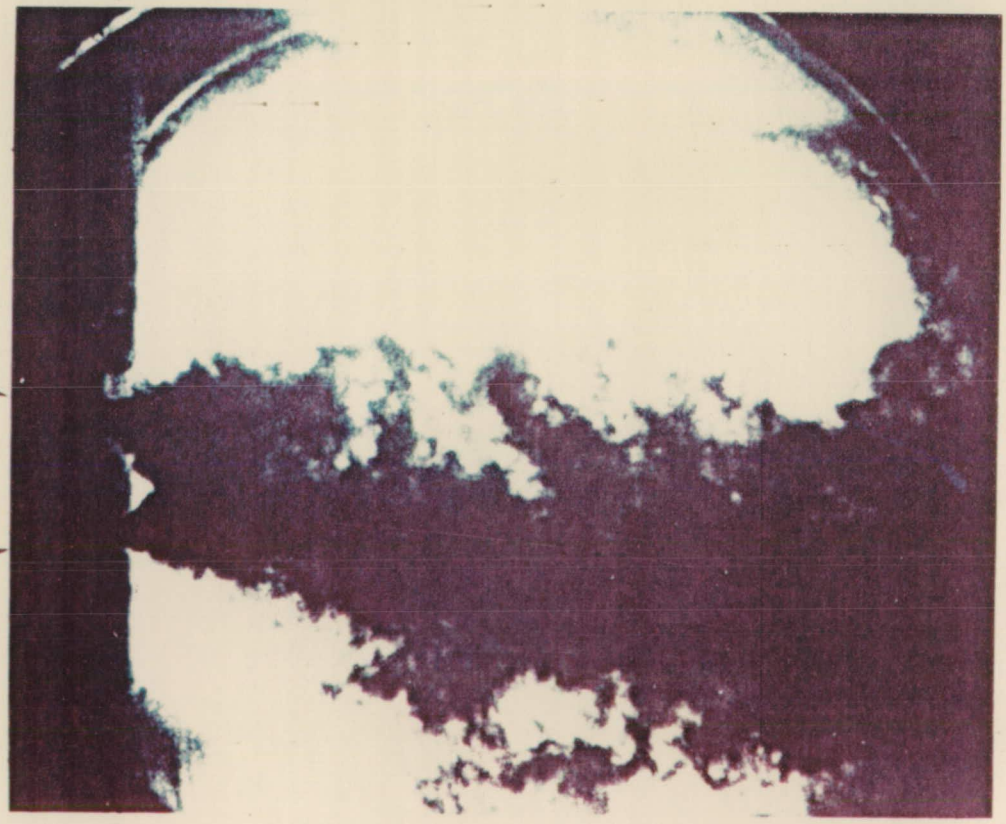

Test No. 124
Fuel Type: RP-1
Injector Element: TLOL
Pc = 475 psia
O/F = 2.65

Figure 38. TLOL, RP-1 Fuel Combustion (Sheet 2 of 4)

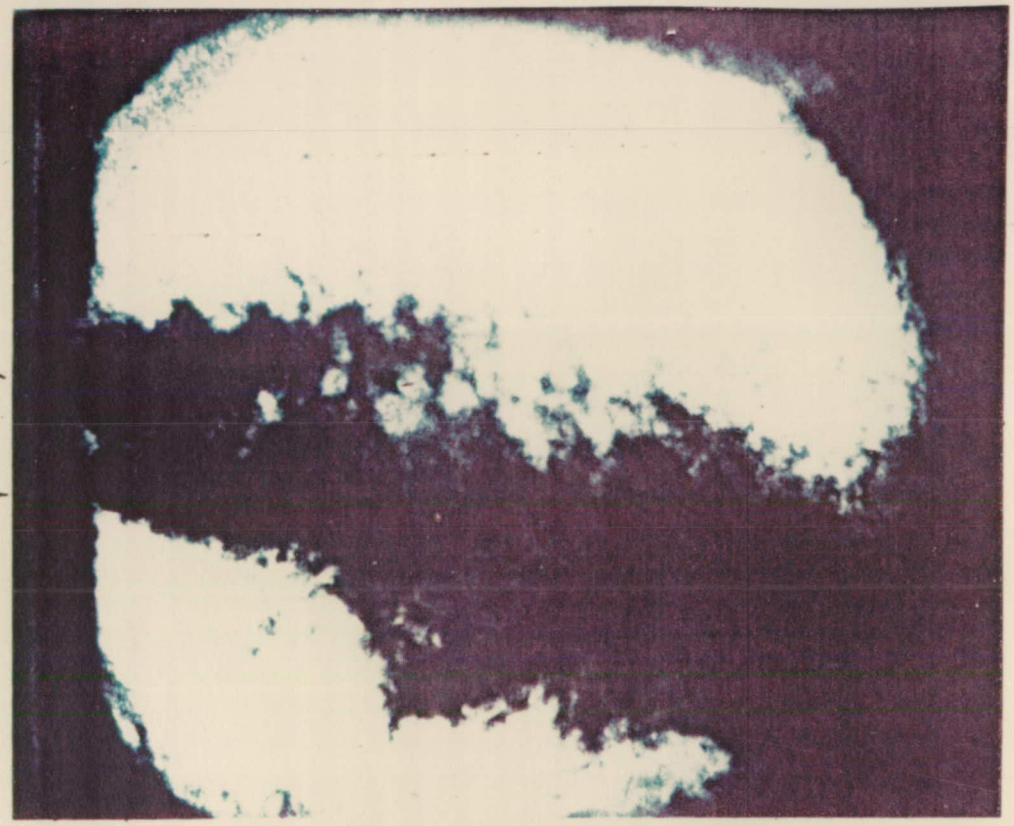

Test No. 125
Fuel Type: RP-1
Injector Element: TL
Pc = 472 psia
O/F = 2.50

Test No. 127
Fuel Type: RP-1
Injector Element: TLOL
Pc = 250 psia
O/F = 2.85

Figure 38. TLOL, RP-1 Fuel Combustion (Sheet 3 of 4)

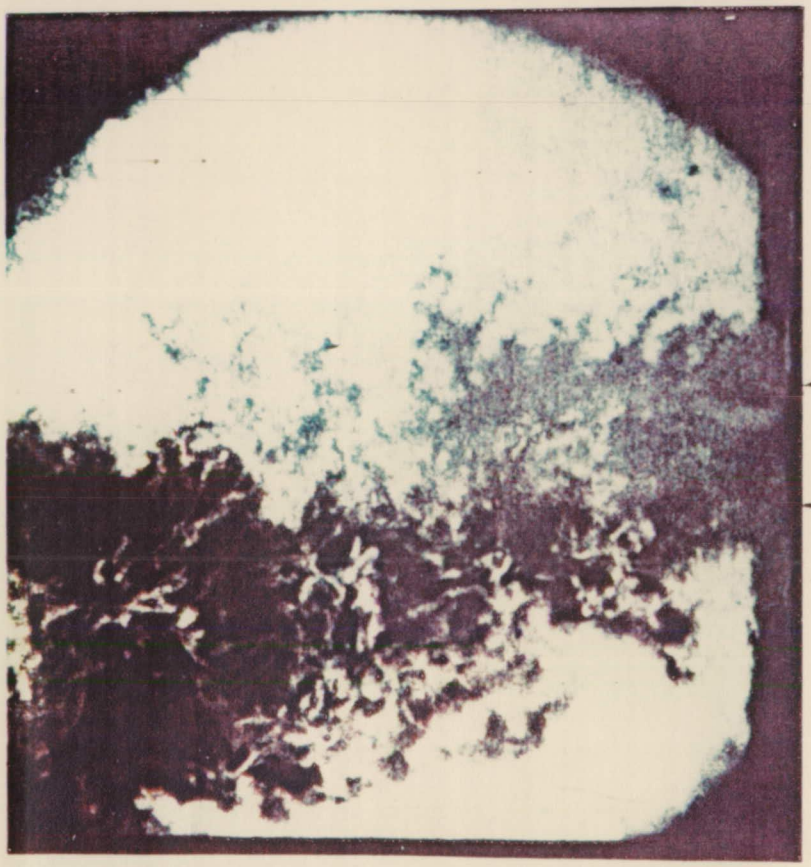

Test No. 128
Fuel Type: RP-1
Injector Element: TLOL
Pc = 400 psia
O/F = 3.10

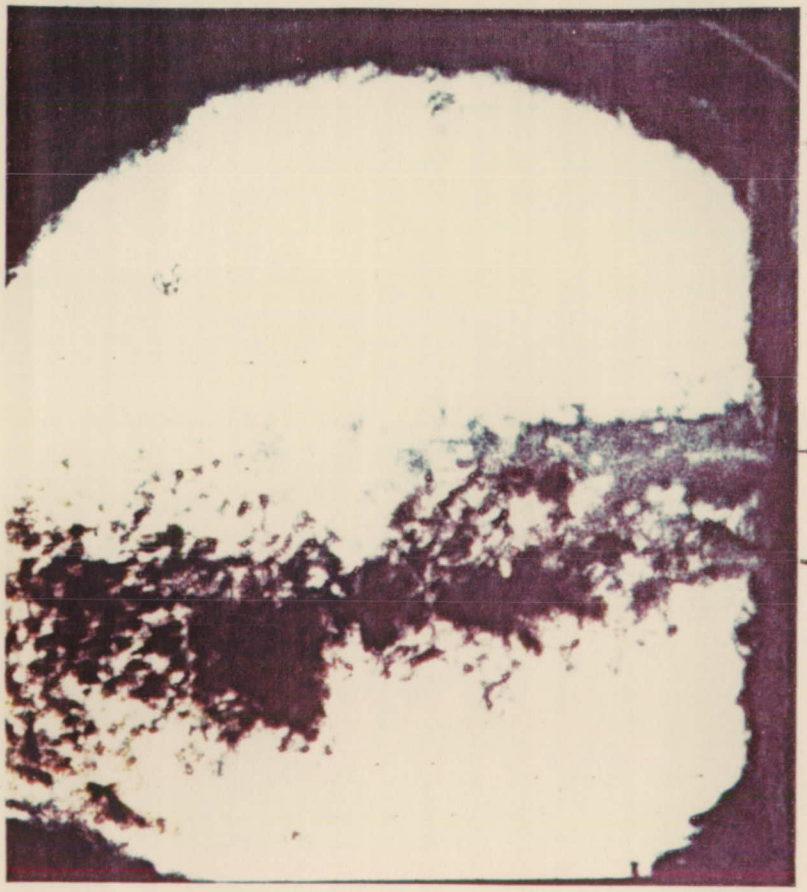

Test No. 129
Fuel Type: RP-1
Injector Element: TLOL
Pc = 800 psia
O/F = 2.8

Figure 38. TLOL, RP-1 Fuel Combustion (Sheet 4 of 4)

V, C, Test Results (cont.)

d. TLOL with Propane

The TLOL tests with propane (Tests 130-133) are photographically summarized in Figure 39. The TLOL tested with propane shows much less brilliant combustion flame, producing much less carbon-particle emission than the LO_2/RP-1 combustion (Tests 130-133). The fuel fans exhibit a grayish-brown color before unlike impingement, indicating less thermal decomposition than the RP-1. Combustion light also increased with chamber pressure, but to a lesser degree than with LOX/RP-1. A brownish vapor is visible in the low pressure tests (Test 130), resulting from propane's high vapor pressure. In comparison with the RP-1 tests, posttest carbon decomposition or sooting in the chamber was negligible.

e. RUD with Propane

Seven LOX/C_3H_8 tests (Tests 134-141) were fired with the RUD operating as a main chamber element. These tests covered a chamber pressure range from 150 psia to 800 psia and were markedly different from the TLOL LOX/C_3H_8 tests. These movies (Test 136-141) shown, in Figure 40, were darker than the TLOL LOX/C_3H_8 movies even though the lens was opened two stops. The pictures shown in Figure 40 were taken during the test start transient, before complete clouding occurred. The pictures subsequently went black. The obscured pictures are the result of greater formation of unburned carbon. The increased carbon formation observed with the RUD is believed to be a result of its superior mixing characteristics which cause chilling of the fuel. The reduced fuel temperature delays vaporization and combustion and apparently leads to carbon formation. The external lighting did not yield the same quality of picture as with the TLOL and OFO triplet since the vapor and unburned combustion intermediates formed a sort of opaque mixture which would not allow the penetration of external light. As a result, details of the combustion could not be ascertained.

f. RUD with Propane, Gas Generator Conditions

The fuel and oxidizer circuits were switched on the RUD and tested at fuel-rich gas generator conditions (Tests 142-144). The first valid test (No. 143) fired for 2 seconds at Pc = 860 psia and MR = 0.55. Excessive sooting was experienced, and the window inserts had to be replaced. Carbon deposits were cooked onto the glass and could not be removed. Since the windows were completely black, no photographic data could be obtained. Test 144 was a repeat of Test 143, using conventional lighting for a comparison. After ignition, the chamber immediately filled with soot, thus nothing more could be seen.

Test No. 130
Fuel Type: C_3H_8
Injector Element: TLOL
Pc = 134 psia
O/F = 2.50

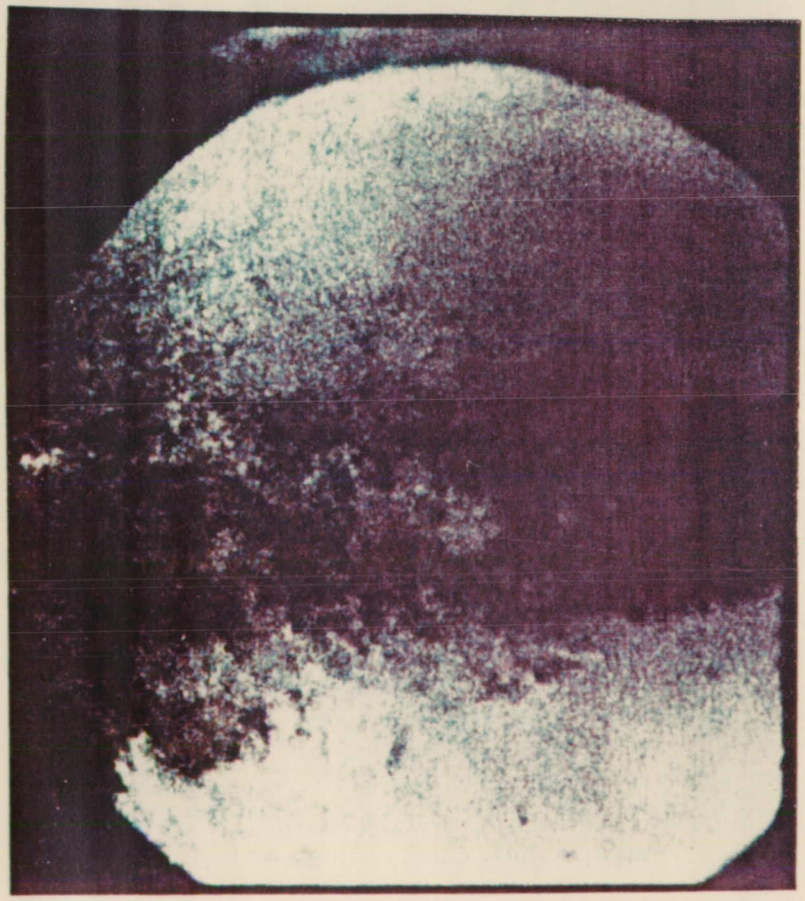

Test No. 131
Fuel Type: C_3H_8
Injector Element: TLOL
Pc = 290 psia
O/F = 2.65

Figure 39. TLOL, Propane Fuel Combustion (Sheet 1 of 2)

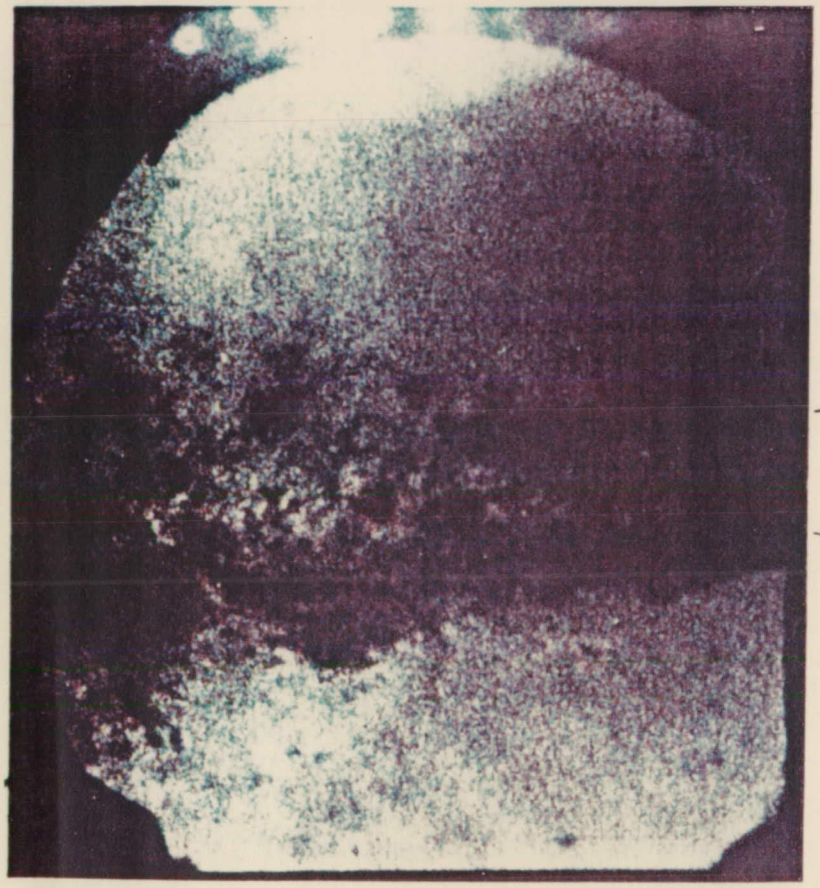

Test No. 132
Fuel Type: C_3H_8
Injector Element: TLOL
Pc = 540 psia
O/F = 3.00

Test No. 133
Fuel Type: C_3H_8
Injector Element: TLOL
Pc = 785 psia
O/F = 2.80

Figure 39. TLOL, Propane Fuel Combustion (Sheet 2 of 2)

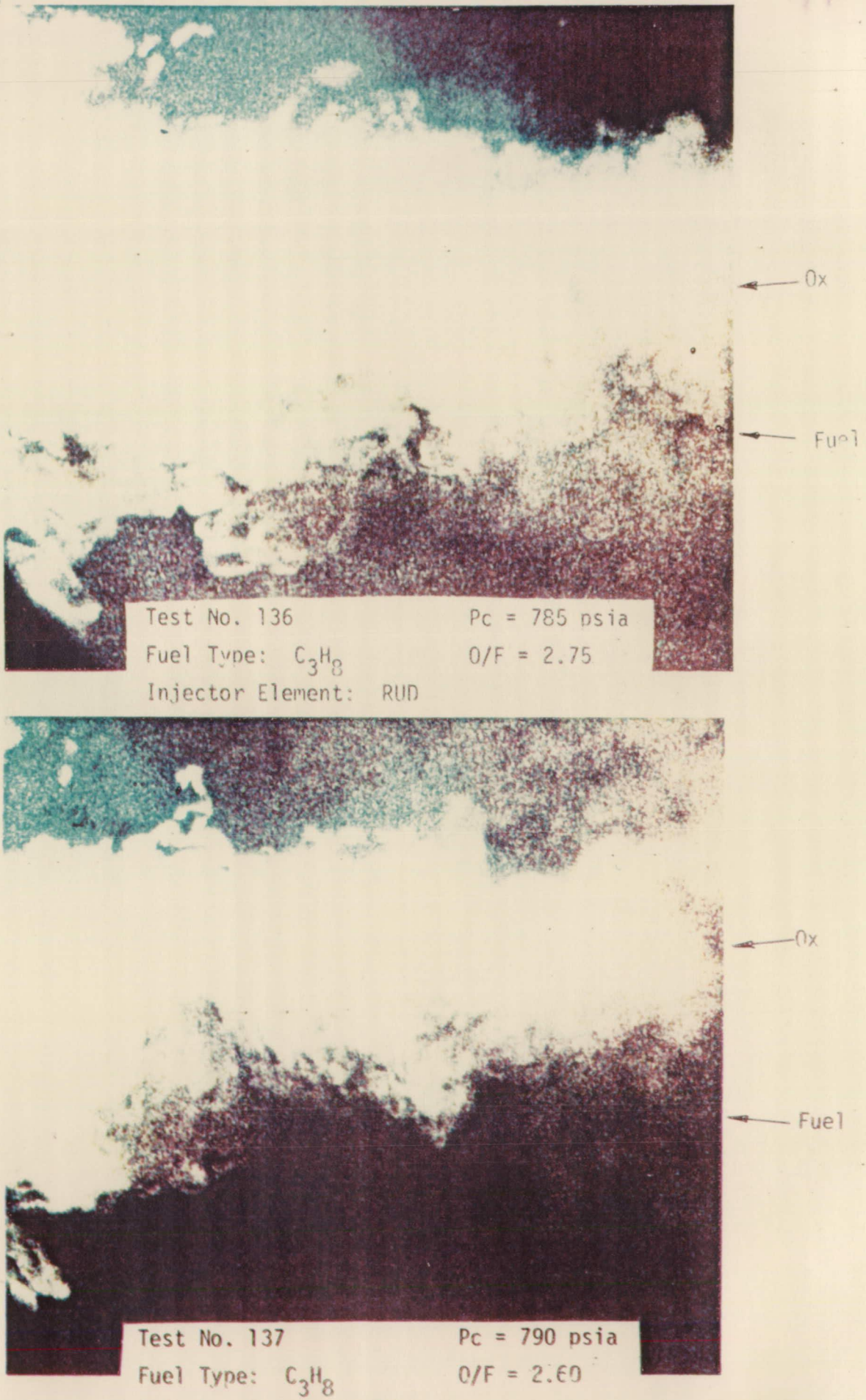

Figure 40. RUD, Propane Fuel Combustion (Sheet 1 of 3)

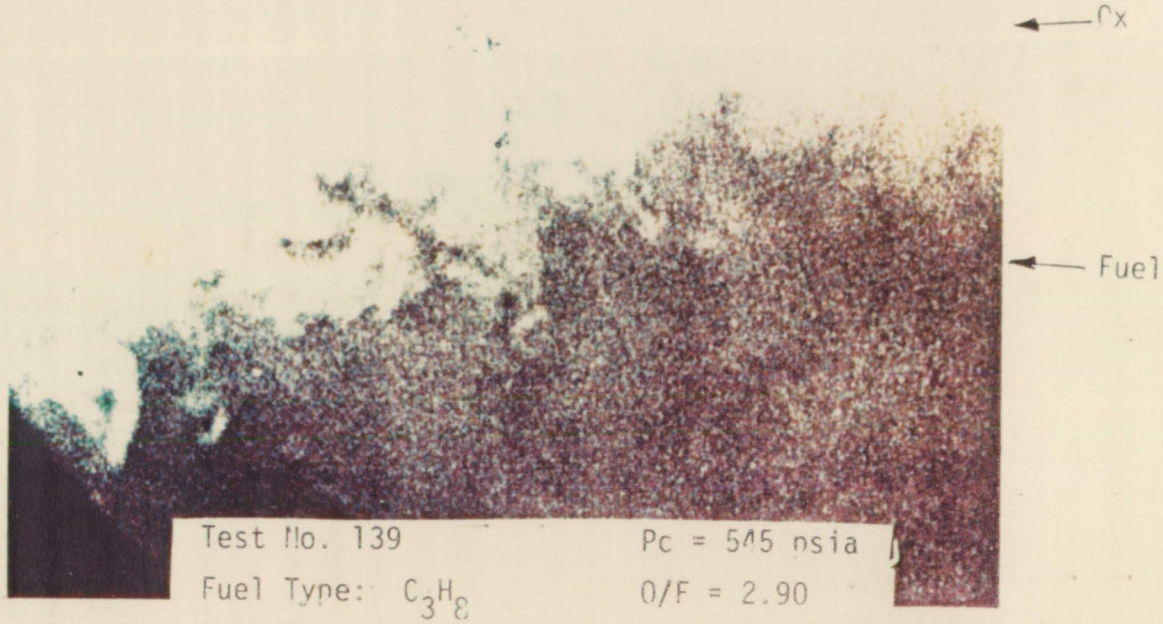

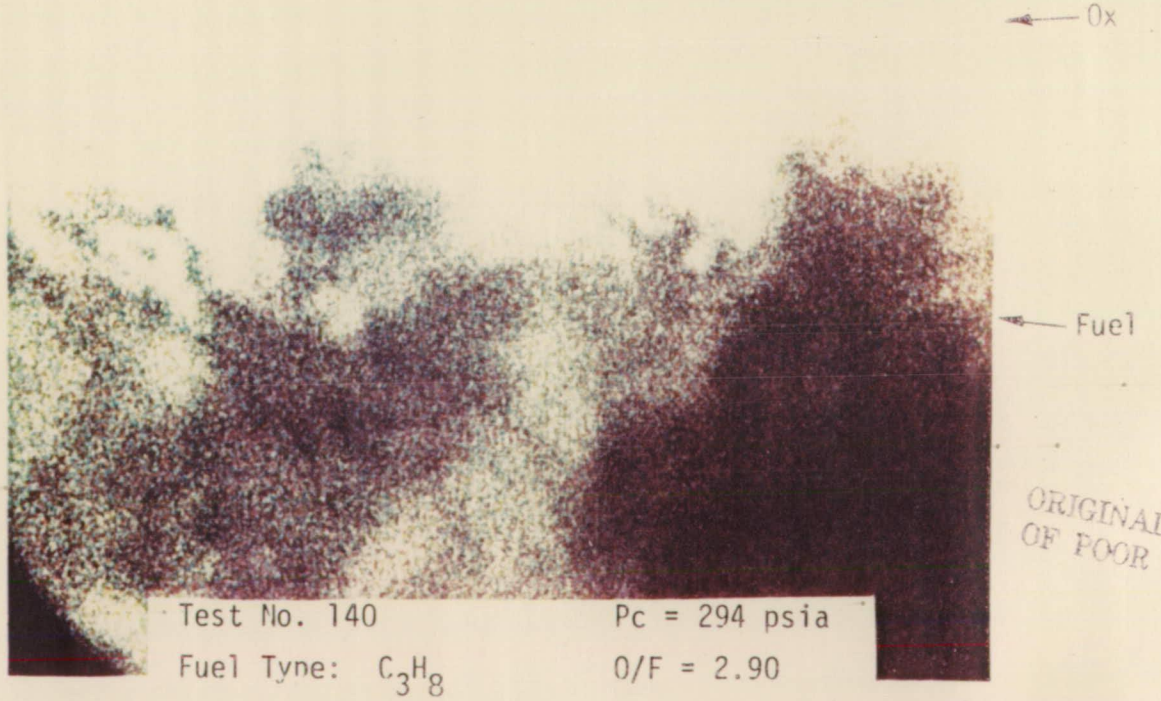

Figure 40. RUD, Propane Fuel Combustion (Sheet 2 of 3)

Test No. 141 Pc = 150 psia

Fuel Type: C_3H_8 O/F = 3.10

Injector Element: RUD

Figure 40. RUD, Propane Fuel Combustion (Sheet 3 of 3)

V, C, Test Results (cont.)

g. Unlike Doublet with Ammonia

Twelve tests (Tests 145-156) were conducted with the Unlike Doublet injector element using LOX/NH_3 propellants. Despite differences in Pc, MR, and stream velocities all tests appeared remarkably similar on film (Figure 41). Both propellant streams had a light gray color before impingement and formed an evenly dispersed, well-mixed fan at each test condition. No changes in light intensity or tendencies toward separation were identified. Tests 149-156 examined extremes of velocity, MR, and Pc with much the same results. In each instance, the LOX/NH_3 combination seemed to display a benign "well-behaved" type of combustion that was apparently insensitive to operating conditions. While there was very little color differentiation to help identify possible RSS, the existence of liquid droplets squirting from the impingement point towards the injector face would indicate that no combustion (and no RSS) was occurring at the impingement point. Ammonia is observed to be less reactive from an RSS standpoint than RP-1 or propane. The fact that the spontaneous ignition temperature of ammonia is greater than the respective values for RP-1, Propane, and Methane may explain its lower reactivity (see Section V.D.).

h. LOL-EDM with Propane

Twenty tests (Tests 157-176) were fired with the LOL-EDM and LOX/C_3H_8 at main engine conditions. These tests (Figure 42) showed well-mixed spray fans which resulted in great quantities of carbon formation, similar to those of the RUD injector. Tests were run with the propane heated to 130°F-150°F (Tests 165, 168, 169, 171, 172) to determine its effect on the carbon formation, since carbon formation seemed to center around the inability to vaporize the propane rapidly. It was found that raising the fuel temperature to around 150°F eliminates most of the propane carbon formation which had obscured the picture in previous tests (Test 169). The pictures became clearer as the chamber pressure was reduced toward the vapor pressure of propane at 150°F (approx. 320 psia). These results tend to support the hypothesis that the carbon formation is caused by delayed vaporization.

With this injector, mixture ratio effects were found to be a significant factor in carbon formation. Low mixture ratios produced more carbon, and high mixture ratios (Test 175) tended to burn more cleanly. The LOL-EDM tends to burn cleanly above 600 psia, regardless of fuel temperature or mixture ratio (Test 161).

Test 176 is an interesting study of temperature and pressure effects on vaporization and black cloud formation. The test began

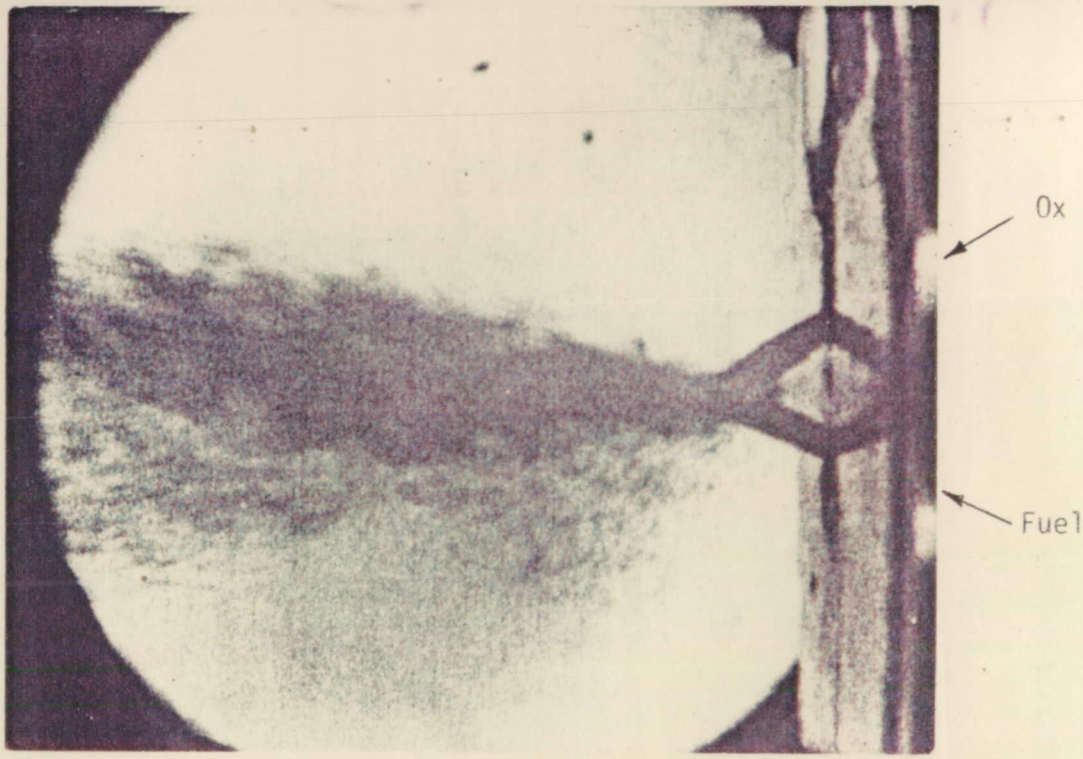

Test No. 145 Pc = 505 psia
Fuel Type: NH_3 O/F = 1.48
Injector Element: Unlike Doublet

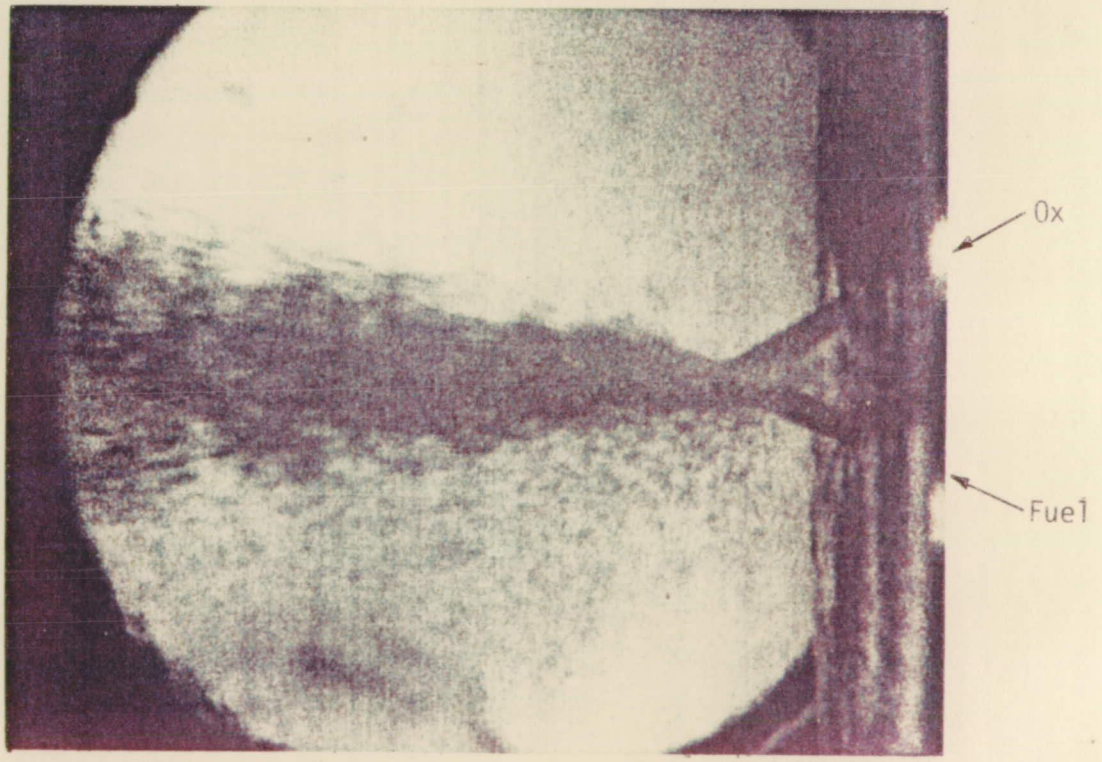

Test No. 147 Pc = 245 psia
Fuel Type: NH_3 O/F = 1.35
Injector Element: Unlike Doublet

Figure 41. Unlike Doublet, Ammonia Fuel Combustion (Sheet 1 of 5)

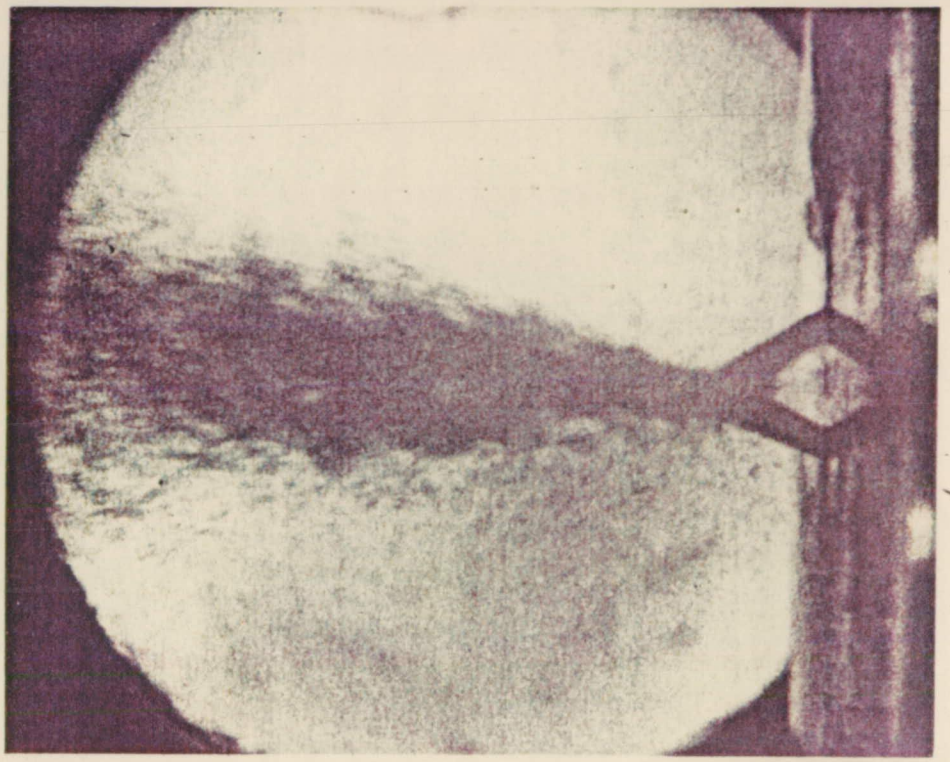

Test No. 148 Pc = 350 psia

Fuel Type: NH_3 O/F = 1.48

Injector Element: Unlike Doublet

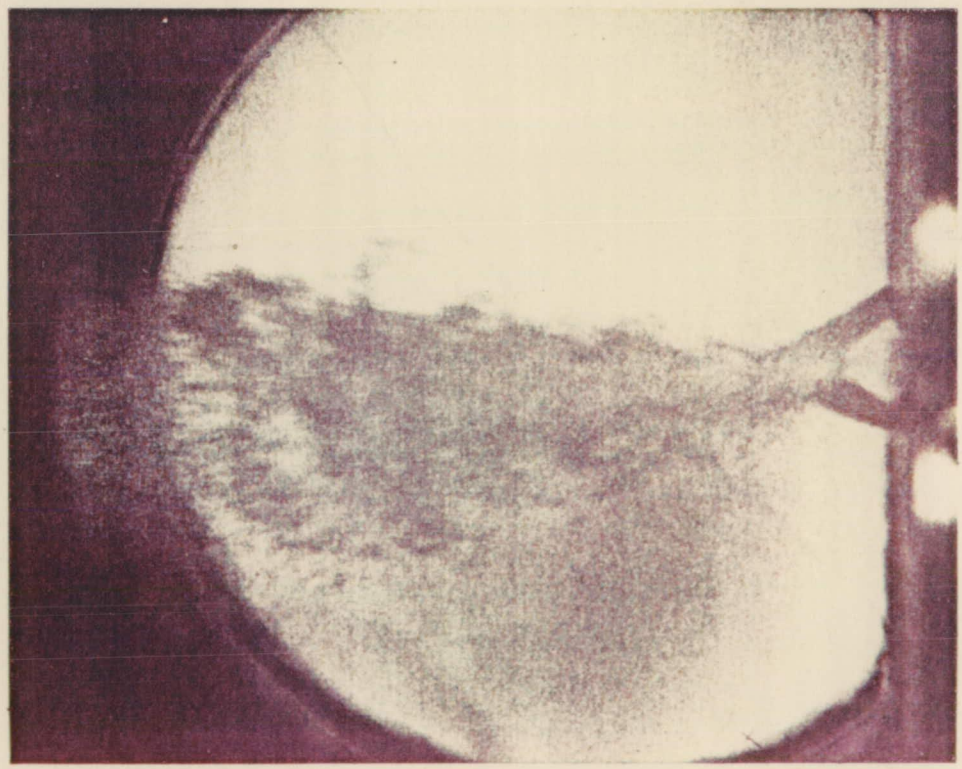

Test No. 149 Pc = 490 psia

Fuel Type: NH_3 O/F = 1.35

Injector Element: Unlike Doublet

Figure 41. Unlike Doublet, Ammonia Fuel Combustion (Sheet 2 of 5)

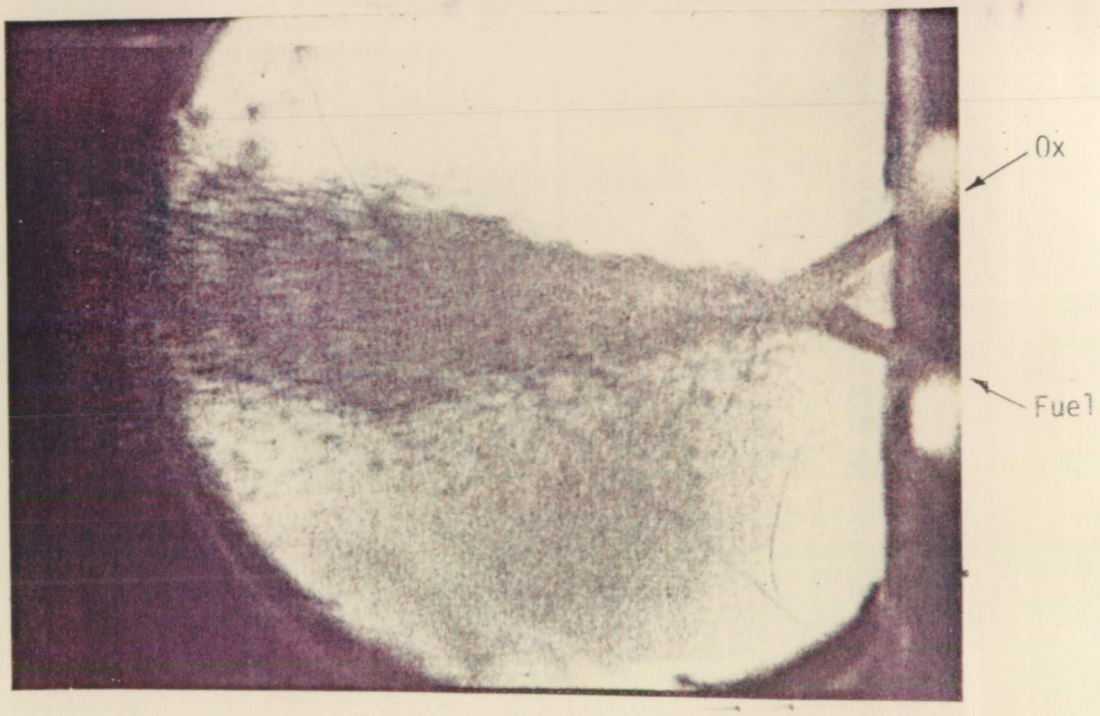

Test No. 150 Pc = 250 psia
Fuel Type: NH_3 O/F = 1.38
Injector Element: Unlike Doublet

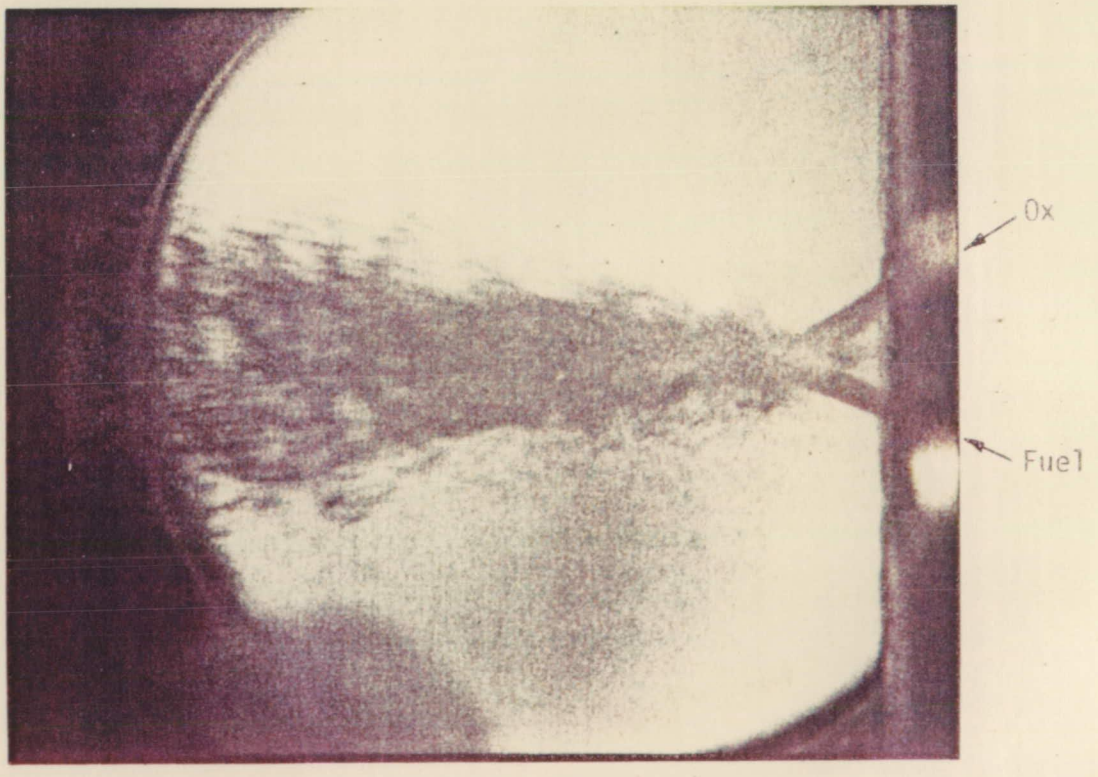

Test No. 151 Pc = 150 psia
Fuel Type: NH_3 O/F = 1.35
Injector Element: Unlike Doublet

Figure 41. Unlike Doublet, Ammonia Fuel Combustion (Sheet 3 of 5)

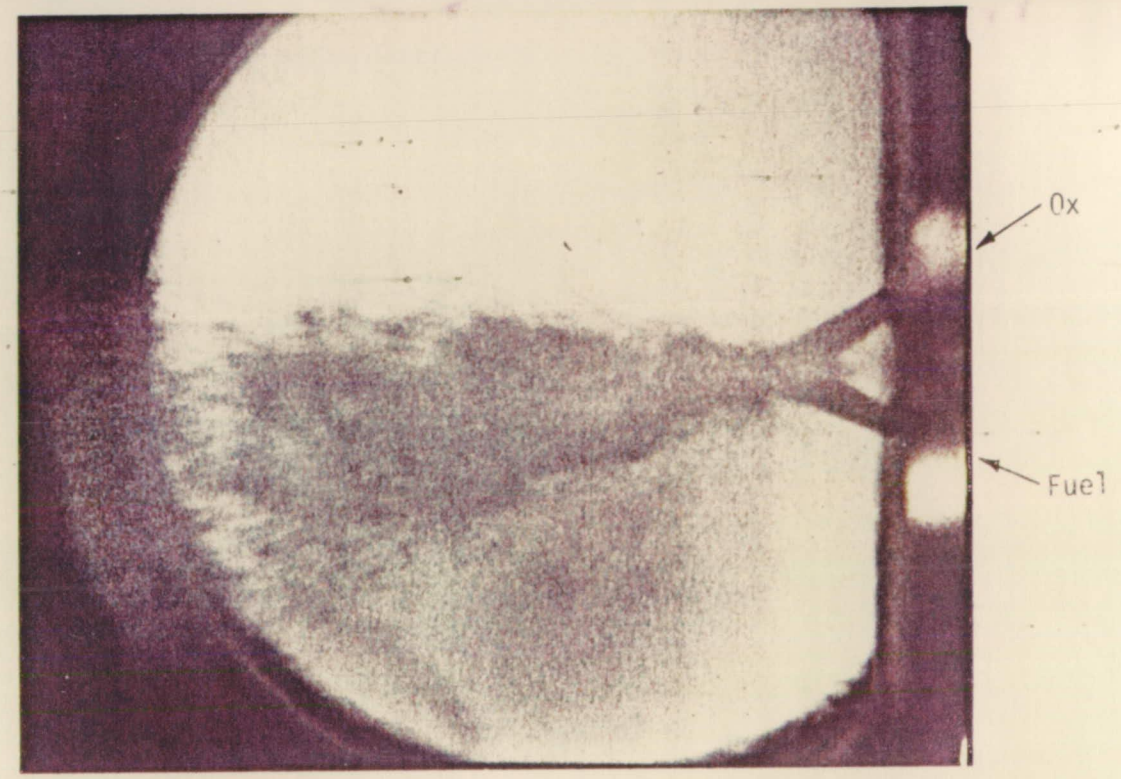

Test No. 152 Pc = 505 psia
Fuel Type: NH_3 O/F = 1.10
Injector Element: Unlike Doublet

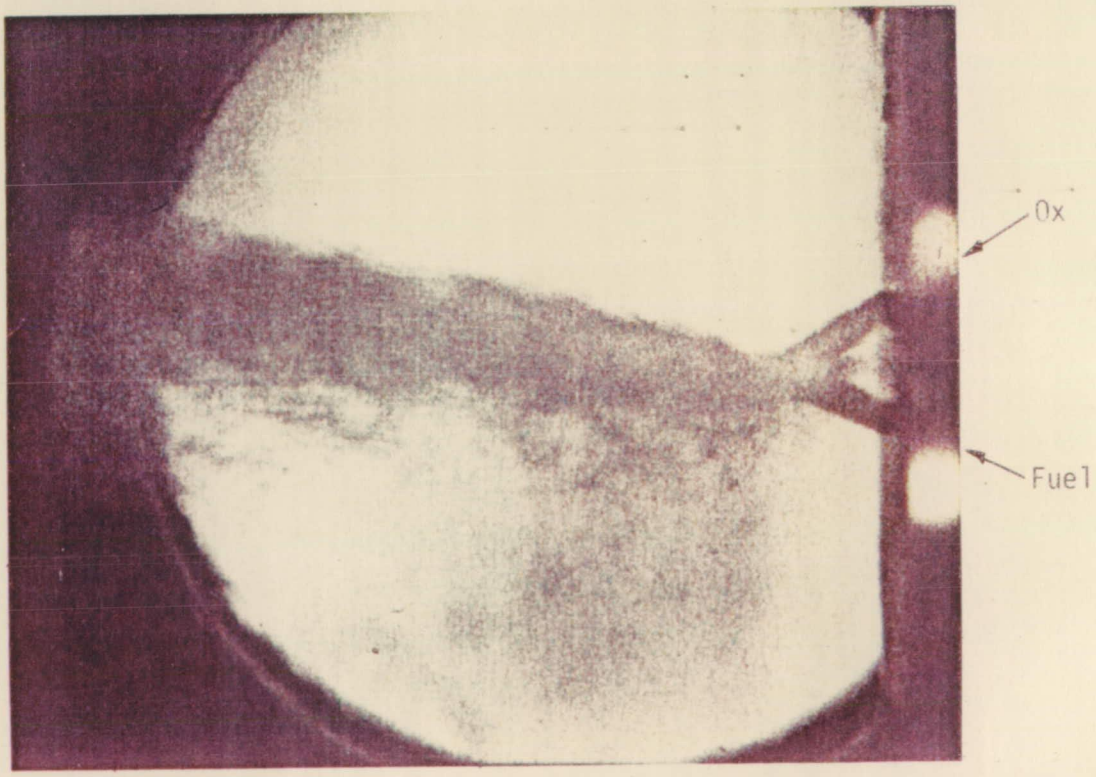

Test No. 153 Pc = 505 psia
Fuel Type: NH_3 O/F = 1.67
Injector Element: Unlike Doublet

Figure 41. Unlike Doublet, Ammonia Fuel Combustion (Sheet 4 of 5)

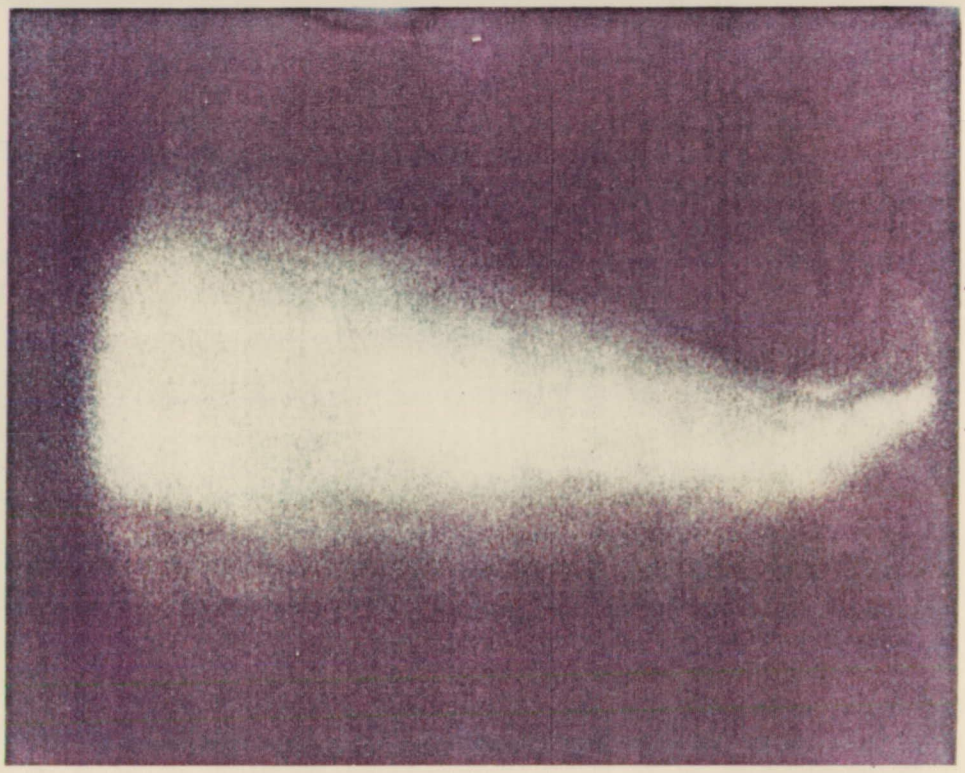

Test No. 154 Pc = 505 psia

Fuel Type: NH_3 O/F = 1.64

Injector Element: Unlike Doublet

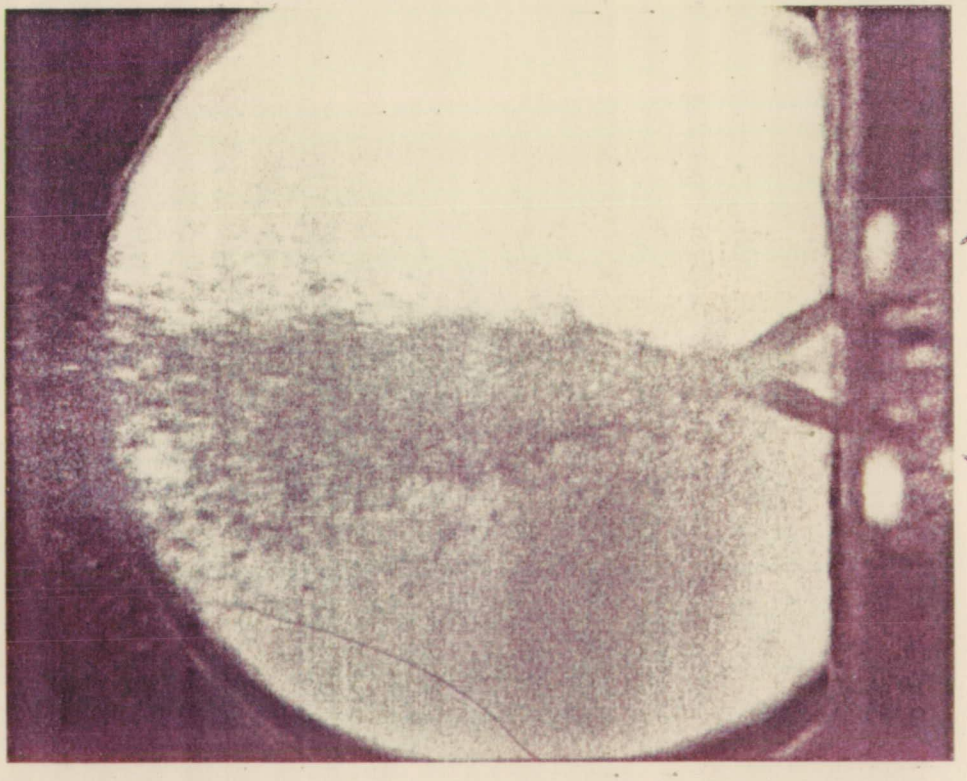

Test No. 155 Pc = 485 psia

Fuel Type: NH_3 O/F = 1.36

Injector Element: Unlike Doublet

Figure 41. Unlike Doublet, Ammonia Fuel Combustion (Sheet 5 of 5)

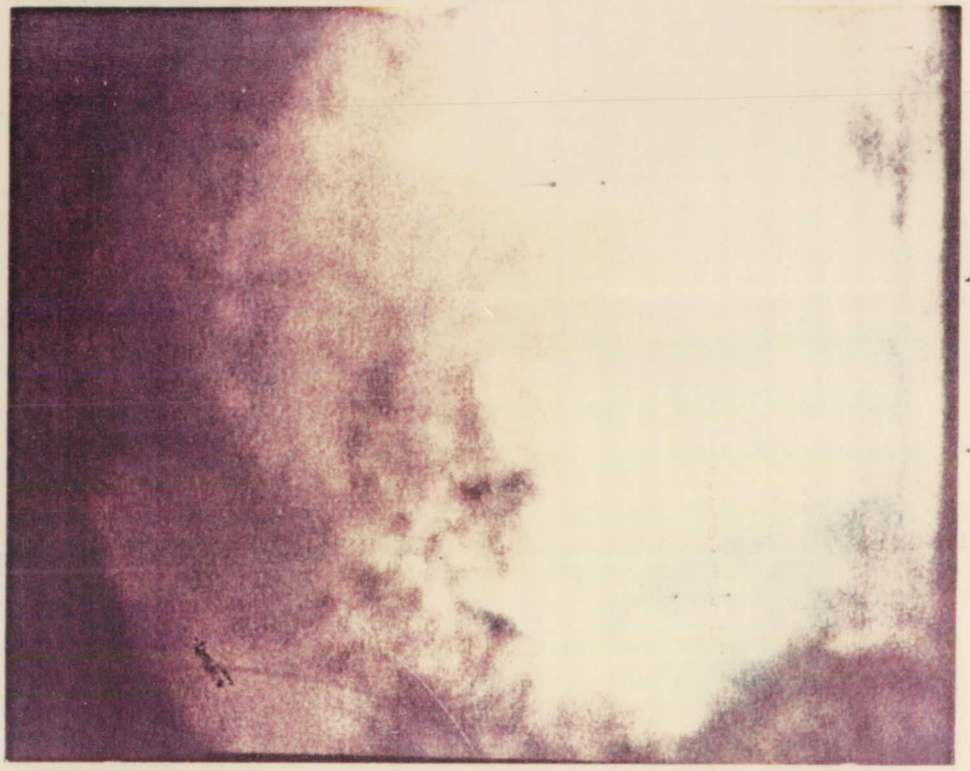

Test No. 158 Pc = 560 psia

Fuel Type: C_3H_8 O/F = 2.85

Injector Element: Like-on-Like EDM

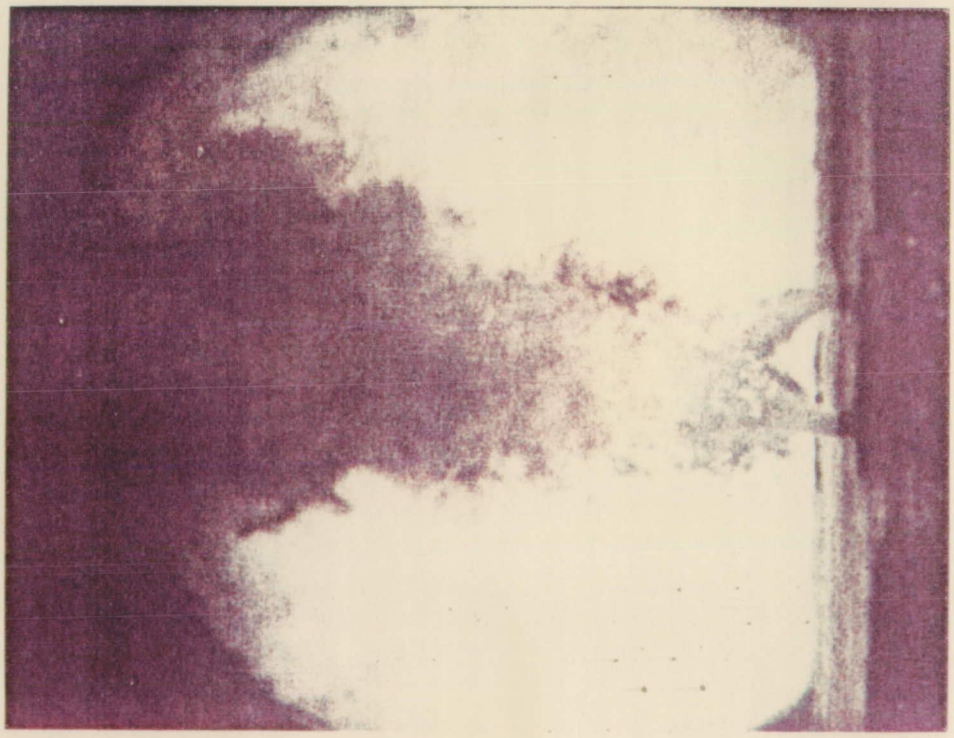

Test No. 161 Pc = 800 psia

Fuel Type: C_3H_8 O/F = 2.90

Injector Element: Like-on-Like EDM

Figure 42. LOL-EDM, Propane Fuel Combustion (Sheet 1 of 4)

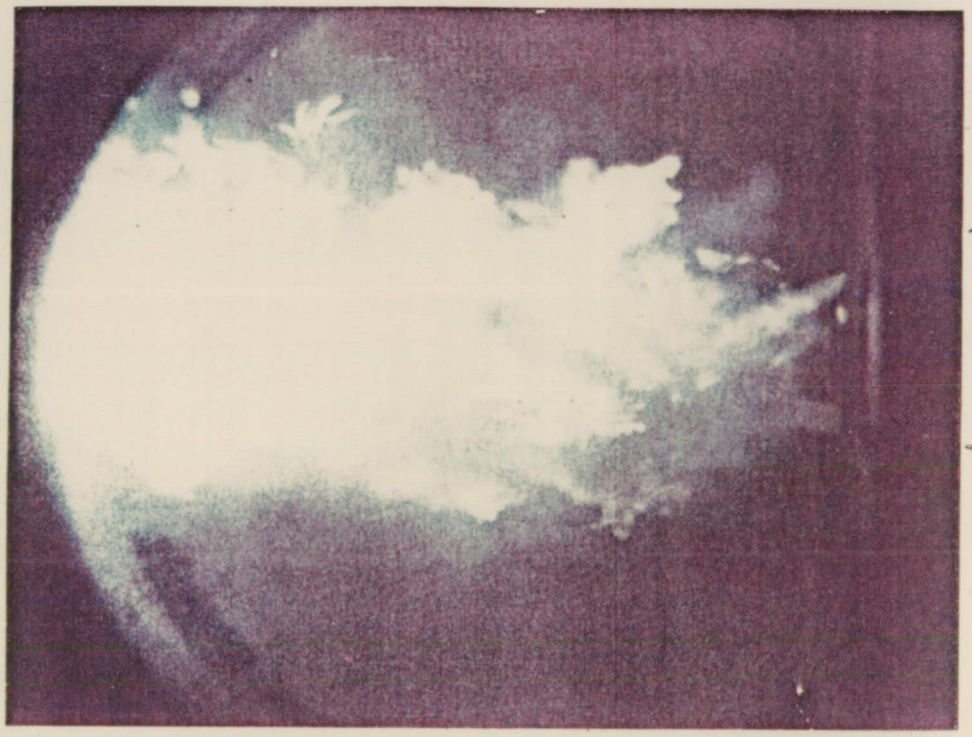

Test No. 169 Pc = 320 psia

Fuel Type: C_3H_8 O/F = 3.10

Injector Element: Like-on-Like EDM

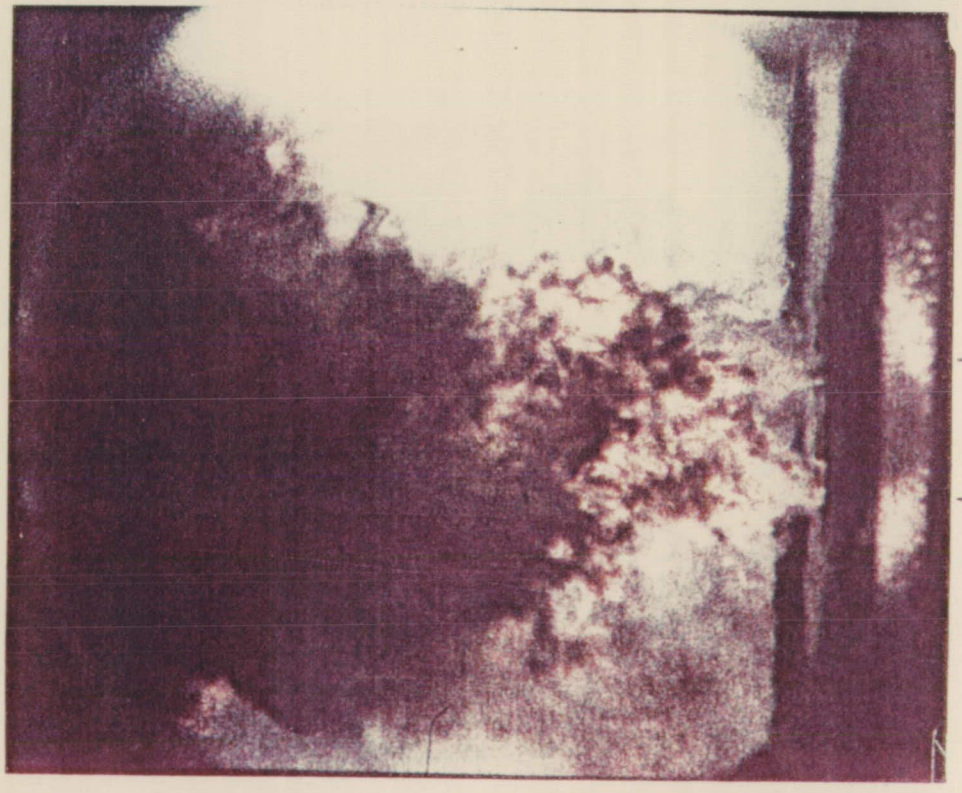

Test No. 171 Pc = 640 psia

Fuel Type: C_3H_8 O/F = 2.80

Injector Element: Like-on-Like EDM

Figure 42. LOL-EDM, Propane Fuel Combustion (Sheet 2 of 4)

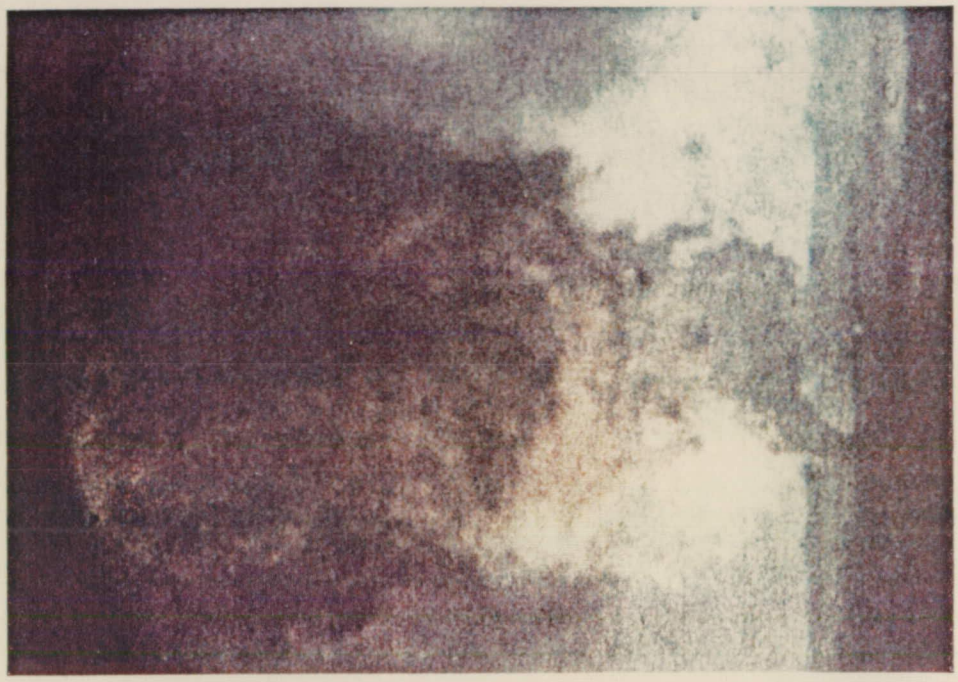

Test No. 172 Pc = 610 psia

Fuel Type: C_3H_8 O/F = 2.95

Injector Element: Like-on-Like EDM

Test No. 175 Pc = 545 psia

Fuel Type: C_3H_8 O/F = 4.10

Injector Element: Like-on-Like EDM

Figure 42. LOL-EDM, Propane Fuel Combustion (Sheet 3 of 4)

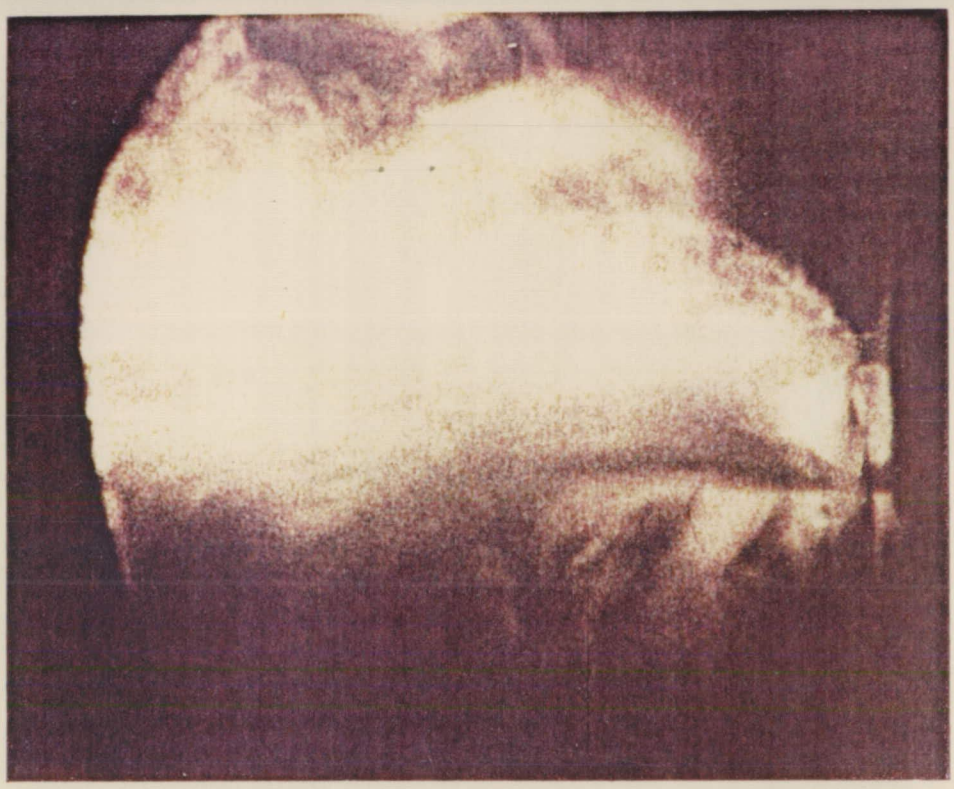

Test No. 176A Pc = 150 psia

Fuel Type: C_3H_8 O/F = 2.90

Injector Element: Like-on-Like EDM

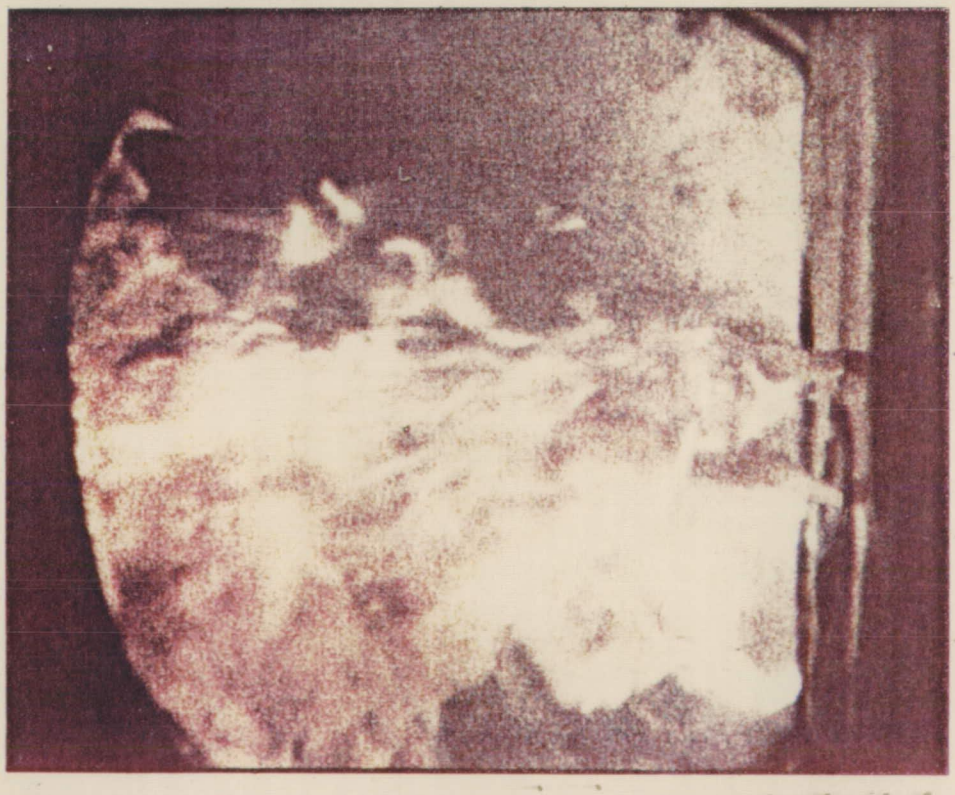

Test No. 176B Pc = 108 psia

Fuel Type: C_3H_8 O/F = 2.90

Injector Element: Like-on-Like EDM

Figure 42. LOL-EDM, Propane Fuel Combustion (Sheet 4 of 4)

above the propane vapor pressure at 75°F, with the combustion field obscured by dark clouds. During the test, the chamber pressure dropped below the vapor pressure at 75°F, at which point the dark clouds disappeared, showing the impingement of two partially vaporized propellant fans. This test result reinforces the theory that the black cloud and carbon formation mechanism is directly related to fuel vaporization. Vaporization in turn is primarily effected by pressure, temperature, mixture ratio, and injector type.

i. PAT with Propane

Twenty-one tests were conducted with the PAT (Tests 177-197). Figure 43 shows the movie results. The combustion field of the PAT, in contrast to the LOL-EDM, showed very little carbon formation until Pc dropped to around 150 psia. Posttest carbon deposits were almost nonexistent at any of the pressures. This apparent complete burning and lack of soot is believed to result from the long free-stream length and the pre-atomization of the propellants which enhances vaporization. Further testing of the PAT examined the effects of varying MR, Pc, fuel temperature, and fuel velocity. The test movies showed remarkable uniformity in view of the wide range of test conditions examined. The injector demonstrated no proclivity towards depositing carbon at any time and showed dark recirculation clouds only at low pressures and low velocities. Low mixture ratios did not seem to affect the carbon formation (down to MR = 2.2). Heating the propane to 120°F caused it to vaporize upon injection and, as evidenced by a slight decrease in C* (RSS), may have affected the liquid phase mixing slightly. Another indication of RSS with this injector is the fact that the fuel impingement angle varied between 30° on Test 189 and almost 0° on Test 195 (parallel fuel streams) as pressure increased from 150 psia to 800 psia. This phenomenon is not observed during cold-flow while increasing ΔP.

j. LOL-EDM with Propane, Gas Generator Conditions

Gas generator tests with C_3H_8 (Tests 198 and 199) were fired at a mixture ratio of 0.72 and chamber pressures of 810 psia and 510 psia, respectively. Both tests exhibited excessive sooting, completely coating the chamber with a fine black powder and precluding any photography immediately after ignition. Further testing in this configuration was deemed counterproductive.

k. Slit Triplet with Gaseous Methane

The Slit Triplet was fired twenty-two times (Tests 200-221), with chamber pressures ranging between 125-810 psia and mixture ratios varying from 2.75 to 4.7. The outstanding characteristic of this testing,

Test No. 179 Pc = 300 psia

Fuel Type: C_3H_8 O/F = 2.85

Injector Element: Pre-Atomized Triplet

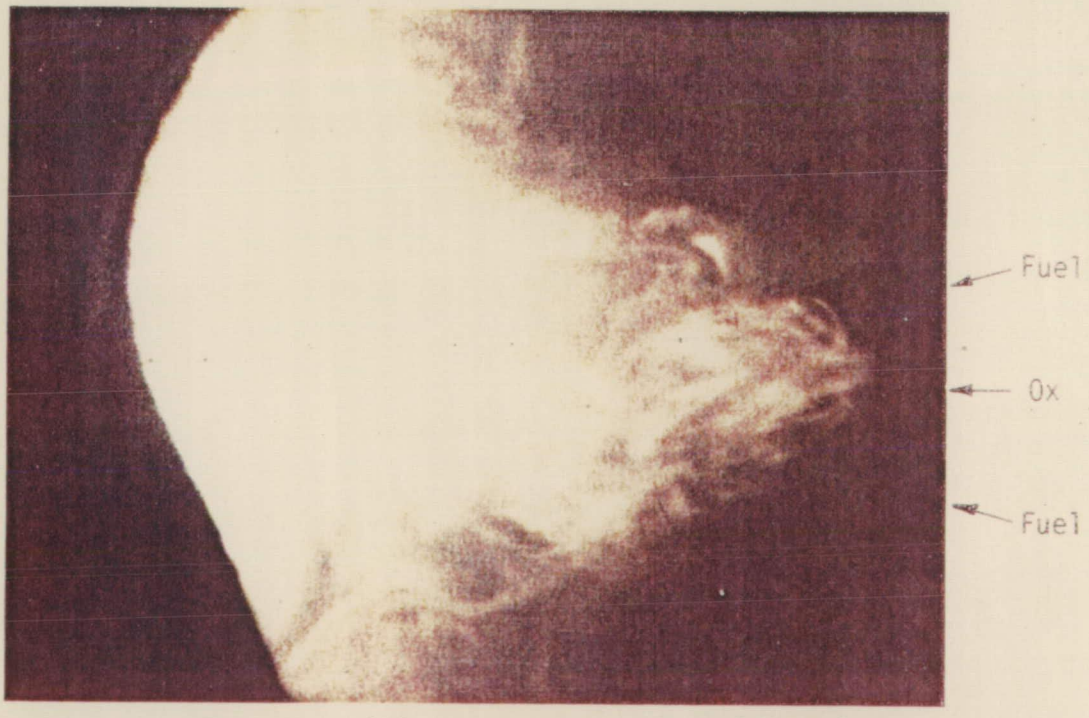

Test No. 182 Pc = 150 psia

Fuel Type: C3H8 O/F = 2.90

Injector Element: Pre-Atomized Triplet

Figure 43. PAT, Propane Fuel Combustion (Sheet 1 of 6)

Test No. 184 Pc = 300 psia

Fuel Type: C_3H_8 O/F = 2.85

Injector Element: Pre-Atomized Triplet

Test No. 187 Pc = 800 psia

Fuel Type: C_3H_8 O/F = 2.90

Injector Element: Pre-Atomized Triplet

Figure 43. PAT, Propane Fuel Combustion (Sheet 2 of 6)

C-2

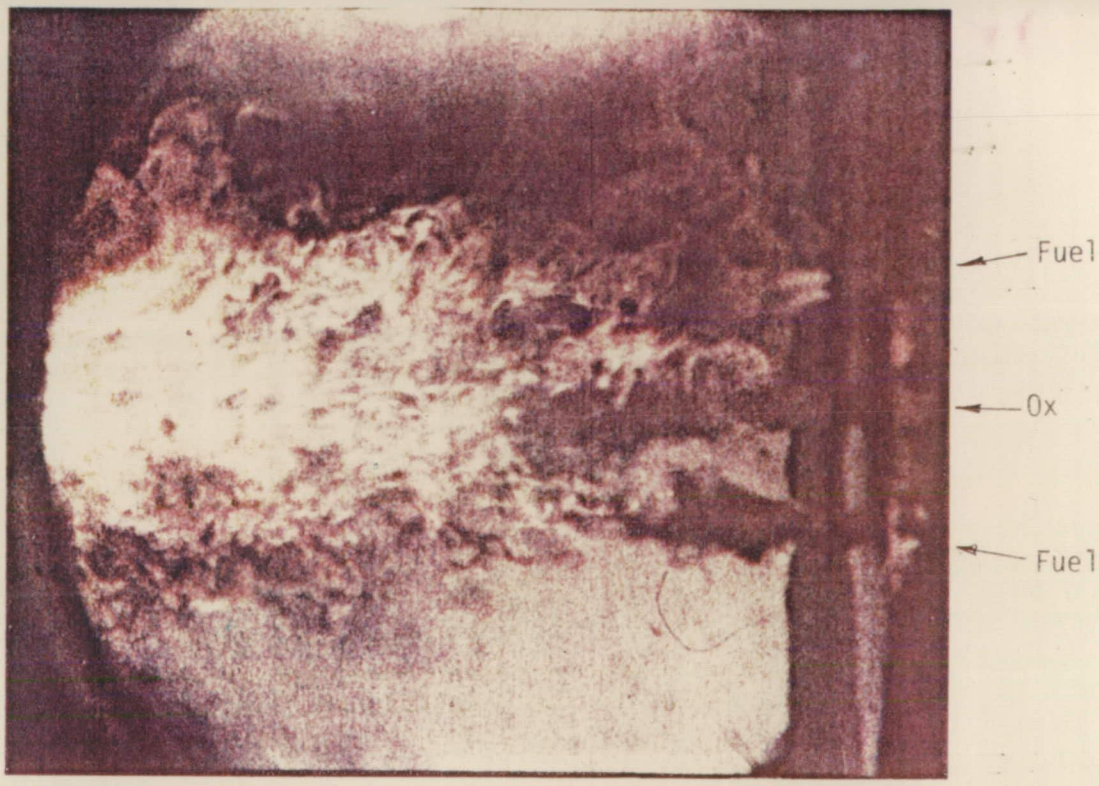

Test No. 188 Pc = 540 psia

Fuel Type: C_3H_8 O/F = 3.00

Injector Element: Pre-Atomized Triplet

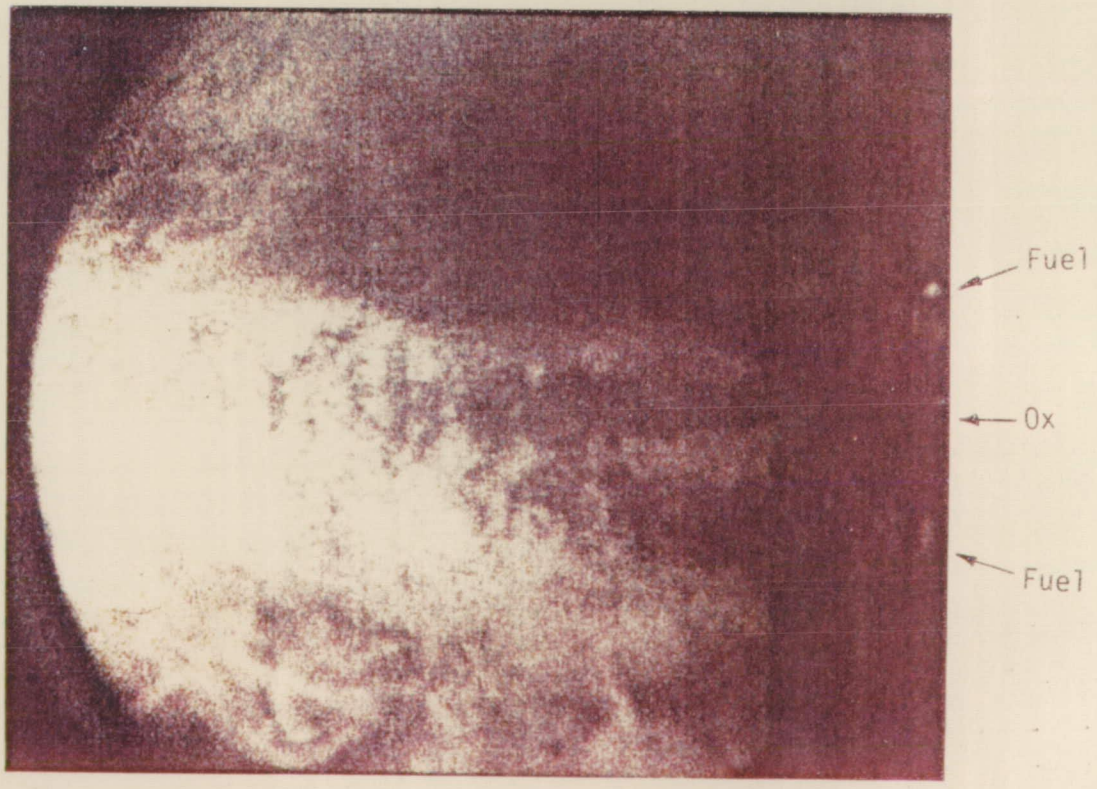

Test No. 189 Pc = 155 psia

Fuel Type: C_3H_8 O/F = 2.80

Injector Element: Pre-Atomized Triplet

Figure 43. PAT, Propane Fuel Combustion (Sheet 3 of 6)

Test No. 191 Pc = 700 psia

Fuel Type: C_3H_8 O/F = ——

Injector Element: Pre-Atomized Triplet

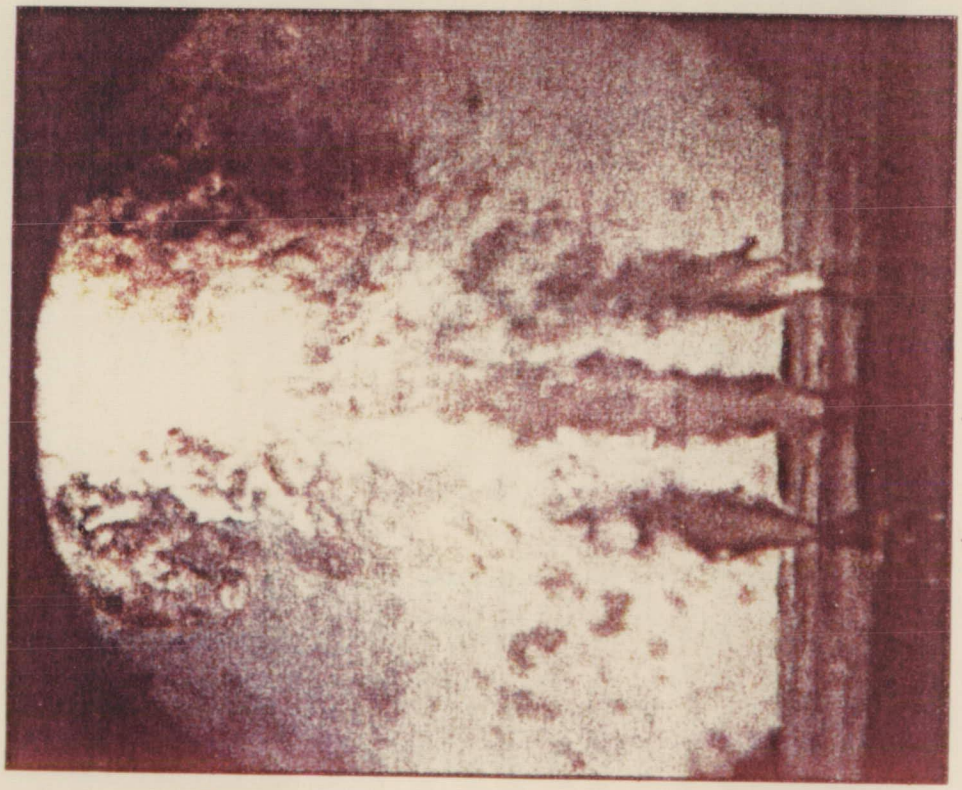

Test No. 193 Pc = 560 psia

Fuel Type: C_3H_8 O/F = 2.80

Injector Element: Pre-Atomized Triplet

Figure 43. PAT, Propane Fuel Combustion (Sheet 4 of 6)

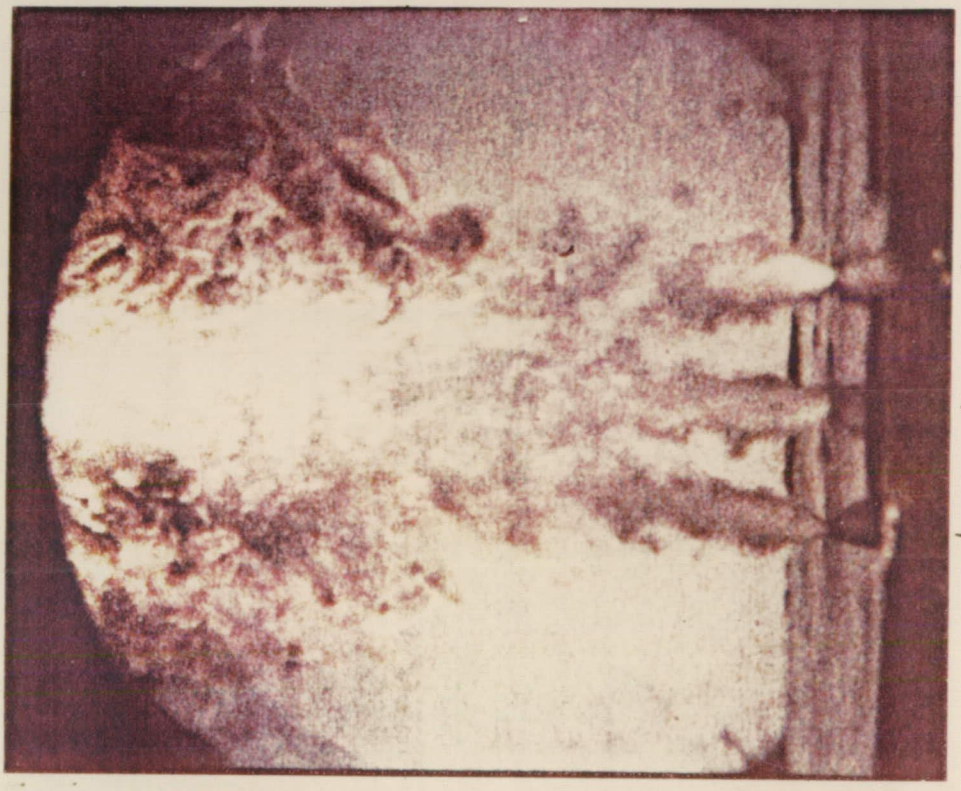

Test No. 194 Pc = 340 psia

Fuel Type: C_3H_8 O/F = 3.00

Injector Element: Pre-Atomized Triplet

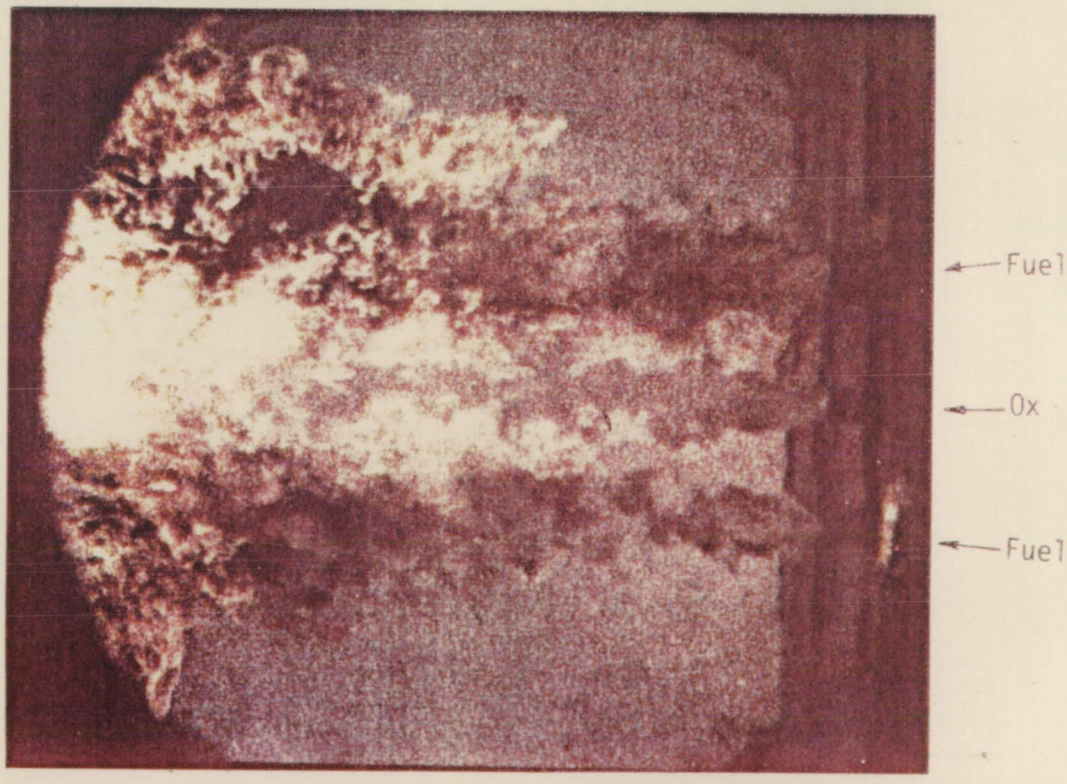

Test No. 195 Pc = 670 psia

Fuel Type: C_3H_8 O/F = 2.85

Injector Element: Pre-Atomized Triplet

Figure 43. PAT, Propane Fuel Combustion (Sheet 5 of 6)

Test No. 196 Pc = 630 psia

Fuel Type: C_3H_8 O/F = 3.20

Injector Element: Pre-Atomized Triplet

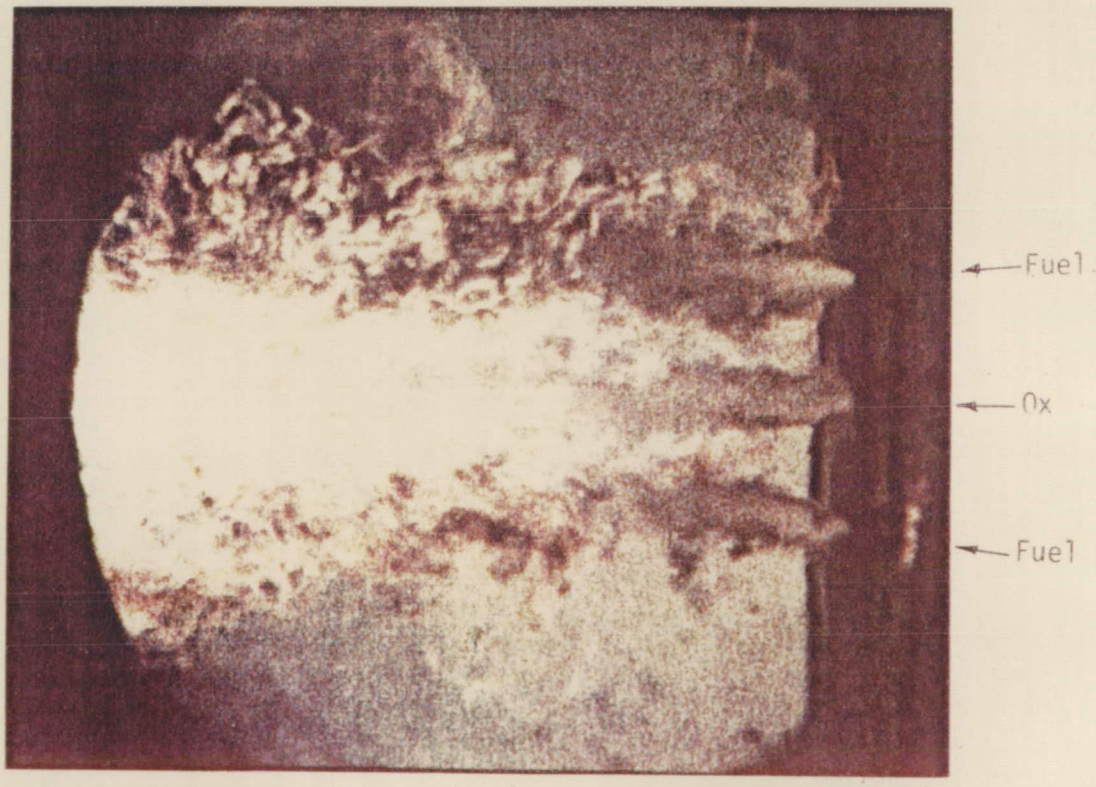

Test No. 197 Pc = 505 psia

Fuel Type: C_3H_8 O/F = 3.00

Injector Element: Pre-Atomized Triplet

Figure 43. PAT, Propane Fuel Combustion (Sheet 6 of 6)

shown in Figure 44, was the complete lack of dark recirculation gases or posttest carbon deposits in the chamber. The C* efficiency was greatly influenced by chamber pressure in all of the gaseous methane tests. This can probably be explained best in terms of the poor mixing qualities of this injector that had been observed in cold-flow testing (see Section V.C.1). RSS is evident at the higher pressures, with combustion occurring at the impingement interface between the gaseous methane and the liquid oxygen. Combustion is evidenced by the blue emission at the interface, as shown on Tests 216 and 217.

1. LOL-EDM with Liquid Methane, Gas Generator Conditions

Six gas generator tests (Tests 222-227) were fired with ℓCH_4. A chamber pressure range of 500 to 800 psia was tested, and mixture ratios were varied between 0.82 and 0.44. Surprisingly, no soot or carbon deposits of any sort were found in the chamber posttest, as can be seen in Figure 45. This is a significant finding when contrasted with the propane gas generator firings (LOL-EDM Tests 198 and 199; RUD Tests 142 to 144) which had generated such excessive quantities of soot that the chamber and injector face became coated with a fine black powder.

D. DEVELOPMENT OF CORRELATIONS AND TREND CURVES

Carbon formation and RSS were found to be the most prominent observable combustion phenomena with LO_2/HC propellants. The objective of the data analysis effort was to develop an understanding of these processes. The data analysis involved literature review, study of high-speed color movies of single element firings, and analytical modeling. The correlations and trends developed for carbon formation and RSS are discussed below.

1. Carbon Formation

A good deal of information about the carbon formation mechanism was gained during this study. All of the testing pointed toward the theory that carbon formation is directly related to fuel vaporization. Vaporization, in turn, is primarily affected by chamber pressure, fuel temperature, mixture ratio, fuel type, and injector element. If the fuel vaporization and combustion are slowed for whatever reason (intimate contact with LOX, short free stream length, low chamber pressure and heat flux, coherent jet versus spray fan with large surface area, low fuel temperature, etc.), carbon formation will result. The low temperature carbon formation may be related to the coking or gumming observed with hydrocarbon fuels in heated tube testing (see Figure 46) or to some flame-quenching reaction. Further study is required to define the physico-chemical mechanisms. Each test was

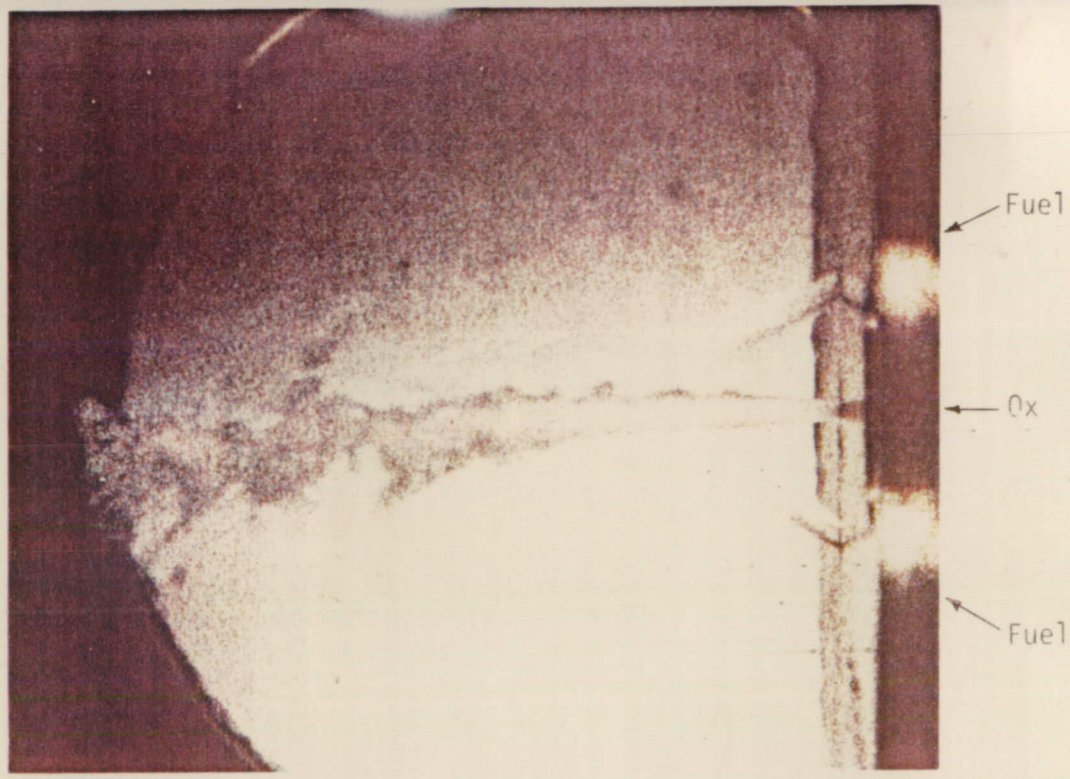

Test No. 202 Pc = 540 psia
Fuel Type: gCH_4 O/F = 4.20
Injector Element: Slit Triplet

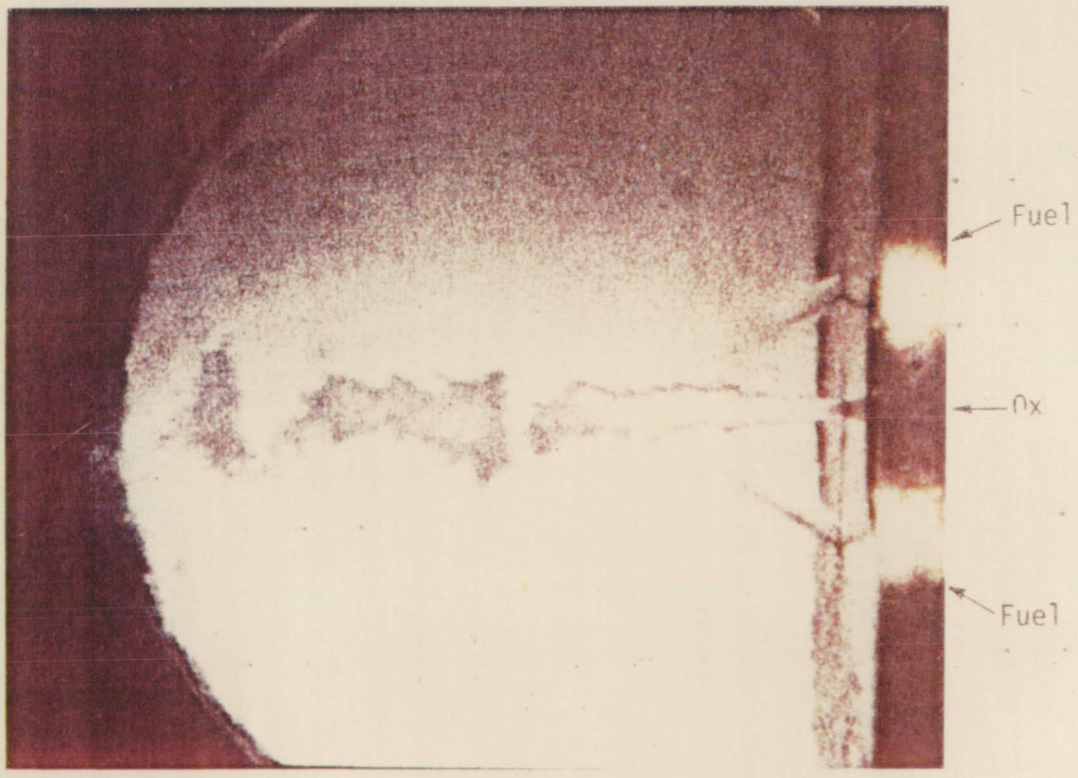

Test No. 203 Pc = 535 psia
Fuel Type: gCH_4 O/F = 3.50
Injector Element: Slit Triplet

Figure 44. Slit Triplet, Gaseous Methane Fuel Combustion (Sheet 1 of 8)

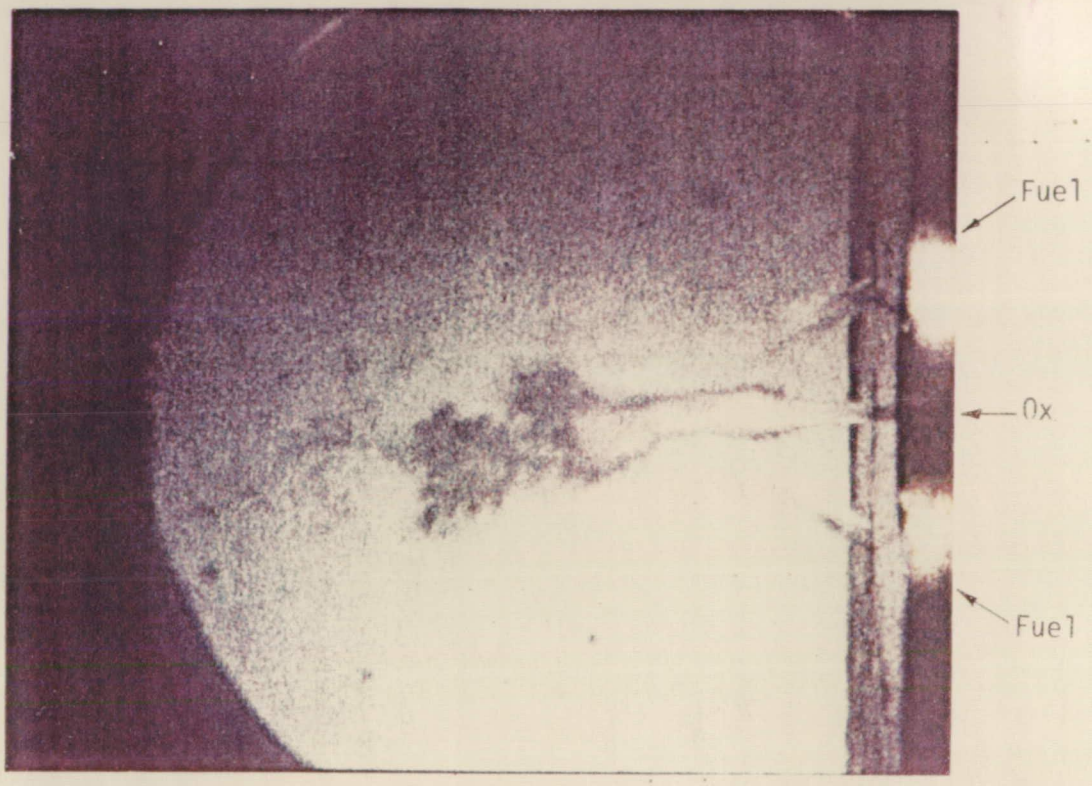

Test No. 204 Pc = 290 psia
Fuel Type: gCH_4 O/F = 3.70
Injector Element: Slit Triplet

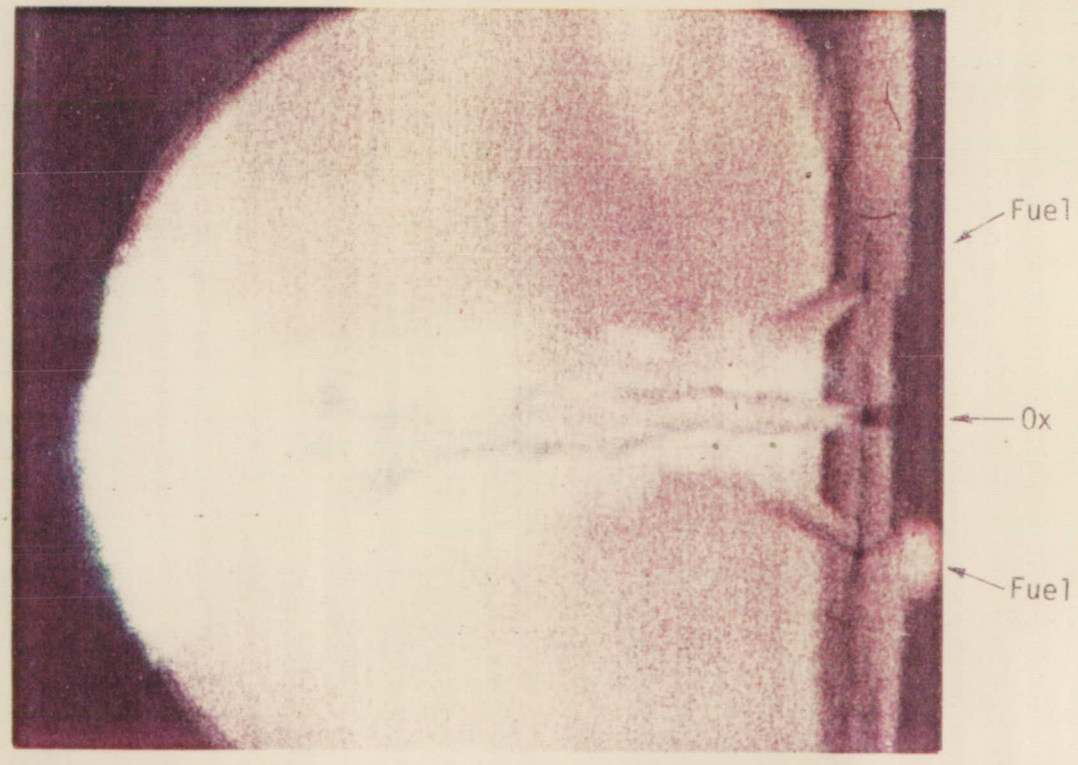

Test No. 206 Pc = 630 psia
Fuel Type: gCH_4 O/F = 3.60
Injector Element: Slit Triplet

Figure 44. Slit Triplet, Gaseous Methane Fuel Combustion (Sheet 2 of 8)

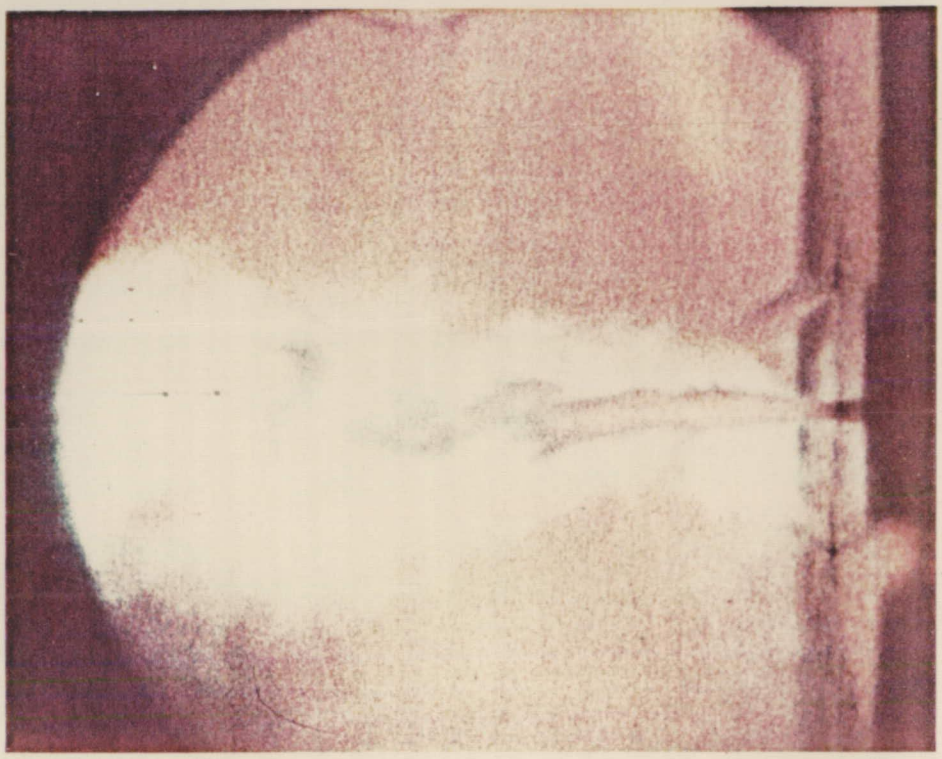

Test No. 207 Pc = 620 psia
Fuel Type: gCH_4 O/F = 3.00
Injector Element: Slit Triplet

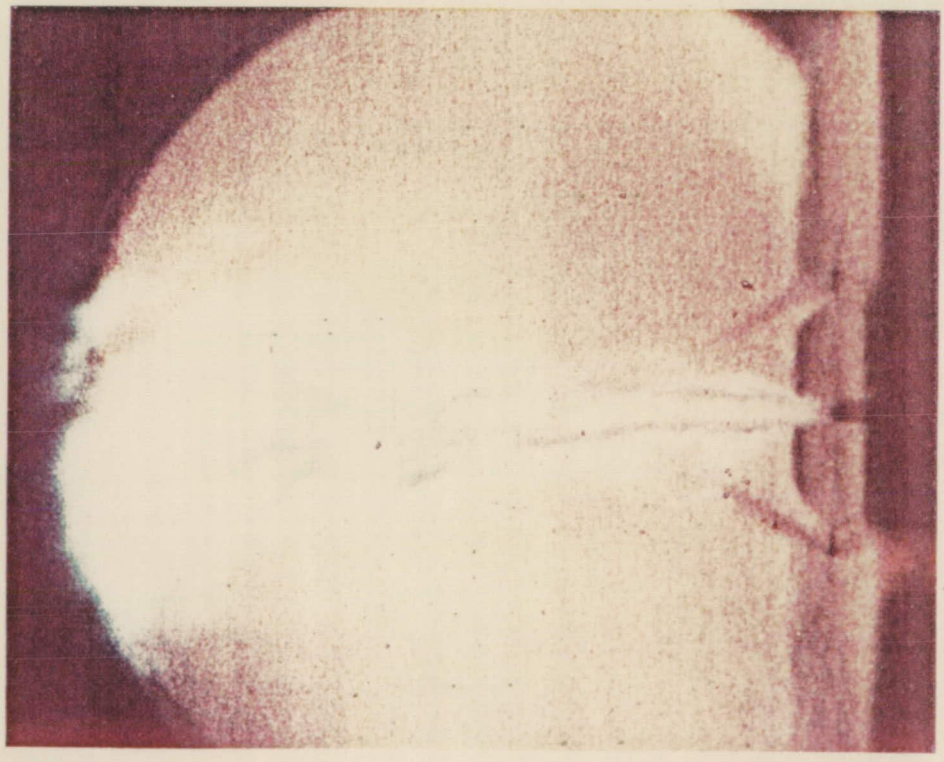

Test No. 209 Pc = 700 psia
Fuel Type: gCH_4 O/F = 3.00
Injector Element: Slit Triplet

Figure 44. Slit Triplet, Gaseous Methane Fuel Combustion (Sheet 3 of 8)

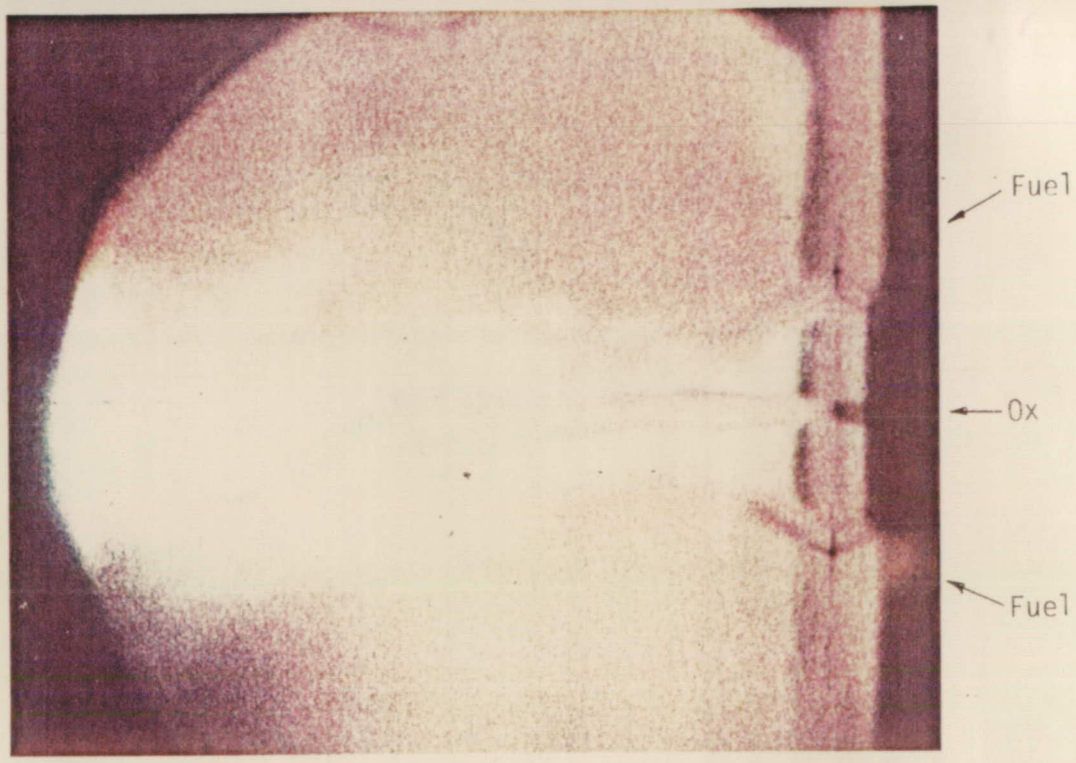

Test No. 212 Pc = 690 psia

Fuel Type: gCH_4 O/F = 3.35

Injector Element: Slit Triplet

Test No. 214 Pc = 310 psia

Fuel Type: gCH_4 O/F = 3.45

Injector Element: Slit Triplet

Figure 44. Slit Triplet, Gaseous Methane Fuel Combustion (Sheet 4 of 8)

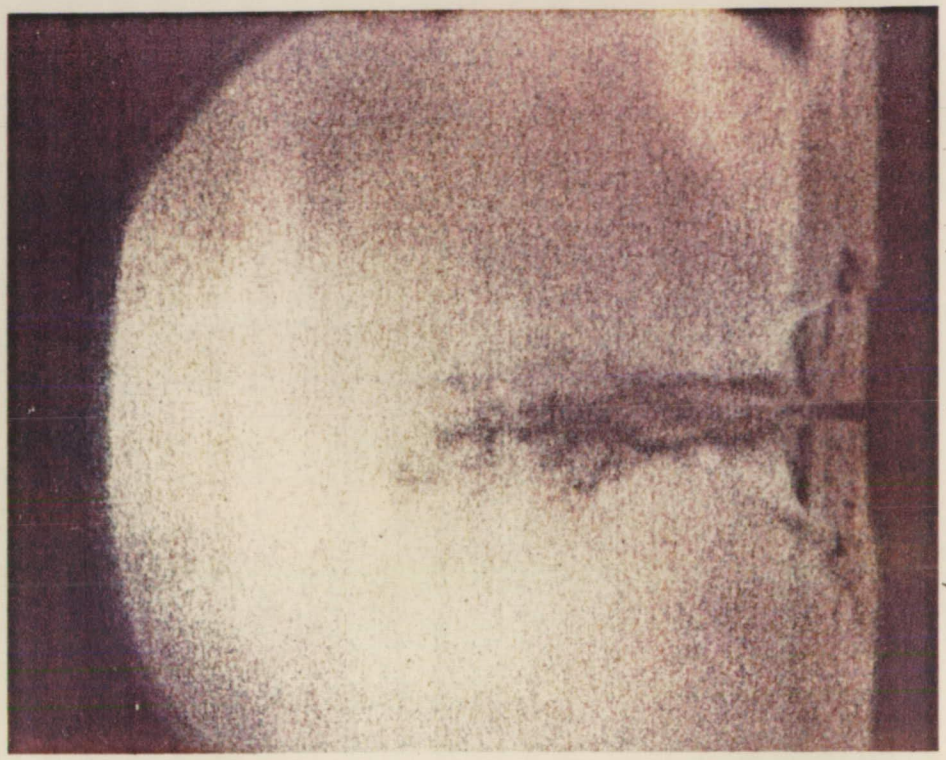

Test No. 215 Pc = 125 psia
Fuel Type: gCH_4 O/F = 4.50
Injector Element: Slit Triplet

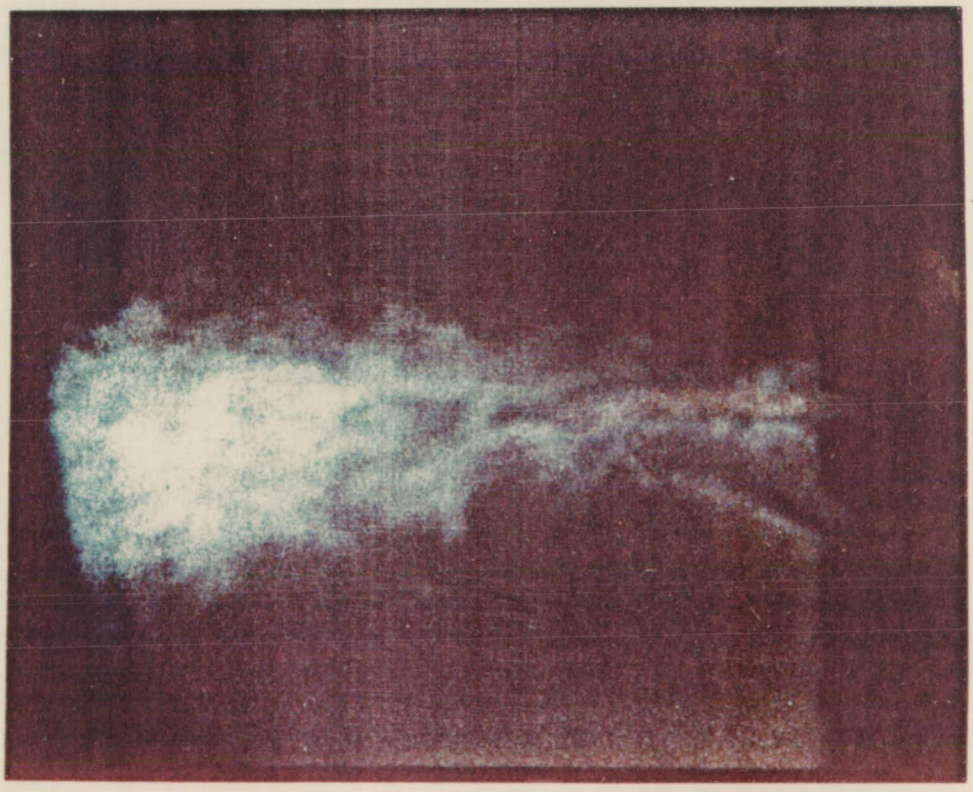

Test No. 216 Pc = 790 psia
Fuel Type: gCH_4 O/F = 2.75
Injector Element: Slit Triplet

Figure 44. Slit Triplet, Gaseous Methane Fuel Combustion (Sheet 5 of 8)

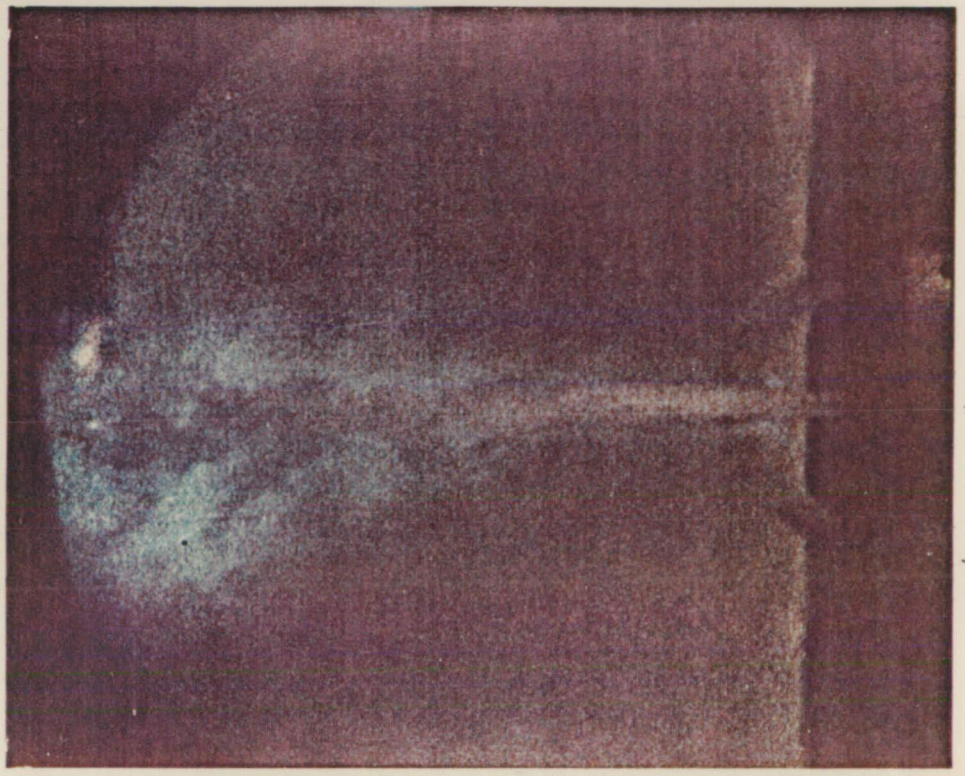

Test No. 217 Pc = 405 psia
Fuel Type: gCH_4 O/F = 4.70
Injector Element: Slit Triplet

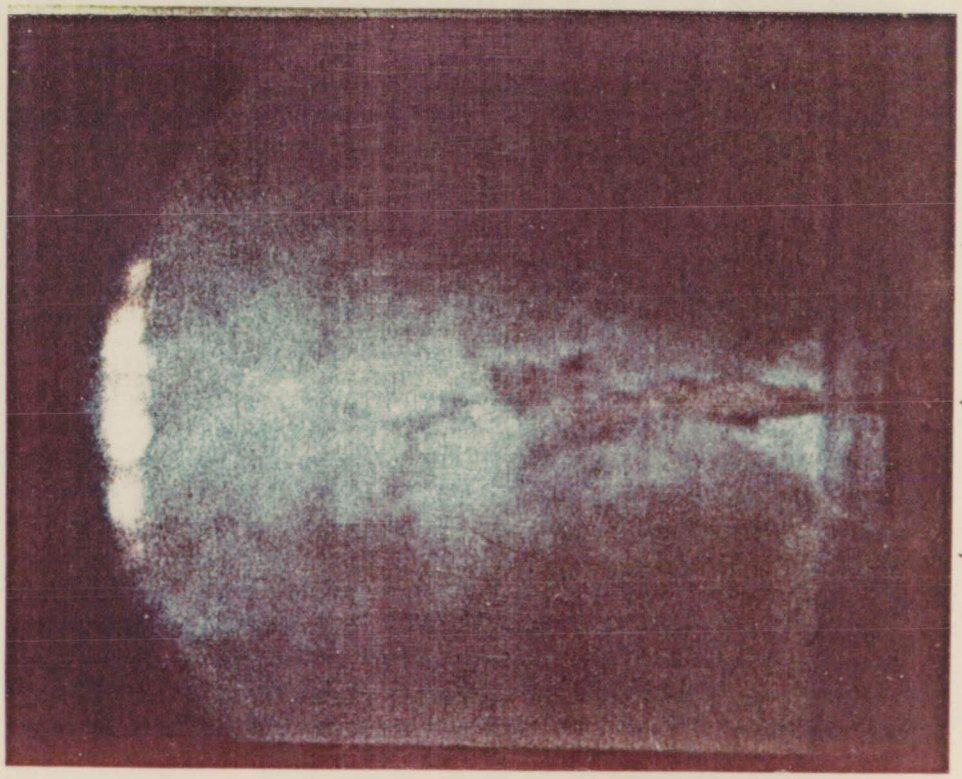

Test No. 218 Pc = 405 psia
Fuel Type: gCH_4 O/F = 2.75
Injector Element: Slit Triplet

Figure 44. Slit Triplet, Gaseous Methane Fuel Combustion (Sheet 6 of 8)

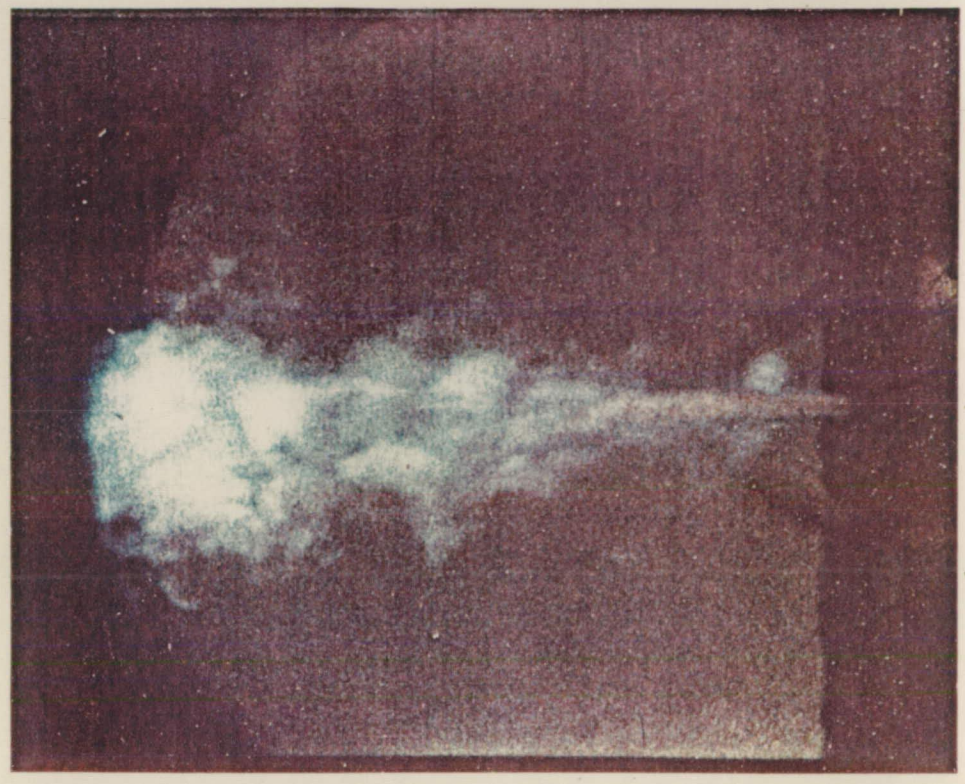

Test No. 219 Pc = 790 psia
Fuel Type: gCH_4 O/F = 3.20
Injector Element: Slit Triplet

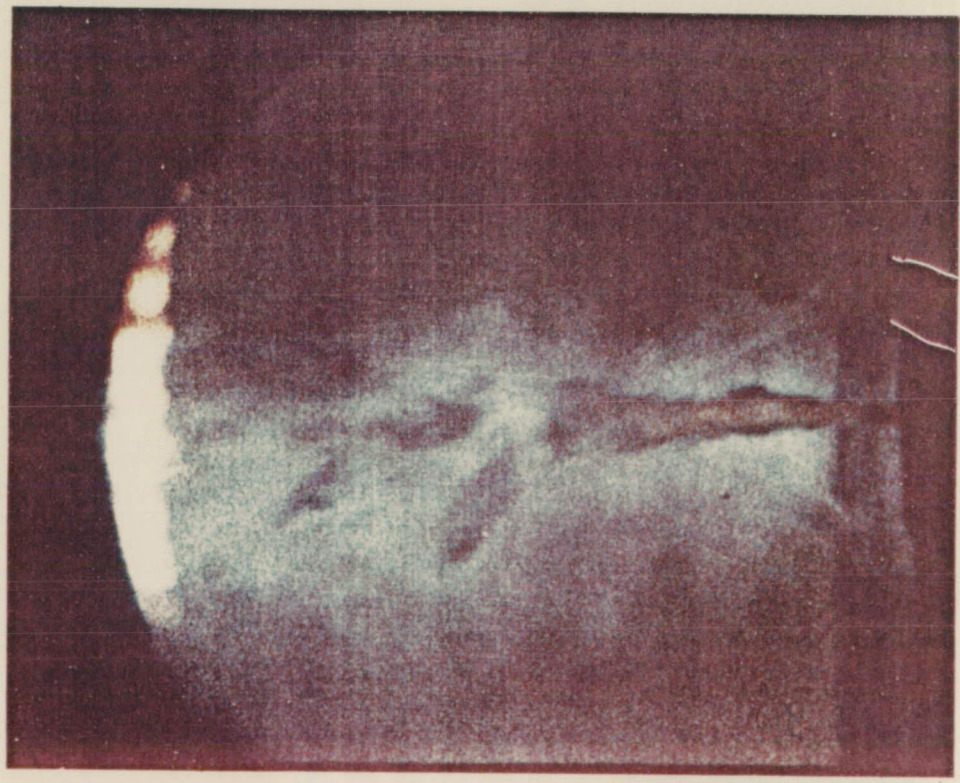

Test No. 220 Pc = 450 psia
Fuel Type: gCH_4 O/F = 3.00
Injector Element: Slit Triplet

Figure 44. Slit Triplet, Gaseous Methane Fuel Combustion (Sheet 7 of 8)

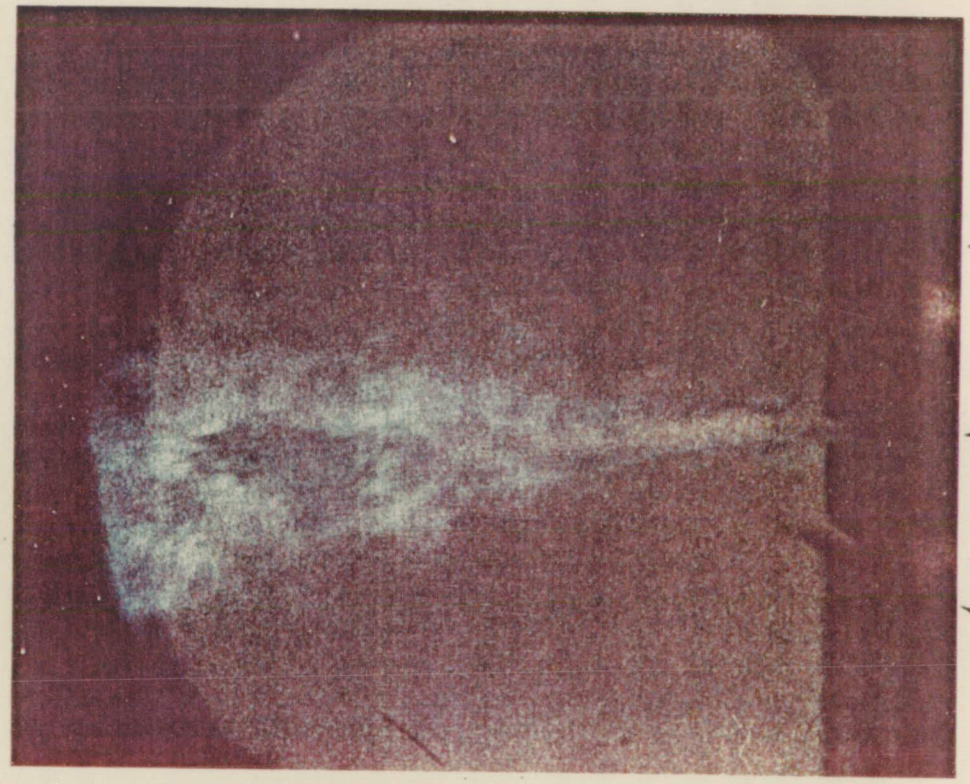

Test No. 221 Pc = 410 psia

Fuel Type: gCH_4 O/F = 4.00

Injector Element: Slit Triplet

Figure 44. Slit Triplet, Gaseous Methane Fuel Combustion (Sheet 8 of 8)

Test No. 223 Pc = 775 psia

Fuel Type: ℓCH_4 O/F = 0.61

Injector Element: Like-on-Like EDM Gas Generator

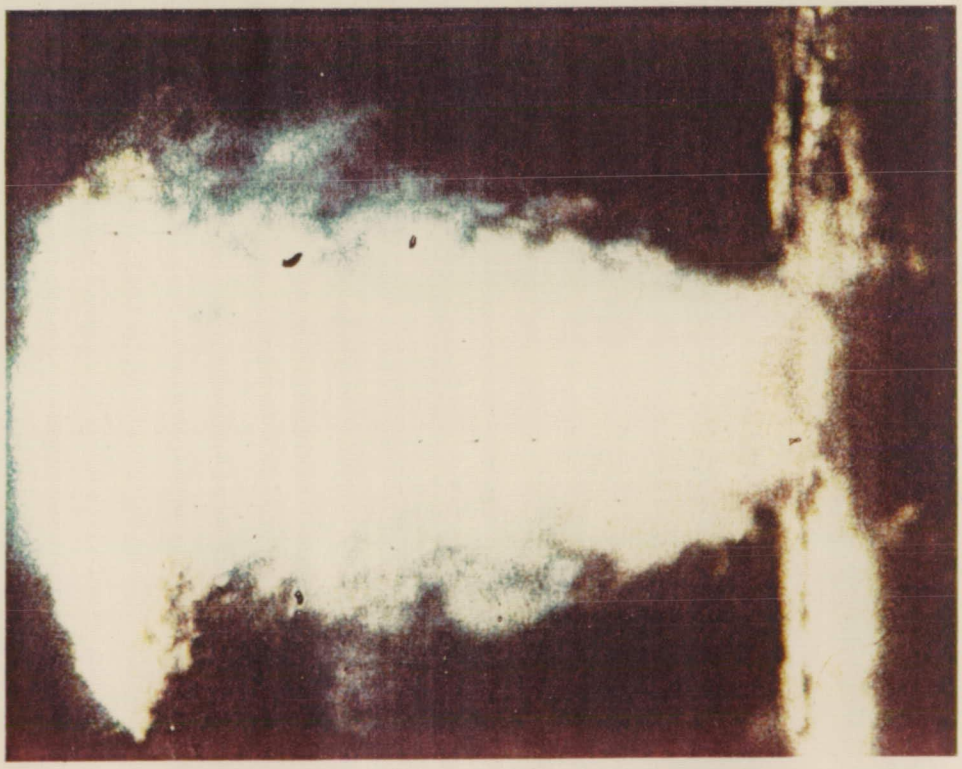

Test No. 225 Pc = 515 psia

Fuel Type: ℓCH_4 O/F = 0.78

Injector Element: Like-on-Like EDM Gas Generator

Figure 45. LOL-EDM Gas Generator, Liquid Methane Combustion (Sheet 1 of 2)

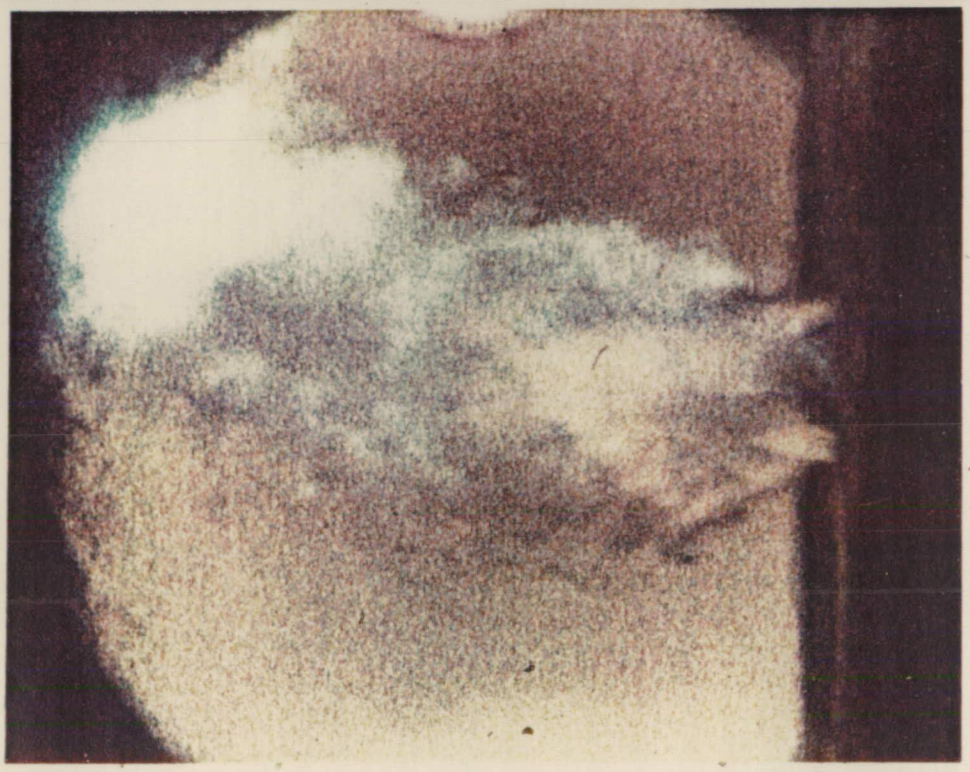

Test No. 226 Pc = 495 psia

Fuel Type: ℓCH_4 O/F = 0.60

Injector Element: Like-on-Like EDM Gas Generator

Test No. 227 Pc = 485 psia

Fuel Type: ℓCH_4 O/F = 0.44

Injector Element: Like-on-Like EDM Gas Generator

Figure 45. LOL-EDM Gas Generator, Liquid Methane Combustion (Sheet 2 of 2)

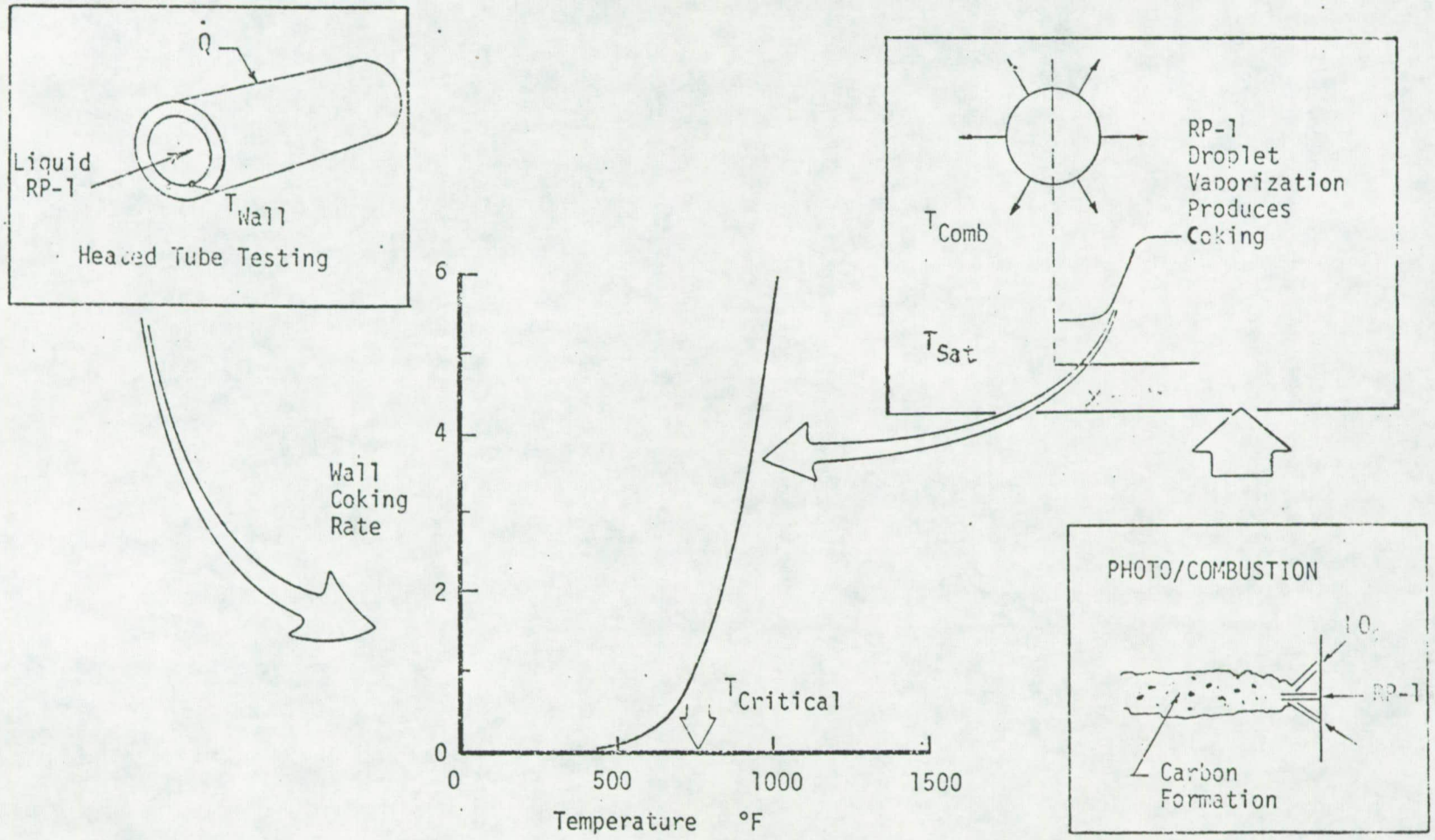

Figure 46. Carbon Formation Mechanism

rated according to the degree of carbon formation observed. Figure 47 illustrates how ratings of "Clear," "Partially Obscured," and "Obscured" appear with a simple unlike doublet injector element.

In an attempt to characterize the carbon formation mechanism, twelve combustion correlations were plotted from the data for each of the twelve injector/propellant combinations (see Table VII). Each of the data points was a symbol representing a certain degree of carbon formation, thereby making carbon formation trends easier to identify. A study of these correlations shows that a plot of "Pc -vs- T_f" gives the best correlation for the twelve injector/propellant combinations (Appendix III). Further study revealed that these twelve plots can be reduced to only three on the basis of carbon formation similarities between fuels and injector spray patterns.

Figure 48 correlates carbon formation for all of the injectors fired with LOX/RP-1. Chamber pressure is seen to be the dominant force in the change from excessive carbon formation to fairly clean combustion. Jet surface area and free stream length were not found to be important factors in the carbon formation at the conditions tested. Most RP-1 tests were fired with fuel temperatures near ambient, so the effect of fuel heating could not be observed.

Figure 49 correlates carbon formation for the short impingement height injectors (RUD and LOL-EDM) fired with LOX/C_3H_8. Both chamber pressure and temperature are seen to influence carbon formation, reinforcing the vaporization theory. The two tests fired at temperatures above the saturation temperature in Figure 45 were clear, even though they were at relatively low pressures. However, this occurred because the fuel was already in the vapor state and ready to burn.

Figure 50 correlates carbon formation for the long impingement height injectors (TLOL and PAT) fired with LOX/C_3H_8. Both chamber pressure and fuel temperature are seen to influence carbon formation. These injectors, however, show a definite tendency to remain more clear at low pressures than did the short impinging injectors. This is believed to be due to the increased vaporization of the pre-atomized long fuel free stream before impingement.

There were no carbon formation correlations for the UD injector since it was fired only with NH_3.

Carbon formation in the LOX/C_3H_8 fuel-rich gas generators was excessive, mainly because of the low mixture ratio (0.4 to 0.7) in addition to the above-mentioned reasons.

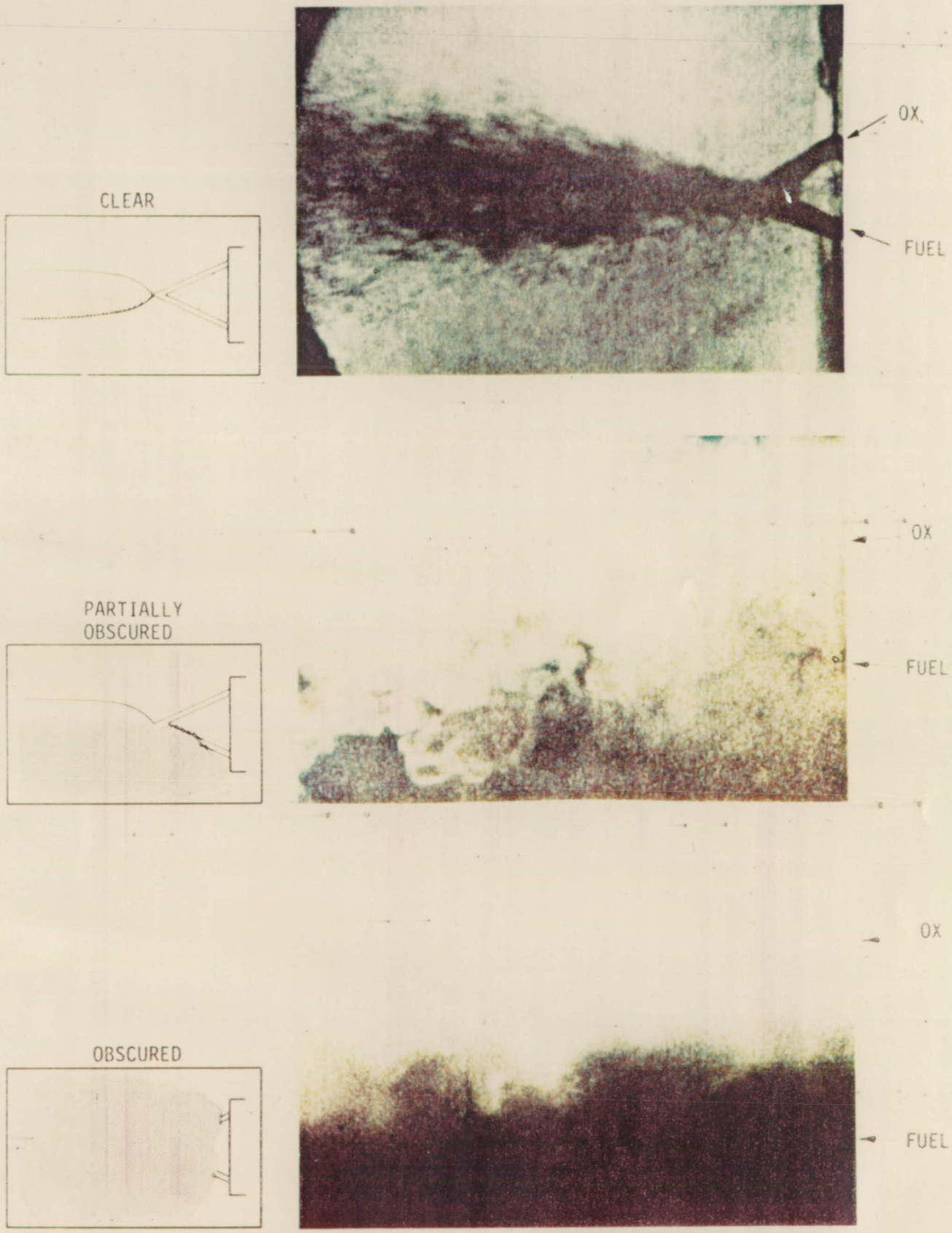

Figure 47. Modes of Carbon Formation

TABLE VII

COMBUSTION CORRELATIONS FROM LOX/HC PHOTOGRAPHIC CHARACTERIZATION PROGRAM

1. C*-vs-Pc
2. C*-vs-$\dot{V}_f$
3. C*-vs-W_T
4. C*-vs-T_f
5. C*-vs-MR
6. C*-vs-Fuel Rey. No.
7. Pc-vs-Fuel Rey. No.
8. Pc-vs-T_f
9. Pc-vs-$\dot{V}_f$
10. Pc-vs-W_f
11. Pc-vs-MR
12. Fuel Rey. No.-vs-MR

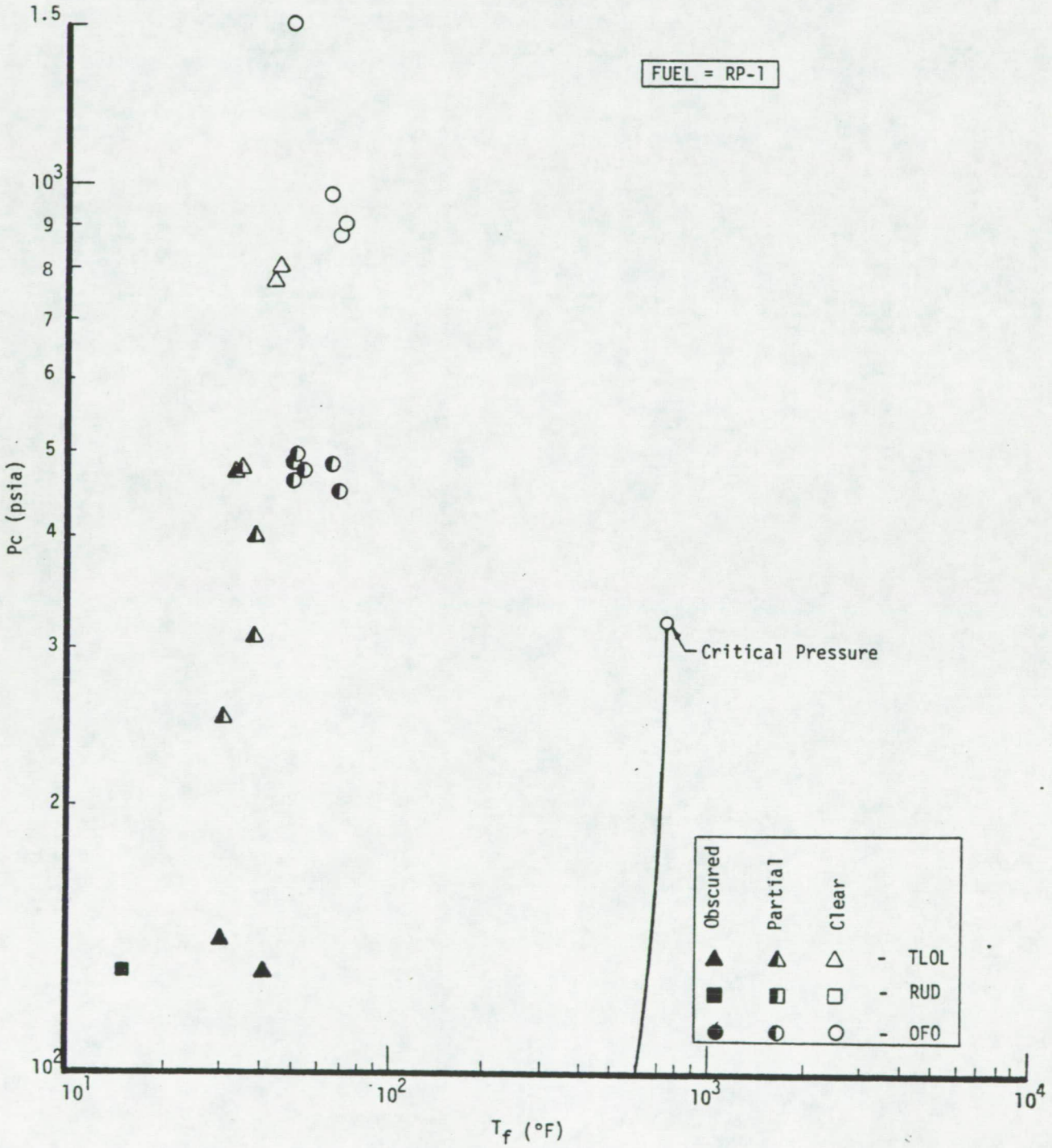

Figure 48. LOX/PR-1 Injectors Coking Correlations

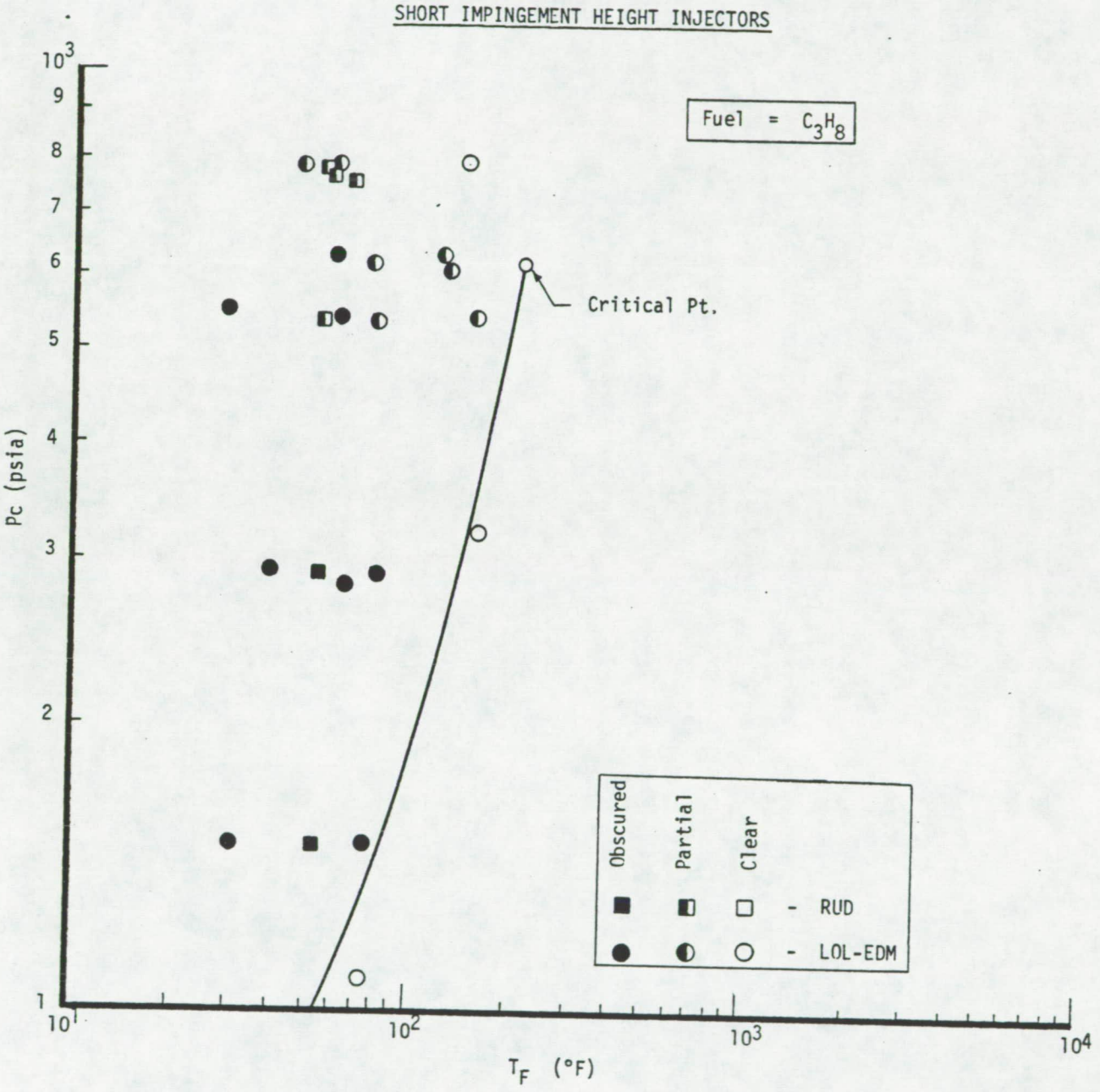

Figure 49. LOX/C_3H_8 Short Impingement Height Injectors Coking Correlations

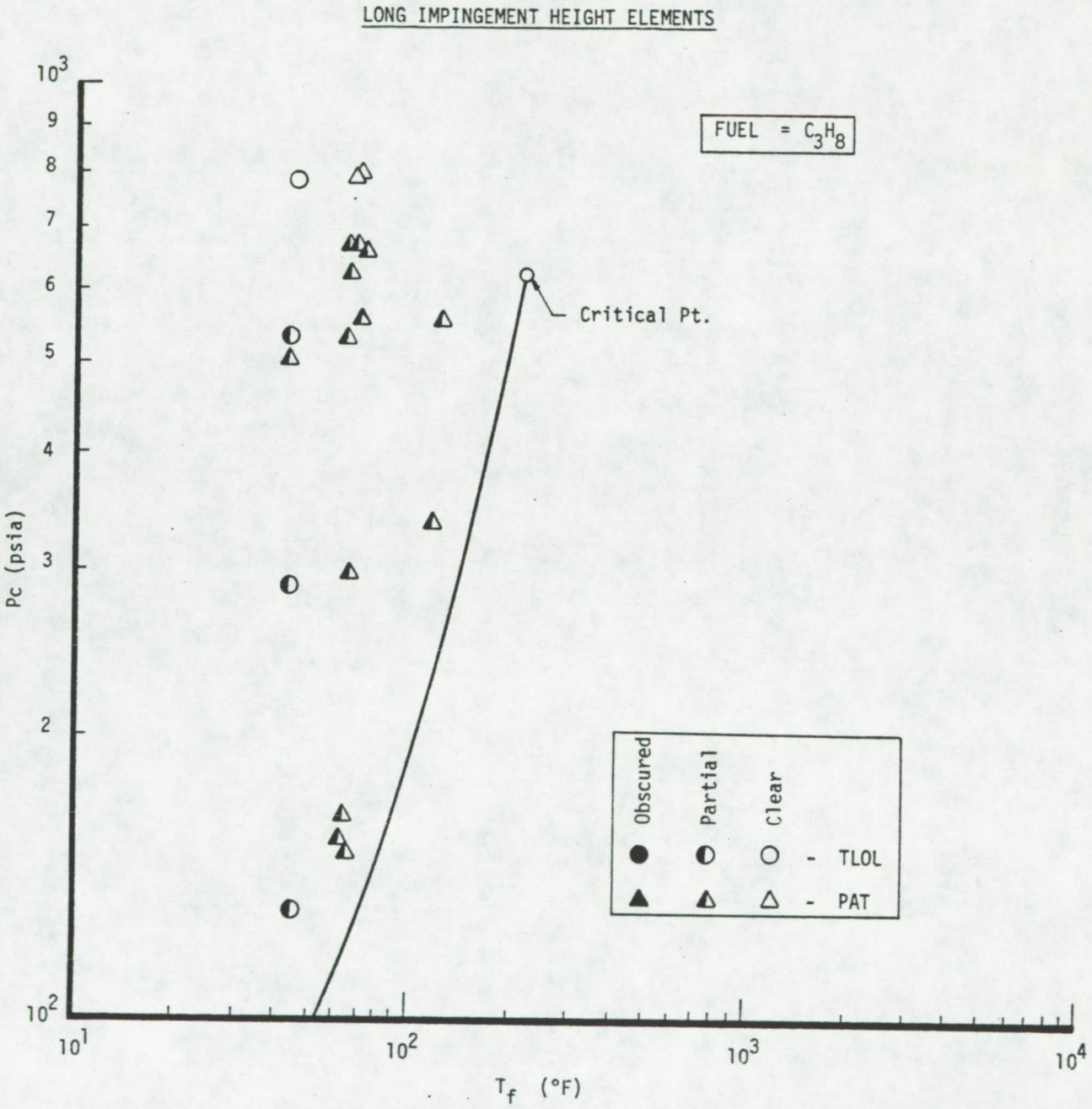

Figure 50. LOX/C_3H_8 Long Impingement Height Injectors Coking Correlations

V, D, Development of Correlations and Trend Curves (cont.)

No carbon formation was experienced with the use of either gaseous or liquid methane. Propane decomposition and reaction result in a higher C_2 species concentration than methane. The C_2 species are very active and, through a process of polymerization, build up into particulate matter. Full-scale multi-element methane gas generators may produce small amounts of carbon, but the quantity would be minuscule in comparison to the carbon production of a propane gas generator.

2. Reactive Stream Separation (RSS)

Previous analysis and testing with storable propellants have shown RSS to be controlled by a vaporization-controlled combustion mechanism (Ref. 1). Data correlations for the storable propellants showed that regimes of RSS could be correlated with chamber pressure and fuel Reynolds number, with chamber pressure exhibiting the strongest influence on RSS. Since vaporization is the controlling mechanism for the storable propellants, it is reasonable to assume that non-hypergolic impingement may also experience RSS. With these facts in mind, two hypotheses were postulated to explain RSS observed with LOX/HC propellants.

a. The first hypothesis is that LOX/HC RSS is also caused by vaporization-controlled combustion at the impingement interface. An attempt at correlating the hydrocarbon data with the storable fuel parameters (Pc -vs- Fuel Reynolds number) was unsuccessful. There was a definite Pc dependence, but the Reynolds number influence is less for the following reasons:

(1) Storable propellants are hypergolic and are not dependent on reaching an ignition temperature for combustion to occur.

(2) Hypergolic propellants are forced toward RSS by increasing velocity. Increased velocity causes increased interfacial surface area, which leads to a greater evaporation rate and more combustion. This is only a second-order effect with LOX/HC propellants, however, since the increased interfacial surface area means greater contact between the ambient temperature fuel and the cryogenic oxidizer. Cooling of the fuel slows vaporization and combustion, thus RSS is likely to occur.

V, D, Development of Correlations and Trend Curves (cont.)

(3) Evaporation of the surface of the fuel stream by hot gas recirculation heating plays a major role in causing RSS with hydrocarbon propellants. Not only is it necessary that some minimum amount of fuel be vaporized before impingement, but also that it be heated to its auto-ignition temperature for RSS to occur. The amount vaporized is a function of fuel free stream length, chamber pressure, fuel velocity, fuel temperature, and type of fuel (see Figure 51). In this respect, one can see the similarity between the influence of chamber pressure on RSS in storable and hydrocarbon propellants alike. Mathematically, this concept can be described as shown below:

$$\dot{W}_V = f\,(Pc, \tau_r, \tau_{ign}, T_f, \text{Fuel Type})$$

where

$\dot{W}_V$ = evaporation rate

Pc = chamber pressure

τ_r = Time between injection and impingement (residence time)

T_f = Fuel temperature

τ_{ign} = Ignition delay time.

High chamber pressure and long residence time obviously increase heat input to the fuel stream and promote evaporation and RSS. If the fuel is pre-heated, it serves to lessen the amount of time and pressure necessary to cause RSS. The type of fuel is an important factor because of heat of vaporization and auto-ignition temperatures (see below):

Fuel	Heat of Vaporization (cal/gr)	Auto-Ignition Temperature (°C)
Ammonia	328.3	651.1
RP-1	69.5	250
Propane	101.7	504.4
Methane	121.7	632.2

Both the heat of vaporization and the spontaneous ignition temperature of ammonia are greater than the respective values for RP-1, Propane, and Methane. RSS was seen to occur with all of the hydrocarbon fuels but not with ammonia. The fact that ammonia seems far less

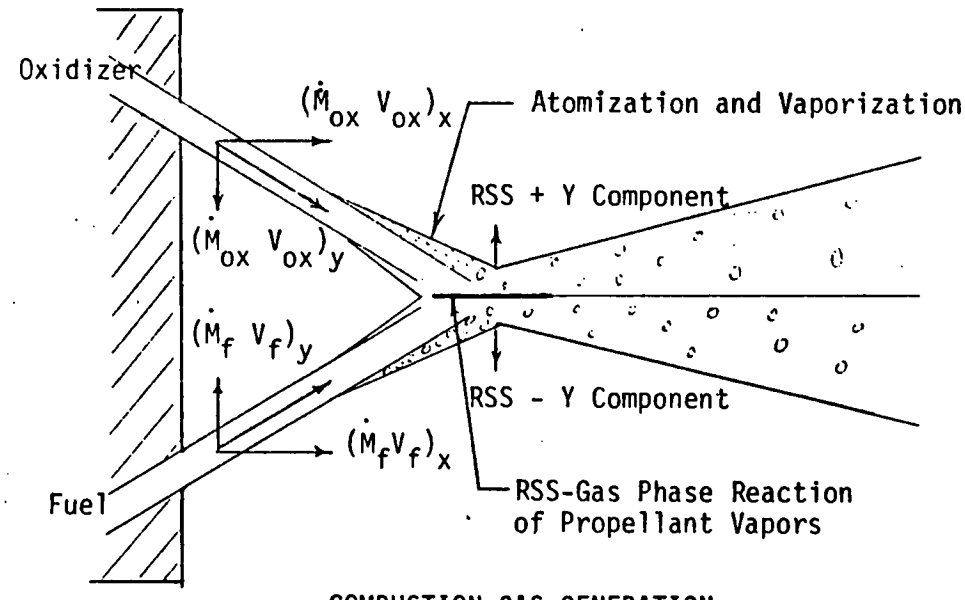

COMBUSTION GAS GENERATION

$\dot{W}_g = (P_c, \tau_{ign}, \tau_r, T_f, \text{Fuel Type})$

W_g = Combustion Gas Generation

P_c = Chamber Pressure

τ_{ign} = Ignition Delay Time

T_f = Fuel Temperature

τ_r = Residence Time

- Highly Dependent on Chamber Pressure and Hot Gas Recirculation Heating to Vaporize Fuel Stream Surface.
- Not as Dependent on Fuel Reynolds Number Because Increasing Velocity Increases the Surface Area, Chilling the Fuel and Retarding RSS.
- Dependent on Fuel Ignition Delay Time and Fuel Type

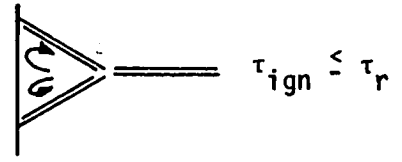

- Sufficiently Large Impingement Angles can Retard RSS when Flow Components $[(\dot{M}_f\ V_f)_y$ and $(\dot{M}_{ox}\ V_{ox})_y]$, are greater than RSS Components.

Figure 51. Vaporization-Controlled Hydrocarbon RSS

reactive from an RSS standpoint than the hydrocarbons fits in well with the theory of vaporization-controlled combustion causing separation.

There is also evidence that when fuel residence times (τ) are short (as in the case of the two Like-on-Like injectors), the impingement angle has an influence on whether or not the streams will separate. The LOL-EDM (32° included) always seemed mixed, while the TLOL (15° included) always fired in the separated mode at the same test conditions and with the same fuel. The hydrocarbon RSS combustion is apparently weak in comparison to its more reactive hypergolic counterpart, and it can be negated or overcome by propellant flow components which forcefully counteract the RSS vector (see Figure 47). This line of reasoning indicates that the PAT injector, which operated in the separated regime at high pressures, could take on better hotfire mixing characteristics if the included angle of impingement were increased and its free length were reduced.

b. The second RSS mechanism theory postulated states that the change in mixing characteristics with chamber pressure and fuel temperature is dependent on gas dynamic effects related to the Weber No. The Weber No. effect at higher chamber pressures may cause faster spray breakup and atomization, which changes the mixing patterns.

Most of the test movies show a trend away from RSS into a well-mixed regime occurring at chamber pressures between 100-300 psia for the fuels exhibiting RSS. The major exception to this rule was the LOL-EDM, which had a free-stream of only 0.1" before fan impingement and an included angle of 32° (cooling the propellant and retarding RSS). Very limited testing was performed between 100-300 psia because the heavy carbon formation precluded photography. At the lower pressures, the better mixing and lower heat flux maintained a cooler fuel temperature and encouraged carbon formation. Although RSS trends are observable, and although possible mechanisms for its occurrence may be postulated, more testing at lower pressure, different impingement angles, and varied fuel temperatures is necessary to formulate correlations and design curves.

3. Summary of Data Trends

The preceding discussions centered around characterizing and correlating carbon formation and RSS mechanisms. Data trends evident during testing are summarized in Figure 52.

a. Carbon Formation Trends

The hydrocarbon fuels tested showed increasing carbon formation in the following order: CH_4, C_3H_8, RP-1. As the C

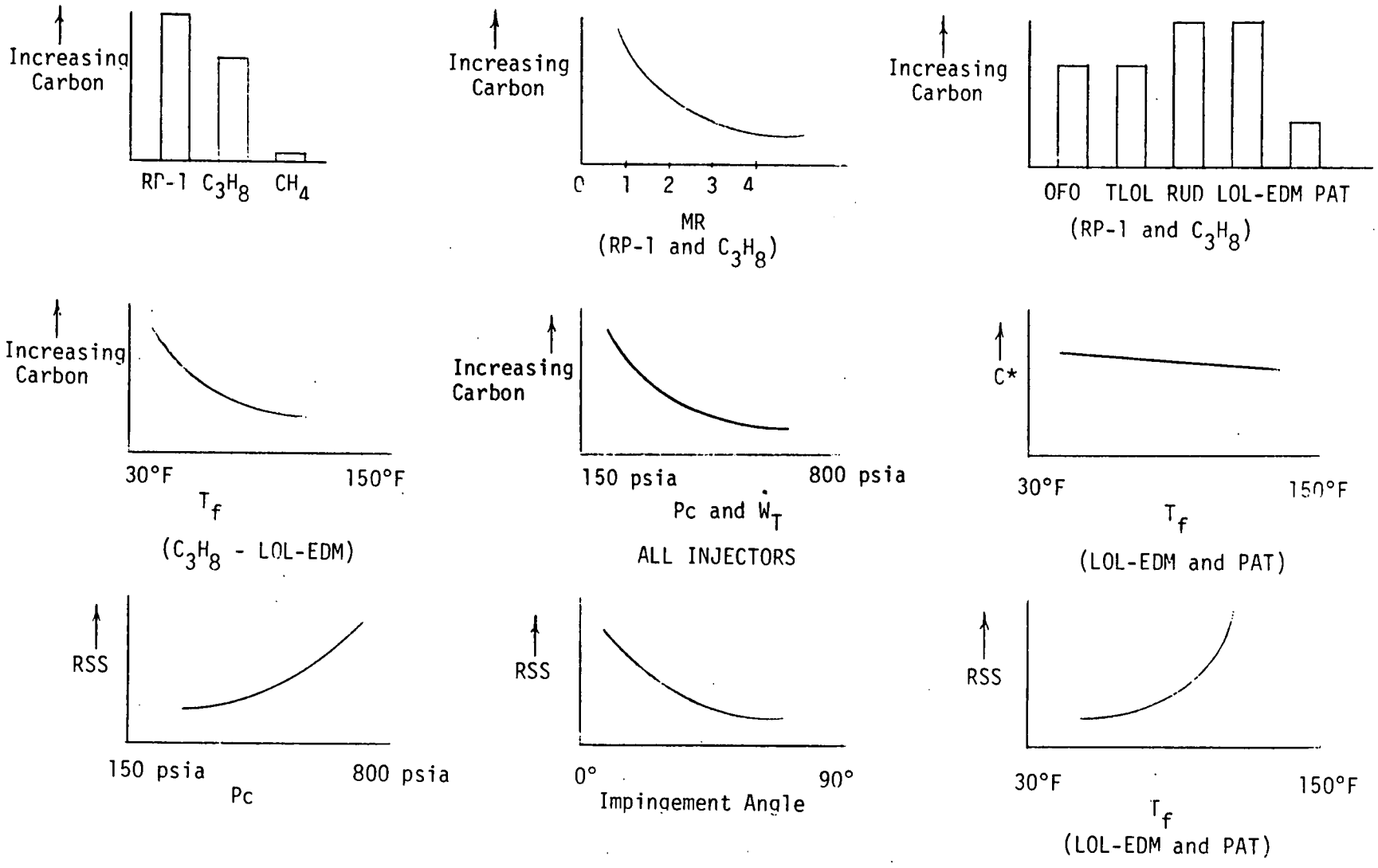

Figure 52. Data Trends

concentration of the HC molecule increases, decomposition results in increased C_2 species that initiate the polymerization process. In an associated manner, it follows that as the mixture ratio is decreased (increased carbon species concentration), the carbon formation rate increases.

The coherent jet impingement injector elements (RUD, LOL-EDM, OFO), showed increased carbon formation. It can be assumed that fuel droplet heating is delayed because of increased atomization time lag and increased mixing with the cryogenic oxidizer that results in fuel chilling. The delay in fuel droplet heating results in delayed fuel vaporization. The pre-atomized triplet element (PAT) caused the least amount of carbon formation. It is noteworthy that the PAT was the least mixed of all the injectors. This finding agrees with the theory that more rapid fuel atomization and vaporization minimizes carbon formation. The carbon formation trend curves for fuel temperature and chamber pressure (shown in Figure 48) also agree with this theory. As fuel temperature is decreased, the vaporization rate decreases and carbon formation increases. The vaporization rate also decreases with decreasing chamber pressure.

b. RSS Trends

Increasing incidence of RSS (i.e., decreased mixing) occurs as the fuel vaporization rate increases. This can be seen from the chamber pressure and fuel temperature trend curves in Figure 48. Fuel vaporization increases with increasing pressure and fuel temperature, resulting in more severe RSS. RSS increases as the unlike impingement angle decreases because of a decreased tangential momentum ratio (i.e., the fuel and oxidizer fans become more parallel).

E. COMBUSTION EVALUATION CRITERIA DEVELOPMENT AND RESULTS

A major objective of Task II was to develop combustion evaluation criteria based on analysis and testing, and to use it to evaluate, select and characterize test results with several combinations of LOX/HC propellants, injector elements, and operating conditions. Complete criteria development and Phase II selection results are given in Ref. 4. The results are summarized below in three subsections:

(1) Combustion Evaluation Criteria Development

(2) Phase II Fuels, Injector Elements, and Operating Conditions Selection

(3) Phase II Test Results Evaluation

V, E, Combustion Evaluation Criteria Development and Results (cont.)

This evaluation, together with the correlations shown previously in this report, provide data to aid in the rational selection of the most promising propellant/injector combinations for future technology and development efforts.

1. Combustion Evaluation Criteria Development

The basic sources of data for development of the criteria are recently conducted LOX/HC technology programs, the N_2O_4/Amine fuels "Blowapart" program (Ref. 1), and the results from the program Phase I testing. The criteria were separately developed for fuel and injector element selection and evaluation.

a. Fuel Evaluation

The primary factors considered for selection of propellants for long-life reusable engine application were subdivided into two major categories: (1) System and (2) Test. System considerations are those which describe the performance and operational characteristics of a fuel in a given system. Test considerations describe the effect of numerous combustion related phenomena which may affect engine operation.

Six criteria were selected for system evaluation. These criteria, along with the characteristics which would be considered desirable for each criterion, are as follows:

(1) Isp - High specific impulse is desired.

(2) Regenerative Chamber Cooling Capability - High thermal conductivity and high heat capacity are desired. Capability of withstanding high temperatures without thermal decomposition.

(3) Bulk Density - High bulk density is desired to maximize vehicle payload and minimize vehicle gross lift-off weight.

(4) Cost - Low cost propellants are required for economical, long life, reusable engine systems.

(5) Toxicity - Toxicity is an important operations and maintenance issue for reusable engine systems.

(6) Corrosiveness - Corrosiveness affects propellant storability.

V, E, Combustion Evaluation Criteria Development and Results (cont.)

Five criteria were selected for test evaluation. These criteria, along with the characteristics which would be considered desirable for each criterion, are as follows:

(1) Fuel Freezing - Fuel freezing should be avoided to preclude spray explosions and unsteady combustion similar to pops.

(2) Pops - It is desirable to operate with steady combustion and no pops.

(3) Carbon Formation - Control of gas-side carbon formation is desirable. It is undesirable at gas-generator conditions. It may be advantageous as a chamber wall insulator at main chamber conditions. Also, its impact on main chamber performance is not well understood.

(4) Reactive Stream Separation - It is desirable to predict the range of operating conditions and injector types which result in RSS so that injectors can be designed to operate entirely in either a separated mode or a mixing mode. Shifting between these two modes is undesirable.

(5) Supercritical Pressure Operation - It is desirable to be able to operate at supercritical pressures and subcritical injection temperatures without flash vaporization causing resurge instabilities.

b. Injector Element Evaluation

Nine criteria were selected for injector element evaluation. These criteria, along with the characteristics which would be considered desirable for each criterion, are as follows:

(1) Atomization - Small drop size is desired.

(2) Mixing - Uniform mixing is desired for high efficiency and complete combustion.

(3) Injector Face Compatibility - A low heat flux is necessary to preclude damage to the injector face.

(4) Chamber Wall Compatibility - The element must produce a uniform, well-mixed combustion zone to preclude local hot spots or chamber streaks.

(5) Chug Stability - Short combustion time lags are desirable to preclude chugging.

(6) Hi-Frequency Combustion Stability - Uniform atomization distribution is desired to facilitate damping device design.

(7) Injector Momentum Balance - A resultant axial momentum is desirable at all operating conditions. Elements insensitive to MR changes are desired.

(8) Fuel Freezing - Fuel freezing should be avoided to preclude spray explosions and popping.

(9) Meaningful Photographic Results - The injector must be capable of demonstrating combustion phenomena in a manner that can be photographed and analyzed.

2. Phase II Fuels, Injector Elements, and Operating Conditions Selection

a. Fuel Selection

Seven fuels were selected for the Phase II evaluation and recommendation: 1) Methane (CH_4); 2) Ethane (C_2H_6); 3) Propane (C_3H_8); 4) Butane (C_4H_{10}); 5) Heptane (C_7H_{16}); 6) RP-1; 7) Ammonia (NH_3). Numerical values were assigned to the various evaluation criteria for each fuel. These numerical values reflect the rating of a specific fuel with respect to those criteria. In this report, all criteria were given equal weight to make the valuation as general as possible. Weighting factors could be used when detailed system requirements are defined.

Results of the fuel evaluation are presented in Table VIII. The rankings are based on a scale of 1 to 10. A fuel ranked as a 10 with respect to a certain criterion would be the best fuel in that category, whereas a ranking of 1 would indicate total unsuitability. The data that form the basis for each ranking are shown below.

TABLE VIII

FUEL EVALUATION CRITERIA
AND SELECTION

Fuel	Isp	Regen Cooling Capability	Bulk Density	Cost	Toxicity	Corrosiveness	Fuel Freezing	Pops	Coking	RSS	Supercritical Pressure Operation	Numerical Average
Methane (CH_4)	10	7	2	5	10	10	10	10	9	8	10	8.3
Ethane (C_2H_6)	9	4	6	1	8	10	10	10	6	8	10	7.5
Propane (C_3H_8)	8	5	8	8	8	10	10	10	6	8	10	8.3
Butane (C_4H_{10})	7	3	5	8	8	10	10	10	5	8	10	7.6
Heptane (C_7H_{16})	7	3	7	1	8	10	10	10	4	8	10	7.1
RP-1	7	4	10	5	8	10	10	10	4	8	10	7.8
Ammonia (NH_3)	4	5	3	10	2	8	10	10	10	10	10	7.5
	SYSTEM							TEST				

V, E, Combustion Evaluation Criteria Development and Results (cont.)

(1) System Parameters

Specific Impulse - The theoretical ODE Isp's of the seven fuels considered were determined at the maximum Isp mixture ratios and are shown in Figure 53. CH_4 (the highest) has a 5.5 percent higher ODE Isp than NH_3 (the lowest).

Regenerative Cooling - The regenerative cooling of high pressure LOX/HC engines is characterized by the great disparity between coolant heat flux capabilities and the cold wall gas-side heat fluxes. Coolant heat flux limits arise from the coolant-side wall temperature limits proposed by fuel decomposition (coking) and poor coolant physical properties. Ammonia, of course, would experience no problem with coking since past experience has shown that hydrocarbon coking or ammonia decomposition takes place at the following approximate temperatures:

RP-1	1060°R
Refined RP-1	1260°R
Propane	1320°R
Methane	1760°R
Ammonia	1510°R

The properties of the seven hydrocarbon fuels are summarized in Table IX. Consideration of each in terms of weight flow and specific heat indicates the LOX to be the poorest coolant and the ammonia to be the best. It is appropriate to note that this cooling study pertains only to nickel chambers, as copper chambers and ammonia are not compatible.

Bulk Density - Using the optimum mixture ratio and referenced Isp values the relative tankage volumes were calculated (see Figure 53). It can be seen that although CH_4 has a 2.7 percent higher Isp than RP-1, it requires 21% greater tank volume. It is noteworthy that propane only requires 3% greater tank volume than RP-1. Ammonia requires 17% greater tank volume than RP-1.

Cost - The cost of hydrocarbon is another important aspect in the selection criteria for propellants. The price listings shown in Table X are the lowest which could be obtained after contacting many large petroleum corporations and refineries. Recent changes in the situation of many oil exporting countries make it difficult to extrapolate 1980 prices to 1990 prices; however, a rate of 9% a year is currently being used by ALRC Procurement. The costs shown are for commercially available "natural" grades

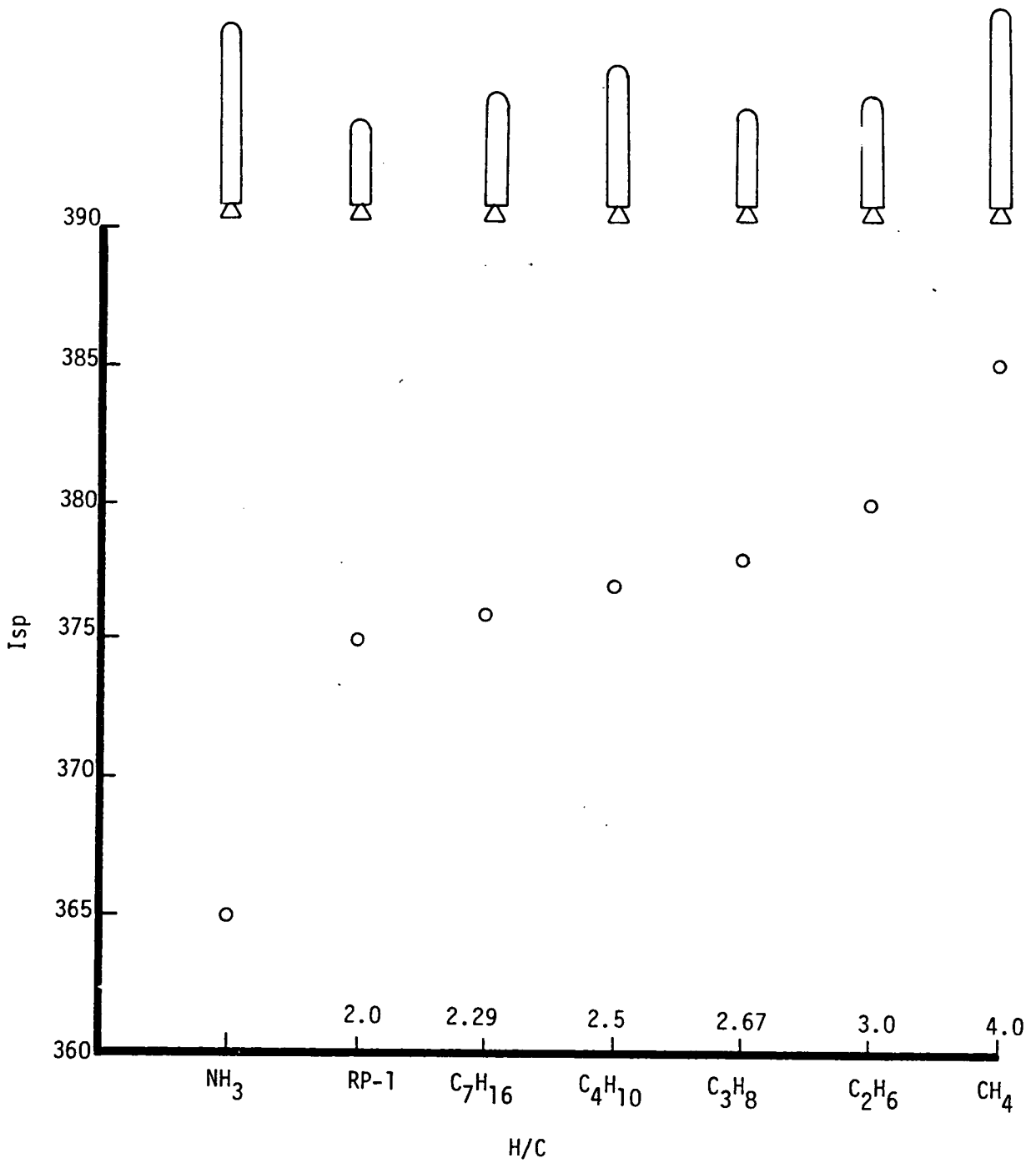

Figure 53. Isp and Relative Tankage Volumes

TABLE IX

FUEL PROPERTIES

PROPERTY	LO_2	Methane CH_4	Ethane C_2H_6	Propane C_3H_6	n-Butane C_4H_{10}	n-Heptane C_7H_{16}	RP-1	Ammonia NH_3
Molecular Weight	32.00	16.04	30.07	44.09	58.12	100.2	172	17.032
C	-	1	2	2	4	7	12	-
H/C	-	4	3	2.67	2.5	2.28	2.0	-
T_{Crit} (°F)	-182	-117	90	206	306	513	758	270
P_{Crit} (psia)	731	673	708	617	551	397	315	1636
SG_f	1.14	.422	.548	.578	.601	.684	.80	.68
N.B.P. (°F)	-297	-259	-128	-44	-31	+209	+422	-29°F
N.F.P. (°F)	-362	-296	-298	-306	-217	-131	-100 to -50	-108°F
Viscosity ($\frac{lb}{ft\text{-}sec}$) at Boiling Point	1.316×10^{-4}	7.76×10^{-5}	1.1×10^{-4}	1.404×10^{-4}	1.3×10^{-4}	3.32×10^{-4}*	1.4×10^{-4}	1.7×10^{-4}
Heat Capacity (Btu/lb-°F) at Boiling Point	.405	.835	.53	.538	.54	.47*	.66	1.07
Thermal Conduct. (Btu/ft-sec-°F) at Boiling Point	2.4×10^{-5}	3.1×10^{-5}	2.44×10^{-5}	1.56×10^{-5}	2.16×10^{-5}	2.02×10^{-5}*	1.94×10^{-5}	6.11×10^{-5}

*Properties at 100°F and not at the boiling point (209°F)

TABLE X

FUEL PRICES

FUEL	COST $/LB	SOURCE OF DATA
PROPANE	0.087	CALIF. LIQUID GAS CORP.
BUTANE	0.087	CHEVRON
RP-1	0.12	ALRC PROCUREMENT
METHANE	0.12	NASA/MSFC
ETHANE	0.35	UNION CARBIDE (SAN FRANCISCO)
AMMONIA	0.0675	USS AGRACAM

that may have unacceptable levels of impurities (e.g., oxygen, sulphur and other hydrocarbon compounds). The level of purity significantly influences cost. As an example, an instrument grade propane that is 99 percent pure costs about 10 times as much as commercial propane that may be as low as 86 percent pure.

Toxicity - According to a Union Carbide reference manual (Ref. 7), methane is non-toxic and propane and RP-1 have very low toxicity, but ammonia is highly toxic at levels of 25 ppm. Ammonia also causes burns on contact with eyes, skin, and mucous membranes.

Corrosiveness - The hydrocarbon fuels are easily contained in metal containers for long periods of time without any corrosion. Ammonia, on the other hand, will corrode a very important metal such as copper.

(2) Test Parameters

Fuel Freezing - It was anticipated that fuel freezing could be a problem with RP-1 and ammonia, particularly while using coherent jet impingement type injectors. No occurrence of freezing was noted during any of the testing. It is still possible, however, that the use of larger orifices could promote fuel freezing. Larger streams would receive proportionately less heat from recirculation gases of their reduced surface area to volume ratio.

Pops - Pops and unsteady combustion with the use of LOX/HC propellants is usually related to fuel freezing and subsequent detonation. This phenomenon may be encouraged by a number of factors, such as high MR's, low Pc mixing, low injector ΔP, low fuel temperature, and large orifice diameters. As was the case with fuel freezing, no occurrences of popping was noted during any of the testing.

Carbon Formation - Carbon formation was influenced by type of fuel, injector element, mixture ratio, and fuel temperature. (See Section V.D.1.) RP-1 and propane, being the heavier hydrocarbons, produced the most carbon in a given situation. From a chemical standpoint, this is to be expected since RP-1 and propane tend to form unsaturated C_2 species, while methane tends to break into carbon (C) and hydrogen (H_2). The C_2 species are very active and, through a process of polymerization, build up into particulate matter. The methane produced no visible carbon during testing, and ammonia, of course, contains no carbon.

The type of carbon produced in this testing seemed to be related to a low-temperature partial reaction which occurs when the

fuel vaporization is slowed. Coking or gumming could become a serious problem in a high temperature, fuel-rich gas generator or in a high-bulk, temperature-rise regen passage.

Reactive Stream Separation - RSS may be significantly affected by the type of fuel selected. Testing with storable propellants in the past (Ref. 1) as well as current testing with hydrocarbon propellants have shown that chamber pressure and fuel Reynolds number are major factors influencing RSS. There appears to be an RSS type of phenomenon, as evidenced by striations in the spray pattern and by separate areas of fuel- and oxidizer-rich propellants. There does seem to be a Pc dependence with better mixing and less combustion light emission at the lower pressures. Higher pressure seems to promote the apparent separation and greatly enhance the light emission.

Evidence of RSS was seen with each fuel except ammonia. While there was very little color differentiation to help identify possible RSS, the existence of liquid droplets squirting from the impingement point towards the injector face would indicate that no vaporization (and no RSS) was occurring at the impngement point. The fact that ammonia seems far less reactive from an RSS standpoint than RP-1 or propane fits in well with the theory of vaporization-controlled combustion causing separation. Both the heat of vaporization and the auto-ignition temperature of ammonia are greater than the respective values for RP-1, Propane, and Methane.

The hydrocarbons are rated only slightly less desirable than ammonia from an RSS standpoint because an injector can be designed to operate efficiently either with or without RSS.

Supercritical Pressure Operation - No occurrence of flash vaporization leading to resurge phenomena has been experienced at subcritical or supercritical pressure operation. As mentioned previously, there is an increase of light emission and apparent separation with an increase in Pc. This increase, however, is gradual and continuous and seems to bear no relationship to the critical pressure.

(3) Fuel Selection

Table VIII shows that although methane and propane scored differently in the various categories, they were tied for the lead in the overall numerical average. This would indicate that both are highly suited for use in future LOX/HC engines and that the superiority of one over the other could be more clearly determined when detailed system requirements are defined. (In other words, the need for a clean burning fuel with highest possible Isp would indicate a need for methane, whereas the need for greater bulk density - where coking and Isp are not so critical - would indicate propane to be more suitable.) Propane and methane were the two hydrocarbons selected for Phase II testing. Ammonia was selected as the third test fuel for primarily two reasons. First, it contains no carbon and thus would

provide an excellent base for photographic comparison. Secondly, in addition to being extremely low cost, it is a good coolant, indicating two significant advantages for a long-life, reusable engine design.

b. Injector Element Selection

Thirteen injector elements were considered for the Phase II evaluation and selection. These injectors were divided into two categories: main chamber and fuel-rich gas generator. Numerical values were assigned to the various evaluation criteria for each element (Table XI). These numerical values reflect the rating of a specific injector with respect to those criteria. The rankings are based on a scale of 1 to 10. An injector ranked as a 10 with respect to a certain criterion would be the best injector in that category, whereas a ranking of 1 would signify total unsuitability.

Table XI indicates that many of the candidate elements could be successfully used for Phase II testing. Schedule and budgetary restraints, however, required that certain hardware items (already fabricated) and certain injectors be used for both main chamber and gas generator applications. The injectors which best meet the above mentioned criteria and are recommended for Phase II testing are shown in Table XII. The specific reasons for each of the selections are given below.

LOL-EDM - This element provides spray-on-spray unlike impingement for good mixing and has historically been used successfully with LOX/HC propellants. Data from the LOL-EDM testing would also be very complementary to data gained from the Transverse Like-on-Like (TLOL) injector in Phase I testing.

Pre-Atomized Triplet (PAT) - The PAT consists of two fuel splash plate elements which impinge on one centrally located oxidizer x-doublet (XDT) element. Both of these platelet element concepts are analytically well characterized at ALRC for performance efficiency, combustion stability, and thermal compatiblity with storable propellants. The intent of pre-atomization of the propellants prior to impingement is to promote propellant heating and mixing. This should prevent possible fuel freezing associated with coherent stream impingement. PAT Phase II testing would also provide a basis for comparison with the Phase I OFO Triplet combustion data.

Unlike Doublet (Using NH_3) - The main reason for the selection of this element is the fact that it was residual hardware from Contract NAS 9-14186 and was readily adaptable to firing with LOX/NH_3. While the unlike doublet may not be the optimum selection from a performance-, heat transfer-, or compatibility standpoint, it certainly does provide the opportunity for economically exploring LOX/NH_3 combustion phenomena. The unlike doublet also provides the best view of the impingement interaction. External lighting problems encountered with LOX/HC propellants

TABLE XI

INJECTION ELEMENT EVALUATION CRITERIA AND SELECTION

Rating

Excellent	=	10
Good	=	8
Fair	=	6
Poor	=	4
Unacceptable	=	0

Injection Element Concept	Atomization (Small Drop Size)	Mixing (Uniform)	Injector Face Compat. (Low Heat Flux)	Chamber Wall Compat. (no Streaks)	Chug Stability (Short Comb. Time Lags)	Hi Freq. Stab. (Uniform Atom. Distribution)	Inj. Momentum Balance (Axial Resultant)	Fuel Freezing (Coherent Jet NH_3 Only)	Yields Good Photographic Results	Numerical Rating Perfect Inj. = 10.0	Remarks/Cause for Rejection
Main Chamber											
EDM-LOL (C_3H_4)	G	G	F	G-F	G	G	G	G	G	7.7	Recommended
PAT FOF (C_3H_8)	E	E	F-G	G	E	F	E	G	G	8.6	Recommended
U.D. (NH_3)	E	E-G	F	F	G	F-P	F	F	E	7.3	Recommended
Swirl Co-Ax(gCH_4)	E	E	E	G	G	G	G	G	F	8.4	Not easily photographed
VDT (C_3H_8)	G-F	G	F	G-F	G	E	G	G	G	7.8	Larger Engine Application
Splash Plate (C_3H_8)	E	G	F	G	E	F	F	G	G	7.8	
XDT (C_3H_8)	G	F-P	F	E	F-P	F-P	E	G	G	7.2	Stability Problems
FOF Triplet (C_3H_8)	E	E-G	G	F-P	G-E	F-P	G	G	G	8.0	Already building PAT (FOF)
Slit Triplet (gCH_4)	E	E-G	E-G	G	E	G	E	G	G	8.9	Recommended
Showerhead (C_3H_8)	P	P	F	G	P	E	E	G	F	6.7	Poor Atomization & Mixing
Fuel-Rich Gas Generator											
PAT FOF	G	G	F	G	G	G	E	G	P	7.6	
PAT FOF (LCH_4)	F	P	U	P	E	G	E	G	P	-	Lean prop outside Fuel core would not atomize
EDM-LOL (LCH_4)	F	F	F	G-F	F	E	G	G	P	6.8	Recommended
RUD (C_3H_8)	G	F-P	P	F	G	F-P	P	G	P	5.8	Recommended
Coaxial Swirler	E	G	E	G	E	F-G	E	G	P	8.3	2nd Choice
Shear Co-ax	U	U	E	E	P	E	E	G	P	-	Poor Mixing & Atomization
"I" Triplet	E	E	F-P	F	E	F-P	F	G	P	7.1	Stab. & compat. Prob.
FOF Triplet	E	F	F-P	G-F	E	F-P	G	G	P	7.0	
XDT	G	U	F	E	U	F	E	G	P	-	Resurge-Prone
Splashplate	G	F	F	G	G	F	U	G	P	-	Excess. Mom. Imbal.
VDT	F	F	F	F	F	E	G	G	P	6.7	Larger Eng. Appl.
Showerhead	U	U	P	G	P	E	E	G	P	-	Poor Mixing, Resurge-Prone

TABLE XII

PHASE II INJECTOR RECOMMENDATIONS

	INJECTOR	PROPELLANTS	APPLICATION
1.	LOL-EDM	LOX/C_3H_8	Main Chamber
2.	Pre-Atomized Triplet	LOX/C_3H_8	Main Chamber
3.	Unlike Doublet (Existing Hardware)	LOX/NH_3	Main Chamber
4.	Slit Triplet	LOX/gCH_4	Main Chamber
5.	Rectangular Unlike Doublet (Existing Hardware)	LOX/C_3H_8	Fuel-Rich Gas Generator
6.	LOL-EDM (See #1 above)	LOX/LCH_4 and C_3H_8	Fuel-Rich Gas Generator

(Phase I testing) were not anticipated to occur during these tests due to the lack of carbon particle emission.

Slit Triplet - The slit triplet was recommended as a main engine injector to be used with LOX and gaseous methane. This design features a centrally located rectangular LOX orifice (high aspect ratio) which would be impinged upon by gaseous methane exiting from two outside rectangular orifices. The interaction between the methane and the sheet of LOX should produce good atomization, mixing, compatibility, and stability. The Slit Triplet is similar in function to a coaxial swirler element, but is expected to yield better photographic results due to the impingement away from the injector face. Since this element is easily photographed, it should yield new insights into the mixing and combustion of impinging gas and liquid streams.

Rectangular Unlike Doublet (Gas Generator) - The Rectangular Unlike Doublet (RUD) injector from Phase I testing could be utilized as a fuel-rich (C_3H_8) gas generator by switching the oxidizer and fuel circuits. The fact that both of the inlet lines are LN_2 jacketed makes this "switching" possible. Utilization of the existing RUD as a gas generator affords an economical, quick look at the advantages and limitations of high-speed photography at low mixture ratio.

LOL-EDM (Gas Generator) - The switching option mentioned above could also be employed with the LOL-EDM element. Of the five injectors previously described, the LOL-EDM should have the least problems converting to a fuel-rich gas generator. The LOL-EDM could be tested with both Propane and Methane to provide a basis for comparing fuel-related sooting characteristics.

3. Phase II Test Results Evaluation

The following comments regarding application of the combustion evaluation criteria are made on the basis of the Phase II test results and correlations previously described in Sections V.C and V.D.

a. Fuel Evaluation

The criteria selected for test evaluation are commented on below.

(1) Fuel Freezing

No fuel freezing was encountered during Phase I or Phase II testing. This was true even for the highest freezing point fuels

(RP-1 and NH_3) with the use of direct impingement, coherent jet injectors. It is possible, however, that the use of large orifices (e.g., booster engine aplications) could promote fuel freezing because of their reduced surface area to volume ratio (i.e., combustion gases would heat larger orifice jets more slowly).

(2) Pops

No unsteady combustion was experienced during any of the program testing. The testing provided no conclusive information regarding any aspect of combustion stability.

(3) Carbon Formation

The gas-side carbon formation criteria for fuel evaluation proved to be accurate. As the fuel Hydrogen/Carbon ratio decreases (CH_4 = 4.0, C_3H_8 = 2.67, RP-1 = 2.0), carbon formation increases for any given injector element and operating point. The injector type and operating point also significantly influenced carbon formation. As a result of these findings, carbon formation was added to the injector element selection criteria.

(4) Reactive Stream Separation

Propellant mixing limited combustion (i.e., RSS) is sensitive to all parameters that influence fuel vaporization rate. For any operating point, the fuel yielding more rapid fuel vaporization will, in general, increase the degree of RSS. Existing drop size and vaporization models must be utilized to determine the actual vaporization rate for candidate fuels for any application.

(5) Supercritical Pressure Operation

Exceeding the critical pressure did not in itself significantly change the atomization, vaporization, or combustion process for any of the fuels tested. When the fuel injection temperature exceeded the saturation temperature at any pressure, carbon formation was essentially eliminated. This indicates that fuel vaporization rate is the key to carbon formation, and that reaching the critical pressure does not create a discontinuity in the fuel vaporization process.

b. Injection Element Evaluation

The Phase II testing resulted in definitive data on four of the previously described injection element selection criteria. Additionally, as a result of the testing and a subsequent analysis of the

important considerations guiding injector selection, two additional criteria were added.

(1) Mixing

Bipropellant mixing limited combustion (synonymous with RSS in this report) was displayed quite vividly during the Phase II testing. The visual data and subsequent correlations indicate that two factors control mixing: 1) the fuel vaporization rate and 2) the degree of injection orifice or spray fan cant towards the unlike propellant. The most important conclusion was that unlike spray fan impingement elements (i.e., TLOL, PAT and EDM-LOL) promote RSS. With unlike spray fan impingement elements significant vaporization occurs before unlike propellant contact. This gas generation prohibits mixing. When coherent unlike jet impingement occurs, mixing improves. It should be noted that of the unlike spray fan impingement elements tested, only the EDM-LOL had near optimum spray fan cant angles. The TLOL and PAT elements had too shallow an unlike impingement angle, which undoubtedly promoted RSS. The results agree with this conclusion. The EDM-LOL showed a higher degree of mixing than the PAT and TLOL. As a result it was concluded that PAT and TLOL mixing could have been improved with increased unlike impingement angles.

(2) Injector Momentum Balance

The photographic results confirmed the pretest conclusions regarding momentum balance. Symmetric unlike jet elements (e.g., FOF triplets, OFO triplets, slit triplets, pentads, etc.) are totally insensitive to mixture ratio. Asymmetrical unlike jet elements (e.g., unlike doublets) exhibit the most unfavorable characteristics with respect to axial momentum balance. Unlike spray fan impingement elements (e.g., EDM-LOL, TLOL, PAT) fall in between the above extremes.

(3) Fuel Freezing

It seems reasonable to assume that unlike coherent jet impingement would promote fuel freezing because of intimate contact. However, no incidences of fuel freezing occurred during the testing. As a result of this testing, it was concluded that fuel freezing is not an important design consideration for injectors in the low-thrust per element design range (approximately 1-50 lbF/element).

(4) Meaningful Photographic Results

The testing confirmed that excellent photographic results could be achieved for those elements where unlike jet or spray fan impingement occurred in a plane normal to the plane of view.

V, E, Combustion Evaluation Criteria Development and Results (cont.)

(5) Carbon Formation

The photographic test results indicated conclusively that the injector element type directly influences carbon formation. Unlike spray fan impingement elements reduce carbon formation because they induce a relatively rapid fuel vaporization rate. Coherent jet impingement elements, in contrast, exhibit increased carbon formation.

(6) Fabrication Complexity

Pre-atomized (i.e., platelet or swirler) elements are inherently more insensitive than coherent jet orifices to orifice size and alignment tolerances. This factor should be considered during injector element selection.

REFERENCES

1. Lawver, B.R., "High Performance N_2O_4/Amine Elements-Blowapart," Final Report, Contract NAS 9-14186, Report 14186-DRL-5, ALRC, March 1979.

2. Judd, D.C. and Lawver, B.R., "Phase I-1 Test Plan for Photographic Characterization of LOX/HC Type Propellants," Contract NAS 9-15724, ALRC, 22 Dec 1978.

3. Judd, D.C., "Phase I-2 Test Plan for Photographic Characterization of LOX/HC Type Propellants," Contract NAS 9-15724, ALRC, 8 Jan 1979.

4. Judd, D.C., "Phase II Propellant, Injector and Test Condition Recommendation," Contract NAS 9-15724, ALRC, 13 July 1979.

5. Lawver, B.R., "High Performance N_2O_4/Amine Elements-Blowapart," Injector Element Design Criteria, Contract NAS 9-14186, ALRC, 15 Nov 1978.

6. Walker, R.E., ITIP Phase 0 Uni-Element Cold Flow Test Results," Report No. ADR:9734:0140, 22 Jan 1976.

7. Judd, D.C., "Phase I Data Dump Report DM-1113T-1," Contract NAS 9-15724, 27 July 1979.

8. Union Carbide, "Specialty Gases and Equipment," Volume IV, Dec. 1977.

APPENDIX I

EQUATIONS FOR SPECIFIC GRAVITY, VISCOSITY, AND SURFACE TENSION

```
TN,L,T,C
      SUBROUTINE PROPT (F,P,TF,SG,ST,VS)

         THIS SUBROUTINE COMPUTES SPECIFIC GRAVITY, VISCOSITY, AND
         SURFACE TENSION FOR SOME STANDARD ROCKET PROPELLANTS
         THE TEMPERATURE MUST BE PROVIDED IN DEGREES FAHRENHEIT.
         OUT-OF-RANGE SPECIFIC GRAVITY OR VISCOSITY IS RETURNED
         AS A VALUE OF 88888.  OUT-OF-RANGE SURFACE TENSION IS
         RETURNED AS A NEGATIVE REAL NUMBER OR ZERO.

      SG=88888.
      VS=88888.
      TR=TF+459.7
      TK=TR/1.8
      GO TO (10,20,30,40,50) F

         COMPUTE SG,ST,VS FOR RP-1

   10 SG=-.000388*TF+.82828
      ST=1.-TK/679.25
      IF(ST.GT.0.) ST=ST**1.2671*53.5055*6.85195E-5
      Z=(TF-68.)/97.
      IF(ABS(Z).GT.1.) GO TO 100
      VS=((((-1.956135E-4*Z+7.867826E-4)*Z-1.303092E-3)*Z+1.322725E-3)
     1    *Z-1.255994E-3)*Z+1.144314E-3
      GO TO 100

         COMPUTE SG,ST,VS FOR METHANE

   20 ST=1.-TK/190.555
      IF(ST.GT.0.) ST=ST**1.23625*40.322*6.85195E-5
      Z=(TR-252.632)/89.388
      IF(ABS(Z).GE.1.) GO TO 100
      VS=((((((-7.190261E-2*Z+2.45455E-2)*Z+0.1088466)*Z-1.784053E-2)
     1    *Z-8.52951E-2)*Z+3.547601E-2)*Z-4.333652E-2)*Z+7.088399E-2
      VS=VS/1.4881639
      SG=((((((-6.849984E-2*Z-5.252717E-2)*Z+7.200876E-2)*Z+3.821812E-2)
     1    *Z-3.900402E-2)*Z-3.324897E-2)*Z-8.740642E-2)*Z+.3773215
      GO TO 100

         COMPUTE SG,ST,VS FOR PROPANE

   30 ST=1.-TK/369.8
      IF(ST.GT.0.) ST=ST**1.24821*51.492*6.85195E-5
      Z=(TR-422.84)/242.82
      IF(ABS(Z).GE.1.) GO TO 34
      VS=((((((-3.516625*Z+3.172092)*Z+3.215512)*Z-2.325508)
     1    *Z-1.378224)*Z+0.8517147)*Z-0.1949874)*Z+0.1816328
      VS=VS*.001/1.4881639
   34 Z=(TR-405.44301)/251.577
      IF(ABS(Z).GE.1.) GO TO 100
      SG=((((((-7.27397E-2*Z-5.84529E-2)*Z+7.127882E-2)*Z+3.560425E-2)
     1    *Z-4.879066E-2)*Z-3.866206E-2)*Z-0.157346B)*Z+0.5883114
      GO TO 100

         COMPUTE ST,VS FOR OXYGEN

   40 CALL OXY (P,TF,SG)
      ST=1.-TK/154.576
      IF(ST.GT.0.) ST=ST**1.22222*38.461*6.85195E-5




      Z=(SG-.9790199)/.3275971
      IF(ABS(Z).GE.1.) GO TO 100
      VS=((((((8.694109E-6*Z+3.157964E-5)*Z+3.500642E-5)*Z+4.602466E-5)
     1    *Z+8.467757E-5)*Z+8.153158E-5)*Z+6.243964E-5)*Z+6.625252E-5
      GO TO 100

         COMPUTE ST,VS,SG FOR AMMONIA

   50 ST=0.0020787-8.9888E-6*TF
      VS=1.E-5/(0.072471+0.00044197*TF)
      TSAT=(((-7.3826E-10*P+1.53233E-6)*P-1.29498E-3)*P+0.675)*P+1.90664
      IF((TSAT-TF).LT.1.) GO TO 100
      SG=0.6621185-(1.132834E-6*TF+6.937453E-4-5.336631E-8*P)*TF
     1    +2.473552E-6*P
  100 RETURN
      END
      ENDS
```

APPENDIX II

TEST RESULTS

JUDD

LOX/HYDROCARBON TYPE PROPELLANTS TESTING DATA

INVESTIGATOR JUDD

FUEL TYPE	TEST NO.	INJECTOR TYPE	PC (PSIA)	MR	TF (F)	REYN	WT (LB)	CSTRE (SEC)	VF (FT/S)	MODE
RP-1	101	9-F-0 TRIPLET	460.	2.40	50.	10100.	.093	4850.	120.	SLICOK
RP-1	102	9-F-0 TRIPLET	0.	.00	0.	0.	.000	0.	0.	UNDEF
RP-1	103	9-F-0 TRIPLET	0.	.00	0.	0.	.000	0.	0.	UNDEF
RP-1	104	9-F-0 TRIPLET	462.	2.60	50.	11343.	.101	4250.	127.	UNDEF
RP-1	105	9-F-0 TRIPLET	480.	2.80	50.	10321.	.100	4600.	116.	SLICOK
RP-1	106	9-F-0 TRIPLET	485.	2.75	50.	10053.	.099	4650.	116.	SLICOK
RP-1	107	9-F-0 TRIPLET	870.	2.60	70.	20636.	.160	0.	200.	CLEAR
RP-1	108	9-F-0 TRIPLET	450.	1.70	70.	8039.	.047	4000.	76.	SLICOK
RP-1	109	9-F-0 TRIPLET	475.	2.40	55.	9382.	.053	4650.	89.	SLICOK
RP-1	110	9-F-0 TRIPLET	420.	2.70	67.	16826.	.137	4750.	165.	SLICOK
RP-1	111	9-F-0 TRIPLET	480.	2.70	67.	16826.	.137	4750.	165.	SLICOK
RP-1	112	9-F-0 TRIPLET	900.	2.60	72.	13840.	.097	0.	120.	CLEAR
RP-1	113	9-F-0 TRIPLET	0.	.00	0.	0.	.000	0.	0.	UNDEF
RP-1	114	9-F-0 TRIPLET	970.	2.75	66.	10315.	.075	4000.	100.	CLEAR
RP-1	115	9-F-0 TRIPLET	0.	.00	0.	0.	.000	0.	0.	UNDEF
RP-1	116	9-F-0 TRIPLET	1500.	2.60	50.	8470.	.082	4600.	100.	CLEAR
RP-1	117	R UNLIK DOUBLET	130.	2.80	15.	2498.	.000	0.	57.	OBSCUR
RP-1	118	R UNLIK DOUBLET	0.	.00	0.	0.	.000	0.	0.	UNDEF
RP-1	119	TRANSVERSE LOL	0.	.00	0.	0.	.000	0.	0.	UNDEF
RP-1	120	TRANSVERSE LOL	135.	2.35	41.	3815.	.062	4300.	58.	OBSCUR
RP-1	121	TRANSVERSE LOL	310.	2.90	38.	3140.	.064	5300.	53.	MODCOK
RP-1	122	TRANSVERSE LOL	780.	2.75	44.	6014.	.113	4750.	95.	CLEAR
RP-1	123	TRANSVERSE LOL	475.	2.65	35.	4705.	.095	4450.	82.	SLICOK
RP-1	124	TRANSVERSE LOL	475.	2.65	34.	4797.	.095	4450.	83.	SLICOK
RP-1	125	TRANSVERSE LOL	472.	2.65	33.	4776.	.094	4450.	83.	SLICOK
RP-1	126	TRANSVERSE LOL	140.	2.10	30.	2533.	.052	4000.	49.	OBSCUR
RP-1	127	TRANSVERSE LOL	250.	2.85	30.	2495.	.058	4800.	48.	MODCOK
RP-1	128	TRANSVERSE LOL	400.	3.10	39.	3426.	.077	4900.	63.	SLICOK
RP-1	129	TRANSVERSE LOL	800.	2.80	45.	5985.	.110	5100.	90.	CLEAR
C3H8	130	TRANSVERSE LOL	135.	2.50	45.	41607.	.044	4000.	63.	SLICOK
C3H8	131	TRANSVERSE LOL	290.	2.65	43.	49666.	.057	4500.	76.	CLEAR
C3H8	132	TRANSVERSE LOL	540.	3.00	43.	64458.	.079	4600.	98.	CLEAR
C3H8	133	TRANSVERSE LOL	790.	2.60	45.	78710.	.094	4650.	120.	CLEAR
C3H8	134	R UNLIK DOUBLET	0.	.00	0.	0.	.000	0.	0.	UNDEF
C3H8	135	R UNLIK DOUBLET	770.	2.80	68.	137923.	.095	4600.	166.	MODCOK
C3H8	136	R UNLIK DOUBLET	780.	2.75	58.	121770.	.095	4600.	158.	MODCOK
C3H8	137	R UNLIK DOUBLET	790.	2.80	54.	55464.	.042	4600.	73.	MODCOK
C3H8	138	R UNLIK DOUBLET	0.	.00	0.	0.	.000	0.	0.	UNDEF
C3H8	139	R UNLIK DOUBLET	545.	2.40	54.	95993.	.091	4600.	128.	MODCOK
C3H8	140	R UNLIK DOUBLET	290.	3.45	54.	74006.	.063	4150.	98.	OBSCUR

JUDD

LOX/HYDROCARBON TYPE PROPELLANTS TESTING DATA

INVESTIGATOR JUDD

FUEL TYPE	TEST NO.	INJECTOR TYPE	PC (PSIA)	MR	TF (F)	REYN	WT (LB)	COTRE (SEC)	VF (FT/S)	MODE
C3H8	141	R UNLIK DOUBLET	150.	3.15	52.	47125.	.043	4000.	63.	OBSCUR
C3H8	142	RUD - GAS GEN	0.	.00	0.	0.	.000	0.	0.	UNDEF
C3H8	143	RUD - GAS GEN	860.	.50	61.	128737.	.058	2900.	110.	OBSCUR
C3H8	144	RUD - GAS GEN	850.	.46	59.	133986.	.059	2850.	116.	OBSCUR
NH3	145	UNLIKE-DOUBLET	505.	1.48	65.	164142.	.117	4850.	112.	CLEAR
NH3	146	UNLIKE-DOUBLET	0.	.00	0.	0.	.000	0.	0.	UNDEF
NH3	147	UNLIKE-DOUBLET	245.	1.35	45.	129509.	.095	4650.	92.	CLEAR
NH3	148	UNLIKE-DOUBLET	350.	1.50	45.	126174.	.100	4850.	92.	CLEAR
NH3	149	UNLIKE-DOUBLET	490.	1.35	63.	145380.	.099	4750.	100.	CLEAR
NH3	150	UNLIKE-DOUBLET	250.	1.38	57.	133739.	.095	4650.	94.	CLEAR
NH3	151	UNLIKE-DOUBLET	150.	1.35	48.	137729.	.100	3900.	100.	CLEAR
NH3	152	UNLIKE-DOUBLET	505.	1.10	54.	161571.	.102	4650.	115.	CLEAR
NH3	153	UNLIKE-DOUBLET	505.	1.67	56.	154827.	.128	5100.	109.	CLEAR
NH3	154	UNLIKE-DOUBLET	505.	1.64	58.	157936.	.127	5100.	111.	CLEAR
NH3	155	UNLIKE-DOUBLET	485.	1.36	64.	105097.	.073	4500.	73.	CLEAR
NH3	156	UNLIKE-DOUBLET	500.	1.40	59.	215544.	.155	4950.	150.	CLEAR
C3H8	157	LOL - EDM	800.	2.80	47.	89923.	.106	5150.	130.	MODCOK
C3H8	158	LOL - EDM	560.	2.85	29.	65659.	.090	5000.	100.	OBSCUR
C3H8	159	LOL - EDM	295.	2.90	39.	56494.	.072	4500.	84.	OBSCUR
C3H8	160	LOL - EDM	150.	2.80	30.	39452.	.050	4100.	60.	OBSCUR
C3H8	161	LOL - EDM	800.	2.90	60.	97117.	.107	5100.	132.	MODCOK
C3H8	162	LOL - EDM	550.	2.95	61.	79565.	.088	4900.	106.	OBSCUR
C3H8	163	LOL - EDM	285.	3.25	64.	61592.	.074	4300.	81.	OBSCUR
C3H8	164	LOL - EDM	290.	2.90	80.	78058.	.075	4350.	91.	OBSCUR
C3H8	165	LOL - EDM	800.	2.85	147.	208855.	.097	4650.	144.	CLEAR
C3H8	166	LOL - EDM	0.	.00	0.	0.	.000	0.	0.	UNDEF
C3H8	167	LOL - EDM	0.	.00	0.	0.	.000	0.	0.	UNDEF
C3H8	168	LOL - EDM	550.	2.90	155.	157079.	.082	4600.	120.	MODCOK
C3H8	169	LOL - EDM	320.	3.10	158.	154762.	.088	3400.	117.	CLEAR
C3H8	170	LOL - EDM	0.	.00	0.	0.	.000	0.	0.	UNDEF
C3H8	171	LOL - EDM	640.	2.80	124.	104571.	.059	4900.	71.	SLICOK
C3H8	172	LOL - EDM	610.	2.95	130.	250770.	.123	4350.	165.	MODCOK
C3H8	173	LOL - EDM	640.	2.20	60.	8777.	.083	4300.	119.	OBSCUR
C3H8	174	LOL - EDM	625.	4.00	76.	83921.	.100	4250.	97.	SLICOK
C3H8	175	LOL - EDM	545.	4.10	79.	73611.	.090	4150.	85.	MODCOK
C3H8	176A	LOL - EDM	150.	2.90	75.	47110.	.047	4100.	56.	OBSCUR
C3H8	176B	LOL - EDM	108.	2.90	72.	75477.	.000	2000.	91.	CLEAR
C3H8	177	PRE ATOM TRIP	805.	2.75	70.	104118.	.086	5100.	155.	CLEAR
C3H8	178	PRE ATOM TRIP	560.	2.75	70.	87702.	.070	5400.	130.	SLICOK
C3H8	179	PRE ATOM TRIP	300.	2.85	66.	64553.	.055	4750.	99.	SLICOK

JUDD

LOX/HYDROCARBON TYPE PROPELLANTS TESTING DATA

INVESTIGATOR JUDD

FUEL TYPE	TEST NO.	INJECTOR TYPE	PC (PSIA)	MR	TF (F)	REYN	WT (LB)	CSTRE (SEC)	VF (FT/S)	MODE
C3H8	180	PRE ATOM TRIP	0.	.00	0.	0.	.000	0.	0.	UNDEF
C3H8	181	PRE ATOM TRIP	0.	.00	0.	0.	.000	0.	0.	UNDEF
C3H8	182	PRE ATOM TRIP	150.	2.90	65.	44283.	.038	4400.	69.	MODCOK
C3H8	183	PRE ATOM TRIP	0.	.00	0.	0.	.000	0.	0.	UNDEF
C3H8	184	PRE ATOM TRIP	300.	2.85	66.	64553.	.055	4750.	99.	SLICOK
C3H8	185	PRE ATOM TRIP	665.	2.20	72.	122300.	.083	5400.	178.	SLICOK
C3H8	186	PRE ATOM TRIP	670.	3.50	69.	70033.	.073	5250.	105.	SLICOK
C3H8	187	PRE ATOM TRIP	800.	2.90	66.	60800.	.055	4600.	93.	CLEAR
C3H8	188	PRE ATOM TRIP	540.	3.00	64.	64082.	.060	5000.	100.	SLICOK
C3H8	189	PRE ATOM TRIP	155.	2.80	62.	58165.	.050	4700.	91.	MODCOK
C3H8	190	PRE ATOM TRIP	165.	2.75	63.	89331.	.078	4750.	140.	SLICOK
C3H8	191	PRE ATOM TRIP	700.	.00	110.	0.	.000	0.	0.	UNDEF
C3H8	192	PRE ATOM TRIP	0.	.00	0.	0.	.000	0.	0.	UNDEF
C3H8	193	PRE ATOM TRIP	560.	2.80	120.	170305.	.074	5150.	142.	SLICOK
C3H8	194	PRE ATOM TRIP	340.	3.00	115.	143277.	.068	4450.	122.	SLICOK
C3H8	195	PRE ATOM TRIP	670.	2.85	66.	95525.	.084	5400.	146.	SLICOK
C3H8	196	PRE ATOM TRIP	630.	3.20	66.	50112.	.051	4000.	78.	SLICOK
C3H8	197	PRE ATOM TRIP	505.	3.00	43.	68435.	.074	4700.	120.	SLICOK
C3H8	198	LOL-EOM GAS GEN	810.	.72	79.	137519.	.079	3250.	113.	OBSCUR
C3H8	199	LOL-EOM GAS GEN	510.	.73	75.	103371.	.063	3100.	88.	OBSCUR
GCH4	200	SLIT TRIPLET	770.	3.90	67.	269842.	.101	5150.	271.	CLEAR
GCH4	201	SLIT TRIPLET	760.	3.60	67.	277992.	.101	5100.	279.	CLEAR
GCH4	202	SLIT TRIPLET	540.	4.20	70.	173026.	.070	4300.	248.	CLEAR
GCH4	203	SLIT TRIPLET	535.	3.50	71.	211659.	.075	4000.	308.	CLEAR
GCH4	204	SLIT TRIPLET	290.	3.70	72.	136406.	.050	3300.	363.	CLEAR
GCH4	205	SLIT TRIPLET	125.	4.70	73.	103524.	.043	2200.	622.	CLEAR
GCH4	206	SLIT TRIPLET	630.	3.60	55.	283078.	.101	3500.	325.	CLEAR
GCH4	207	SLIT TRIPLET	620.	3.00	54.	345763.	.105	3300.	405.	CLEAR
GCH4	208	SLIT TRIPLET	0.	.00	0.	0.	.000	0.	0.	UNDEF
GCH4	209	SLIT TRIPLET	700.	4.00	56.	267785.	.105	5250.	279.	CLEAR
GCH4	210	SLIT TRIPLET	0.	.00	0.	0.	.000	0.	0.	UNDEF
GCH4	211	SLIT TRIPLET	0.	.00	0.	0.	.000	0.	0.	UNDEF
GCH4	212	SLIT TRIPLET	690.	3.35	50.	454803.	.150	5200.	471.	CLEAR
GCH4	213	SLIT TRIPLET	685.	2.80	45.	211966.	.060	4650.	216.	CLEAR
GCH4	214	SLIT TRIPLET	310.	3.45	44.	160539.	.051	4150.	363.	CLEAR
GCH4	215	SLIT TRIPLET	125.	4.50	40.	131234.	.050	2450.	707.	CLEAR
GCH4	216	SLIT TRIPLET	790.	2.75	38.	306921.	.087	5100.	260.	CLEAR
GCH4	217	SLIT TRIPLET	405.	4.70	38.	132693.	.054	4500.	225.	CLEAR
GCH4	218	SLIT TRIPLET	405.	2.75	38.	150993.	.041	4000.	257.	CLEAR
GCH4	219	SLIT TRIPLET	790.	3.20	40.	215515.	.067	4900.	183.	CLEAR

JUDD

LOX/HYDROCARBON TYPE PROPELLANTS TESTING DATA

INVESTIGATOR JUDD

FUEL TYPE	TEST NO.	INJECTOR TYPE	PC (PSIA)	MR	TF (F)	REYN	WT (LB)	CSTRE (SEC)	VF (FT/S)	MODE
GCH4	220	SLIT TRIPLET	450.	3.00	40.	303088.	.098	4900.	468.	CLEAR
GCH4	221	SLIT TRIPLET	410.	4.00	46.	101752.	.036	4400.	174.	CLEAR
LCH4	222	LOL-EDM GAS GEN	805.	.82	-220.	189924.	.092	3050.	140.	CLEAR
LCH4	223	LOL-EDM GAS GEN	775.	.61	-230.	194587.	.084	2900.	157.	CLEAR
LCH4	224	LOL-EDM GAS GEN	805.	.50	-206.	210361.	.068	2875.	146.	CLEAR
LCH4	225	LOL-EDM GAS GEN	515.	.78	-226.	145129.	.066	3200.	113.	CLEAR
LCH4	226	LOL-EDM GAS GEN	495.	.60	-245.	132636.	.066	2900.	120.	CLEAR
LCH4	227	LOL-EDM GAS GEN	495.	.44	-211.	212882.	.070	2700.	150.	CLEAR

$FIN

APPENDIX III

CARBON FORMATION CORRELATIONS USING "Pc versus T_f"

INVESTIGATOR JUDD

INJECTOR = OFO TRIPLET

FUEL = RP-1

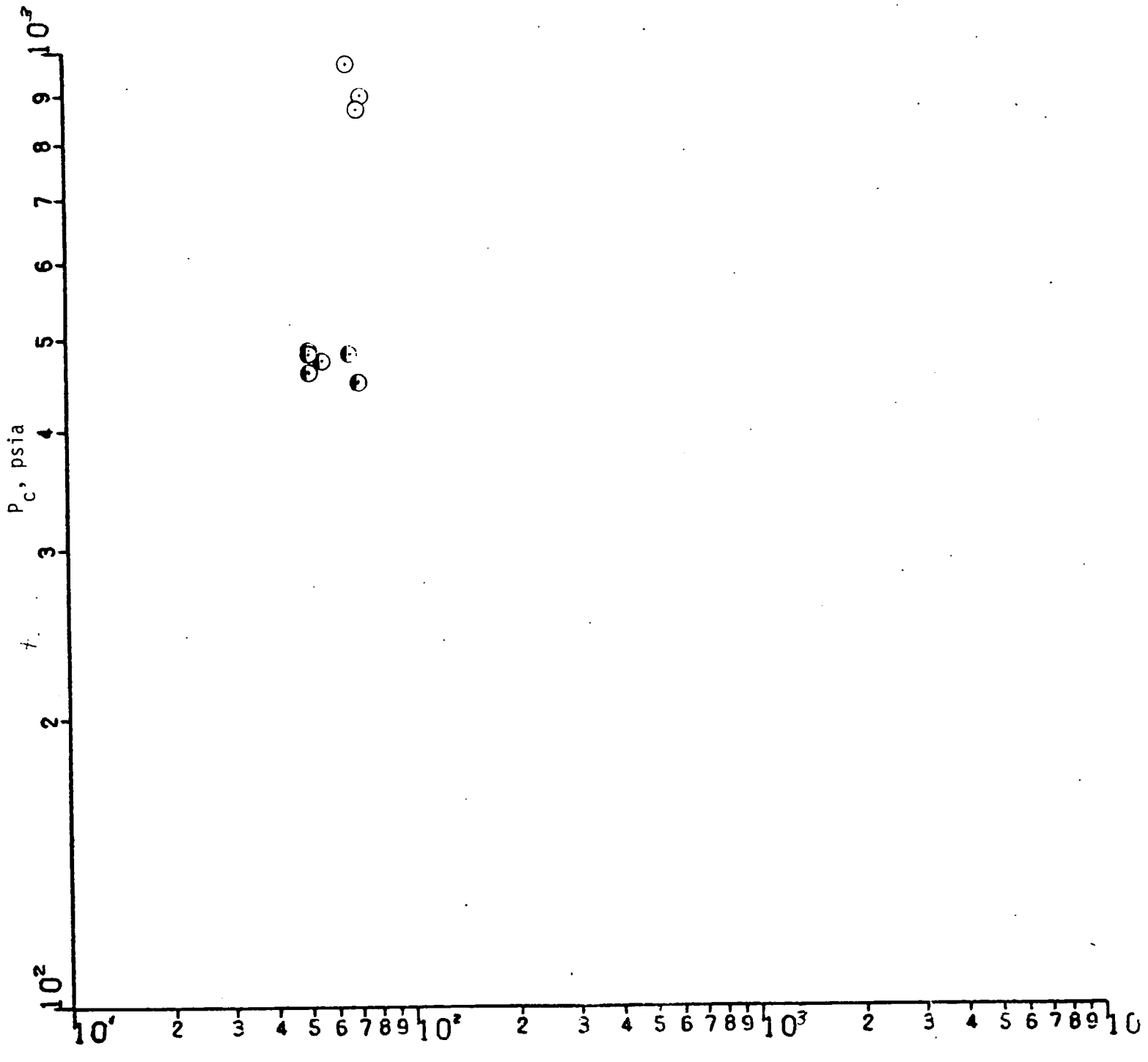

INVESTIGATOR JUDD

INJECTOR = R UNLIKE DOURLET

FUEL = RP-1

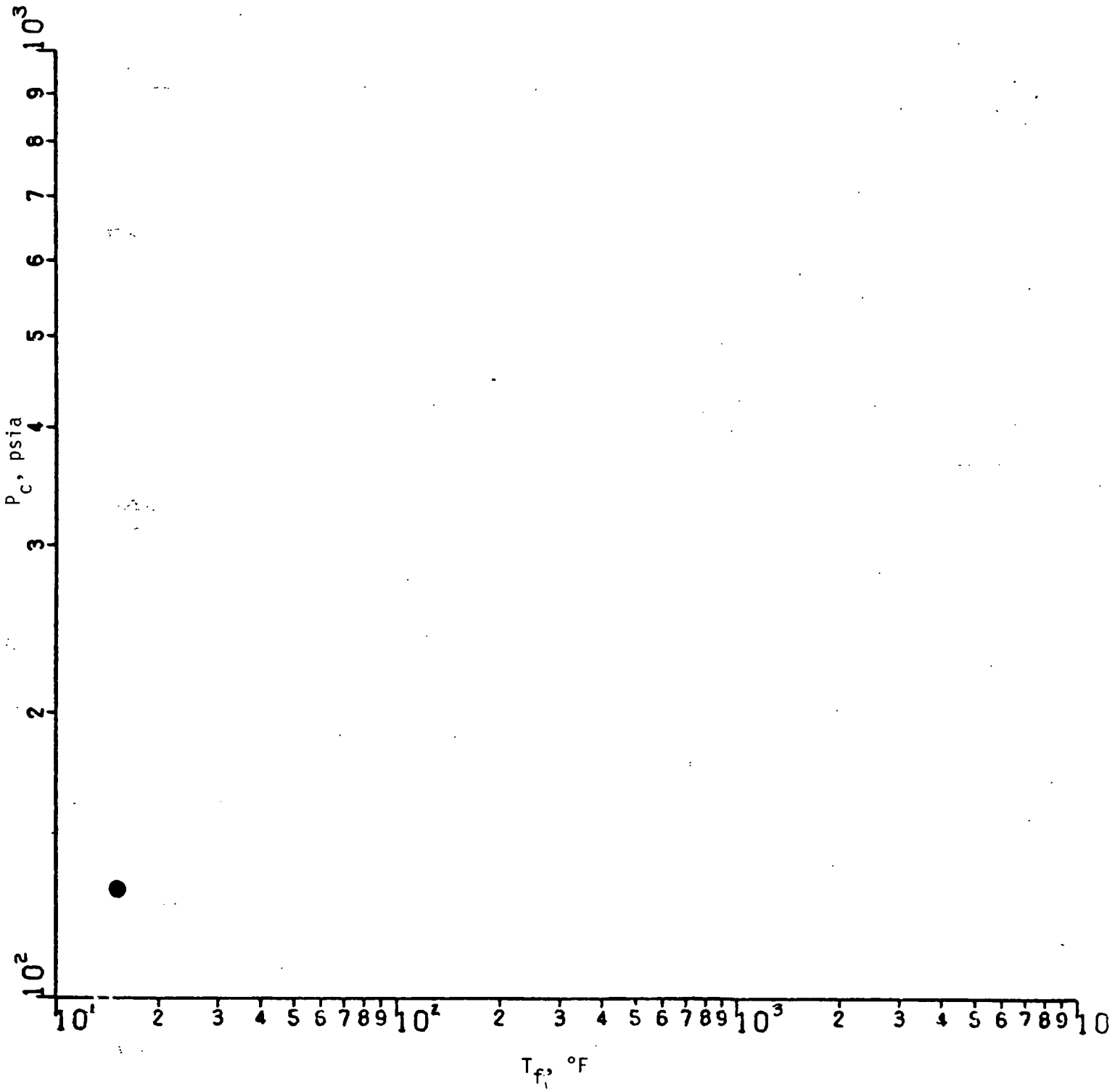

INVESTIGATOR JUDD

INJECTOR = TRANSVERSE LOL

FUEL = RP-1

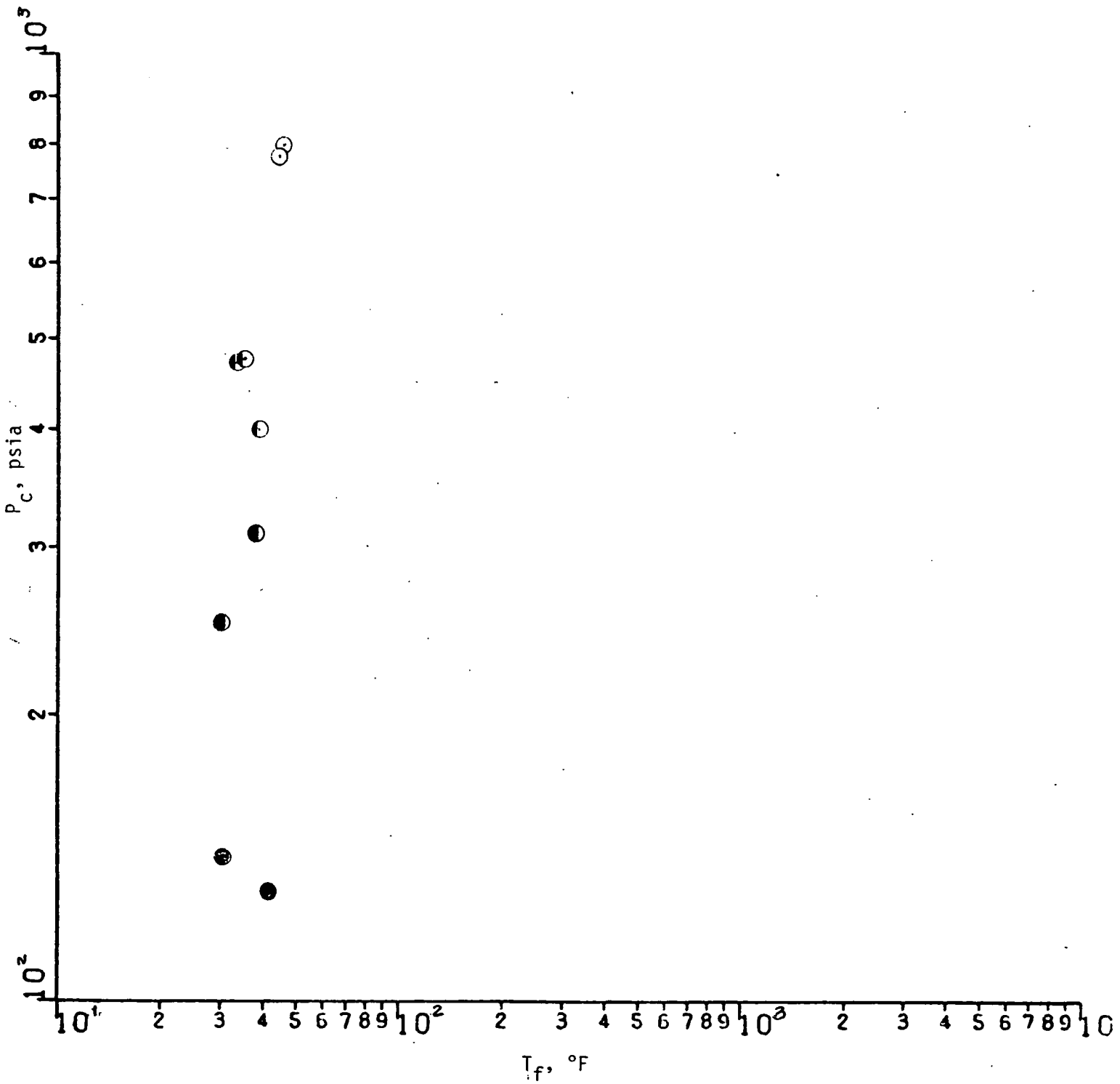

INVESTIGATOR JUDO

INJECTOR = R UNLIKE DOUBLET

FUEL = C_3H_8

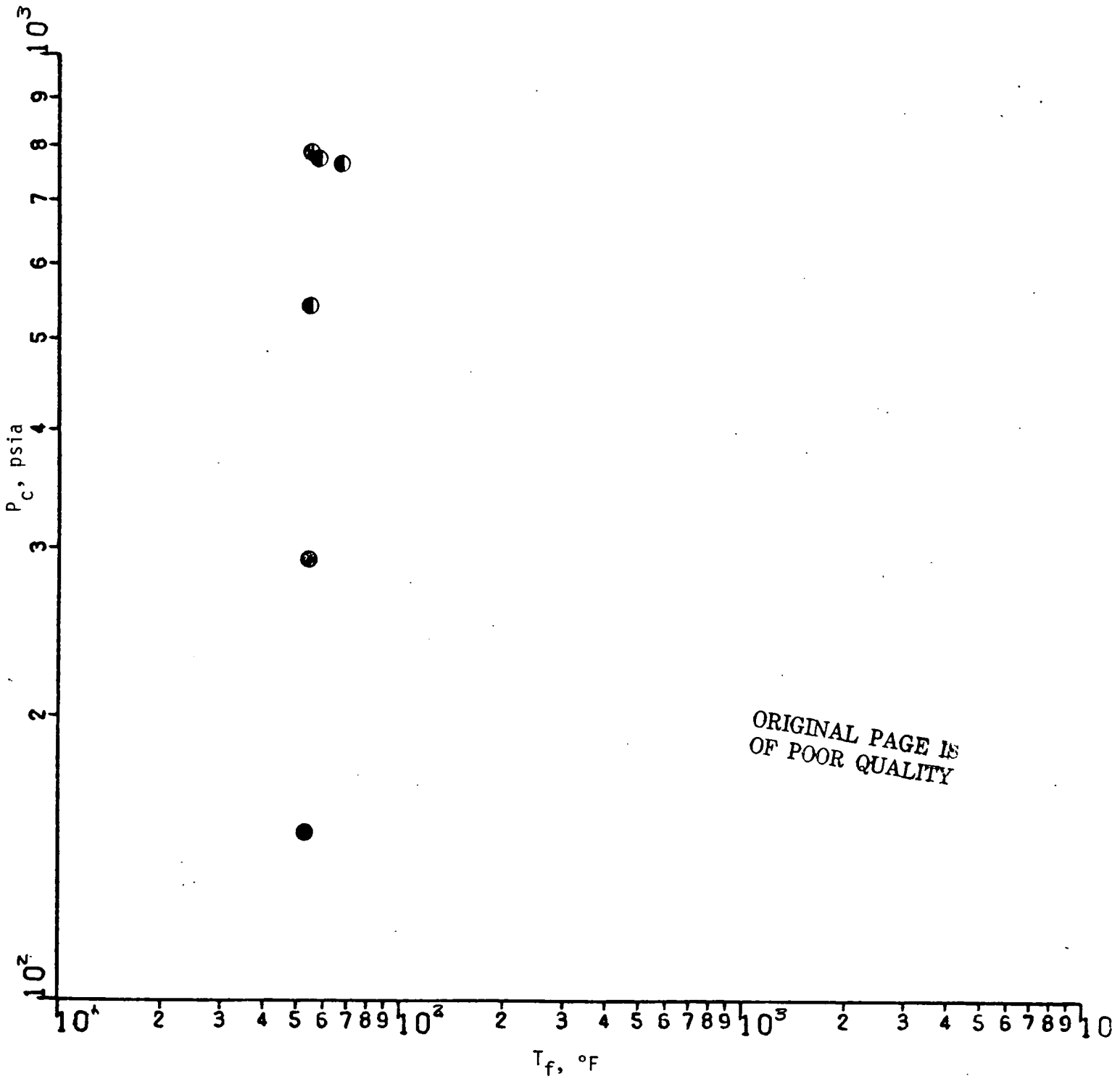

INVESTIGATOR JUDD

INJECTOR = LOL-EDM

FUEL = C_3H_8

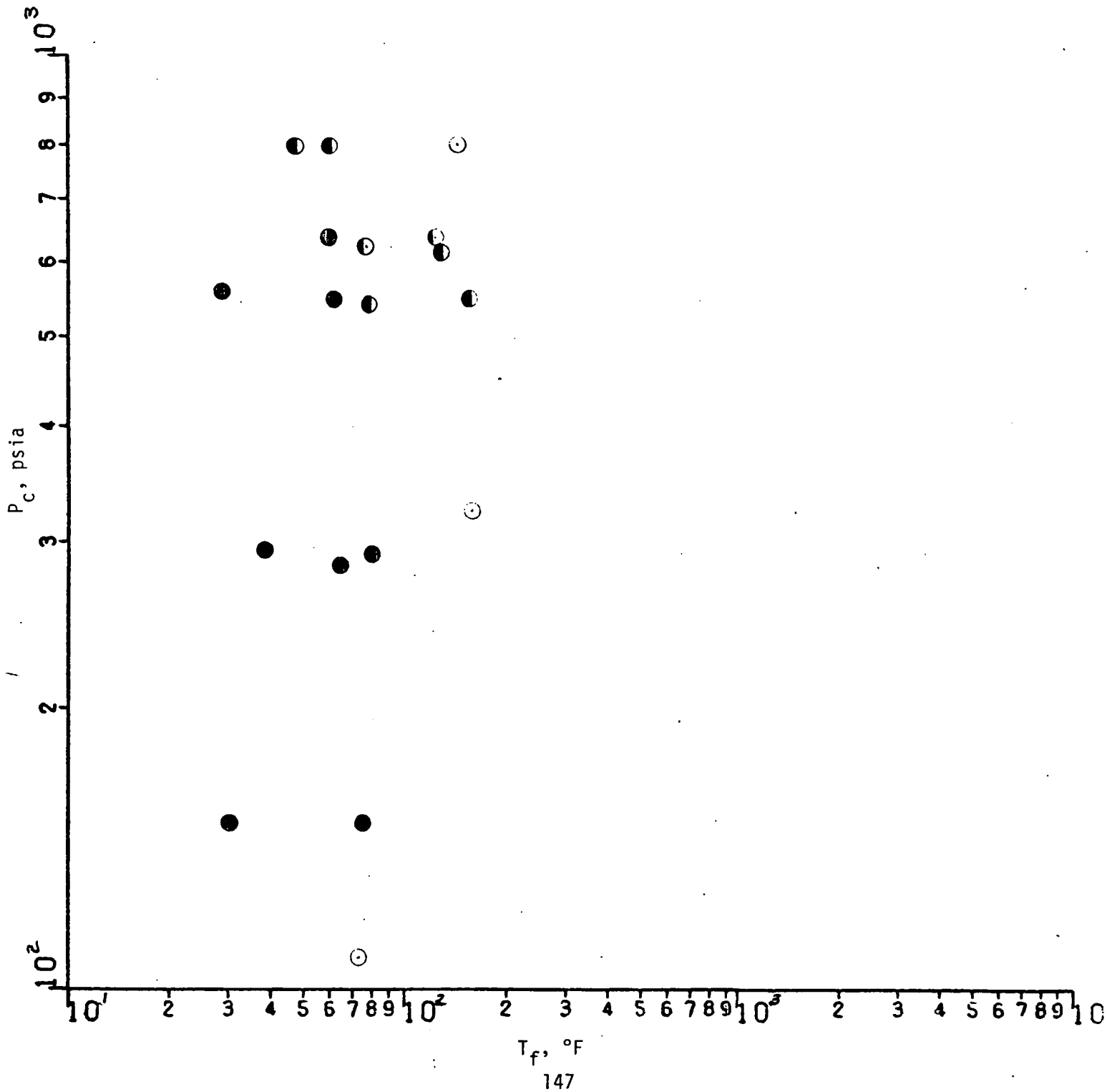

INVESTIGATOR JUDD

INJECTOR = PRE-ATOMIZED TRIPLET

FUEL = C_3H_8

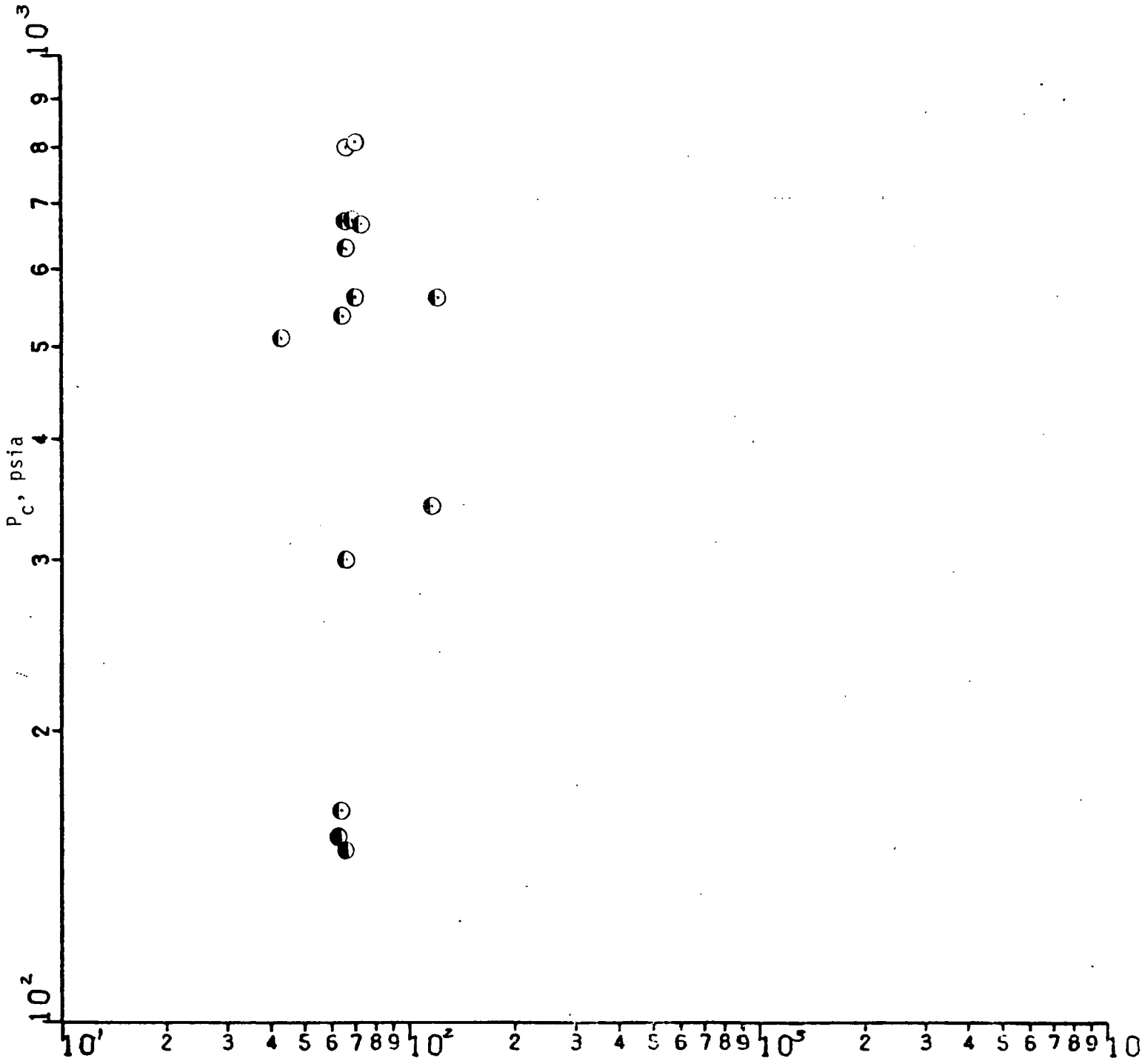

INVESTIGATOR JUDD

INJECTOR = TRANSVERSE LOL

FUEL = C_3H_8

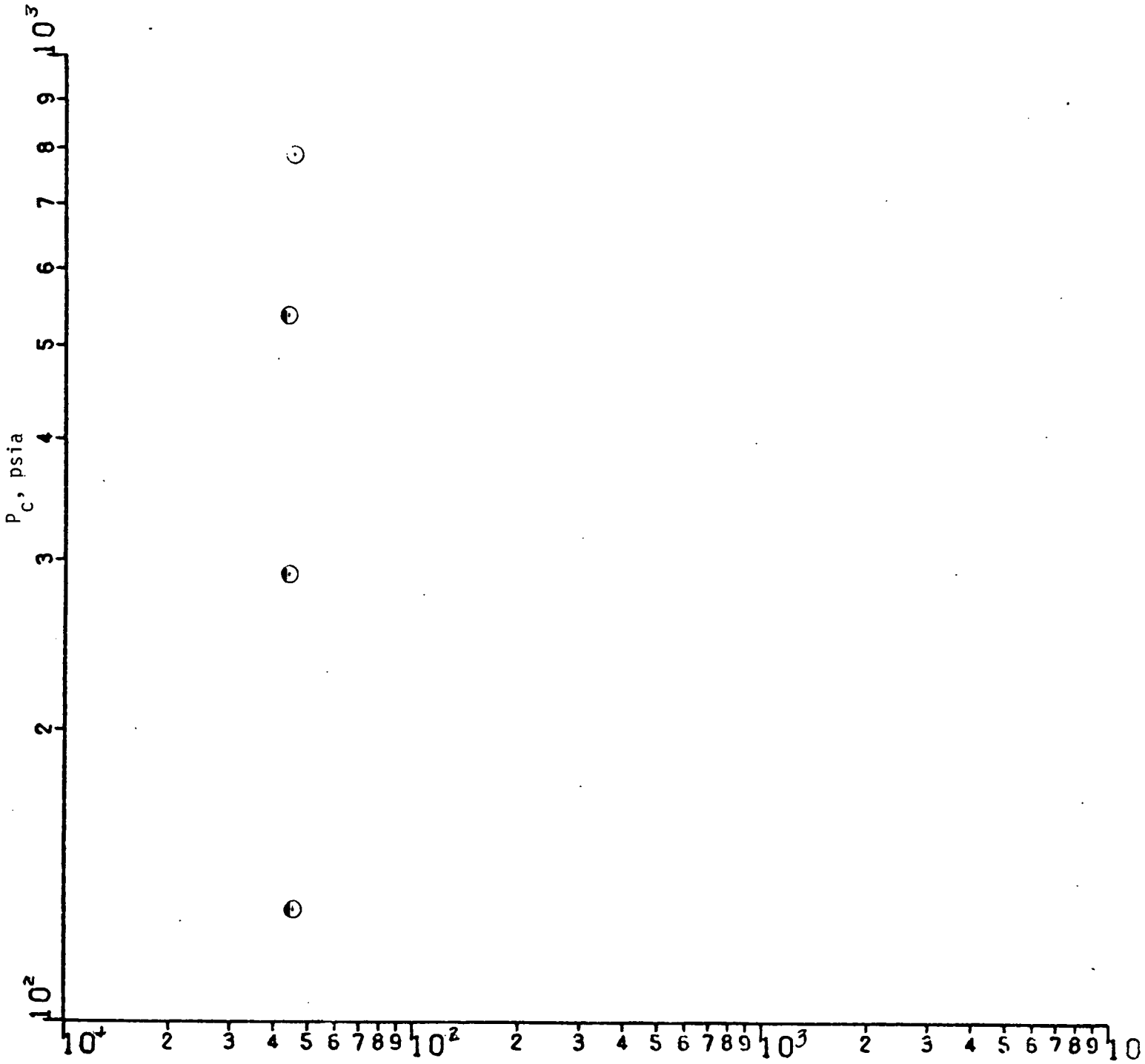

INVESTIGATOR JUDD

INJECTOR = UNLIKE DOUBLET

FUEL = NH_3

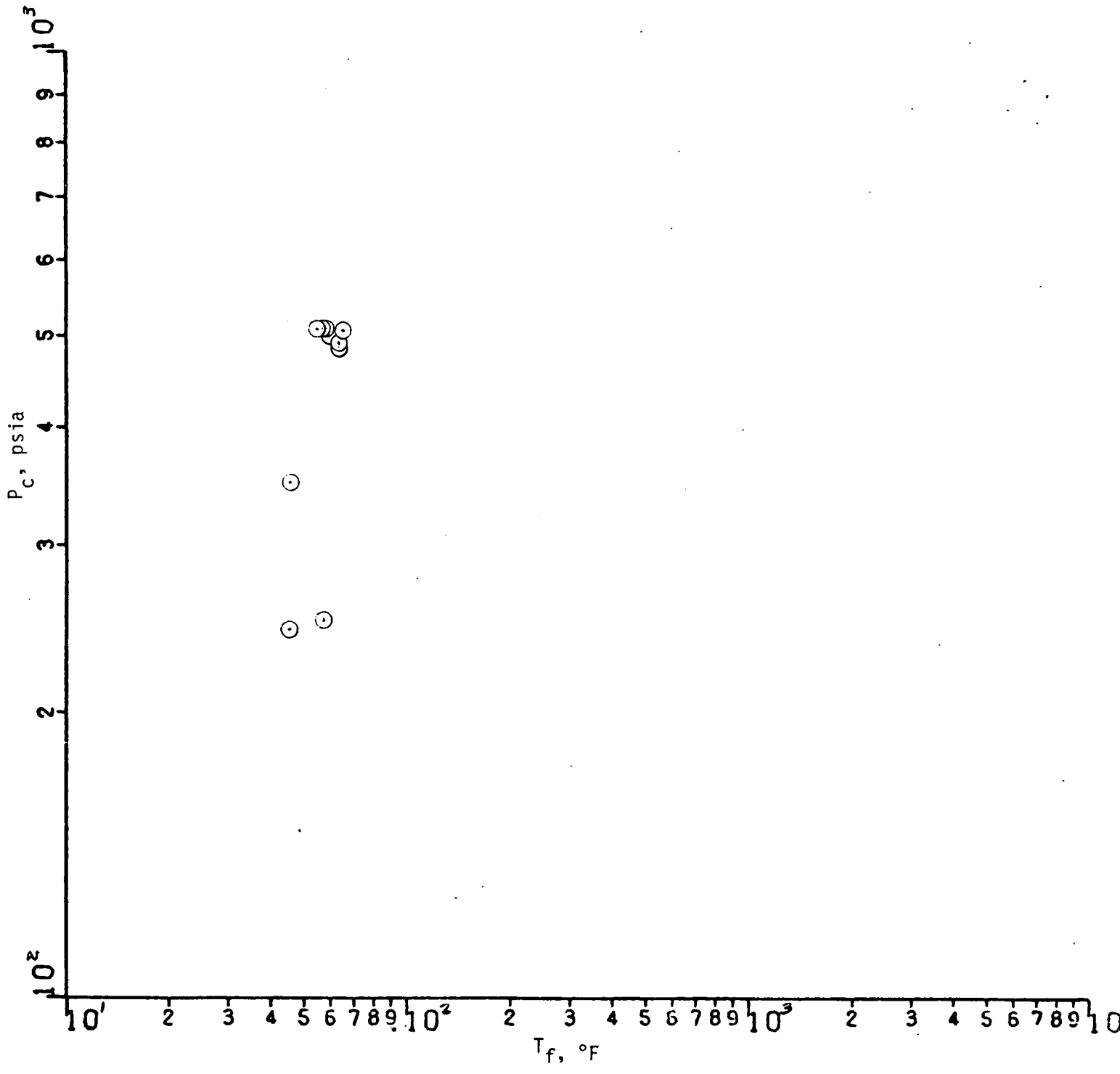

INVESTIGATOR JUDD

INJECTOR = RUD GAS GENERATOR

FUEL = C_3H_8

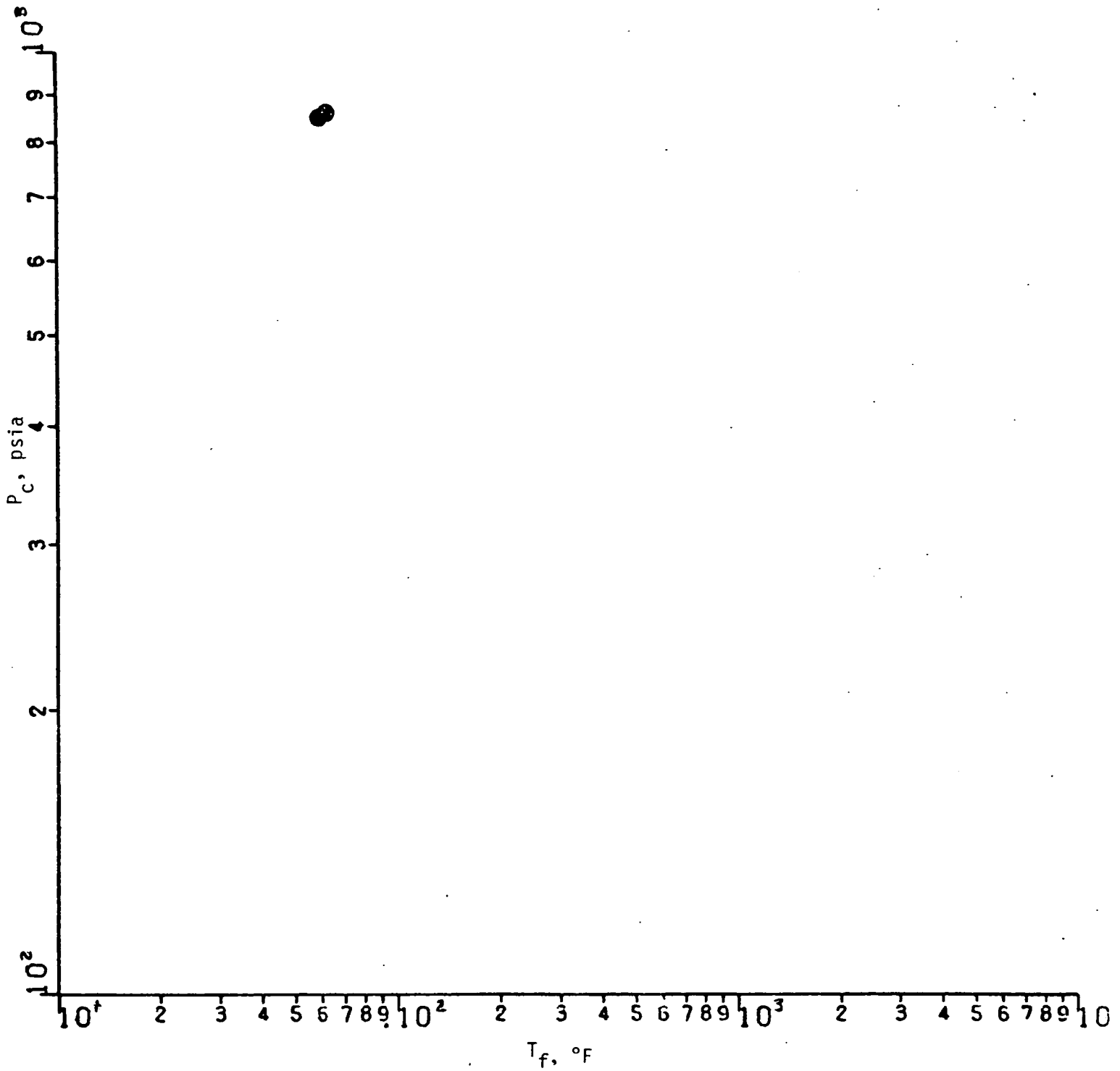

INVESTIGATOR JUDD

INJECTOR = LOL-EDM GAS GENERATOR

FUEL = C_3H_8

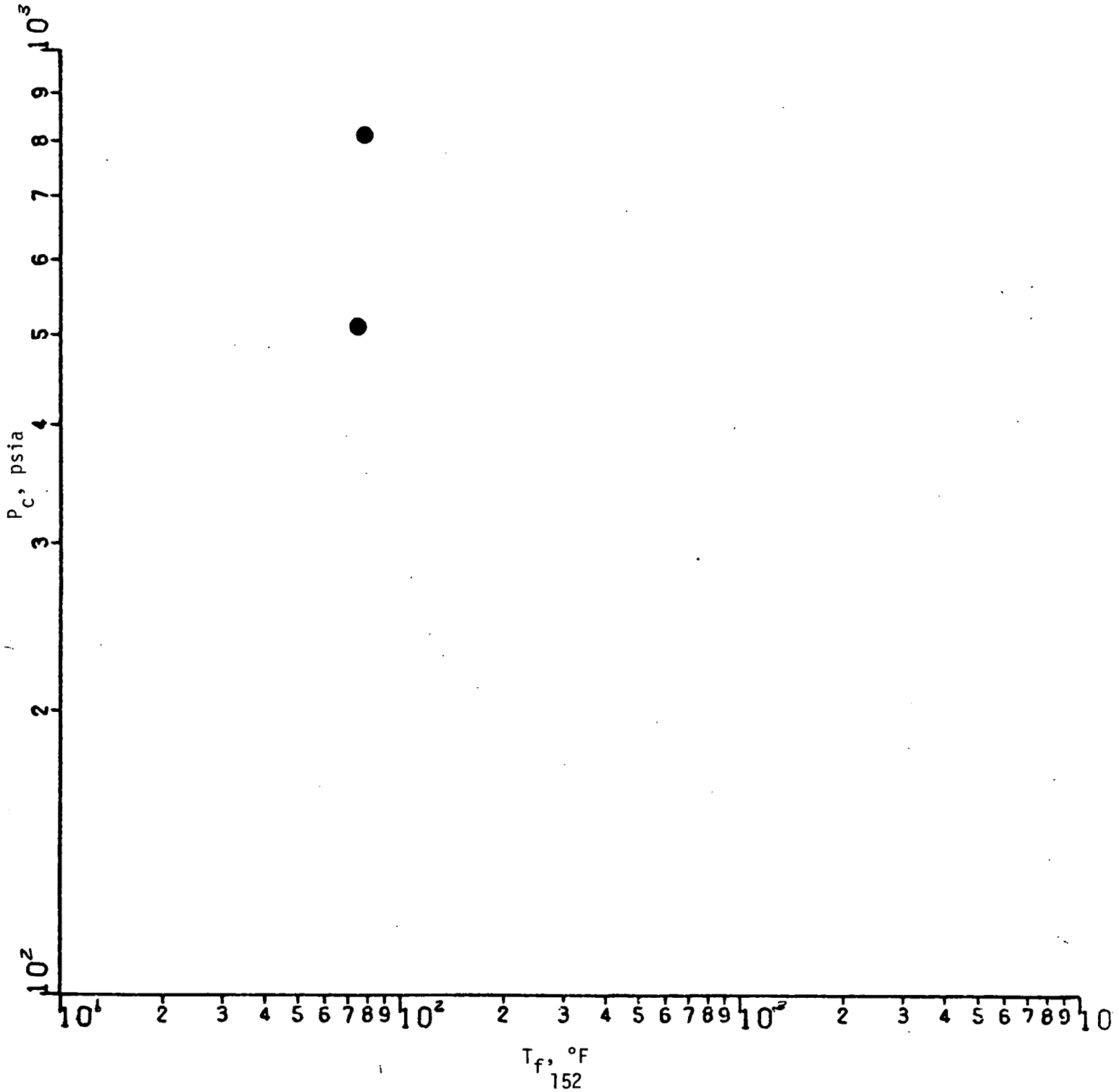

INVESTIGATOR JUDD

INJECTOR = SLIT TRIPLET

FUEL = GCH_4

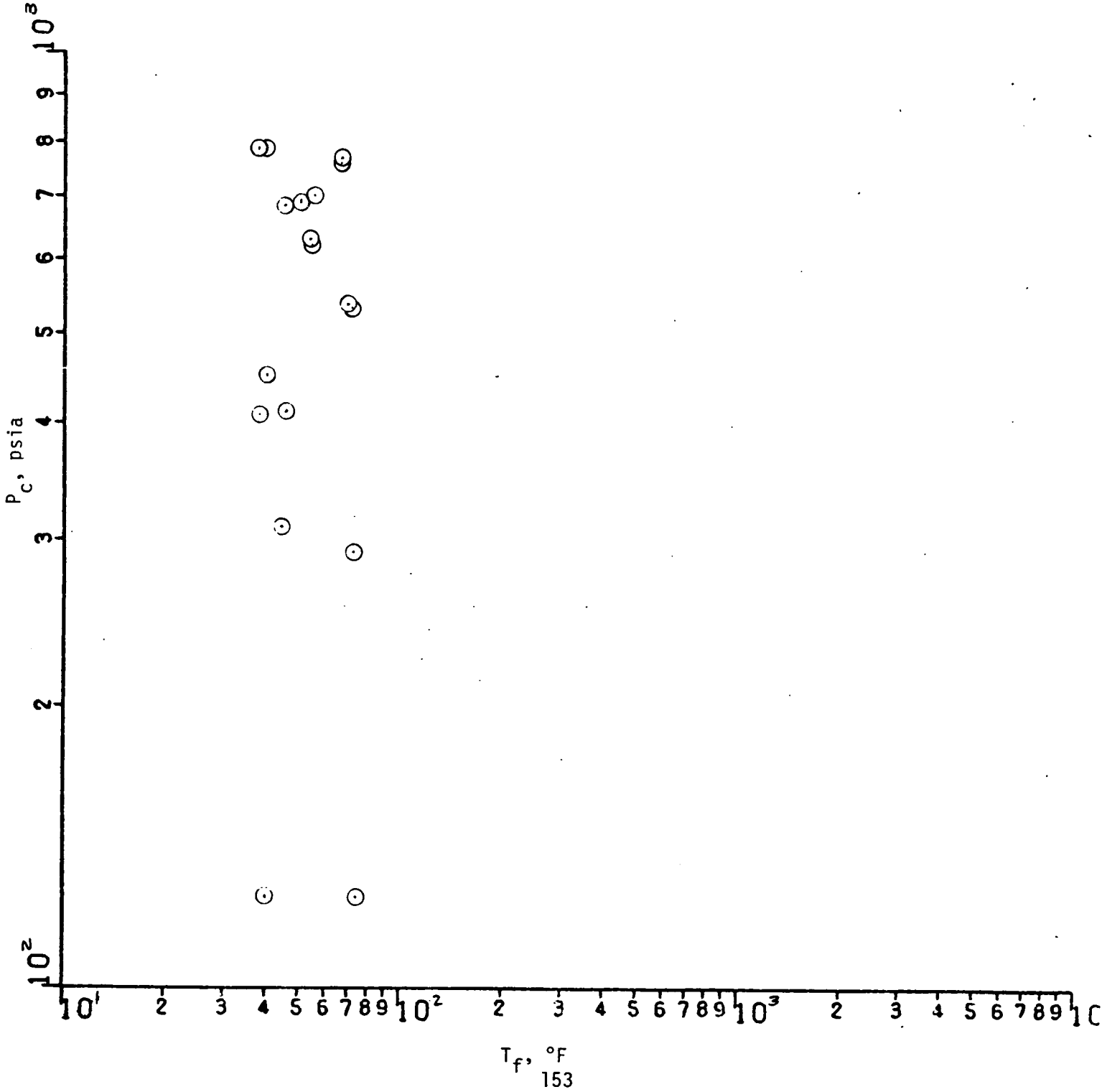

INVESTIGATOR JUDD

INJECTOR = LOL-EDM GAS GENERATOR

FUEL = LCH_4